

**Morphological, Physiological, Biochemical
and Molecular Response of Rice Seedlings to
Metallo-Nanoparticles**

THESIS SUBMITTED TO GOA UNIVERSITY
FOR THE DEGREE OF

DOCTOR OF PHILOSOPHY

IN
BOTANY

581
DAC / MOR

By

Maria Vera Jesus Da Costa

M.Sc. Biotechnology



Under the guidance of

Prof. Prabhat K. Sharma
Department of Botany
Goa University
Goa 403 206
India

T- 772
772

July 2016

STATEMENT

As required under the university ordinance OB-09, I state that the present thesis entitled “Morphological, physiological, Biochemical and Molecular Response of Rice Seedlings to Metallo-Nanoparticles” is my original contribution and that the same has not been submitted on any previous occasion to the best of my knowledge, the present study is the first comprehensive study of its kind from the area mentioned.

The literature conceiving the problem investigated has been cited. Due acknowledgements have been made wherever facilities have been availed.



Maria Vera Jesus Da Costa

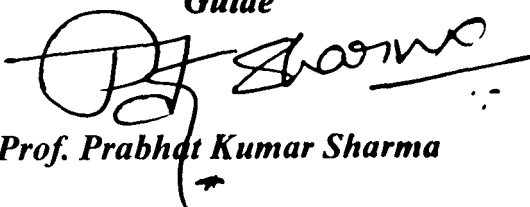
Place: Goa University, Goa

Date: July 2016

CERTIFICATE

This is to certify that the thesis entitled “Morphological, physiological, Biochemical and Molecular Response of Rice Seedlings to Metallo-Nanoparticles” submitted by Ms. Maria Vera Jesus Da Costa for the award of the degree of Doctor of Philosophy in Botany is based on the results of experiments carried out by her under my supervision. The thesis or any part thereof has not previously been submitted for any other degree or diploma.

Guide



Prof. Prabhakar Kumar Sharma

Place: Goa University, Goa

Date: July 2016



Boat on the water

Dedicated to

My beloved grandmother

Late. Mrs. Bela Rubertina Carneiro e Rodrigues

&

My loving parents

CONTENTS

	Page number
Acknowledgment	i
List of figures	iii
List of tables	viii
Abbreviations	x
Abstract	xii
Introduction	1- 45
Materials and Methods	46-71
Results	72-128
Discussion	129-152
References	153-182
List of Publications	183
Awards	

ACKNOWLEDGMENT

I would like to express my deepest sense of gratitude to my mentor and research guide Prof. Prabhat Kumar Sharma, Department of Botany, Goa University for his valuable guidance, encouragement and endless support.

My sincere thanks to Prof. B. F. Rodrigues (Head), Department of Botany for providing the Departmental facilities and Prof. M. K. Janarthanam, Dean, Faculty of Environment and Life Sciences for his constant support and encouragement. I would also like to thank Prof. S. K. Dubey (VC's nominee), Dept. of Microbiology for his encouragement.

I am grateful to The Indian Council of Agricultural Research (ICAR), Goa and Goa Bagayatdar Sahakari Kharedi Vikri Sauntha Maryadit, Ponda, Goa for providing rice seeds, Prof. Tapas Nag and team, All India Institute Of Medical Science (AIIMS), New Delhi for Transmission Electron Microscopy (TEM) sample preparation and imaging, Dr. V. K Banakar (Scientist), NIO for his help in using the Inductively Coupled Plasma Atomic Emission Spectroscopy (ICP-OES) facility; Dr. Anelia Mesquita (Retd. Scientist), Dr. Blasco Fernandes, NIO, Goa and Prof. G. N. Nayak, Dept. of Marine Science, Goa University for providing Atomic Absorption Spectroscopy (AAS) facility; Dr. Girish Kunte (CeNSE, IISc, Bangalore) for Dynamic Light Scattering (DLS) facility; Prof. Priolkar and Ms. Elaine Dias, Dept. of Physics, Goa University for X-ray Diffraction (XRD) analysis and Mr. Amit Tripathi (CDRI, Lucknow) for help with statistical software and literature collection.

My sincere gratitude to Dr. Nandkumar Kamat, Prof. S. Krishnan and Prof. Vijaya Kerkar for their good wishes and reassurance. I also wish to thank all the non-teaching staff namely Mr. Tari, Mr. Vithal Naik, Mrs. Nutan Chari, Mr. Dilip and Mr. Gaonkar for their continuous help and co-operation.

This acknowledgement would be incomplete without the mention of my dear lab mates, Ms. Nisha Kevat, Mrs. Smita Srisvastava, Ms. Prabha Tiwari (Plant Physiology Laboratory, Goa University) and Dr. Rupali Bhandari for their constant support, help and encouragement. A special thanks to Mr. Anup Despande, Ms. Rosy D'Souza and Mr. Ravi

Kiran Pagare for their help whenever I asked them. I also extend my sincere thanks to all the Ph. D and post-doctoral students, Department of Botany, Goa University (2011-2016) for their support.

I am extremely thankful to the Department of Science and Technology (DST), New Delhi (SR/SO/PS-63/2009) and UGC SAP [F. 3-50/2009 (SAP-II)] to PKS (2011-2013) and UGC Maulana Azad National Fellowship Programme grant to MVJDC for providing financial assistance for the year (2013-2016).

Last but not the least I would like to thank my late grandmother and my loving parents, my father who has been a constant support and my mother for accompanying me out of Goa for experimental work. I thank my sister and close friends Samuel Rodrigues and Noel Soares for their co-operation, moral support and for keeping my spirits high during the course of my work.

Maria Vera Jesus Da Costa

LIST OF FIGURES

Sr.No	Title	Page no
1.1.1	A visual display of natural and manufactured objects that fall in the “nano” (<100 nm) and “micro” (>100 nm) size ranges.	4
1.1.2	Engineered nanoparticles (A) and typical synthetic methods for nanoparticles for the top-down and bottom-up approaches (B).	6
1.1.3	Applications of Nanoparticles	8
1.3	Series of events accounting for the toxicity of NPs starting with the sources to the entry into the ecosystem	12
1.4	Probable modes of nanoparticle uptake in a plant cell.	15
1.5	The uptake, translocation and biotransformation pathway of various nanoparticles in a plant system. Plant showing the selective uptake and translocation of nanoparticles (A) and transverse cross section of the root absorption zone showing the differential nanoparticle interaction on exposure (B).	17
1.7.1	Schematic diagram representing the organization of the membranes in the chloroplast (A) the protein complexes of the thylakoid membranes (B) and the photosystem II complex (C).	26
1.7.2	Non-cyclic photophosphorylation (Z scheme) (A) and Carbon dioxide fixation (B) of photosynthesis in plants.	29
1.8.1	The Reactive Oxygen Species (ROS) cycle in plants (A) and the formation of different ROS (B).	31
1.8.2	Lipid peroxidation mechanism in plants	34
1.9	The antioxidant system	40
2.2.1	Setting up of the hydroponic system from early seed stage to final stage of growth.	49
2.2.2	Comparison of the Standardized hydroponic system used for the study (A) with the unsuccessful techniques tried, Petriplate method (B) and broad based glass dish method (C) used for growth of rice plants at a temperature of $25 \pm 2^{\circ}\text{C}$ and a 16 h photoperiod (light intensity $200 \mu\text{mol m}^{-2} \text{s}^{-1}$) with additional incandescent light (20W bulbs).	51

Sr.No	Title	Page no
2.3	Pictorial depiction and the diagrammatic representation of the working principle of SEM (A), XRD (B) and DLS (C).	53
2.4	Inductively coupled plasma mass spectroscopy	55
2.5	Diagram representing parts of rice plant at 6 d (A) and 30 d (B, C) used in the study. The 6 d plants show the emergence of two leaves (first and second) and 30 d plant show three leaves (first, second and third).	57
2.6	Transmission Electron Microscope used in this study.	59
2.7	Tools to study the photosynthetic response of rice plants to Metallo-nanoparticles.	61
2.9	Real time PCR, BioRad, MJ Mini Opticon (A), PCR Corbett Research, Gradient Palm Cycler (B).	70
3.1	Scanning electron microscope images (30,000 X) and X-ray Diffractometer (Rigaku, Japan) pattern taken at room temperature in the range $2\theta=20^{\circ}$ - 80° with a step of 0.02° and a speed= $2^{\circ}/\text{min}$ using Cu $k\alpha$ radiation ($\lambda=0.15406$ nm) to determine the size and shape of MNPs. X-ray diffraction pattern of CuO NPs showing spherical shape and size of <50 nm size (A), X-ray diffraction pattern of ZnO <50 nm showing non-spherical shape and <50 nm size (B), X-ray diffraction pattern of ZnO <100 nm showing non-spherical shape and size of 100 nm (C).	73
3.3.1	Pictorial diagram showing shoot and root length in 6 d (A) and 30 d (B) old rice seedlings treated with CuO NPs in a hydroponic culture system.	81
3.3.2	Pictorial diagram showing shoot and root length in 6 d (A, C) and 30 d (B, D) old rice seedlings treated with ZnO NPs of size < 50 nm (A, B) and 100 nm (C, D) in a hydroponic culture system.	82
3.3.3	SEM images of leaf (adaxial) surface showing number and size of stomata and trichomes (A-C), size of stomata (D-F) and external morphology of roots (G-I) of plants treated with CuO NP for 30 d.	84
3.3.4	SEM images of leaf (adaxial) surface showing number and size of stomata and trichomes (A-C), size of stomata (D-F) and external morphology of roots (G-I) of plants treated with ZnO NP for 30 d.	85

Sr.No	Title	Page no
3.3.5	Cross section (40 X) of mature rice leaf treated with CuO (A-F) and ZnO (G-K) NPs at different concentrations after 30 d of growth.	86
3.3.6	Cross section (40 X) of mature rice leaf treated with CuO (A-O) and ZnO (a-o) NPs at different concentrations [10 x magnification (A-E; a-e) and 40 x magnifications (F-O; f-o)].	87
3.4.1	Electron photomicrographs of leaf (A-I) and roots (J-L) of <i>O. sativa</i> showing changes in organelles and accumulation of CuO NPs. Whole cell of untreated leaf (A); treated leaf showing number of chloroplast, c and mitochondria, m (B); intact bundle sheath cells (C); accumulation of CuO NPs in cytosol (D-F); fully stacked thylakoids (G), partially stacked and accumulation of CuO NPs (H), destacked (2-3 thylakoids per granum) and distorted arrangement of thylakoids (I), images of root showing CuO NP aggregation and cluster formation (J-L) in roots.	93
3.4.2	Electron photomicrographs of leaf (A-I) and roots (J-L) of <i>O. sativa</i> showing changes in organelles and accumulation of ZnO NPs in leaf and root. Whole cell of untreated leaf (A); number of chloroplast at low concentration (B); intact bundle sheath cells (C); presence of starch granules, s (D); chloroplast number, c (E); number of mitochondria, m (F); fully stacked thylakoids (G), partially stacked (H-I) and accumulation of ZnO NPs in roots (J-L).	94
3.5	Photosynthetic rate (P_N), stomatal conductance (g_s), and transpiration rate (E) of rice plants treated with CuO (A) and ZnO of <50 nm size (B) and ZnO of 100 nm size (C) NPs after 30 d.	96
3.6.1	Maximum quantum efficiency of PSII (F_v/F_m), photochemical quenching (q_P) and non-photochemical quenching (q_N) (A); quantum efficiency of PSII (B) of rice plants treated with CuO NPs for 30 d.	98
3.6.2	Maximum quantum efficiency of PSII (F_v/F_m), photochemical quenching (q_P), non-photochemical quenching (q_N) (A) and quantum efficiency of PSII (B) of rice plants treated with ZnO (<50 nm) NPs for 30 d.	99

Sr.No	Title	Page no
3.6.3	Maximum quantum efficiency of PSII (F_v/F_m), photochemical quenching (q_p), non-photochemical quenching (q_N) (A) and quantum efficiency of PSII (B) of rice plants treated with ZnO (100 nm) NPs for 30 d.	100
3.7.1	HPLC Profile extracted at 445 nm of photosynthetic pigments in rice plants after 30 d of CuO NP treatment.	101
3.7.2	HPLC Profile extracted at 445 nm of photosynthetic pigments in rice plants after 30 d of ZnO (<50 nm) NP treatment.	102
3.7.3	HPLC Profile extracted at 445 nm of photosynthetic pigments in rice plants after 30 d of ZnO (100 nm) NP treatment.	103
3.8.1	Malondialdehyde (MDA) content in rice plants treated with CuO (A) and ZnO of <50 nm size (B) and ZnO of 100 nm size (C) NPs after 30 d.	109
3.8.2	Protein carbonyl content in rice plants treated with CuO (A) and ZnO of <50 nm size (B) and ZnO of 100 nm size (C) NPs after 30 d.	110
3.8.3	Proline content in rice plants treated with CuO (A) and ZnO of <50 nm size (B) and ZnO of 100 nm size (C) NPs after 30 d.	111
3.9.1	Ascorbate content (A) and Superoxide dismutase (SOD) activity (B) of rice plants treated with CuO and ZnO (100 nm) nanoparticles for 30 d.	113
3.9.2	Spermine (A) and spermidine (B) content of rice plants treated with CuO and ZnO (100 nm) nanoparticles for 30 d.	114
3.10	Gene expression of Superoxide dismutase (A), Ascorbate peroxidase (B), Glutathione reductase (C) and Phytochelatin synthase (D) in rice plants treated with CuO and ZnO (100 nm) nanoparticles for 30 d.	117
3.11.1	The maximum quantum efficiency of PSII (F_v/F_m ; A), photochemical quenching (q_p ; B), non-photochemical quenching (q_N ; C), photosynthesis rate (P_N ; D), transpiration rate (E; E) and stomatal conductance (g_s ; F) of rice plants treated with bulk Cu and CuO NPs.	123
3.11.2	Photosynthetic rate (P_N ; A), transpiration rate (E; B), and stomatal conductance (g_s ; C) of rice plants treated with ZnO (<50, 100 nm) NP and bulk Zn.	124

Sr.No	Title	Page no
3.11.3	Malondialdehyde (A), proline (B), ascorbate (C) content and superoxide dismutase activity (D) of rice plants treated with CuO NPs and bulk Cu; Percent MDA content (E) and proline content (F) of rice treated with ZnO NPs and bulk Zn	126
4.7	Mechanism of Metallo-nanoparticle (MNP) effect (A) and Bulk metal (Cu & Zn) effect (B) in <i>Oryza sativa</i> grown hydroponically.	152

LIST OF TABLES

Sr.No	Title	Page no
2.1	Metallo- nanoparticles specification as mentioned by supplier.	47
2.2	Composition of Hoagland's Plant Nutrient Solution (Hoagland and Arnon 1950)	48
2.9	List of anti-oxidant primers (Reverse and Forward) used to study gene expression by real time analysis procured from Pharmoids and Equipments Pvt. Ltd.	71
3.2	Amount of ions released from MNP and its bulk counterpart in water and Hoagland's solution (A) and percent ions released from MNPs and bulk metals at 100 and 1000 mg L ⁻¹ weight bases (B).	75
3.3.1	Percent germination, shoot, root length (6 d old plants) and biomass (30 d old plants) of <i>Oryza sativa</i> var. Jyoti grown at different concentrations of CuO NPs.	77
3.3.2	Percent germination, shoot, root length (6 d old plants) and biomass (30 d old plants) of <i>Oryza sativa</i> var. Jyoti grown at different concentrations of ZnO (<50 nm) NPs.	78
3.3.3	Percent germination, shoot, root length (6 d old plants) and biomass (30 d old plants) of <i>Oryza sativa</i> var. Jyoti grown at different concentrations of ZnO (100 nm) NPs.	79
3.4.1.1	Cu content in leaf and root of <i>O. sativa</i> plants treated with CuO NPs at 0–1000 mg L ⁻¹ concentrations for 30 d.	89
3.4.1.2	Zn content in <i>O. sativa</i> treated with ZnO NPs at 0–1000 mg L ⁻¹ concentrations for 30 d.	91
3.7.1	The Car content and relative Chl content of <i>O. sativa</i> leaves treated with CuO NPs at 0–1000 mg L ⁻¹ concentrations for 30 d. β -carotene was used as standard.	105
3.7.2	The Car content and relative Chl content of <i>O. sativa</i> leaves treated with ZnO (<50 nm) NP at 0–1000 mg L ⁻¹ concentration after 30 d of growth.	106

Sr.No	Title	Page no
3.7.3	The Car content and relative Chl content of <i>O. sativa</i> leaves treated with ZnO (100 nm) NP treated rice plants at 0-1000 mg L ⁻¹ concentration after 30 d of growth.	107
3.11.1	Percent germination, shoot, root length (6 d), biomass (30 d), content of copper (Cu) in leaf and root tissue and the Chl ratio, Chl/ Car ratio of <i>O. sativa</i> treated with bulk Cu at different concentrations.	120
3.11.2	Percent germination, shoot, root length (6 d) and biomass (30 d) of <i>O. sativa</i> treated with bulk Zn at concentration of 0-1000 mg L ⁻¹ .	121

ABBREVIATIONS

$^1\text{O}_2$	Singlet oxygen
AAS	Atomic absorption spectrophotometer
ABA	Abscisic acid
AIDS	Acquired immune deficiency syndrome
APX	Ascorbate peroxidase
ASA	Ascorbic acid
ATP	Adenosine triphosphate
BADH	Betaine aldehyde dehydrogenase
CAT	Catalase
CeO_2	Cerium dioxide
Chl_3	Triplet Chlorophyll state
CNT	Carbon nanotubes
CO_2	Carbon dioxide
CoFe_2O_4 NPs	Cobalt ferrite nanoparticles
CuO NPs	Copper Oxide nanoparticles
DHA	Dehydroascorbate
DHAR	Dehydroascorbate reductase
<i>E</i>	Transpiration rate
ENM	Engineered nanomaterial
EPA	Environmental protection agency
ETC	Electron transport chain
Fd	Ferredoxin
Fe_3O_4 NPs	Iron oxide nanoparticles
F_m	Maximum fluorescence
FMS	Fluorescence monitoring system
F_v	Variable fluorescence
F_v/F_m	Maximal quantum yield of PSII photochemistry
GB	Glycine betaine
GPX	Glutathione peroxidase
GR	Glutathione reductase
g_s	Stomatal conductance
GSH	Glutathione
GSSG	Glutathione disulphide (oxidized)
H_2O_2	Hydrogen peroxide
$\text{HO}^{2\cdot}$	Per hydroxyl radical
IRGA	Infra-red gas analyzer
MDA	Malondialdehyde
MDHA	Mono-dehydroascorbate
MDHAR	Mono-dehydroascorbate Reductase
Mn_2O_3	Manganese oxide nanoparticles
MNP	Metallo-nanoparticles/ metal oxide nanoparticles
MRSA	Methicillin-resistant <i>Staphylococcus aureus</i>

MTs	Metallothioneins
MWCNT	Multi-walled carbon nanotubes
NADP ⁺	Nicotinamide adenine dinucleotide phosphate
Ni (OH) ₂ NPs	Nickel dioxide nanoparticles
NP	Nanoparticles
O ₂ ⁻	Superoxide radical
OAT	Ornithine-delta-aminotransferase
PCs	Phytochelatin
PCS	Phytochelatin synthase
PIXES	Proton induced X-ray emission spectroscopy
P _N	Photosynthetic rate
PSI	Photosystem I
PSII	Photosystem II
PUFA	Polyunsaturated fatty acid
Put	Putrescine
q _P	Photochemical quenching
RAPD	Random Amplification of Polymorphic DNA
RDM	Root dry mass
RFM	Root fresh mass
RO [•]	Alkoxy radical
ROS	Reactive oxygen species
SDM	Shoot dry mass
SEM	Scanning electron microscope
SFM	Shoot fresh mass
SiO ₂	Silicon dioxide
SOD	Superoxide dismutase
Spd	Spermidine
Spm	Spermine
SWNT	Single walled nanotubes
tAPX	Thylakoid bound APX
TBA	Thiobarbituric acid
TEM	Transmission electron microscope
TiO ₂ NPs	Titanium dioxide nanoparticles
XRD	X-Ray diffraction
ZnO	Zinc oxide nanoparticles

Elements of the Periodic Table

Ba	Barium	Ra	Radium
Be	Beryllium	Rf	Rutherfordium
Ca	Calcium	Sc	Scandium
Cu	Copper	Sr	Strontium
Hf	Hydrogen fluoride	Ta	Tantalum
Lr	Lawrencium	V	Vanadium
Lu	Lutetium	Y	Yttrium
Nb	Niobium	Zr	Zirconium

ABSTRACT

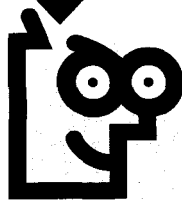
The dawn of nanotechnology has seen an ever increasing use of metallo-nanoparticles (MNPs) in various industrial sectors including agriculture. The excessive usage of these MNPs results in their inevitable release into the environment subsequently entering into plants with effects unknown. It was therefore, imperative to explore the effects of MNPs on food crops and detect their threshold level of toxicity. The present investigation was conducted in order to assess the influence of Copper and Zinc oxide (50 and 100 nm) NPs on various morphological, physiological, biochemical and molecular parameters in *Oryza sativa* var. Jyoti grown hydroponically at a concentration range of 0-1000 mg L⁻¹ for a growth period of 30 d and to compare its behaviour with bulk metals. Nanoparticle characterization studies with X-ray diffraction showed that the particle size of CuO NPs, ZnO (50 nm) NPs and ZnO (100 nm) NPs was 50 ± 2, 35 ± 2 and 100 ± 2 nm respectively, the sizes obtained were in accordance to the specifications given by the supplier. Dissolution studies revealed that MNPs released relatively smaller amounts of metal ions in Hoagland's solution at high concentrations as compared to metal ions released by bulk metals. The toxicity threshold of CuO NPs was found to be 100 mg L⁻¹ and the threshold level for ZnO NPs (50 and 100 nm) was 50 mg L⁻¹ in treated rice plants. Metallo-NPs accumulated in leaves and roots with increase in concentration, however, increase of MNPs in roots was many fold greater than in leaves indicating an exclusion mechanism at root level. Accumulation of MNPs in leaves was observed in the chloroplast resulting in destacking and distortion of thylakoids (wavy arrangement) leading to decreased photosynthesis and productivity. Photosynthetic measurements taken using the Fluorescence Monitoring System showed a decrease in maximum quantum efficiency of PSII (F_v/F_m ratio), photochemical quenching (q_p) and quantum efficiency of PSII (Φ_{PSII})

whereas Infra-Red Gas analysis revealed a decline in photosynthetic rate (P_N), transpiration rate (E) and stomatal conductance (g_s). An increase in the Chl *a/b* ratio at high concentrations was also observed using high performance liquid chromatography technique. Increased MNP treatment also resulted in osmotic stress indicated by decreased number and size of stomata, increased number and size of trichomes, reduction in E , g_s and elevated proline levels. Increase in ascorbate content, spermine content and gene expression of enzymatic antioxidants (SOD, APX and GR) indicated mitigation of metabolic ROS generation resulting in suppressed oxidative stress upon MNP treatment. Increased gene expression of phytochelatin at the highest concentration of MNP reveals a plants defense mechanism to actively chelate the metal particles in leaves by compartmentalization of metal-PC complexes preventing MNP induced damage. The results showed that unlike bulk metals, MNPs did not release excess metals ions to generate ROS thereby resulting in negligible oxidative stress indicated by absence of oxidation to lipids and proteins. The mechanism of phytotoxicity observed as a result of MNP treatment in this study was mainly due to MNP accumulation in the chloroplast causing destacking and distortion of thylakoid membranes and not due to the metal ions released from MNP.

CHAPTER

1

INTRODUCTION



“Environmental pollution is an incurable disease. It can only be prevented”

Barry Commoner

INTRODUCTION

TABLE OF CONTENTS

Sr. No	Title of the topic	Page No.
1.1	What Are Nanoparticles?	2
1.1.1	Classification of Nanoparticles	2
1.1.2	Nanoparticle Synthesis	5
1.1.3	Applications of Nanoparticles	7
1.2	Metallo- Nanoparticles	10
1.3	Nanoparticles in the Environment	11
1.4	Internalization and Uptake of Metallo-Nanoparticles in Plants	13
1.5	Localization and Storage of Metallo-Nanoparticles in Plants	16
1.6	Effect of Metallo-Nanoparticles in Plants	18
1.6.1	Copper Oxide Nanoparticle (CuO MNPs)	18
1.6.2	Zinc Oxide Nanoparticle (ZnO MNPs)	20
1.7	Photosynthesis	24
1.8	Mechanism of metal stress	30
1.8.1	Lipid Peroxidation	32
1.8.2	Protein Oxidation	35
1.8.3	DNA Damage	35
1.9	ROS Scavenging Antioxidant Defense Mechanism	36
1.9.1	Enzymatic Anti-Oxidant Systems	36
1.9.2	Non -Enzymatic Anti-Oxidant Systems	38
1.9.3	Other Cellular Mechanisms For Metal Detoxification	41
1.10	<i>Oryza Sativa</i> (Rice) As A Model Plant	43
1.11	Aim And Objectives	44

Nano-biotechnology was born as a hybrid discipline, a combination of biotechnology and nano-science. It is a field of applied sciences which encompasses the construction of materials, devices and systems by virtue of nanoscale control and manipulation of matter. Although new, the history of nano-materials began in 1959, when Richard P. Feynman, a physicist at California Institute of Technology (Pasadena, CA, USA) predicted the dawn of nano-materials while saying there is plenty of room at the bottom in one of his class and proposed that scaling down to nano level and starting from the bottom was essential for the upcoming technological development (Mody et al., 2010). In 2000, the US established the National Nanotechnology Initiative (NNI) to study the commercial and environmental impact of the nanoparticles including metallo-nanoparticles and this was followed by a plethora of nanotechnology projects funded by NNI and others over the last 13 years (www.nano.gov). Nanotechnology has rapidly been expanding ever since producing a number of engineered nanomaterials (ENMs; Damoiseaux et al., 2011) which include materials such as metals/ metal oxides, quantum dots, fullerenes, carbon nanotubes, dendrimers etc. These ENMs can be produced to exhibit different crystallinity, aspect ratios, shapes, sizes, surface modifications or hybridization with other nanomaterials. Thus, the number of commercially produced nanomaterials which are inclusive of ENMs has surpassed 1000 consumer products in 2009 and could grow to 10^4 materials within a decade. Due to these applications the global investment in the production of nanoparticles (NPs) is set to cross \$1 trillion by 2015 (Roco 2005) and nanotechnology-related products are expected to reach 58,000 tons by 2020 (Maynard 2006). A recent report suggested that the magnitude of NP exposure to soil was five orders higher than that in air and water, with the annual input of NPs in soil alone predicted to be $\sim 1.01\text{-}2380 \text{ mg kg}^{-1}\text{yr}^{-1}$ (Schwab et al., 2015). Literature shows that research on NPs interaction with plant system is limited and the consequences of ENMs in the plants unknown. This warrants the need to understand

the interactions of NPs with plants and its consequent effects. In this study, an attempt was made to understand the effect of metallo- nanoparticles or metal oxide nanoparticles (MNP) in *Oryza sativa*, its uptake, translocation, changes in the internal and external morphology and influence on photosynthesis, in-addition to enzymatic and non-enzymatic anti-oxidant response upon MNP treatment.

1.1. What Are Nanoparticles?

Many organizations have defined NPs based on its particle dimensions and/or diameter. The International Organization for Standardization (ISO) defines NPs as a particle spanning 1–100 nm in diameter to which Roco (2005) added that it can be a small entity that acts as a complete unit with respect to its transport and properties. The American Society of Testing and Materials (ASTM) defines NP as an ultrafine particle of 1-100 nm in length with 2 or 3 dimensions in the range of 1–100 nm. A similar definition has been given by National Institute of Occupational Safety and Health (NIOSH) stating NPs is a particle with diameter between 1–100 nm or a fiber spanning the range 1–100 nm. The Scientific Committee on Consumer Products (SCCP) defines NPs as a particle with at least one side in the range of 1–100 nm in size while British Standards Institution (BSI) describes it as having all the dimensions between 1 and 100 nm in size. In this study, throughout the text, metallo– nanoparticles (MNP) refers to metal oxide NPs of size ranging between 1–100 nm and bulk metals refers to the metal salt such as CuSO_4 and ZnSO_4 (heavy metal; www.sciencedaily.com) which easily ionize unlike MNPs.

1.1.1. Classification of Nanoparticles

A significant fraction of solid matter on the earth surface is found as colloids and NPs (Wiggington et al., 2007). A pictorial representation of natural and manufactured objects that fall in the “nano” (<100 nm) and “micro” (>100 nm) size ranges is shown in Figure

1.1.1. Nanoparticles are characterized into three main sub categories, naturally occurring, incidental/unintentional and engineered. **Naturally occurring NPs** are produced as aerosols during volcanic eruptions, pollen fragments, forest fires, viruses and hydrothermal vent systems (Luther and Rickard 2005). **Incidental/ unintentional NPs** are produced through emissions from vehicles, coal combustion, power plants, welding generating soot and elemental carbon. **Engineered nanoparticles (ENPs)** are intentionally produced or designed at the atomic scale with very specific properties (shape and/or size) required for the purpose of commercial applications. ENPs can also be bought from vendors or produced experimentally (<https://web.stanford.edu>) and are used in detergents, sunscreens, printer inks, paints, tires, coatings, cement etc. (<https://web.stanford.edu>). Examples of ENPs are metals, metal oxides, quantum dots, bucky balls/ nanotubes, sunscreen pigments and nanocapsules (Navarro et al., 2008a). Nanoparticles produced from unintentional sources are mostly heterogenous or polydispersed particles having irregular shapes whereas ENPs are monodispersed or homogenous having constant shapes (Sioutas et al., 2005).

Engineered NPs can be further classified into six categories consisting of fullerenes and carbon nanotubes (CNTs), ceramic NPs, quantum dots, polymeric NPs and dendrimers (Fig 1.1.2 A). **Fullerenes and carbon nanotubes** are similar to each other. Fullerenes are hollow spheres comprising of $28 \geq 100$ atoms of crystalline forms of carbon while carbon nanotubes (CNTs) are tubular cylinders of carbon atoms. Both fullerenes and CNTs can be linked with organic or inorganic groups to form numerous products. **Ceramic NPs** are objects composed of inorganic and non-metallic materials. They are relatively flexible and therefore can form coatings and nanomaterials at lower temperatures. **Quantum Dots** are combinations of elements from Group II (Alkaline earth metals such as Be, Mg, Ca, Sr, Ba, Ra) and IV (Transition metals such as Ti, Zr, Hf, Rf)

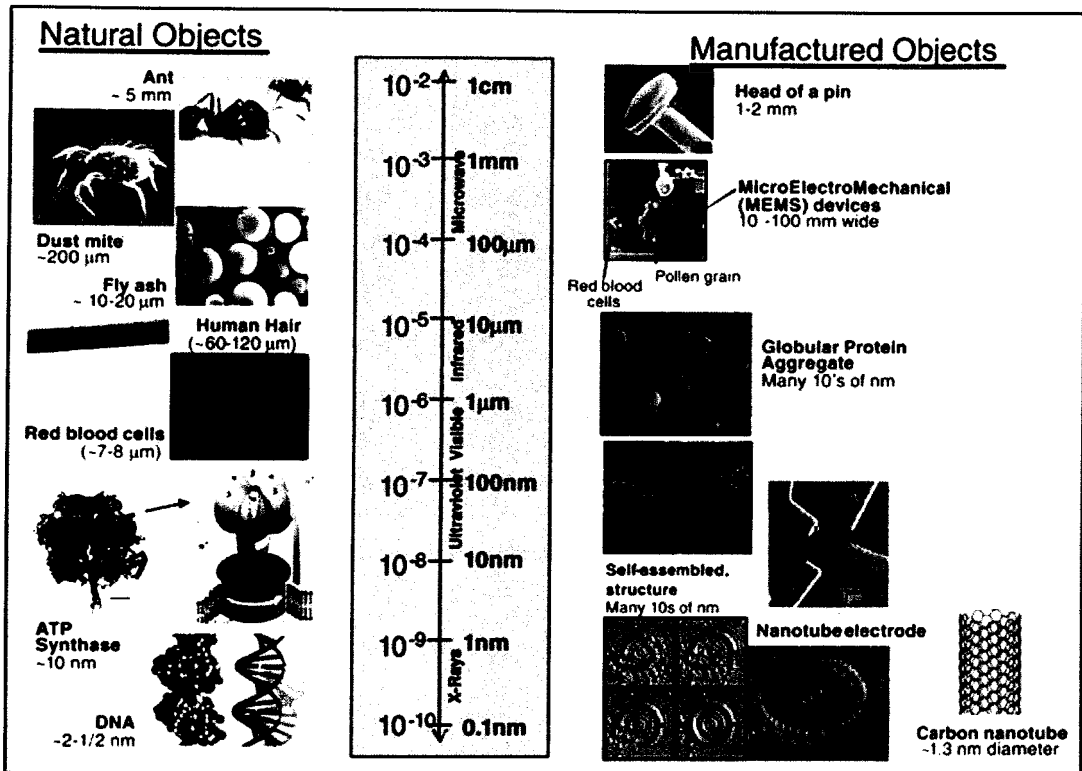


Fig 1.1.1. A visual display of natural and manufactured objects that fall in the “nano” (<100 nm) and “micro” (>100 nm) size ranges. “Adapted from Institute of Medicine (US) Food Forum, Nanotechnology in Food Products: Workshop Summary, Washington (DC): National Academies Press (US); 2009. Chap 1, Introduction)”

or Groups III (Sc, Y, Lu, Lr) and V (Transition metals such as V, Nb, Ta, Db) of the periodic table and have sizes ranging from 1-10 nm. They display unique optical and electronic properties used for a number of applications. **Polymeric NPs** are prepared from polymers such as synthetic plastics (polystyrene) and natural biopolymers (DNA and proteins) having NPs dispersed in the polymer matrix; for example, nano-spheres and nano-capsules. Nano-spheres are matrix particles whose entire mass is solid with the surface of the sphere adsorbed by molecules or encapsulated within the particle (Kumari et al., 2010). Nano-capsules are vesicular systems which entrap substances and confine them to a cavity consisting of a liquid core enclosed by a solid shell. **Dendrimers** are nano-sized and radially symmetric NPs that have well-defined, monodisperse and homogeneous structures and usually possess a symmetric core, an inner shell and an outer shell (Abbasi et al., 2014) and are constructed by the sequential addition of layers of bifurcating functional groups whose molecular surface dominates the properties of dendrimers.

1.1.2. Nanoparticle Synthesis

Synthesis of NPs requires a process that fulfils the following criteria. Firstly, regulators to control the particle (crystal) size, distribution, shape and aggregation of NPs; Secondly, an enhancement technique for nanoparticle purity; thirdly, stability of the physical and chemical properties of NPs and fourthly, greater reproducibility and production with reduced costs. Two approaches have been used to synthesize engineered NPs in industries, the top- down method and the bottom-top method (Fig 1.1.2 B). The top-down method is the application of an external force to a solid that leads to its disintegration into smaller particles and the bottom-up method that produces NPs beginning from atoms based on atomic alterations or molecular condensations. The techniques and methods used to synthesize NPs have been summarised in Fig 1.1.2 B.

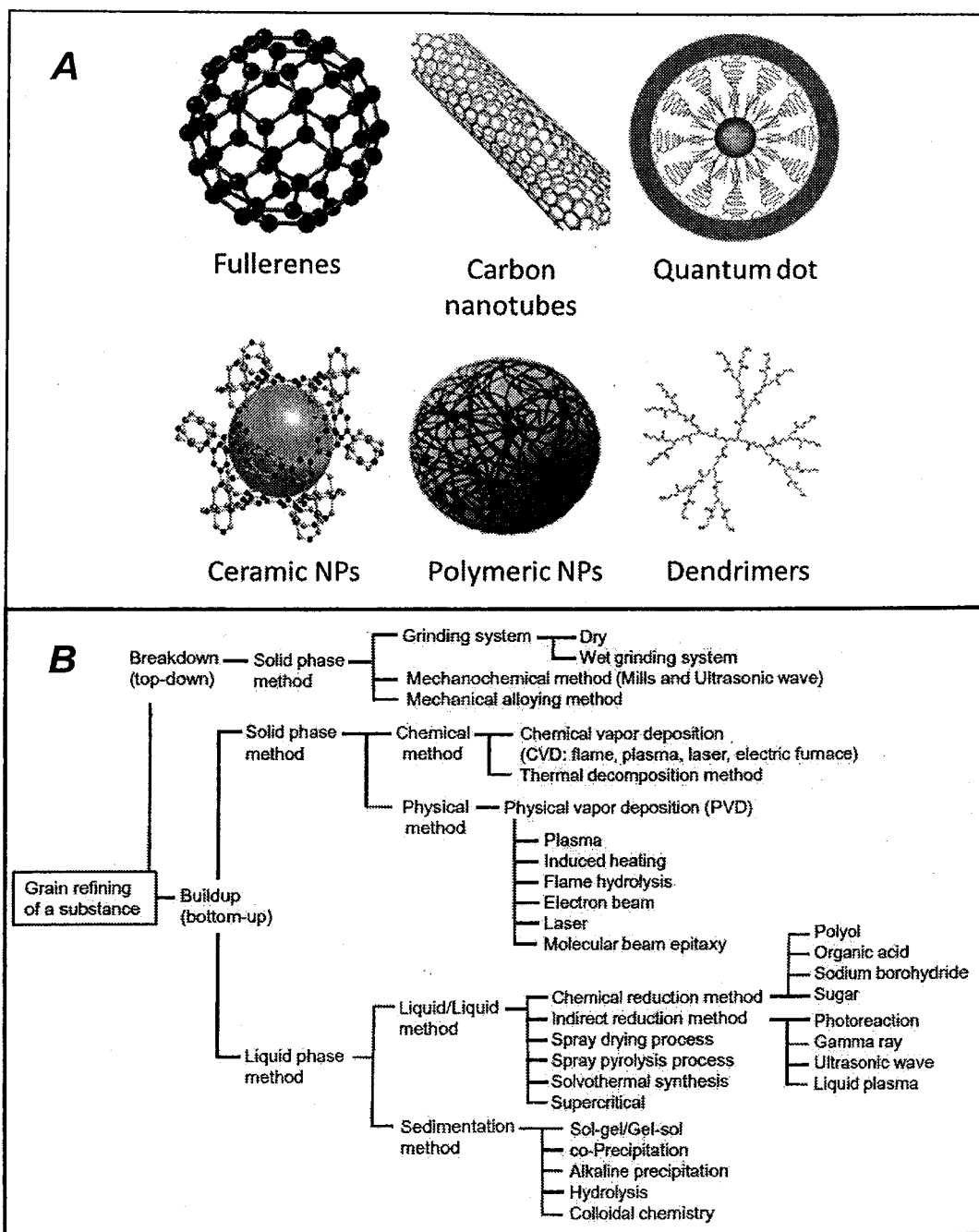


Fig 1.1.2. Engineered nanoparticles (A) and typical synthetic methods for nanoparticles for the top-down and bottom-up approaches; adapted from Horikoshi & Serpone 2013 (B).

1.1.3. *Applications of Nanoparticles*

Nanoparticles have multidisciplinary applications due to their unique properties (Fig 1.1.3), few of which are described below. **Metals oxides nanoparticles, fullerenes and carbon nanotubes** have a number of applications based on its function and are being used in the construction of microelectronic circuits, piezoelectric devices, sensors, fuel cells, chemiresistors, photonics, coatings for the surfaces against corrosion and as catalysts on a large scale. In medicine, the property of surface plasmon resonance of carbon nanotubes, quantum dots and fullerenes has been widely used in the treatment of diseases such as cancer and AIDS. Metallo-NPs, in particular, copper (II) oxide (CuO) /cupric oxide and zinc oxide (ZnO) nanoparticles are used for a variety of applications. CuO NPs are semiconducting compounds with a monoclinic structure (Ren et al., 2009) and has attracted particular attention because it displays a range of potentially useful physical properties such as high temperature superconductivity, electron correlation effects and spin dynamics (Ren et al., 2009). As an important p-type semiconductor, CuO has found many diverse applications in gas sensors, catalysis, batteries, high-temperature superconductors and solar energy converters. In the energy-saving area, energy transferring fluids filled with nano CuO particles can increase fluid viscosity and boost thermal conductivity. CuO crystal structures possess a narrow band gap giving useful photovoltaic or photocatalytic properties as well as photoconductive functionalities. CuO NPs is used in electronics due to its toughness and ductility, electrical conductivity, increased hardness and semiconductor luminescence efficiency. CuO NPs are also used as anti-microbial agents against a number of bacterial pathogens such as *Escherichia coli* and meticillin-resistant *Staphylococcus aureus* (MRSA; Ren et al., 2009). On the other hand, zinc oxide (ZnO) nanoparticles are used as chemical sensors, gas sensors and bio-sensors. They are also used in photonics, cosmetics, storage, optical, electrical devices and solar cells (Vaseem et al.,

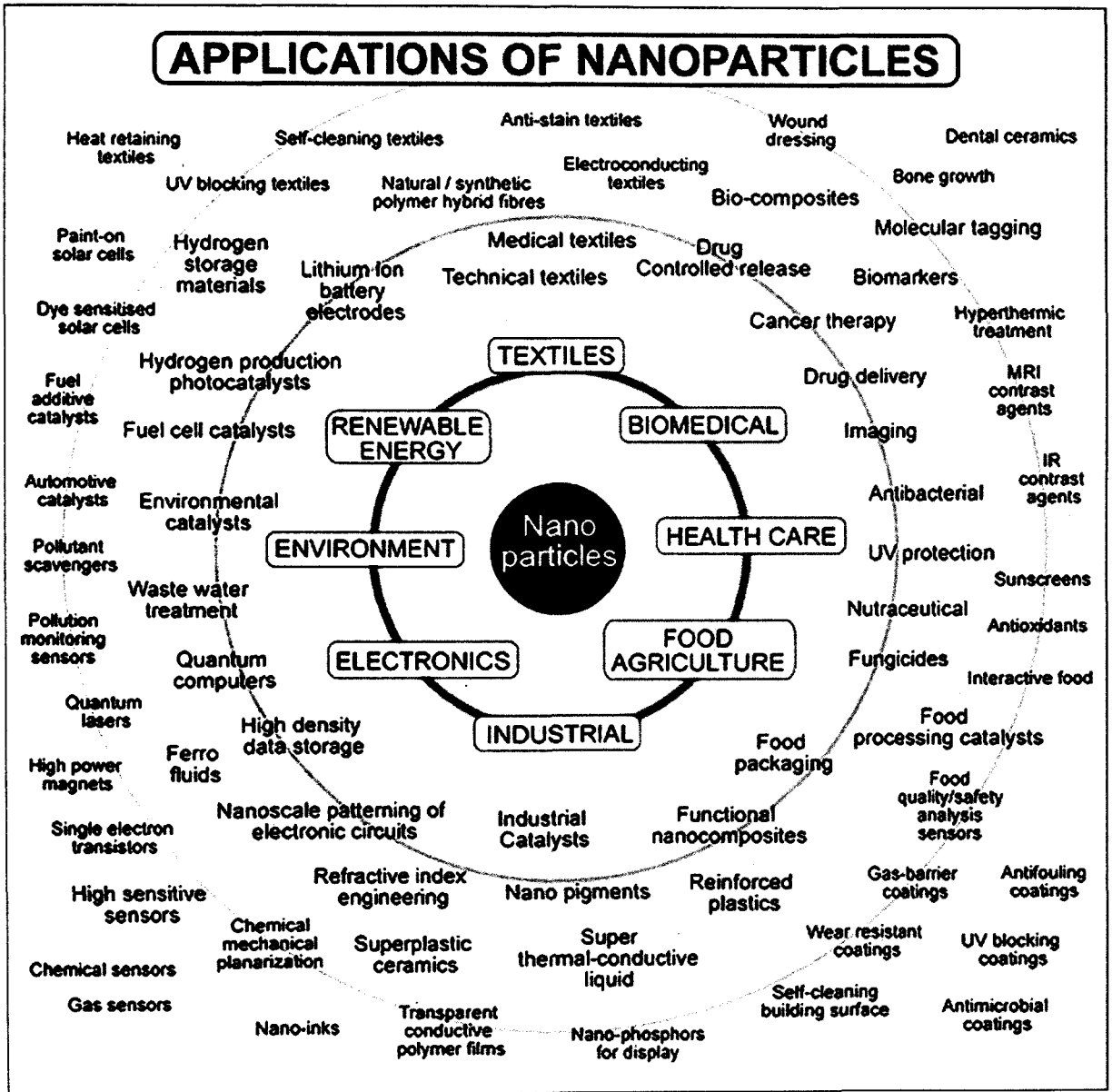


Fig 1.1.3. Applications of Nanoparticles (Tsuzuki 2009)

2010). ZnO NPs is an attractive material for short-wavelength optical/ electronic uses owing to its wide band gap 3.37 eV, large bond strength, and large exciton binding energy (60 m eV) at room temperature. As a wide band gap material, ZnO is used in solid state blue to ultraviolet (UV) optoelectronics, including laser developments. In addition, due to its piezoelectric property, ZnO NPs are very useful for the fabrication of devices, such as electromagnetic coupled sensors and actuators. ZnO NPs can act as alpha-amylase inhibitors for controlling Diabetes (Dhobale et al., 2008). ZnO NPs has been used for its antifungal (He et al., 2011) and antibacterial activity (You et al., 2011) and for the treatment of cancer by stimulation of apoptosis killing the cancer cells (Premanathan et al., 2011). Zinc oxide NPs are also used in coatings and paints due to their UV absorbing efficiency (Becheri et al., 2008) and limpidity to visible light (Franklin et al., 2007).

Ceramic nanoparticles are used in mining, aerospace, refinery, chemical and food industries, packaging science, electronics and transmission industry. **Quantum dots** are used in medicine, for imaging, high-speed and high-resolution screening, drug vectors, diagnostic tools and solar batteries. They are also used in the production of insulators, metals, semiconductors and magnetic materials. **Polymeric nanoparticles** are used in drug targeting, gene therapy and delivery of proteins, peptides and genes via administration through the oral route. **Dendrimers** are used in detecting agents (dye), affinity ligands, radio ligands, imaging agents, targeting components, pharmaceutically active compounds (drug and gene delivery) and solubilizing agents. In agriculture, dendrimers such as nanocapsules have been used for delivery of pesticides, fertilizers, growth hormones, vaccines and other agrichemicals more efficiently. Nanosensors are used for monitoring soil conditions, crop growth and detection of plant/animal pathogens and nanochips for identity preservation and tracking.

1.2. Metallo-Nanoparticles

The term metallo-nanoparticle is used to describe nano-sized metal oxides with dimensions within the nano-meter scale which is the focus of this study. Metal elements are known to be capable of forming a wide range of oxide compounds such as copper, copper oxide; zinc, zinc oxide; iron, iron oxide; magnesium, magnesium oxide; silver, silver oxide; cerium, cerium dioxide; titanium and titanium dioxide etc. Metal NPs have diverse physical and chemical properties when compared to their bulk counterparts e.g., lower melting points, higher specific surface area per unit mass, possessing abundant reactive sites, catalytic properties, specific optical properties, magnetizations, mechanical strengths as well as mobility (Maynard et al., 2006; Weisner et al., 2006; Horikoshi and Serpone 2013). Particle mobility in turn depends on gravitational forces, buoyancy and Brownian motion (Christian et al., 2008). Metal nanoparticles also possess optical properties arising due to its ability to confine its electrons not observed with bulk metals (Horikoshi and Serpone 2013). This property has been used to produce quantum effects, quantum confinement in semiconductor particles and super-para magnetism in magnetic materials as well as surface plasmon resonance in certain metal particles (Hewakuruppu et al., 2013). For instance, Au and Ag express various colours by changing the size, shape and rate of condensation, therefore, is highly recommended in paints. Engineered metal nanoparticles may possibly react with other metals based on either its surface chemical components and/or depending upon factors such as environmentally induced changes, deliberate and accidental coating (Baer et al., 2010). Also, Solubility is reported to be enhanced when particle size decreases below 100 nm exhibiting greater surface reactivity (Auffan et al., 2009).

Metal and metal oxide nanoparticles are thermodynamically unstable as it can undergo chemical dissolution by change in factors such as temperature and pressure

(Tourinho et al., 2012). The release of ions from nanoparticles termed dissolution occurs when the ion detaches from the particle and drifts into the solution. It has been shown that the mobility, bioavailability and toxicity of nanoparticles are influenced in aquatic (Kim et al., 1999; Long et al., 2004; Witters et al., 1998) and soil (Kahru et al., 2005) environments by a range of varying physicochemical parameters such as pH, temperature, soil type, dissolved organic matter, humic acids, suspended solids etc. However, information based on the release of ions from MNP and its effects is scarce. Few reports have shown that MNPs are able to release only a small amount of ions in the medium insufficient to cause any negative effect (Lee et al., 2008; Lee et al., 2013; Lin and Xing 2008) whereas other studies have suggested that MNP released ions that possibly could generate ROS causing oxidative damage (Lalau et al., 2015; Navarro et al., 2008b; Perreault et al., 2010). Much debate still exists regarding the dissolution of metallo- nanoparticles and the cause of toxicity (whether due to MNP or ions) in plants. Thus in the present study, the extent of MNP dissolution and its subsequent effect in rice was investigated.

1.3. Nanoparticles in the Environment

Metallo-nanoparticles (MNPs) can enter the environment either through air, water or soil. In the atmosphere, NPs can enter through combustion of vehicles which are primary sources of NPs (Navarro et al., 2008a). Metallo-NP entry into the atmosphere may result in its deposition in soil and water bodies (e.g. waste incineration). Admission of metallo-NPs in soil could also occur through soil and water remediation processes (Barnes et al., 2010; Mueller and Nowack 2008) and through agricultural amendments (e.g., as fertilizers; Mueller and Nowack 2008; Johnson et al., 2011). Another source of input of metal NPs to the soil is due to treated wastewater effluent and sewage sludge (Gottschalk and Nowack 2011). For instance, washing of textiles results in the release of Ag NPs (Geranio et al., 2009) while usage of paints release TiO₂ NPs (Kaegi et al., 2008). These NPs are retained

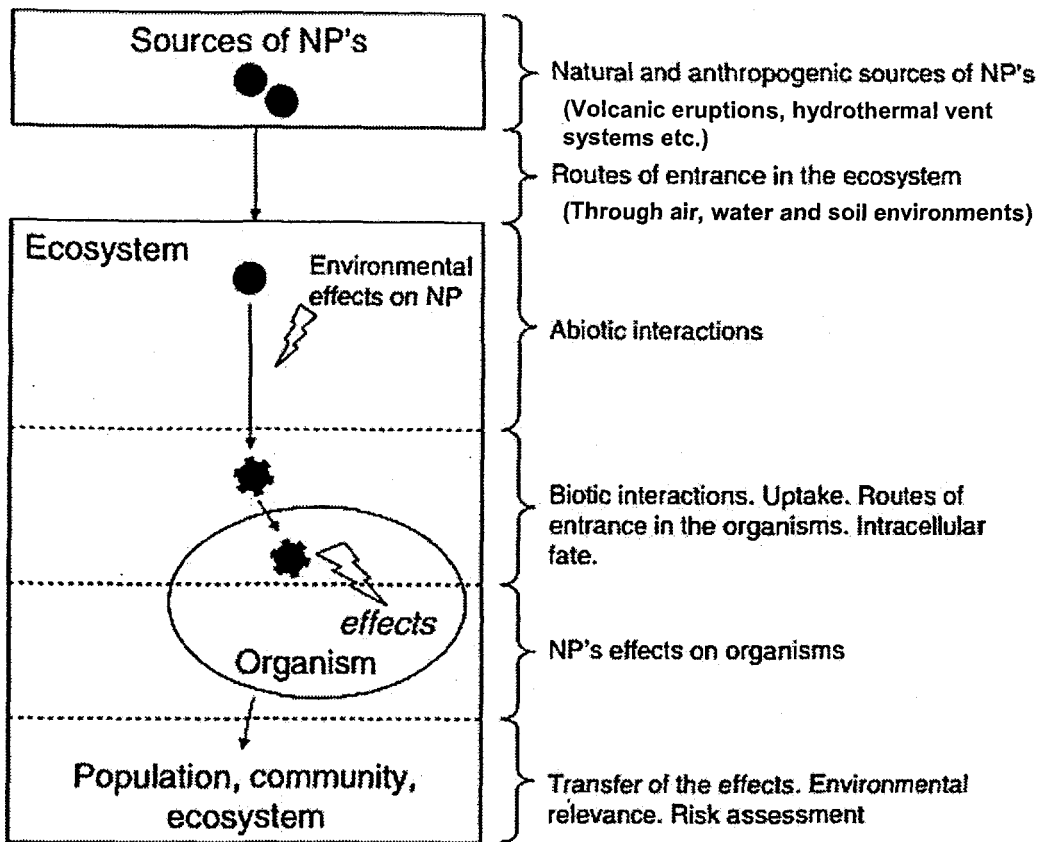


Fig 1.3. Series of events accounting for the toxicity of NPs starting with the sources to the entry into the ecosystem (Navarro et al., 2008a). In the ecosystem, NPs encounter abiotic interactions due to different atmospheric, aquatic and terrestrial environments, resulting in physical and chemical alterations (change in size, shape and surface properties). The alterations significantly govern the fate of the NPs in the environment and its bioavailability to various organisms. The NP-organism communications might occur at biological interfaces causing its entry into the organisms exhibiting unknown effects which may be transferred through food webs affecting communities and ecosystems at large.

in the sludge phase during wastewater treatment entering into the soil (Johnson et al., 2011). Once released into the ecosystem these metallo-NPs then experience abiotic interactions in different environments leading to its physical and chemical alterations such as change of size and surface charge (Navarro et al., 2008a). The behavior of metallo- NPs in the atmosphere depends on chemical reactions such as temperature, relative humidity and atmospheric turbulence (Biswas and Wu 2005). In water and soil environments, NP behavior is governed by size and surface area, agglomeration/aggregation, dissolution rate and dispersability (Stone et al., 2010). Transportation of metallo-NPs in water and soil occurs due to the influence of both environmental conditions (entrapment of NPs in porous soils and changes in flow rate) and the physicochemical characteristics (Brownian motion, gravity, ionic strength and charged surface) of the particles (Tourinho et al., 2012). Besides the above factors, metallo-NPs are also dependent on surface properties of acidity constants and zero point of charge (Giammer et al., 2007). For example, TiO₂ NPs are positively charged at pH <6 and negatively charged at pH >7 (Guzman et al., 2006; Ridley et al., 2006). Despite our knowledge of potential environmental release pathways (Gottschalk et al., 2009; Johnson et al., 2011) also shown in Fig 1.3, little is known about the extent of NPs reaching the environment.

1.4. Internalization and Uptake of Metallo-Nanoparticles in Plants

Organisms such as algae and plants are expected to interact strongly with their immediate environment being affected as a result of their direct exposure to NPs (Navarro et al., 2008a). There are several publications reporting the uptake and accumulation of metallo-NPs in plant leaf and root tissue. For instance, uptake of ZnO NPs (8 nm) in *Glycine max* (Lopez-Moreno et al., 2010), carbon coated magnetic NPs in *Cucurbita pepo* (Gonzalez-Melendi et al., 2008), Pd uptake in *Hordeum vulgare* (Battke et al., 2008) and copper uptake in *Phaseolus radiates* and *Triticum aestivum* (Lee et al., 2008) have been reported,

however, the exact mechanism of NP uptake, particularly transport of metallo-NPs of a specified size in plants is yet to be investigated. Rico et al. (2011) in a review article explained various probable modes of uptake of nanoparticles/nanotube and natural organic matter in plant cells (Fig 1.4). Metallo-NPs can travel passively by simple diffusion, facilitated diffusion, and osmosis into the plant system (Rico et al., 2011) or into the cell, causing internal and external structural modifications which not only depends upon the surface characteristics, particle size, temperature, pH and ionic strength (Maynard et al., 2006; Wiesner et al., 2006) but also on lipid and protein interface such as electrostatic, hydrophobic interactions and hydrogen bonding (Ojamae et al., 2006). Nanoparticles of smaller sizes can easily pass through the plant cell membranes which passively allow the passage of small molecules; whereas larger NPs are proposed to trigger an unknown cellular mechanism resulting in formation of new pores which might be larger than usual increasing uptake of larger NPs (Navarro et al., 2008a). Other probable modes of NP uptake in plant cells are through carrier protein, aquaporin and ion channels, all of which are pore-forming integral membrane proteins that facilitate the movement of different molecules across a biological membrane (Rico et al., 2011). Fluid phase endocytosis (via clathrin-coated vesicles), plasmodesmata transport and entry facilitated via natural organic matter have also been proposed (Rico et al., 2011). Internalization of metallo-NPs into plants may also occur based on cell wall composition, symbiotic microorganism interactions, and absence of cuticle in submerged plants (Schwab et al., 2015). Additionally, NP entry could occur via mucilage (exopolysaccharide) and exudates which contain secondary metabolites such as phenols, terpenoids, phytoalexins, phenyl propanoids excreted by the root caps into the rhizosphere (Schwab et al., 2015).

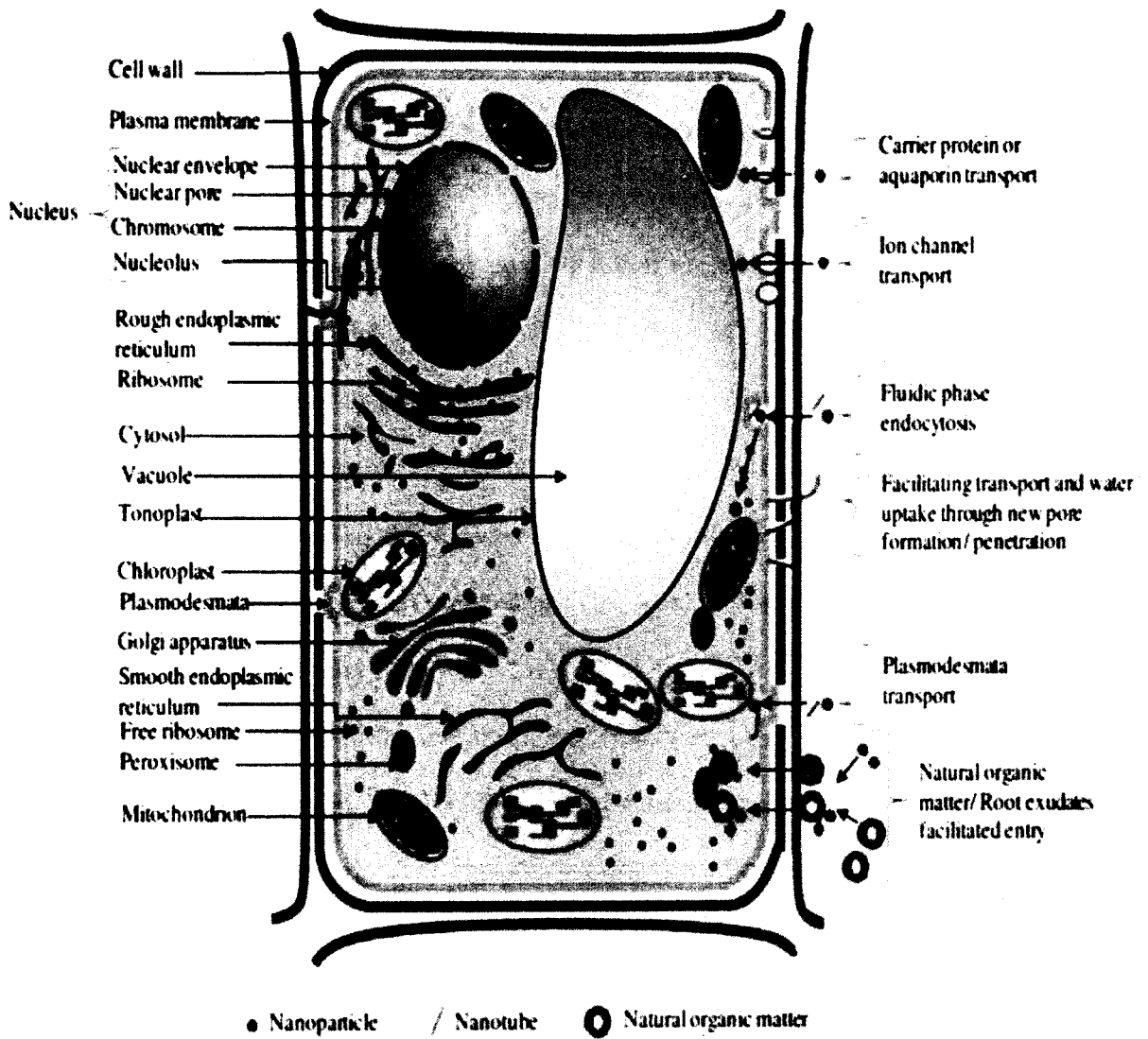


Fig 1.4. Probable modes of nanoparticle uptake in a plant cell. "Adapted with permission from Rico et al. (2011)"

1.5. Localization and Storage of Metallo-Nanoparticles in Plants

There are few concerns arising from the observation that MNPs are accumulated in plants. Current available literatures showed vaguely that MNPs are found in the plant cell, however, there are no specific studies on how the nanoparticles get stored in these tissues. Figure 1.5 shows the uptake, translocation and biotransformation pathway of various nanoparticles in a plant system. Cu NPs were reported to be found in the cytoplasm and cell wall of *Phaseolus radiatus* (mung bean) and in the roots of *Triticum aestivum* upon NP treatment by Lee et al. (2008). It was also reported that CuO (<50 nm) and ZnO (<100 nm) NPs were detected in the shoots of wheat (*Triticum aestivum*) in the form of Cu (I)-sulfur complexes and as Zn-phosphate (Dimkpa et al., 2012). Other studies showed that single walled carbon nanotubes (SWCNTs) were found in vacuoles as well as in cytoplasmic strands of *N. tabacum* plant cell suspensions (Liu et al., 2009). Micro X-ray fluorescence studies revealed the presence of Ti (TiO₂ NPs) in the roots of cucumber that were consequently transported to the leaf trichomes (Servin et al., 2012). Parsons et al. (2010) studied the biotransformation of Ni (OH)₂ NPs by mesquite plants (*Prosopis* sp.) using X-ray absorption spectroscopy. They reported localization of NP in plant tissue based on the oxidation state of Ni. For instance, uncoated Ni NPs were observed in roots and shoots, whereas leaves showed the presence of a Ni (II)-organic acid type complex. In alfalfa, Ag NPs could accumulate in the stems (Gardea-Torresdey et al., 2003) while Platinum (Pt) was uniformly distributed in the epidermal, cortical and vascular tissue within the roots of *Medicago sativa* and *Brassica juncea* assessed using proton induced X-ray emission (PIXE) spectroscopy (Bali et al., 2010). Accumulation of C₇₀ NPs in edible rice plants has been reported to be transmitted to the second generation (Lin et al., 2009). This could possibly produce plants adaptive to NPs which may be more responsive accumulating large amounts of the respective NPs (Rico et al., 2011). Furthermore, studies have shown uptake

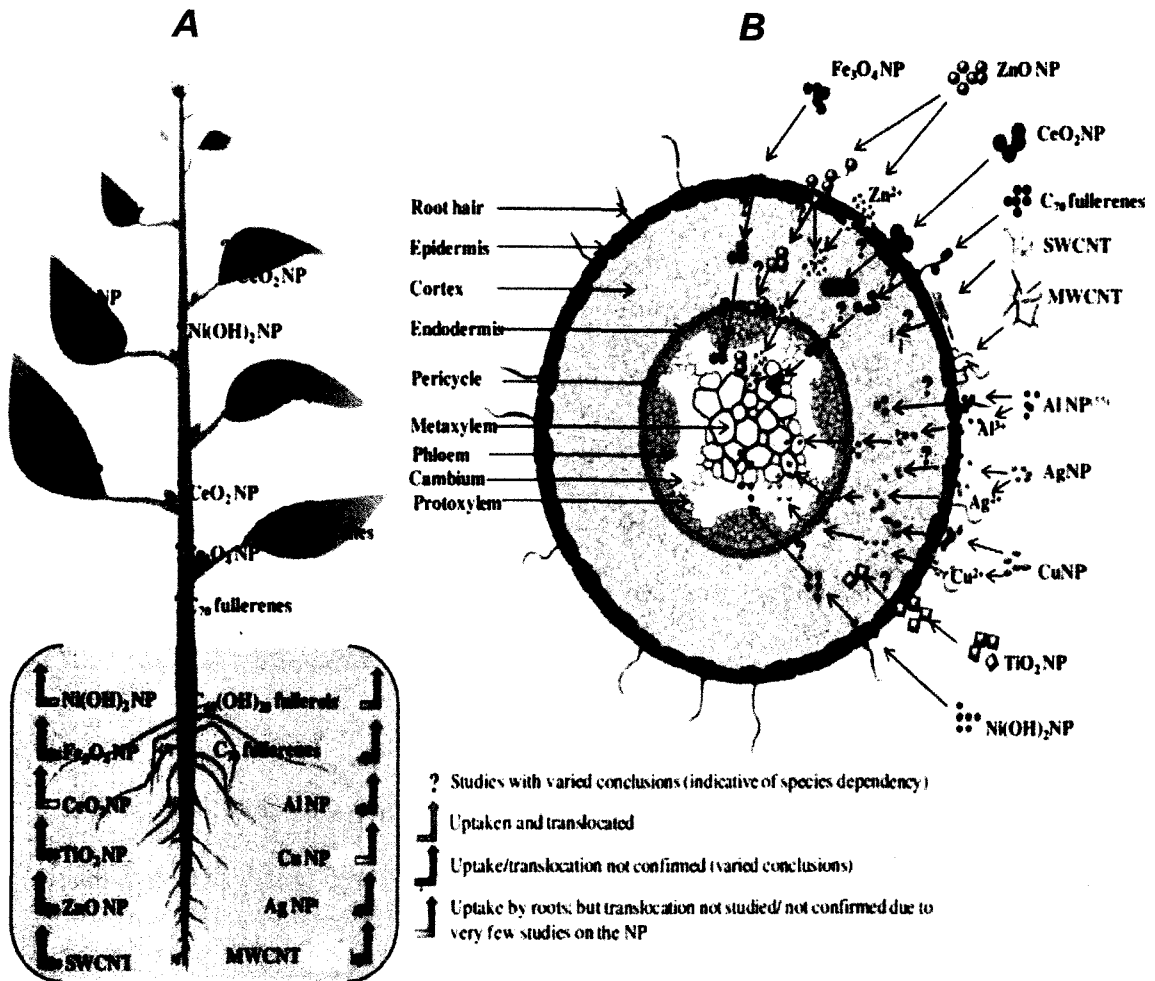


Fig 1.5. The uptake, translocation and biotransformation pathway of various nanoparticles in a plant system. Plant showing the selective uptake and translocation of nanoparticles (A) and transverse cross section of the root absorption zone showing the differential nanoparticle interaction on exposure (B). "Adapted with permission from Rico et al. (2011)"

of NPs in algae and tobacco and its bioaccumulation to the next trophic level i.e. humans (Navarro et al., 2008a; Judy et al., 2011).

1.6. Effect of Metallo-Nanoparticles in Plants

Studies on the toxicity of metallo-nanoparticles in crop plants are limited and only few reports on Fe₃O₄, CeO₂, SiO₂ and TiO₂ NPs are available. Furthermore, reports beyond germination and growth are currently lacking. Reduced seed germination in alfalfa, soybean, tomato and cucumber was observed with nano ceria at 4000 mg L⁻¹ concentration (Lopez-Moreno et al., 2010). On the other hand, iron oxide NPs have been found to increase soybean pod and leaf dry weight (Sheykhbaglou et al., 2010) and are also observed to facilitate iron and photosynthate transfer to the leaves of peanut (Liu et al., 2005). Similarly, TiO₂ NPs was beneficial to plant growth showing an increase in the Hill's reaction, increased acceleration of electron transport and oxygen evolution in chloroplasts of *Spinacia oleracea* (Hong et al., 2005) leading to elevated Rubisco carboxylase activity, 2.67 times the control (Gao et al., 2006). An increase in the protein expression of Rubisco by 40% as compared to its control in spinach was also reported by Xuming et al. (2008).

1.6.1. Copper Oxide Nanoparticle (CuO MNPs)

Copper is indispensable for plant growth. It is involved in several physiological processes in plants as it can exist in multiple oxidation states (Cu²⁺, Cu⁺) *in vivo* (Yruela 2005). Cu acts as a structural component in regulatory proteins and participates in photosynthetic electron transport, mitochondrial respiration, cell wall metabolism, oxidative stress responses and hormone signalling (Marschner 1995; Raven et al., 1999). At cellular level, Cu plays a significant role in signalling of transcription, protein trafficking machinery, oxidative phosphorylation and iron mobilization. At concentrations beyond the threshold,

Cu can be toxic to the organism. Consumption of Cu beyond 1–2 mg L⁻¹ in drinking water could result in toxicity symptoms in humans (OJEC 1998; EPA 2003). Likewise, freshwater organisms experience acute toxic effects at concentrations as low as 10 µg L⁻¹ (EPA 2007). The redox properties of Cu can also contribute to its toxicity, as a free ion it can catalyse production of damaging radicals (Manceau et al., 2008). Accumulation of Cu in plants is reported to occur in the chloroplast as it is a part of plastocyanin involved in the photosynthetic electron transport chain (ETC). The functional association of Cu in ETC inside PSII was described by Barr and Crane (1973). The mechanism of Cu toxicity on ETC *in vitro* was studied by Ouzounidou et al. (1997) and it was found that PSII site was more sensitive than PSI. Copper in excess, is known to reduce biomass and cause chlorotic symptoms in plants. Copper is also known to interfere with photosynthesis and respiration (Marschner 1995; Prasad and Strzalta 1999) by modifying pigment and protein composition of photosynthetic membranes (Maksymiec et al., 1994). Copper can also pass through membranes disturbing calcium flow, result in enhanced H₂O₂ synthesis affecting NADPH oxidase activity and triggering a chain of antioxidative mechanisms. Besides, antioxidants, metal chelators also play an important role in detoxification of metals and include metallothioneins (MTs) and phytochelatins (PCs) which are reported during Cu stress by Yruela (2005).

The environmental concentration of CuO NPs is unavailable, however, bulk or ionic form of copper (Cu), is present at an optimum level of 10 µg g⁻¹ dry weight in plant tissue (Yruela 2005). The critical free Cu concentration in nutrient media ranges from 10⁻¹⁴ to 10⁻¹⁶ M and that of soil ranges from 10⁻⁶ to 10⁻⁹ M (Yruela 2005). Unlike bulk metals, NPs show different properties based on size and surface characteristics. Copper oxide NPs are reported to decrease growth and biomass in *Cucurbita pepo* (zucchini) plants (Stampoulis et al., 2009; Musante and White 2012) and in rice by Lidon and Henriques

(1998). Decrease in photosynthesis as a result of CuO NP treatment was reported to be due to reduction in chlorophyll content of *Landoltia punctata* (Shi et al., 2011) and also due to inhibition of photosystem II quantum yields in *Lemna gibba* (Perreault et al., 2010), in *Chlamydomonas reinhardtii* (Perreault et al., 2012) and in *Elodea densa* (Nekrasova et al., 2011). Haverkamp and Marshall (2009) has experimentally shown the limit of metal NP accumulation with different metals and proposed that uptake was controlled by the total reducing capacity of the plant for the reduction potential of the metal species. Uptake of Cu in plants is reported in by various researchers (Lin and Xing 2008; Lidon and Henriques 1998; Lee et al., 2008), however, Cu uptake in the roots was seen to a greater extent than in the aerial parts signifying an exclusion mechanism for toxicity tolerance against heavy metal stress (Wang et al., 2004).

1.6.2. Zinc Oxide Nanoparticles (ZnO MNPs)

The crucial role of Zinc (Zn) in plants was first shown in maize, later in barley and dwarf sunflower (Sommer and Lipman 1926). Zinc is an indispensable element for plant growth and plays an important role in numerous biological processes, mainly due to its fundamental role in stabilizing the structural domains of proteins (Tapiero and Tew 2003). Zinc is the second most abundant transition metal in organisms after iron (Fe), and the lone metal characterized in all six enzyme classes (Enzyme Commission number, EC 1–6; oxidoreductases, transferases, hydrolases, lyases, isomerases, ligases). Zn plays a role as a cofactor for enzymes such as peroxidases (Vallee and Auld 1990; Aravind and Prasad 2003), anhydrases (Aravind and Prasad 2004a; 2005a), dehydrogenases and oxidases. Also, Zn is reported to be beneficial for the photosynthetic machinery of the plant system (Aravind and Prasad 2004b) as it can increase the biosynthesis of photosynthetic pigments i.e. chlorophyll and carotenoids and is responsible for accurate protein folding (e.g. alcohol dehydrogenases, protein kinases). Zinc also plays an important role in PSII repair

processes, structural integrity of Rubisco, modulation of carbonic anhydrase activity, maintaining HCO_3^- substrate level for PEP carboxylase as well as in stomatal opening (Tsonev and Lidon 2012). Zinc finger domain containing proteins is the largest class of Zn-binding proteins in organisms which can control transcription directly through effects on DNA/RNA binding, and also through regulation of chromatin structure, site-specific modifications, RNA metabolism and protein-protein interactions (Englbrecht et al., 2004). Peroxidases that possess Zn as cofactor have numerous physiological roles in plant cells (physiological processes such as respiration, photosynthesis and transpiration) participating in many reactions including lignification, cell elongation and growth reductions (Mocquot et al., 1996; Aravind and Prasad, 2005b). Zinc at high concentrations could become toxic to plants exhibiting symptoms of growth inhibition (Barceló and Poschenrieder 1990), changes in the leaf morphology, chlorosis, necrosis and impairment of photosynthesis (Cherif et al., 2010; Hermle et al., 2007).

Based on manufacturer information (using the market study) collected through surveys and interviews, Keller et al. (2013) estimated that the annual global production of zinc oxide nanoparticles (ZnO NPs) in 2010 was more than 30,000 metric tons which included ZnO emissions during manufacturing (32-680 tons/year) and emissions into the atmosphere (90-578 tons/year), water bodies (170-2985 tons/year), soils (3100-9283 tons/year) and landfills (21,153-28171 tons/year). However, the manufacturing rate of NPs is estimated to near 58,000 tons by 2020 (Maynard et al., 2006). The actual concentration of ZnO NPs in soil has not been reported, however, bulk Zn is shown to be present in typical uncontaminated soils and in agricultural crops in the concentration range of 10-300 mg kg^{-1} and 15-200 mg kg^{-1} dry mass (DM) respectively (Nagajyoti et al., 2010).

Concern regarding the effect of NPs in living organisms is growing in both the scientific and public communities. Literature on the effects of ZnO NPs in plants is limited,

mostly covering areas like germination and growth. Studies have shown that ZnO NPs did not affect seed germination in soybean at 4000 mg L⁻¹ but significantly reduced corn germination even at a concentration of 500 mg L⁻¹ ZnO NPs (Lin and Xing 2008; Lopez-Moreno et al., 2010). ZnO NPs also negatively affected seed germination, root elongation and biomass in *Cucurbita pepo* (zucchini; Stampoulis et al., 2009), in rice by Boonyanitipong et al. (2011) and in radish, lettuce, corn, ryegrass and cucumber by Lin and Xing (2007). Zinc oxide nanoparticles were also reported to inhibited root growth of *Allium cepa* (Ghodake et al. 2011) and root meristem growth in *Allium sativum* L. causing mitosis and mitotic aberrations in a concentration dependent manner (Shaymurat et al. 2012). At concentrations above 400 mg L⁻¹ of ZnO (< 50 nm) NPs, a negative effect on germination rate, leaf number and root length was observed in *Arabidopsis thaliana* (Lee et al., 2010). The decrease in photosynthetic activity of cyanobacteria, *Anabaena flos-aquae* (Brayner et al., 2010) and reduction of enzyme activities such as catalase (CAT) and peroxidase (Du et al. 2011) was also reported to decrease with ZnO NPs.

Besides the reduction in germination, leaf and root length, plant height and biomass, other factors such as variation in number and size of trichomes and stomatal pores on the leaf surface are indicators of stress. Trichomes are hair-like appendages that develop from cells of the aerial epidermis produced by most plant species (Werker 2000). They can range from unicellular to multi-cellular and can be straight, spiral, hooked, branched or unbranched (Werker 2000). Some trichomes have glands that release secondary metabolites such as terpenes and alkaloids which are poisonous, repellent or trap insects or other organisms. The number of trichomes produced and trichome density vary genetically within species. For instance, leaf trichomes may increase due to abiotic stress such as metal, drought, solar UV-radiation and low temperature. Increased leaf trichomes can be generated by the plant only during leaf formation in response to stress and after

subsequent damage (Dalin et al., 2008). A reduction in trichomes may be observed when the stress levels decrease as trichomes are costly to produce requiring higher amounts of substrates for its construction. Leaf trichomes help to decrease the light interception and reduce loss of photosynthesis (Gutschick 1999). They also help in keeping water off the leaf surface and the stomata, helping in maintaining the leaf gas exchange as well as protect the plant against damage from herbivores. Increase in trichomes during heavy metal accumulation in plants has been reported (Emamverdian et al., 2015; Hall 2002).

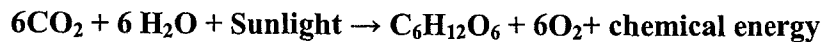
Stomatal pores are present in most plant leaves at densities of several hundred per square millimeter. Stomata are required to control the exchange of CO₂ and water vapour, which is fundamentally associated to transpirational cooling. Stomata can be described by the aerial density or the fraction of epidermal cells that respond to three major physiological state variables such as photosynthetic metabolites, hormones or regulators such as abscisic acid (ABA). It is notable that the upper and lower (adaxial and abaxial) leaf surfaces can differ in stomatal density and in physiological responsiveness (Wang et al., 2008). The three major adaptive functions of stomata are optimization of the interchange of photosynthetic CO₂ gain against the transpiration rate, controlling the risk of dehydration, particularly balancing the leaf water potential and regulating the temperature by transpirational cooling. Although, trichomes and stomata are considered as stress indicators, research on its variation upon MNP stress has not been studied. In the present study, these variations were observed and reported.

With an ever increasing commercial demand for MNPs in the present market, there exists a high risk of MNP exposure to organisms with unknown consequences. Only a few studies have been carried out till date to understand the interaction of metallo-NPs with plants. Therefore, in this study an attempt was made to investigate the effect of CuO and ZnO NPs on plant growth and productivity and also to estimate the threshold level of MNP

toxicity in rice plants as an attempt to facilitate quantitative ecological risk assessment with respect to agricultural food crops.

1.7. Photosynthesis

The conversion of light energy into chemical energy using carbon dioxide and water to produce carbohydrates is a process termed as photosynthesis in plants and is represented as



The process of photosynthesis occurs in two steps. In the first step, light-dependent reactions capture the energy of light and use it to make the energy-storage molecules ATP and NADPH.



During the second step, the light-independent reactions use these products to capture and reduce carbon dioxide synthesizing carbohydrates.

In plants, photosynthesis occurs in the chloroplasts which are 5 to 10 μm long organelles bounded by a chloroplast envelope containing integral and peripheral membrane protein complexes that absorb light energy forming the photosystems (Fig 1.7.1 A). The chloroplasts have three distinct internal compartments, the inter-membrane space between the two membranes of the chloroplast envelope, the stroma, which lies inside the envelope but outside the thylakoid membrane and the thylakoid lumen. The thylakoid membrane forms the third internal membrane system comprising of a network of flattened discs called thylakoids, which are normally organized in stacks called grana (Fig 1.7.1 A). Thylakoid membranes contain pigments such as chlorophylls (chlorophyll *a* and *b*) and carotenoids that help in light harvesting during photosynthesis. Carotenoids are further divided into pure hydrocarbon carotenes (β -carotene) and the oxygen containing xanthophyll's (neoxanthin, antheraxanthin, violaxanthin, zeaxanthin, and lutein). Carotenoids (Car) are lipid soluble antioxidant that absorbs light and pass it to the Chl molecule. Besides its light

harvesting function, carotenoids (Car) such as β -carotene, zeaxanthin and tocopherols play an important photo-protective role in all photosynthetic organisms, either by scavenging reactive oxygen species (ROS) or by dissipating excessive energy in the form of heat. Cars are also involved in the stabilization of light harvesting complex (LHC) of photosystem I (PSI) as well as in the ultrastructural organization of the thylakoid membranes. The physical separation of PSI and PSII in the thylakoid membranes prevents the spill over of excitation energy providing fine regulated light for photosynthesis (Horton 1999). Thylakoid membrane stacking is an important factor in regulation of photosynthesis, and depends on van der Waals attractive forces, lateral segregation of protein complexes within the membranes, cation-mediated electrostatic interaction between membranes and steric hindrance (Dekker and Boekema 2005). The shape of grana is also important in thylakoid stacking and depends on the percentage and type of lipids as well as the connection between the protein complexes and the lipids (Dekker and Boekema 2005).

Heavy metals at concentrations above optimum levels are reported to reduce photosynthesis. Copper is reported to reduce the chlorophyll content altering chloroplast structure and thylakoid membrane composition disturbing stacking of grana and stroma lamellae (Yruela 2005) whereas zinc is reported to decrease growth by affecting the photochemical reactions, biosynthesis of chlorophyll pigments, carbonic anhydrase activity and disturbing the cell membrane integrity (Tsonev and Lidon 2012) negatively affecting photosynthesis.

The four major complexes of thylakoids are Photosystem II (P_{680}), Cytochrome b_6 -Cytochrome f complex, Photosystem I (P_{700}) and ATP synthase (Fig 1.7.1 B). Photosystem I and II absorb light at wavelengths of 700 nm (far-red) and 680 nm (red) respectively and are spatially divide in the ratio 1: 1.5 in the thylakoid membrane (Fig 1.7.1 B). The PSII reaction centres are located mostly in the grana lamellae while the PSI reaction centres and

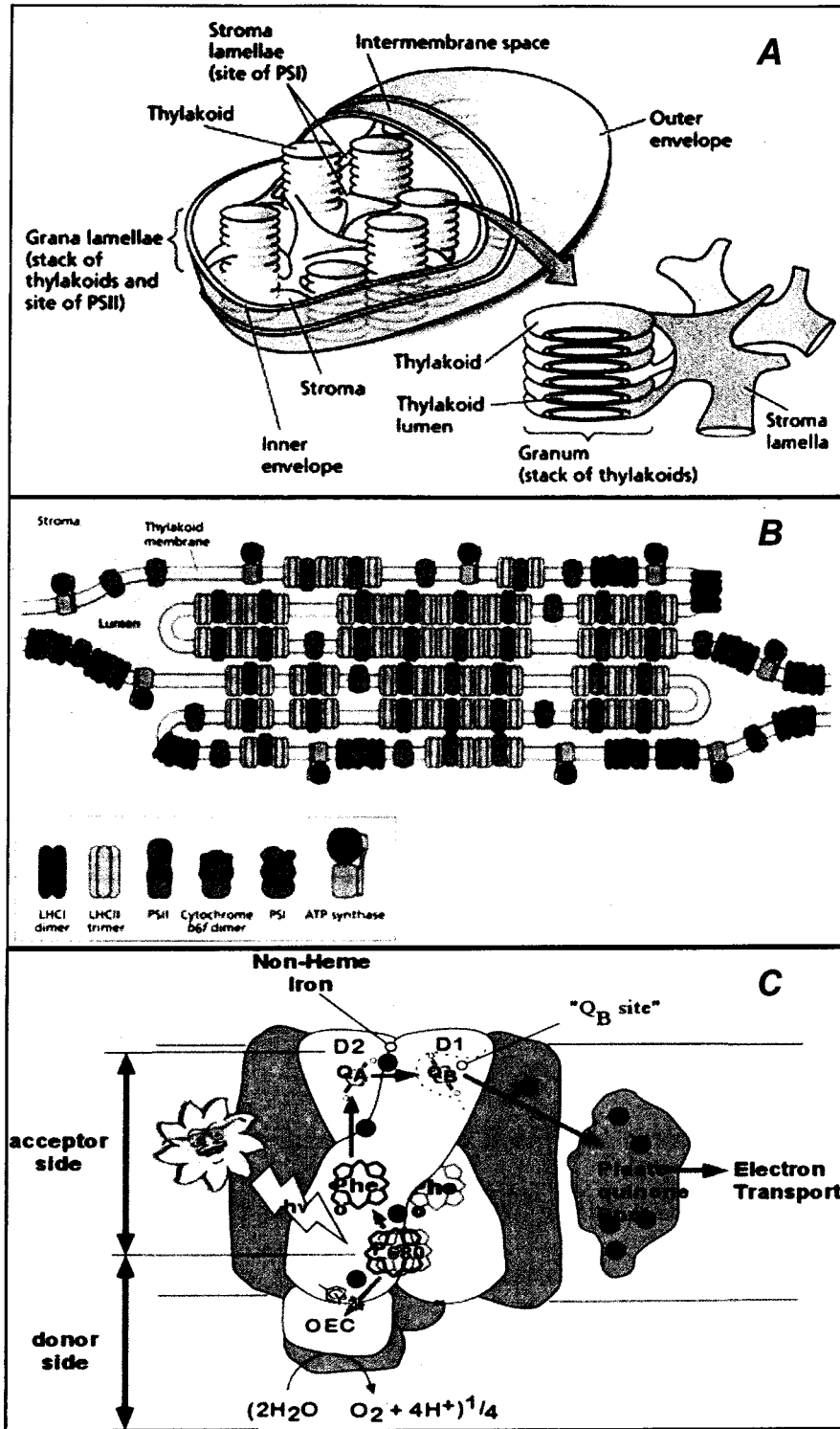


Fig 1.7.1. Schematic diagram representing the organization of the membranes in the chloroplast (A) the protein complexes of the thylakoid membranes (B) and the photosystem II complex (C). "Figure A & B, adapted from Taiz and Zeiger 2010".

ATP synthase enzyme are found in the stroma lamellae (Fig 1.7.1 C). PSII photosystem is an integral membrane protein whose core consists of a pseudo-symmetric heterodimer of two homologous proteins D1 and D2. The polypeptide D1 consist of redox-active tyrosine, YZ, and QB plastoquinone and polypeptide D2 consist of pheophytin and QA (Fig 1.7.1 C). D1 protein of PSII is reported to be the most vulnerable PS for damage by light-induced radicals and active oxygen species (Anderson 1986). Structurally, PS II comprises of >25 polypeptides and is fenced by Chl *a* and *b* binding proteins as light harvesting complexes that capture light for the complex.

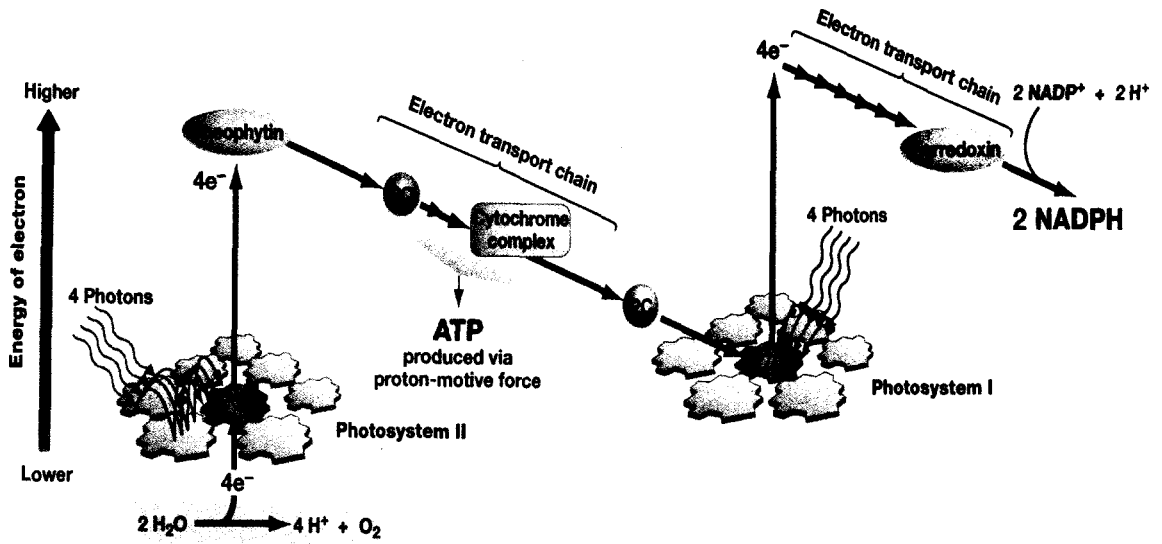
The final stage of NADPH formation from NADP^+ in the light reactions is catalyzed by PSI. PS I comprises of 11-13 polypeptides depending on the plant species. The enzymatic heart of the complex has 3 subunits known as PsaA, PsaB liganded with the prosthetic groups, P700, A₀, A₁, and F_X and F_A and F_B iron-sulfur clusters are found in PsaC. Chl *a* molecules lies at the center of the structure which absorbs light maximally at 700 nm (P₇₀₀). Upon excitation-either by direct absorption of a photon or exciton transfer-P700* transfers an electron through the complex catalyzing the reduction of NADP^+ via ferredoxin: NADP^+ reductase.

The cytochrome b6f complex is evenly distributed between the stroma and the granum lamellae. The Cytochrome b6-Cytochrome f complex (*cyt b₆f*) consists of four different integral polypeptides, *cyt b₆* (*cyt b563*), *cyt f*, iron sulphur protein (a 2Fe-2S protein) and component IV. The main function of this complex is to pass electrons from PSII (LHCII) to PSI (LHCI) by oxidizing PQH₂ and reducing plastocyanin (a copper containing protein), also by transporting H⁺ from stroma into the thylakoid lumen. The electrons are then transferred from PSI down the electron transport chain to reduce 2NADP⁺ to 2NADPH. During this process a proton gradient is generated across the thylakoid membrane that drives the synthesis of ATP. The ATP synthase complex in

thylakoids is a group of polypeptides that convert ADP and inorganic phosphate to ATP and water. It couples ATP formation to transport electrons and H^+ across the thylakoid membrane. It is located along with PSI, only in the stroma thylakoids and non-appressed regions of grana thylakoids.

The light-dependent reaction has two forms: cyclic and non-cyclic photophosphorylation (1.7.2 A). ATP and NADPH generated from the light reaction in the thylakoid membrane flow to the stroma to drive the enzyme-catalysed reduction of atmospheric CO_2 to carbohydrates called the Calvin-Benson cycle (1.7.2 B). The two major products of photosynthetic fixation of carbon dioxide are starch and sucrose, the former is a reserve polysaccharide that accumulates transiently in the chloroplasts and the latter is a disaccharide that is exported from leaves to developing and storage organs of the plant. The Calvin-Benson cycle (elucidated in 1950 by M. Calvin, A. Benson) has three phases carboxylation of the CO_2 acceptor molecule, first step involves generation of two molecules of 3-phosphoglycerate, second step is the reduction of 3-phosphoglycerate and the third step is the regeneration of ribulose 1, 5-bisphosphate (CO_2 acceptor).

Photosynthetic efficiency and chlorophyll *a/b* ratio is considered to be a convenient abiotic stress parameter, however, variable results were obtained with MNPs. Reports have shown that MNPs alter the photosynthetic efficiency and quantum yield upon plant-NP interaction (Rico et al., 2015). For instance, Copper oxide NPs decreased the photochemical quenching and increased the non- photochemical quenching in *Lemna gibba* inhibiting plant growth (Perreault et al., 2010). Reduction in chlorophyll content and increased chlorophyll *a/b* ratio was observed in rice with CeO_2 MNPs (Rico et al., 2013), whereas, decreased Chl content and chlorophyll *a/b* ratio was observed in sunflower seedlings upon exposure to Fe_3O_4 and $CoFe_2O_4$ MNPs (Ursache-Oprisan et al., 2011). Metallo-NPs like superparamagnetic iron oxide nanoparticles (SPIONs) were reported to

A

© 2011 Pearson Education, Inc.

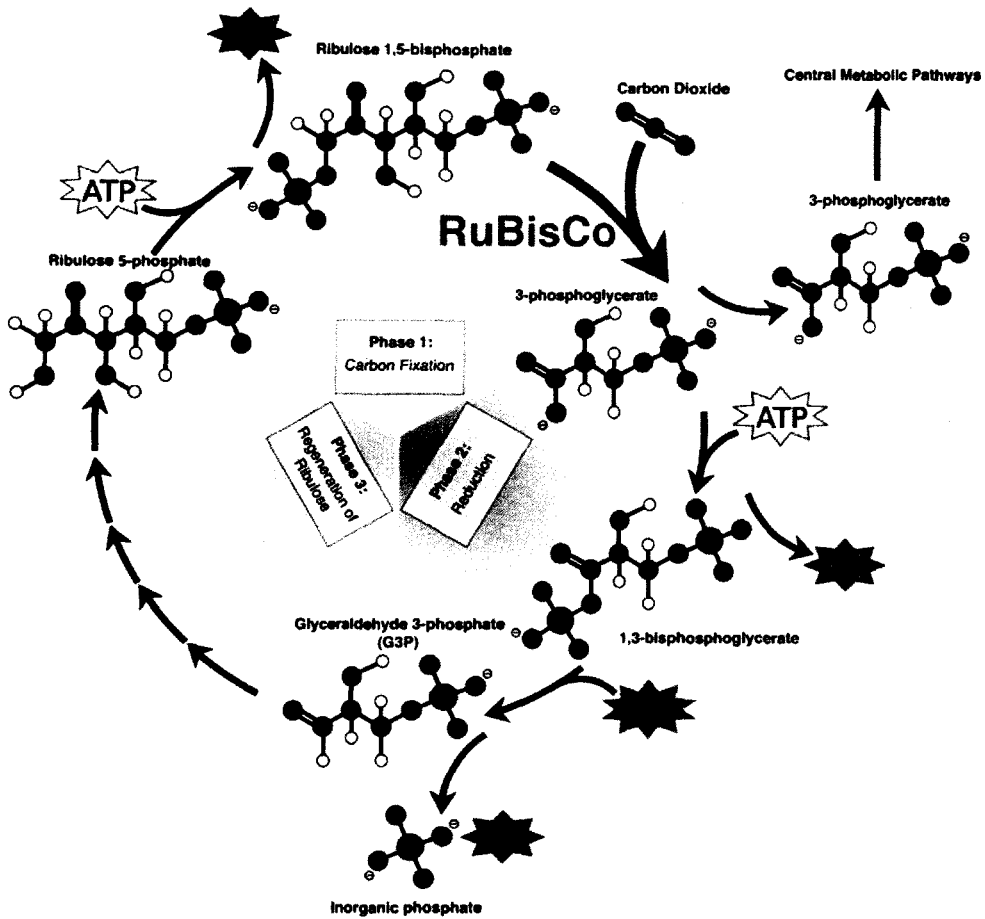
B

Fig 1.7.2. Non-cyclic photophosphorylation (Z scheme) (A; chemistry.about. com) and Carbon dioxide fixation (B; <http://bio100.class.uic.edu>) of photosynthesis in plants. Figure A: Quinone (A/B); Pheo, Pheophytin; OEC, oxygen evolving complex.

cause no changes in the Chl content upon treatment in soyabean (Ghafariyan et al., 2013). Metallo-nanoparticles are also reported to be beneficial to plant growth. For instance, titanium nano anatase (TiO₂ NPs) are involved in activating Rubisco (complex of Rubisco and Rubisco activase) improving the photosynthetic activity in spinach (*Spinacia oleracea*) plants (Gao et al., 2006). Increase in the light absorption of Chl *a*, fluorescence quantum yield in PSII, electron transfer and oxygen evolution rate upon TiO₂ NPs has been reported (Mingyu et al., 2007; Yang et al., 2007a). SiO₂ NPs also improved the photosynthetic rate of *Cucurbita pepo* L. by improving the carbonic anhydrase activity and biosynthesis of pigments (Siddiqui et al., 2014). In chloroplast, single walled carbon nano tubes (SWCNTs) were found to improve the photosynthetic activity and electron transport rates 3-fold higher than in controls (Giraldo et al., 2014). Also, nano mesoporous silica compound (SBA) when bound to PSII was found to induce stable photosynthetic oxygen-evolving reactions (Noji et al., 2011)

1.8. Mechanism of Metal Stress

During the normal cellular metabolism, plants utilize oxygen and reduce it to water and reactive oxygen species (ROS) to produce energy required for its developmental processes (Mittler et al., 2002). Under metal stress conditions, the balance of by-products of normal cell metabolism between production and elimination gets disturbed leading to the additional ROS generation in plants occurring as free radicles such as superoxide radical (O₂^{•-}), hydroxyl radical (•OH), perhydroxyl radical (HO^{2•}), or as non-radical forms such as singlet oxygen (1O₂) and hydrogen peroxide (H₂O₂) (Fig 1.8.1 A). In plants, ROS is produced in chloroplasts, mitochondria, apoplast, peroxisomes, endoplasmic reticulum, plasma membranes and cell wall (Fig 1.8.1 A; Mittler et al., 2002; Asada 2006). Chloroplasts containing chlorophyll are the primary sites for singlet oxygen production during the electron transport chain (ETC) and can affect membranes and lipids located near

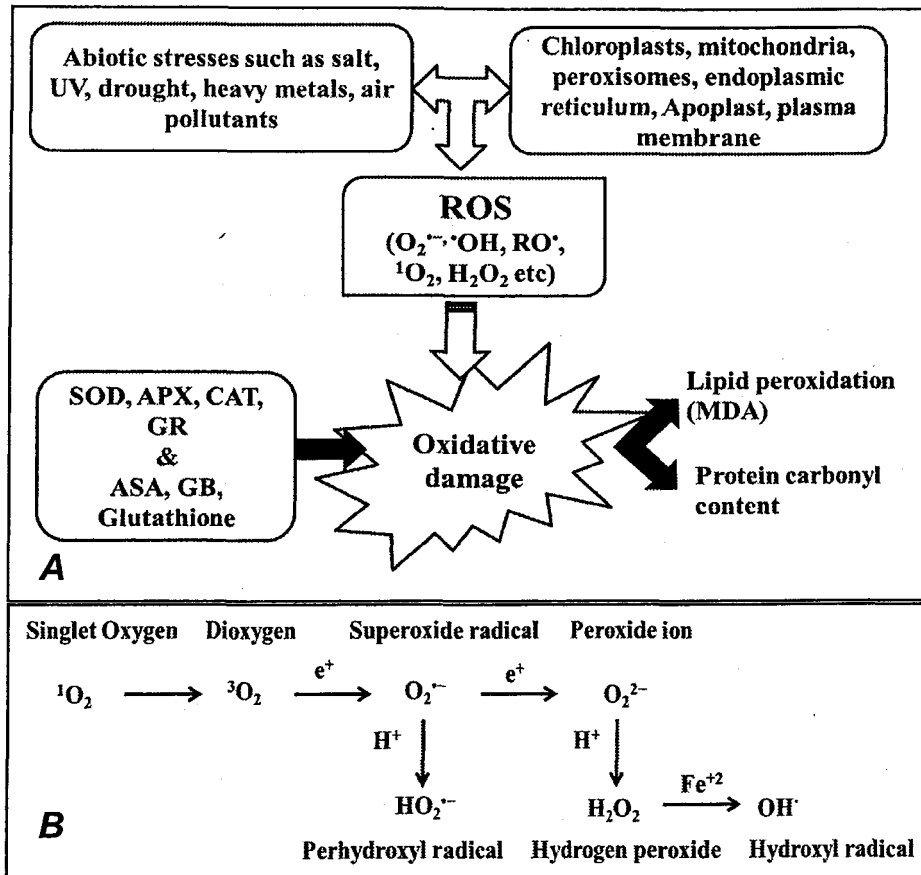


Fig 1.8.1. The Reactive Oxygen Species (ROS) cycle in plants (A) and the formation of different ROS (B). Figure A: SOD, superoxide dismutase; APX, ascorbate peroxidase; CAT, catalase; GR, glutathione reductase; ASA, ascorbate; GB, Glycine Betaine (Gill and Tuteja, 2010).

the site of its production placing PSII in jeopardy (Zolla and Rinalducci 2002). Limited CO₂ fixation results in decreased carbon dioxide fixation and NADP⁺ formation by the Calvin's cycle leading to ROS generation via Mehler's reaction (Makino et al., 2002). Mehler's reaction is the photo-reduction of O₂ at PSI to produce O₂^{•-}, which are detoxified to H₂O₂ and O₂ by superoxide dismutase. Other ROS like •OH or HO₂• are formed via the Haber-Weiss reaction where O₂^{•-} donates an electron to Fe³⁺, reducing ferric ion to ferrous (Fig 1.8.1 B; Kehrer 2000). This reduced form of iron (Fe²⁺) then transfers electrons to H₂O₂ leading to the formation of •OH, a cycle known as Fenton reaction (Fig 1.8.1 B). The H₂O₂ molecules produced in this process are then rapidly detoxified to water by the ascorbate peroxidase pathway. During normal metabolic processes, the ROS generated can act as secondary messengers in the developmental and signal transduction pathways, however, during stress conditions ROS produced in excess can cause damage to lipids, proteins and DNA through the production of peroxides and free radicals (Kehrer 2000).

1.8.1. Lipid Peroxidation

Lipid peroxidation (LPO) refers to the oxidative degradation of lipids in cell membranes as a result of abiotic stress (Fig 1.8.2 A). The free radicals produced in this process can cause damage to proteins, DNA and pigments (Gill and Tuteja 2010). The process of LPO involves three steps: Initiation, propagation and termination (Fig 1.8.2 A). Initiation step involves the removal of a hydrogen atom by a hydroxyl radical (OH•) from an unsaturated fatty acyl chain of a polyunsaturated fatty acid (PUFA) generating a fatty acid radical (R•). This R• then binds to an oxygen molecule in the aerobic environment forming the fatty acid peroxy radical (ROO•). Once initiated, the ROO• radical further propagates the peroxidation chain reaction by attacking the nearby polyunsaturated fatty acid (PUFA) side chains. The resulting lipid hydroperoxide then decomposes into aldehydes (malondialdehyde), lipid alkoxy radicals, alkanes, lipid peroxides and alcohols (Fig 1.8.2

A; Gill and Tuteja, 2010). Malondialdehyde (MDA) is one of the decomposition products of lipid peroxidation and is used as an indicator of oxidative stress (Karuppanapandian et al., 2011). Redox active transition metals such as Cu^{2+} and Fe^{2+} can generate the highly reactive OH^\cdot via the metal-catalyzed Haber-Weiss or Fenton reaction which is able to initiate radical chain reactions responsible for irreversible chemical modification of many cellular components in plants (Mittler et al., 2004). In excess, heavy metals such as copper (Cu) and zinc (Zn) produce ROS resulting in oxidative stress. Copper and zinc in plants can cause LPO and membrane permeability changing the composition of thylakoid membranes, thereby disrupting the photosynthetic electron transport and the oxygen evolving complex by generating free radicals resulting in reduced photosynthesis (Yruela 2005; Glińska et al., 2016). The mechanism of ROS generation leading to oxidative damage upon MNP exposure is still unclear. Studies with MNPs are questionable on whether oxidative damage in plants is due to NPs or NP-released ions (Rico et al., 2015). Reports have shown that both CuO and ZnO NPs by itself increased lipid peroxidation in plants due to limited dissolution in the media (Ghodake et al., 2011; Lee et al., 2013a; Shi et al., 2011). On the contrary, few researchers believe that MNPs release ions that undergo redox potential causing oxidative damage, however, no experimental proof on the MNP induced ROS generation has been shown till date. Higher lipid peroxidation due to ROS generation via Fenton reaction in leaves of *Elodea densa* exposed to CuO NPs was observed by Nekrasova et al. (2011) and in *Allium cepa* treated with ZnO NPs was observed by Kumari et al. (2011). Other MNPs are also reported to generate ROS such as Al_2O_3 NPs in tobacco BY-2 suspension cultures (Poborilova et al., 2013), carbon nanotubes in red spinach (*Amaranthus tricolor* L; Begum and Fugetsu 2012), AgNPs in green algae (Oukarroum et al., 2012) and NiO NPs in tomato root cells was observed (Faisal et al., 2013).

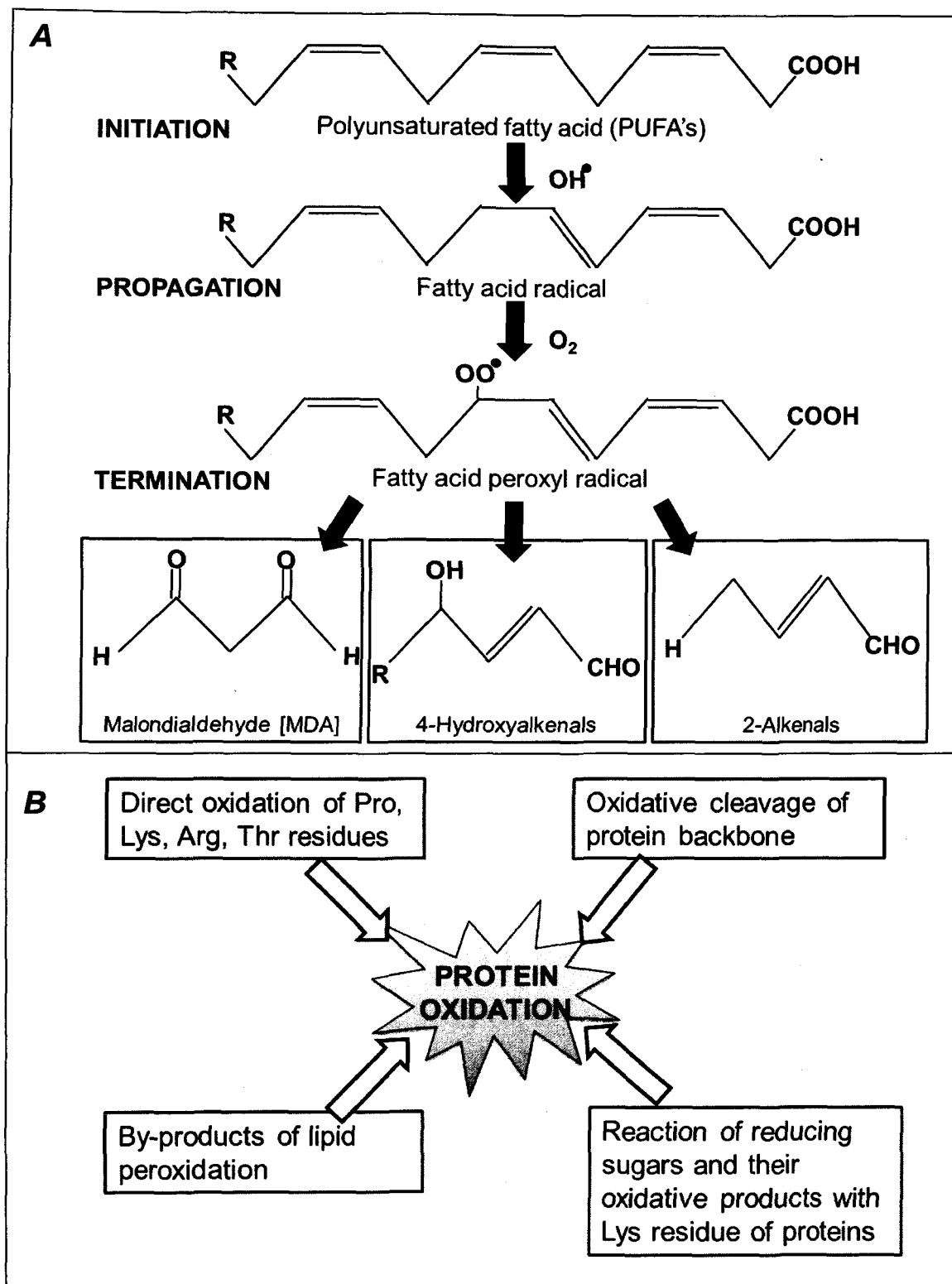


Fig 1.8.2. Lipid peroxidation mechanism (A) and protein oxidation (B) in plants

1.8.2. Protein Oxidation

The covalent modification of protein induced by either ROS or by-products of oxidative stress (LPO) is termed protein oxidation (PO) (Fig 1.8.2 A; Gill and Tuteja 2010). Protein carbonylation assay is widely used as a marker of PO. Protein carbonylation occurs due to direct oxidation of amino acid side chains (eg. arginine, proline, threonine, lysine, tryptophan and histidine) by ROS producing free carbonyl groups. These carbonyl groups have increased susceptibility towards proteolytic attack (Møller et al., 2007). It has been found that carbonylation of protein in tissues occurs due to heavy metals, cold and drought stress (Gill and Tuteja 2010), however, the mechanism behind the protein-NP interaction is not well characterized (Rahming and Fazal 2014). It is believed that nanoparticles upon entry into the biological system are instantly coated by proteins leading to the formation of a protein corona that may lead to modification of protein conformation disturbing the normal protein function by aggregation, misfolding, and deactivation (Lynch et al., 2006). The effect of MNPs on protein carbonylation in plants is still in its infancy, however, MNP induced PO has been studied in animals. Metal and metallo-NPs such as Cu, CuO, Mn₂O₃, and Fe was reported to cause protein oxidation of bovine serum albumin (BSA) via the enzyme-linked immunosorbent assay (ELISA; Sun et al., 2013). Also, increase in protein oxidation, lipid peroxidation and ROS scavenging enzymes was observed upon exposure to CuO NPs in the fish Chinook salmon (*Oncorhynchus tshawytscha*) CHSE-214 cells (Srikanth et al., 2015). Increased protein oxidation upon heavy metal cadmium stress was also reported in peroxisomes of pea plants (Romero-Puertas et al., 2002).

1.8.3. DNA Damage

The most reactive ROS that can cause damage to DNA purine and pyrimidine bases as well as the deoxyribose backbone is OH[•]. Damage to DNA occurs via base deletion, cross-links, base modifications (alkylation and oxidation), strand breaks and pyrimidine

dimers resulting in reduced protein synthesis, cell membrane destruction and damage to photosynthetic proteins. Researchers have shown that metallo-NPs cause DNA damage in plants; however, the mechanism of damage is yet to be elucidated. CuO NPs have been reported to cause oxidative DNA damage in terrestrial plants such as radish, annual ryegrass, and perennial ryegrass (Atha et al., 2012) whereas AgNPs were reported to show cytotoxic and genotoxic impacts in root tips of onion (Kumari et al., 2009). In contrast to the above reports, it was observed that CuO NPs did not cause any cytotoxic effect to A549 and HeLa S3 cells after 24 h incubation but caused insignificant generation of micronuclei and DNA fragments (Semisch et al., 2014). Similarly, TiO₂ NPs caused chromosomal aberrations and DNA damage in *Allium cepa* (Pakrashi et al., 2014) and disturbed the molecular expression profiles of microRNAs in tobacco (*Nicotiana tabacum*; Frazier et al., 2014). Quantum dots also caused damage to DNA suppressing the proliferation of WTK1 cells upon treatment with 25- 400 mg L⁻¹ in aqueous medium (Hoshino et al., 2004). In the present work, the mechanism of DNA damage was not studied.

1.9. ROS Scavenging Antioxidant Defence Mechanism

The excess ROS generated in plant cell organelles such as chloroplasts, mitochondria and peroxisomes during abiotic stress are effectively scavenged by enzymatic and non-enzymatic antioxidants that serves in the detoxification of ROS and protect cells from oxidative damage (Hasegawa et al., 2000; Srivalli et al., 2003).

1.9.1. Enzymatic anti-oxidant systems

Enzymatic antioxidants are key indicators of oxidative stress and include superoxide dismutase (SOD), ascorbate peroxidase (APX), Catalase (CAT), glutathione reductase (GR), Glutathione Peroxidase (GPX), mono-dehydroascorbate (MDHAR) and

dehydroascorbate reductase (DHAR) enzymes that detoxify ROS and lipid peroxidation products generated as a result of metal stress. Superoxide dismutase (SOD) is an active intracellular, metallo-enzymatic antioxidant which is ubiquitous and provides the first line of defense against the toxic effects of elevated levels of ROS. The SODs remove $O_2^{\cdot -}$ by catalyzing its dismutation into H_2O_2 via the metal catalyzed Haber–Weiss-type reaction and Mehler’s reaction (Fig 1.9). SODs are classified into three known types based on the cofactors, the copper/zinc (Cu/Zn-SOD), the iron (Fe-SOD) and the manganese (Mn-SOD) which are localized in different cellular compartments (Mittler 2002). The enhanced SOD activity reveals a protective mechanism adapted towards oxidative stress tolerance due to metal stress. Catalase (CAT) is an enzyme (tetrameric heme-containing) that converts H_2O_2 produced by SOD into H_2O and O_2 (Fig 1.9; Garg and Manchanda 2009). A single molecule of CAT can convert ≈ 6 million molecules of H_2O_2 into H_2O and O_2 per minute, thus having the highest turnover rates compared to all other enzymes. The hydrogen peroxide (H_2O_2) produced by SOD is detoxified into H_2O and mono-dehydroascorbate (MDHA) within the chloroplast and cytosol of plant cells by the enzyme ascorbate peroxidase (APX; Fig 1.9). Besides its H_2O_2 detoxification role, APX (two cytosolic forms and a membrane-bound form) controls the quantum efficiency and modulates the electron transport in union with the ascorbate-glutathione (AsA-GSH) cycle. In chloroplasts, SOD and APX enzymes exist in both soluble and thylakoid-bound forms eliminating $O_2^{\cdot -}$ generated during metabolic processes (Asada 2006). Glutathione reductase (GR) is a flavo-protein oxidoreductase that is found in both prokaryotes and eukaryotes (Romero-Puertas et al., 2006) predominantly localized in chloroplasts, but also in mitochondria and cytosol (Creissen et al., 1994). It plays an essential role in defense system against ROS by sustaining the reduced status of Glutathione (GSH) through the ASH-GSH cycle. GR and

GSH play a crucial role in determining the tolerance of a plant under various stresses (Rao and Reddy 2008).

Few reports have shown that metallo-NPs increase expression levels of SOD, APX and CAT causing oxidative stress. Increase in the expression of SOD-3 in *Caenorhabditis elegans* exposed to AgNPs was observed by Rho et al. (2009). Recently, increase in enzymatic antioxidant activity upon metallo-NP stress has been reported. For instance, increase in SOD and CAT enzyme activities as well as LPO upon exposure to magnetite (Fe_3O_4) NPs compared to its bulk metal on perennial ryegrass (*Lolium perenne* L.) and pumpkin (*Cucurbita mixta*) plants under hydroponic conditions was reported by Wang et al. (2011). Similarly, increase in the SOD and CAT activities at 100 mg L^{-1} of CuO and ZnO NPs in *Cucumis sativus* was reported by Kim et al. (2012a). In another study, TiO_2 NPs showed no effect in total antioxidant capacity (TAC) and SOD activity of *Brassica campestris* (oilseed rape), *Lactuca sativa* L. (lettuce), and *Phaseolus vulgaris* var. *humilis* (kidney bean) at concentrations of 100- 5000 mg L^{-1} (Song et al., 2013a). Also, tomato (*Lycopersicon esculentum*) plants upon treatment with nano- TiO_2 (5000 mg Kg^{-1}) and silver NPs resulted in higher SOD activity (Song et al., 2013b).

1.9.2. Non -Enzymatic Anti-Oxidant Systems

The non-enzymatic antioxidants in plants include ascorbic acid (AA), carotenoids (CARs), glutathione (GSH), tocopherols (TOCs) and phenolic compounds. Ascorbic acid (ASA) is one of the most important antioxidant which is present in most plant organelles especially chloroplast (Smirnoff 2000). ASA has the ability to donate electrons in varied enzymatic and non-enzymatic reactions making it the main ROS- detoxifying compound in the aqueous phase. ASA can directly scavenge $\text{O}_2^{\cdot-}$, OH^{\cdot} , and $^1\text{O}_2$, and can reduce H_2O_2 to H_2O via the APX reaction (Fig 1.9; Noctor and Foyer 1998). In chloroplasts, heat dissipation is carried out by ASA that acts as a cofactor of violaxanthin de-epoxidase, thus,

in addition to regulating other plant metabolic processes, increased endogenous ASA levels in plants are necessary to lessen oxidative stress (Smirnoff 2000). In the oxidation reaction of ASA, mono-dehydroascorbate is formed which dissociates into ASA and dehydroascorbate (DHA). ASA also regulates the pH-mediated modulation of PSII activity and the down-regulation of zeaxanthin production preventing photo-oxidation, in addition to its role as an antioxidant (Gill and Tuteja 2010). Reduced form of Glutathione (GSH; glu-cys-gly) present in the plant cell (Jimenez 1998) plays a major role in the antioxidative defense system by restoring ASA via the ASA-GSH cycle.

Proline (Pro) plays a crucial role for cellular metabolism both as a component of proteins and as free amino acid and acts as an osmoprotectant, a protein stabilizer, a metal chelator, an inhibitor of LPO, OH[•] radical and an ¹O₂ scavenger (Ashraf and Foolad 2007; Bohnert et al., 1995; Sleator and Hill 2002). Pro is reported to be an effective scavenger of OH[•] and ROS formed under metal, salt and water stress conditions in all plants, including algae (Alia and Saradhi 1991). In plants, proline is synthesized mainly from glutamate, which is reduced to glutamate-semialdehyde (GSA) by the pyrroline-5-carboxylate synthetase (P5CS) enzyme, and spontaneously converted to pyrroline-5-carboxylate (P5C) (Savoure et al., 1995). P5C reductase (P5CR) further reduces the P5C intermediate to proline (Verbruggen et al., 1996). Proline catabolism occurs in mitochondria via the sequential action of proline dehydrogenase or proline oxidase (PDH or POX) producing P5C from proline, and P5C dehydrogenase (P5CDH), which converts P5C to glutamate. As an alternative pathway, proline can be synthesized from ornithine, which is transaminated first by ornithine-delta-aminotransferase (OAT) producing GSA and P5C, which is then converted to proline (Kishor et al., 1995). Proline content is found to accumulate during MNP and heavy metal stress (Da Costa and Sharma 2016; Gunjan et al., 2014; Zarafshar et al., 2015). For instance, zucchini plants upon exposure to Cu NPs

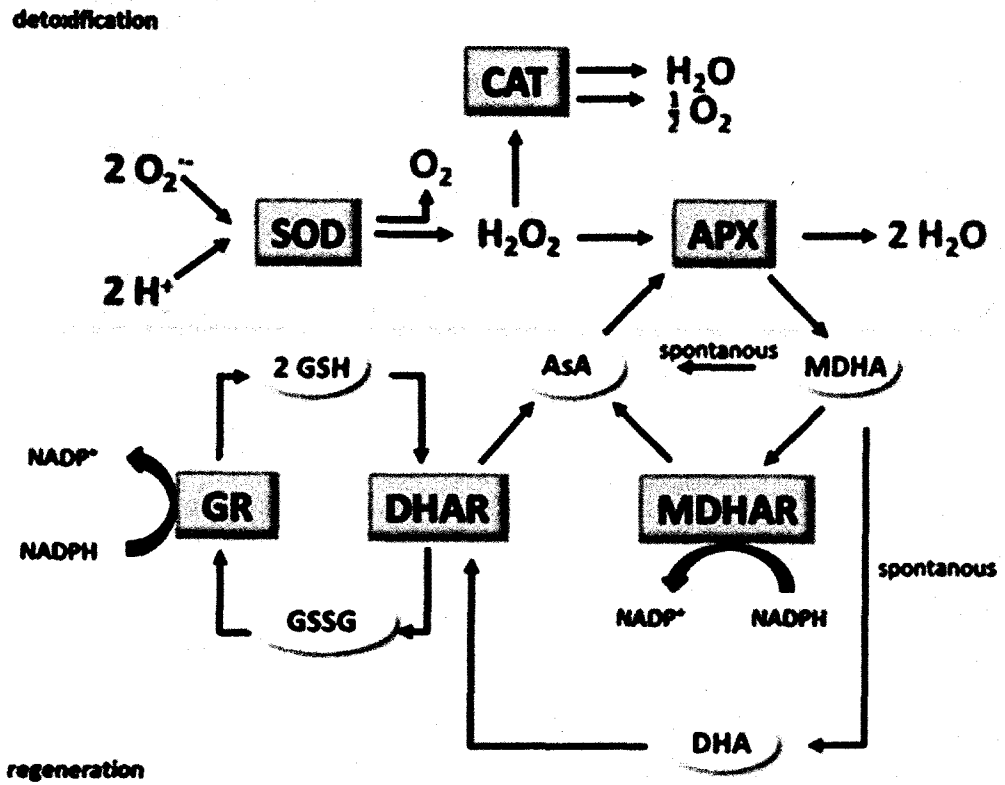


Fig 1.9. The antioxidant system. AsA, ascorbate; DHA, dehydroascorbate; SOD, superoxide dismutase; CAT, catalase; APX, ascorbate peroxidase; MDHA, monodehydroascorbate; MDHAR, MDHA reductase; DHAR, DHA reductase; GR, glutathione reductase; GSH glutathione; GSSG, glutathione disulphide. (Groß et al., 2013)

showed modulation of ascorbate-glutathione cycle, membrane damage and proline accumulation in rice (Shaw and Hossain 2013) and exposure to heavy metal Ni resulted in accumulation of proline and stimulation of GST activity in pea plants (Gajewska and Sklodowska 2005).

1.9.3. Other Cellular Mechanisms for Metal Detoxification

Higher plants contain two main cysteine rich, metal binding peptides, the metallothioneins (MTs) and phytochelatins (PC). MTs are gene encoded polypeptides initially identified in mammals and now have been identified in plants (Prasad & Hagemeyer 1999). Information concerning the metals likely to be bound by MTs is lacking, although Cd has been studied. The role of MTs and its function in metal detoxification in plants are under investigation and therefore predicting its role would be difficult at this point of time, therefore, not included in the present study. PCs on the other hand, have been most widely studied in plants, particularly in relation to cadmium tolerance (Cobbett and Goldsbrough 2002).

Phytochelatins are small, heavy metal-binding, cysteine-rich polypeptides present in plants and other organisms (Grill et al., 1987). PC synthase (PCS) enzyme (M_r 95000) is composed of four subunits with a catalytically active dimer (M_r 50000). PCs are important for detoxification of Cd^{2+} followed by Ag^+ , Bi^{3+} , Pb^{2+} , Zn^{2+} , Cu^{2+} , Hg^{2+} and Au^+ . Most other metals lack significant binding at all. The general structure of PC is $(\gamma\text{-Glu-Cys})_n\text{Gly}$ ($n=2-11$). PCs are synthesized by plants from glutathione (GSH) by phytochelatin synthase (PCS; Grill et al., 1987) forming metal-complexes with metal ions subsequently being transported from the cytosol and often sequestered in the vacuoles (Salt and Rauser 1995). The ubiquitous mechanism for metal detoxification involves metal chelation by a ligand (Cobbett 2000). Organic acids, amino acids, peptides and polypeptides have been described as metal-binding ligands (Rauser 1999). Activation of PCs arises from an interaction between the catalytic active domain of PCS and the free metal ion or metal-

GSH complexes (Cobbett 2000). Besides metal detoxification, PCs are involved in sulphur assimilation, GSH and sulphide biosynthesis.

Polyamines (PAs) occur ubiquitously in nature and are involved in the growth, development and stress metabolism in plants (Evans 1989). PAs play a role in the plant defense mechanism against abiotic and biotic stresses (Ma et al., 2005; Liu et al., 2004) and are responsive to light, temperature, salinity (Maiale et al., 2004), water (Ma et al., 2005), chemical and physical stress agents. The major endogenous PAs are putrescine (Put), spermidine (Spd), and spermines (Spm) are found in either free form or in soluble conjugated or insoluble-conjugated forms (Gemperlová et al., 2006). Spd and Spm are synthesized by Spd synthase and Spm synthase respectively whereas Put can be directly synthesized by ornithine decarboxylase or indirectly from arginine via arginine decarboxylase (Gemperlova' et al., 2006). PAs are implicated in many physiological processes such as morphogenesis, cell division, senescence, apoptosis (Yang et al., 2007b) and development of embryoids or floral primordia in certain vegetative tissue cultures (Galston and Sawhney 1990). Under metal stress, PAs are known to block the major vacuolar channels resulting in metal accumulation and decline in the ion conductance facilitating metal ion compartmentalization reducing toxicity in the photosynthetic tissue (Brüggemann et al., 1998). Stress-tolerant plants enhance PA biosynthesis in responses to stress, up to 2-3 times compared to control plants (Kasukabe et al., 2004). Literature review reveals that no published data regarding the influence of MNP on the polyamine content has been reported, however, heavy metal effect on polyamine content has been studied (Gong et al., 2016; Jacobsen et al., 1992).

Glycinebetaine, the N, N',N''-trimethyl glycine is a quaternary ammonium compound which acts as an osmolyte that accumulates in plants under NaCl and drought stress (Ma et al., 2007). GB accumulates in species of the poaceae and Chenopodiaceae,

however, is lacking in food crops such as rice and tobacco (GB non-accumulators) due to the deficiency of endogenous choline, a precursor of GB (Ma et al., 2007). GB is synthesized from choline to form betaine aldehyde via choline monooxygenase (C_{MO}). The betaine aldehyde thus produced is converted to glycine betaine by the enzyme betaine aldehyde dehydrogenase (BADH). GB is a non-toxic cellular compatible solute that decreases the osmotic potential of the cell in response to stress induced hypertonic conditions. Due to its protective role under various stresses, GB is fetching interest in production of improved GB crop varieties. GB is effective in stabilizing enzymes, membrane integrity and functional units such as oxygen evolving PSII complex, cell membranes, quaternary structures of complex proteins and enzymes such as Rubisco. Plants that are engineered to produce these compounds show increased protection against photo-inhibition and reactive oxygen species (Hasegawa et al., 2000). GB has the capability of storing nitrogen that can be used by plants when the stress is relieved (Schwacke et al., 1999). Also, studies show that GB could trigger the aggregation of soluble sugars, free proline, K⁺, Na⁺ and Cl⁻ (Majid et al., 2012). Due to the established fact that GB is not naturally produced in rice, the approach to investigate its role was ruled out in the present study. However, external application of GB in improving plant tolerance to MNPs is an upcoming interesting area of research.

1.10. *Oryza Sativa* (Rice) as a Model Plant

Rice is the chief crop having the second highest worldwide production after china and is the most widely consumed staple food (cereal grain) for a large part of the world's human population, especially in Asia and particularly India. Rice is the most important grain with regard to human nutrition and caloric intake. It is relatively fast growing annual crop with a high rate of return. One acre of field may yield as much as 8000 pounds of rice, making it an efficient crop to cultivate. It grows best in warm, humid climate, usually in rain fed

areas that receive heavy annual rainfall with standing water about five inches deep. It is also grown through irrigation in areas that receive moderately less rainfall. Since rice can be grown in the flooded areas, the probability of rice plants being exposed to metallo-NPs would be much greater considering direct and indirect land applications. Therefore, rice (*Oryza sativa* var. Jyoti) was selected as a model plant for the present study.

1.11. Aim and Objectives

Metal oxide nanoparticles or metallo-nanoparticles (MNPs) have varied applications in the commercial and agricultural industry. The MNPs manufactured inevitably enter the environment through air, water and soil, especially as fertilizers, growth enhancers or as other nano-agricultural products that hit the market. With research on the effects of these MNPs on plants still being in its infancy, it is unclear whether the entry of the MNPs into the living system could result in a positive or a negative outcome. Thus, it is imperative to carry out a systematic study to address the question whether the use of nanoparticles would be detrimental to plant growth and productivity and if so, then to determine the toxicity threshold of rice to CuO and ZnO NPs (50 and 100 nm). Additionally, does the mechanism of effect of MNPs on plant differ from their bulk counterparts and is this attributed to their nano size? Keeping these questions in mind, the objectives of the present study was designed as follows.

Objective I: To Study the seed Germination rate and external and internal morphological changes

- Germination rate.
- Measurement of root and shoot length.
- Observing the phenotypic changes of the plantlet.
- Observing trichomes, stomatal structure and number through Scanning Electron Microscope (SEM).

Objective II: To study the translocation of nanoparticles within root and shoot

- To estimate the amount nanoparticles in various tissue using atomic absorption spectroscopy.
- Sectioning of root and leaves.
- Internalization studies of nanoparticles in plant tissue through transmission electron microscope (TEM) according to Da Costa and Sharma (2016).

Objective III: To study the responses on photosynthesis

- Carbon dioxide fixation studies using Infrared gas analyzer (IRGA) according to Sharma and Hall (1996).
- Fluorescence measurements (FMS) according to Sharma et al. (1997).
- Extraction and analysis of photosynthetic pigments using HPLC according to Sharma and Hall (1996).

Objective IV: To study the effects of nanoparticles on the ROS generation and subsequent oxidative damage

- Oxidation of lipids according to Sankhalkar and Sharma (2002)
- Estimation of proteins oxidation according to Reznick and Packer (1994)
- Estimation of proline content according to Bates et al. (1973).

Objective V: To study the activity of anti-oxidant enzyme and non-enzyme oxidants and their expression level

- Determination of Ascorbate content based on Kampfenkel et al. (1995).
- Assay of superoxide dismutase (SOD) according to Boveris (1984).
- Estimation and quantification of polyamines (spermine, spermidine) according to Flores and Galston (1982); Redmong and Tseng (1979).
- Gene expression studies of antioxidant enzymes (APX, GR, SOD) and metal chelating enzyme Phytochelatin (PC) by Real Time-PCR

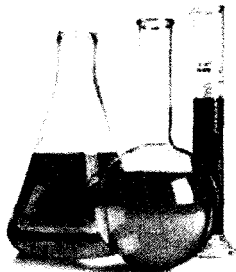
CHAPTER

2

MATERIALS

&

METHODS



“There is one thing even more vital to science than intelligent methods; and that is, the sincere desire to find out the truth, whatever it may be”

Charles Pierce

MATERIALS & METHODS

TABLE OF CONTENTS

Sr.No	Title of the topic	Page no
2.1	Plant Material and Metallo-nanoparticles	46
2.2	Plant growth and treatment under hydroponic system	46
2.3	Characterization of CuO and ZnO NPs	50
2.4	Determination of metal ions released from NP suspensions	54
2.5	Morphological studies of CuO and ZnO NPs	54
2.5.1	Percent germination	54
2.5.2	Shoot and root length measurements	56
2.5.3	Biomass determination	56
2.5.4	External morphological study	56
2.6	Uptake studies of CuO and ZnO NPs	58
2.6.1	Estimation of CuO and ZnO NPs in leaf and root tissue	58
2.6.2	Internal morphological studies using TEM	60
2.7	Photosynthesis studies in response to CuO and ZnO NP treatment	60
2.7.1	Infra-red gas analyser measurement	60
2.7.2	Chlorophyll Fluorescence measurement	63
2.7.3	Extraction and analysis of photosynthetic Pigments using HPLC	64
2.8	Biochemical assays	65
2.8.1	Lipid peroxidation	65
2.8.2	Protein oxidation assay	65
2.8.3	Estimation of Proline content	66
2.8.4	Ascorbic acid assay	66
2.8.5	Superoxide dismutase (SOD) enzyme activity assay	67
2.8.6	Extraction and quantification of polyamines	67
2.9	Gene expression studies	68
2.10	Statistical analysis	69

2.1. Plant Material and Metallo-Nanoparticles

Seeds of *Oryza sativa* (var. Jyoti), a high yielding, salt sensitive rice variety (PTB-10 x IR-8) was obtained from Indian Council of Agricultural Research, Goa and stored in dark at 20°C. Copper (II) Oxide (≤ 50 nm) and ZnO nanopowder (≤ 50 nm and < 100 nm) were obtained from Sigma Aldrich, India (Table 2.1). Plants were grown and treated with metallo-NPs hydroponically.

2.2. Plant Growth and Treatment under Hydroponic System

CuO and ZnO (≤ 50 nm, < 100 nm) NP solution of 0, 2.5, 10, 50, 100 and 1000 mg L⁻¹ at pH 6.5 was prepared separately in Hoagland's solution (Table 2.2). Seeds were surface sterilized using 4% sodium hypochlorite solution and continuously shaken for 3 min. The seeds were then washed 5-6 times and soaked in distilled water for 2-3 d. Germination paper was placed in Petri dishes, rice seeds were sown (100 seeds per Petri dish) and NP suspension of various concentrations of NPs was poured in respective Petri dishes (Fig 2.2.1). The set up was placed in a growth chamber having a temperature of $25 \pm 2^\circ\text{C}$ and 16 h photoperiod of light intensity $200 \mu\text{mol m}^{-2} \text{s}^{-1}$ and allowed to grow for 6 d. Glass beakers of two liter capacity (Borosil) were used as hydroponic vessels for plant growth. Rice plantlets (6 d) were transferred onto perforated thermocol sheets in groups of ten with the roots immersed in Hoagland's nutrient solution (Fig 2.2.1). The untreated (control) plantlets were grown without MNPs in Hoagland's solution while the treated plantlets were grown in Hoagland's solution supplemented with MNPs at different concentrations (2.5-1000 mg L⁻¹) and were allowed to grow for a total period of 30 d. The solution for each NP concentration was replenished individually every third day. Five sets were grown for each NP with respective nanoparticle concentration and analyzed. Proper aeration through tubes was provided from the top to the base of the glass beakers by means of air pumps.

Table 2.1. Metallo- nanoparticles specification as mentioned by supplier.

Product Name:	Copper(II) oxide 99.999% trace metals basis	Zinc oxide nanopowder, <50 nm particle size	Zinc oxide nanopowder, <100 nm particle size
Product Number:	544868	677450	544906
Formula:	CuO	OZn	OZn
Formula Weight:	79.55 g/mol	81.39 g/mol	81.39 g/mol
Appearance (Color)	Black	White to Yellow	White
Appearance (Form)	nanopowder	nanopowder	Powder
Average Particle Size	≤ 50 nm	<50 nm (BET)	≤ 100 nm
Specific Surface Area (m²/g)	25 - 40	>10.8	15 – 25

Table 2.2. Composition of Hoagland's Plant Nutrient Solution (Hoagland and Arnon 1950)

Component	Stock Solution (g/L)	Stock Solution (ml)	mL /1L
2M KNO ₃	202g/l	20.2g/dl	2.5
2M Ca(NO ₃) ₂ x 4H ₂ O	236g/0.5 L	47.2 g/dl	2.5
Iron (Sprint 138 iron chelate)	15 g/l	1.5 g/dl	1.5
2M MgSO ₄ x 7H ₂ O	493 g/l	49.3 g/dl	1
1M NH ₄ NO ₃	80 g/l	8 g/dl	1
H ₃ BO ₃	2.86 g/l	0.286 g/dl	1
MnCl ₂ x 4H ₂ O	1.81 g/l	0.181 g/dl	1
ZnSO ₄ x 7H ₂ O	0.22 g/l	0.022 g/dl	1
CuSO ₄	0.051 g/l	0.0051 g/dl	1
Na ₂ MoO ₄ x 2H ₂ O	0.12 g/l	0.012 g/dl	1
1M KH ₂ PO ₄			
(pH to 6.0 with 3M KOH)	136 g/l	13.6 g/dl	0.5

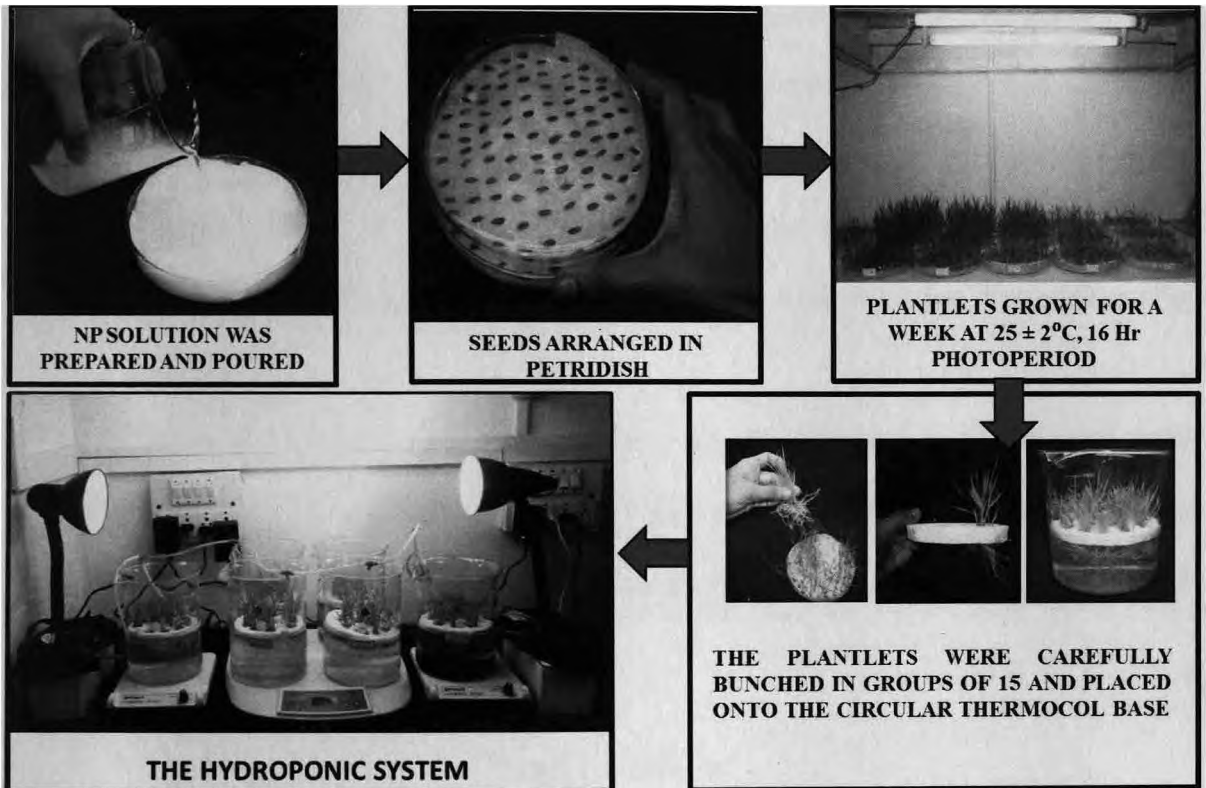


Fig 2.2.1. Setting up of the hydroponic system from early seed stage to final stage of growth.

Continuous stirring of MNPs was achieved using magnetic stirrers. Root damage was completely minimized using this technique and was therefore used for the study (Fig 2.2.2 A). Several other methods were tried. For instance, seed germination and growth on germination paper soaked with MNPs were used; however, even though this method enabled good growth of rice seedlings, the plantlets survived only for a short period due to decomposition of leaves and roots by fungal contamination (Fig 2.2.2 B). Broad based glass dishes (Borosil) of two liter capacity were also used with perforated thermocol sheets, this method was not successful as the plant roots grew to the base of the dish which were mostly physically damaged by magnets used to stir the MNPs, therefore, proper aeration and continuous stirring of MNPs could not be achieved using these dishes (Fig 2.2.2 C).

Bulk Cu ($\text{CuSO}_4 \cdot 5\text{H}_2\text{O}$) and Zn ($\text{ZnSO}_4 \cdot 7\text{H}_2\text{O}$) treatment were also studied at the same concentration to understand the extent of ions released and comparative mechanism of toxicity of bulk metals and MNPs. The growth method and conditions were maintained as described for MNPs.

2.3. Characterization of CuO and ZnO NPs

Scanning Electron Microscope: Size of CuO and ZnO NP powder was characterized using Scanning Electron Microscopy (JSM 5800 LV, JEOL, Japan) operating at a constant acceleration voltage of 10 kV. NPs were ultra-sonicated in 100% ethanol and a drop of this solution was placed onto the stub layered with carbon conductive, double sided adhesive tape (SPI Supplies®, USA). The sample was air-dried and sputter coated with gold for 15 s (SPIMODULE Gold Sputter Coater) under high vacuum and analyzed with INCA viewer software (oxford instruments) at the National Institute of Oceanography, Goa (Fig 2.3 A).

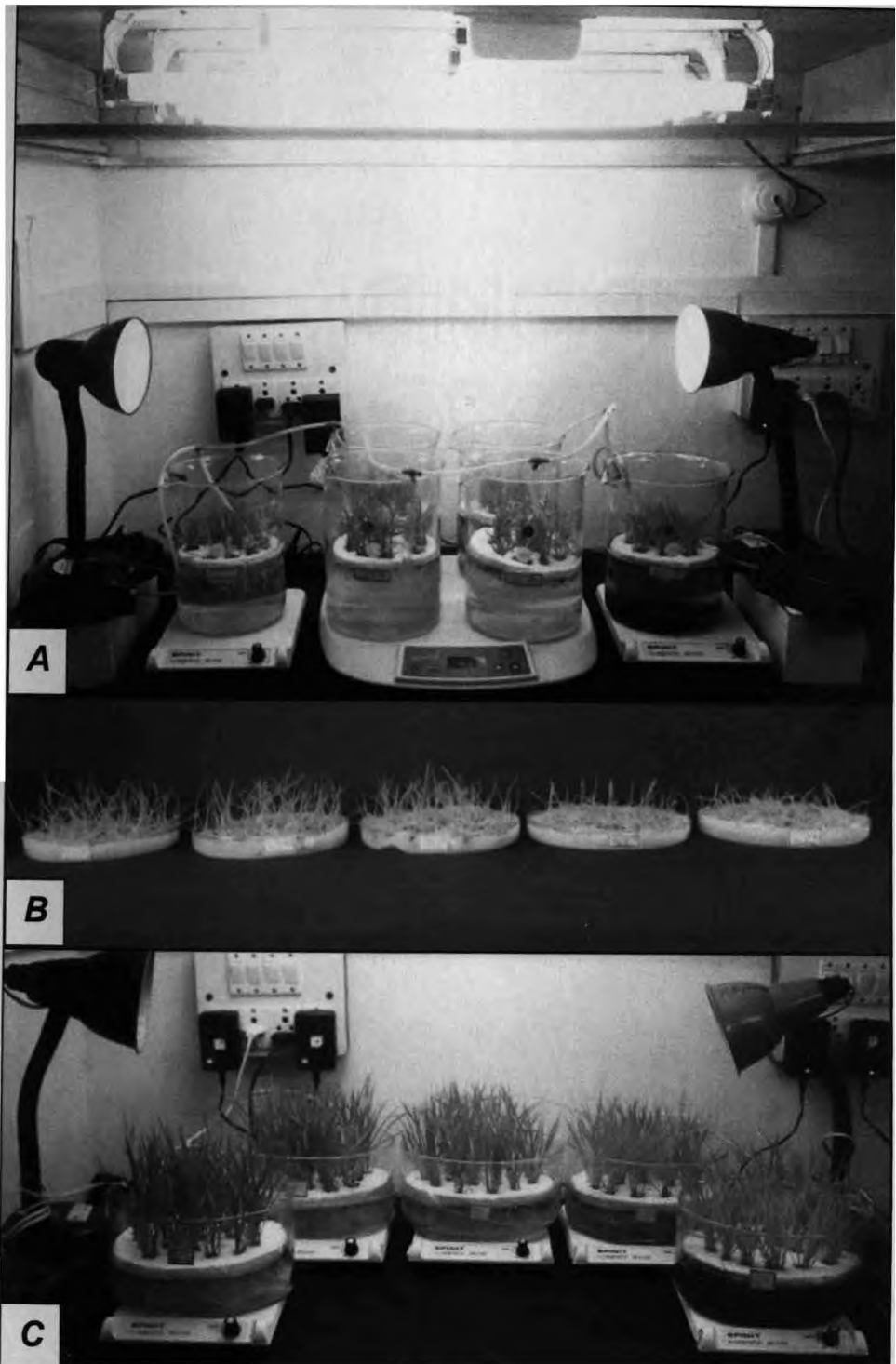


Fig 2.2.2. Comparison of the Standardized hydroponic system used for the study (A) with the unsuccessful techniques tried, Petriplate method (B) and broad based glass dish method (C) used for growth of rice plants at a temperature of $25 \pm 2^\circ\text{C}$ and a 16 h photoperiod (light intensity $200 \mu\text{mol m}^{-2} \text{s}^{-1}$) with additional incandescent light (20W bulbs).

T-7772



X-Ray Diffraction: Nanoparticle powder was characterized using X-ray Diffractometer (XRD) by Rigaku with a scintillation counter probe SC-30 (Deflector) (Fig 2.3 B). The XRD analysis was performed using Traces software (GBC scientific instruments) on powdered samples of CuO and ZnO NPs recorded at room temperature in the range of $2\theta = 20^\circ - 80^\circ$ with a step of 0.02° and a speed of $2^\circ/\text{min}$ to obtain particle size using Cu $K\alpha$ radiation ($\lambda=0.15406$ nm). The XRD patterns obtained was analyzed based on the maximum valued peak among the first three peaks detected by the scintillation counter probe SC-30. The peak at higher 2θ values were not considered as they are inaccurate at high resolution. The particle size was calculated using Scherrer's formula

$$D = \frac{\eta\lambda}{\beta\cos\theta}$$

Where D= particle size

$\eta=0.89$ (Scherrer's constant)

$\lambda=0.154$ nm

β = FWHM (full width half maximum)

θ = diffraction angle ($2\theta/2$)

Scherer's constant (η value) is obtained when the standard (silicon) used gives a 100% intensity peak at full width half maximum (FWHM). The particle size depends on " β " since $\cos \theta$ does not show a large variation at different angles. Therefore, if the width of the peak increases, the particle size becomes smaller. XRD follows a simple principle, when an X ray beam of high intensity (λ) falls on the crystal at an angle θ , it diffracts the beam which is detected by a X- ray detector at 2θ position as shown in Figure 2.3.B. The incident angle is than increased over time while the detector angle always remains 2θ above the source path. When X-rays strike the phosphor present in the detector, it produces flashes of light, which are detected by the photomultiplier tube. The intensities produced are determined by the number of counts in a certain amount of time.

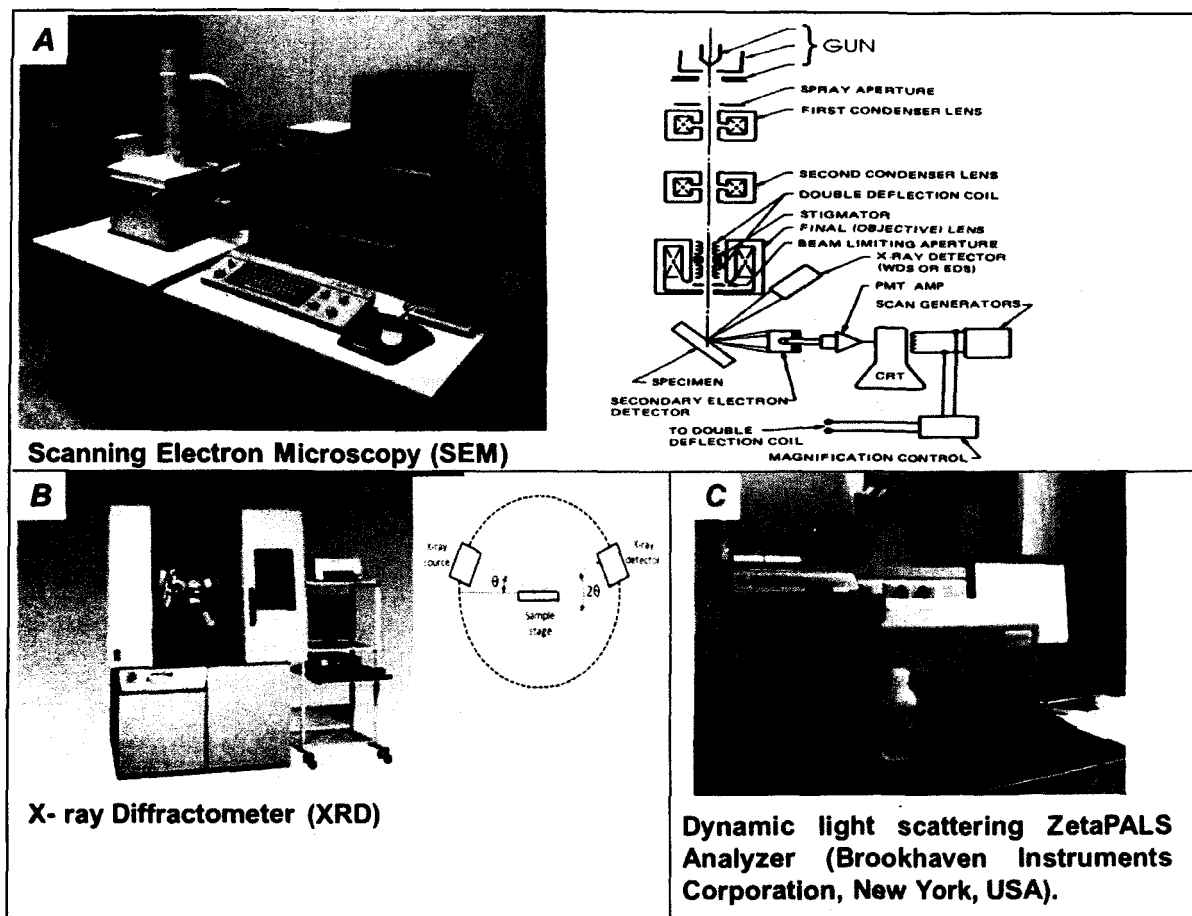


Fig 2.3. Pictorial depiction and the diagrammatic representation of the working principle of SEM (A), XRD (B) and DLS (C). “DLS image taken at Centre for Nano Science and Engineering (CeNSE), Indian Institute of Science, Bangalore, India”.

Dynamic Light Scattering: Size determination of the particle and its behavior in aqueous system was studied using dynamic light scattering ZetaPALS Analyzer (Brookhaven Instruments Corporation, New York, USA) at Centre for Nano Science and Engineering (CeNSE), Indian Institute of Science, Bangalore, India. CuO and ZnO NPs at 1000 mg L⁻¹ concentration were physically dispersed in Hoagland's nutrient solution using an ultrasonicator. Each measurement consisting of five replicates were measured with 10 s duration at 25°C and analyzed using BIC Particle Sizing Software Ver.5.23 (Fig 2.3 C). This size experiment does not differentiate between individual atoms and group of nano sized particles in the nutrient medium. Due to this limitation the particle size measured using DLS is highly variable depending on the elemental form of metallo-NPs and its size may not be in accordance to the supplier due to its interaction with other components of the medium forming agglomerates or aggregates of larger size.

2.4. Determination of metal ions released from NP suspensions

Metal ion concentration released from NP solutions was measured using Inductively coupled plasma mass spectroscopy (ICP-OES, Perkin-Elmer Optima 7300 DV, USA) according to Wu et al., (2012). Aliquots of CuO and ZnO NP metal oxide suspensions (0, 2.5, 10, 50, 100 and 1000 mg L⁻¹) were drawn after the suspensions were incubated in sterile water and Hoagland's nutrient solution at room temperature for 48 h. The extracts were centrifuged at maximum speed for 20 min, and supernatants were collected and filtered with 0.2 µm Ultipor®N66®Nylon 6, 6 membrane filter (Fig 2.4).

2.5. Morphological studies of CuO and ZnO NPs:

2.5.1. Percent Germination:

The percentage of germination was calculated taking average of triplicates for each set of individual MNPs grown separately.



Fig 2.4. Inductively coupled plasma mass spectroscopy. “Image taken at National Institute of Oceanography, Goa”.

2.5.2. Shoot and root measurements were physically taken for individual sets of CuO and ZnO NPs.

2.5.3. Biomass determination: The biomass of 10 plants for each concentration (0- 1000 mg L⁻¹) grown with CuO and ZnO NP concentration was measured after 30 d of growth.

2.5.4. External morphological study: The external root and leaf morphology was studied by visualizing lyophilized segments of root and leaf using (SEM) Scanning Electron Microscopy (JSM 5800 LV, JEOL, Japan; Fig 2.3 A) and analyzed with INCA viewer software (oxford instruments) at the National Institute of Oceanography, Goa. External morphology of 3rd leaf (Fig 2.5) and root treated with CuO, ZnO (< 50 and 100 nm) was also studied by visualizing lyophilized segments of root and shoot tissue with SEM. The treated plantlet was placed at -20^oC for 24 h in glass beakers. The Cool Safe 110 Freeze Dryer (Fisher Scientific Bio-block) was put on and it was allowed to reach a temperature of -110^oC simultaneously the vacuum pump was kept on for 30 min with the external valve connecting to the Freeze dryer closed. The samples were then placed on top of the acrylic plate enclosed within an acrylic chamber. The external valve was opened connecting the freeze dryer to the vacuum pump. It was allowed to undergo sublimation for 4 h. The external valve was closed and the vacuum pump was allowed to run for 40 min. The pressure was equalized by opening the release valve at the lid and the samples were removed, sealed using parafilm and placed in a desiccator until SEM analysis. The adaxial (upper) side of the leaf was carefully placed onto a double sided stick tape, the other side adhered to a specimen mount. This mount was secured to a holder by screws. The stage was set such that the specimen is approx. 50 mm from the bottom of the sputter head. The leak valve was closed and the argon pressure set to 5 psi. The power was switched on, starting the vacuum pump. Once the pressure falls to approximately 600-400 millitorr, the

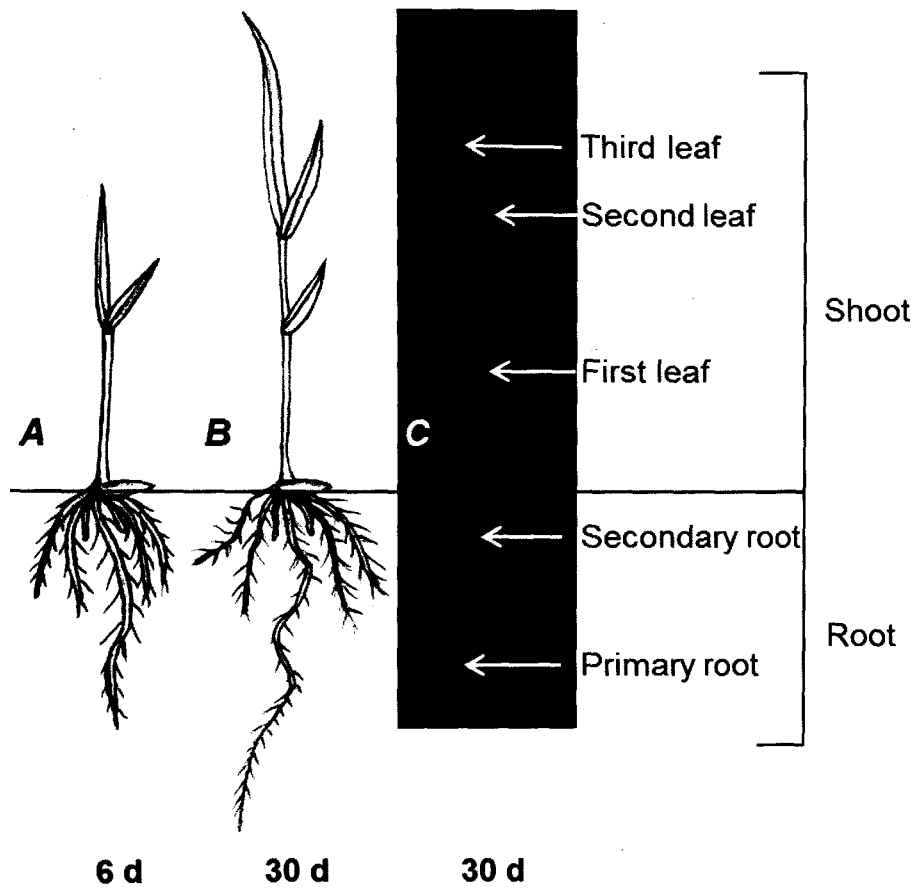


Fig 2.5. Diagram representing parts of rice plant at 6 d (A) and 30 d (B, C) used in the study. The 6 d plants show the emergence of two leaves (first and second) and 30 d plant show three leaves (first, second and third).

gas leak valve was partially opened to flush the work chamber with argon for about 15 sec. The leak valve was closed and the work chamber was allowed to pump down to approximately 80 millitorr. The gas leak valve was opened and adjusted to set the plasma current to 10 mA. A visible discharge was observed in the chamber. The start button was pressed and gold was sputtered onto the specimen for 110 sec. The plasma automatically extinguished at the end of the period. The power was switched off and air was allowed to enter the chamber using the "vent" valve on the top of the sputter head. The gold sputtered specimen mount was fixed onto the sample holder in the SEM sample chamber. A vacuum was created and the SEM was connected to a computer system. The images were obtained at 10 kV and at high magnification.

2.6. Uptake studies of CuO and ZnO NPs

2.6.1. Estimation of MNPs in leaf and root tissue

Uptake of MNPs was determined using atomic absorption spectrophotometer (Flame Furnace system—AA Analyst 200, AAS, Perkin Elmer, USA) at the National Institute of Oceanography, Goa. Fresh tissue (1g) of control and treated plant leaf and root was weighed and dried separately in an oven for 3 d at 65°C. Once drying was complete, the tissue was weighed for dry weight and transferred to crucibles for ash preparation in a furnace at a temperature of 450°C for 8 h. The ash was dissolved in 1% HNO₃ (Merck) solution and filtered through 0.45 µm Whatman filter paper and then used. The filtered sample was used for AAS analysis in whole root and leaf tissues of CuO and ZnO NP exposed plants, as well as in different sections of the leaf (apical, middle, and basal region) at different concentrations of CuO NPs only. Standards used were prepared using CuSO₄ and ZnSO₄ in 1% HNO₃ acid. The AAS data obtained in mg kg⁻¹ (ppm) and multiplied by the appropriate value to convert the obtained data to one gram dry weight basis.

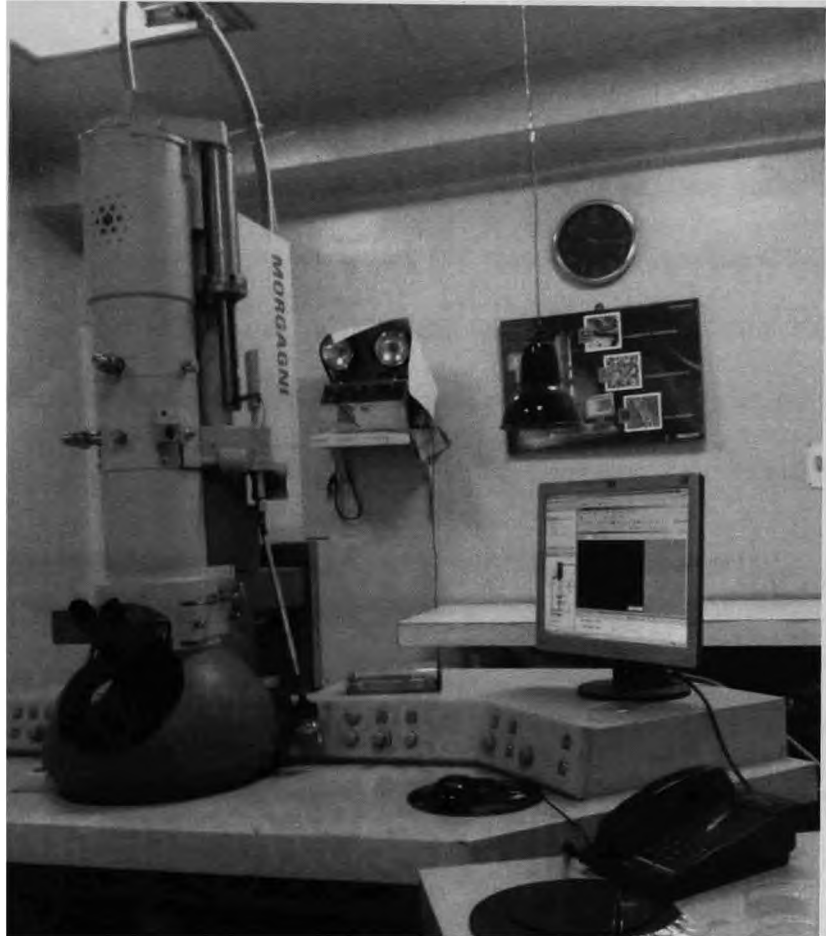


Fig 2.6. Transmission electron microscopy (TEM, FEI Tecnai™, Morgagni 268D). “Image taken at All India Institute of Medical Sciences (AIIMS), New Delhi”.

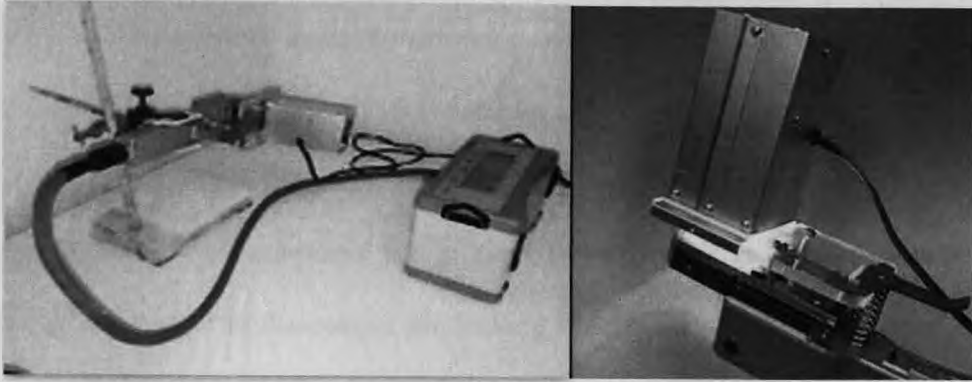
2.6.2. Internal morphological study:

The internal leaf and root morphology was studied using transmission electron microscopy (TEM) at All India Institute of Medical Sciences (AIIMS), New Delhi (Fig 2.6). The leaf and root tissue was cut into 2×2 mm pieces and fixed in a mixture of 2% paraformaldehyde and 2.5% glutaraldehyde in 0.1 M phosphate buffer for 10 h at 4°C. The tissue samples were washed in 0.1 M phosphate buffer at 4°C. Samples were then post fixed at room temperature for 1 h in 1% OsO₄ in 0.1 M phosphate buffer (pH 7.2). Samples were dehydrated in acetone, infiltrated, and embedded in Araldite CY 212. Thin, serial sections were cut (70-80 nm thick) using ultra-microtome (Leica UC6, Leica Microsystems, Germany), collected on copper grids, stained with uranyl acetate and lead citrate, and examined under a TEM (Morgagni 268D, Fei Company, The Netherlands).

2.7. Photosynthesis studies in response to CuO and ZnO NP treatment.

2.7.1. Infra-red gas analyzer measurement

Net photosynthesis, stomatal conductance, and transpiration rate studies were carried out using a portable infra-red gas analyzer (IRGA, ADC Bioscientific, LCI-SD; Fig 2.7 A). Infra-red gas analyzer uses the principle of Non Dispersive Infrared (NDIR) for CO₂ measurement. CO₂ absorbs energy in the infrared region in a proportion directly related to the concentration of gas. The gas to be measured (produced by plants) is passed through a chamber with an infrared source which measures the signal when the CO₂ concentration is present. The reference (To the chamber) and analysis (From the chamber) gases are alternated with zero gas produced by passing air through the soda lime removing all the CO₂. The cycle time allows the cell to refill taking repeated measurements. The Infra-red gas analyzer “Console” contains a large LCD, microprocessor controlled operating system with signal conditioning, air supply unit and PC card data storage (Fig 2.7 A). A leaf chamber is connected to the console by an umbilical cord. The leaf chamber contains the



A. Infra Red Gas Analyzer (LCi-SD, ADC Bioscientific)



B. Fluorescence monitoring system (FMS-1, Hansatech Instruments)



C. High Performance Liquid Chromatography (HPLC, Waters)

Fig 2.7. Tools to study the photosynthetic response of rice plants to Metallo-nanoparticles.

PCA-275A printed circuit board comprising of conditioning and pre-amplifier circuitry for chamber temperature, leaf temperature and PAR (Photosynthetically active radiation) sensors. Two laser-trimmed humidity sensors provide the reference and analysis humidity signals and an infrared optical bench was used for CO₂ analysis. The main console supplies air with a relatively stable CO₂ concentration at a controlled flow-rate to the leaf chamber. The CO₂ and H₂O concentrations are measured and the air is directed over both the surfaces of the leaf. The discharged air leaving the chamber is analyzed, and the CO₂ content and H₂O content determined. From the known airflow rates and the differences in gas concentration, assimilation and transpiration rates are calculated. A small fan in the chamber ensures thorough mixing of the air around the leaf in the leaf chamber. The photosynthesis rate (P_N), transpiration rate (E) and stomatal conductance (g_s) were measured at ambient temperature and carbon dioxide concentration and light intensity of 1200 $\mu\text{mol m}^{-2} \text{s}^{-1}$ using a detachable light source provided by a dichroic lamp (Hansatech, UK) according to Sharma and Hall (1996), calculated using the following formulae.

Molar flow of air per m² of leaf surface μ_s ($\text{mol m}^{-2} \text{s}^{-1}$)

$$\mu_s = \frac{\mu}{\text{Area}}$$

Where μ = molar air flow in mol s^{-1}
 Area = projected leaf area in m^2

Difference in CO₂ concentration Δc ($\text{vpm} = \mu\text{mol mol}^{-1}$)

$$\Delta c = C_{ref} - C'_{an}$$

Where Δc difference in CO₂ concentration, in $\mu\text{mol mol}^{-1}$
 C_{ref} CO₂ flowing into the leaf chamber, in $\mu\text{mol mol}^{-1}$
 C'_{an} CO₂ flowing out of the leaf chamber, in $\mu\text{mol mol}^{-1}$

Photosynthetic rate (Rate of CO₂ exchange in the leaf chamber) A ($\mu\text{mol m}^{-2} \text{s}^{-1}$)

$$A = \mu_s \Delta c$$

Where μ_s = Mass flow of air per m^2 of leaf area, $\text{mol m}^{-2}\text{s}^{-1}$
 Δc = difference in CO_2 concentration, in $\mu\text{mol mol}^{-1}$

Water vapour pressure in and out of the leaf chamber

$$\Delta e = e'_{an} - e_{ref}$$

Where e'_{an} = water vapour pressure out of the leaf chamber, mbar
 e_{ref} = water vapour pressure into the leaf chamber, mbar

Transpiration rate E ($\text{mol m}^{-2}\text{s}^{-1}$)

$$E = \frac{\mu_s \Delta e}{P}$$

Where μ_s = Mass flow of air per m^2 of leaf area, $\text{mol m}^{-2}\text{s}^{-1}$
 Δe = Differential water vapour concentration, mbar
 $P = 1$ (atmospheric pressure, mbar)

Stomatal conductance of water vapour g_s ($\text{mol m}^{-2}\text{s}^{-1}$)

$$g_s = \frac{1}{r_s}$$

Where r_s = Stomatal resistance to water vapour, $\text{mol m}^{-2}\text{s}^{-1} \text{mol}^{-1}$

2.7.2. Chlorophyll Fluorescence measurements: Fluorescence measurements (F_v/F_m , q_p , q_N and Φ_{PSII}) were carried out according to Sharma et al. (1997) using a fluorescence monitoring system (FMS, Hansatech instruments; Fig 2.7 B). The third leaf (mature primary leaf) were dark adapted for 10 min to inhibit all light dependent reactions by completely re-oxidizing PSII electron acceptor molecules, opening the reaction centre's and maximizing probability of photochemistry. A weak modulating beam of intensity $3-4 \mu\text{mol m}^{-2} \text{s}^{-1}$ is focused on the sample to measure initial fluorescence (F_o), followed by exposure to a saturating pulse (approximately $4,000 \mu\text{mol photons m}^{-2} \text{s}^{-1}$ for 0.06 s) to measure the maximum fluorescence (F_m). Variable fluorescence (F_v) was determined by deducting the F_o from F_m ($F_v = F_m - F_o$) and the maximum quantum yield (F_v/F_m) ratio was calculated. Actinic light was provided at an intensity of $1200 \mu\text{mol m}^{-2} \text{s}^{-1}$ and allowed to

reach a steady state fluorescence yield (F_s) after which far red pulse was given for 5 sec which was then used to calculate the relative contributions for photochemical and non-photochemical energy dissipation measured as the photochemical quenching (q_P) and non-photochemical quenching (q_N) using Modfluor32 software as per the equations given below.

Maximum quantum efficiency of photosystem II (no units)

$$F_v/F_m = (F_m - F_o)/F_m$$

Quantum efficiency of PSII (no units)

$$\Phi_{PSII} = (F_m' - F_s)/F_m'$$

Photochemical quenching co-efficient (no units)

$$q_P = (F_m' - F_s)/(F_m' - F_o)$$

Non-Photochemical quenching co-efficient (no units)

$$q_N = (F_m - F_m')/(F_m - F_o)$$

2.7.3. Extraction and analysis of photosynthetic Pigments using HPLC:

Leaf tissue (0.1 g) was ground in 100% acetone (Merck, HPLC grade) making a final volume of 1.5 ml and incubated overnight at 4°C (Fig 2.7 C). The homogenate was centrifuged (Z32HK, HERMLE Labortechnik GmbH, Germany) at 4°C for 10 min at 4,000 × g. One ml of supernatant was collected and filtered through 0.2 µm Ultipor®N66®Nylon membrane filter (PALL Life Sciences, USA) and 10 µl of sample was analyzed in an HPLC system (Waters, USA), using two-solvent gradient as a mobile phase (using Merck HPLC grade chemicals) composed of solution A (ethyl acetate) and solution B (acetonitrile: water, 9:1). The mobile flow rate was 1.2 ml min⁻¹ for a run time of 30 min. The pigments were separated using a C18 column (Waters Spherisorb ODS2 – 250 mm × 4.6 mm × 5 µm). The pigment peaks were determined at 445 nm with a Waters 2996

photodiode array detector based on RT and spectral characteristics. β -carotene was used as an external standard for the relative quantification of pigments (Sharma and Hall 1996).

2.8. Biochemical parameters

2.8.1. Lipid peroxidation

Malondialdehyde (MDA) assay was carried out according to Sankhalkar and Sharma (2002). 0.2 g of plant leaf tissue was taken and ground in 5 ml of 1% trichloroacetic acid (TCA) and centrifuged at 2000 rpm for 3-4 min. 1 ml of supernatant was taken in triplicates and 2.5 ml of incubation buffer (50 mM Tris HCl, 175 mM NaCl; pH 8), 2.5 ml of 0.5% thiobarbituric (TBA) acid prepared in 20% TCA was added to each sample. The mixture was then kept in dry bath (WiseTherm HB-48P) at 95°C for 30 min followed by cooling at room temperature. O.D was taken at 532 and 600 nm using UV-Visible spectrophotometer (UV-2450, Shimadzu, Singapore). Peroxidation of lipids was measured using an extinction coefficient of $155 \text{ mM}^{-1} \text{ cm}^{-1}$.

2.8.2. Protein oxidation assay

Protein carbonyl colorimetric assay method according to Reznick and Packer (1994) was used. Plant tissue (0.1 g) was taken and ground in 2.5 ml of sodium phosphate buffer (pH 7.4, Merck) and centrifuged at 7000 rpm for 15 min at 4°C. 1 ml each of supernatant was used for sample (S) and control (C) reactions separately. To the control reaction, 4 ml of 2.5 N HCl (Merck) was added. To the sample reaction, 4 ml of 0.2 % 2, 4-dinitrophenyl hydrazine (DNPH, Himedia AR grade) prepared in 2.5 N HCl was added. Mixtures were incubated in dark for 1 h at room temperature while keeping stirred at regular intervals. 4 ml of 20% TCA was added, mixed and centrifuged at 7000 rpm for 10 min at 4°C. The supernatant was discarded and the pellet was re-suspended in 1ml of 10% TCA, incubated in ice for 5 min and centrifuged at 7000 rpm for 10 min at 4°C. 1 ml of

ethyl acetate: ethanol (1:1) was carefully added to the pellet, vortexed and centrifuged at 7000 rpm for 10 min at 4°C. The pellet was finally dissolved in 1.5 ml of 6 N Guanidine hydrochloride (Himedia $\geq 99\%$ pure) prepared in sodium phosphate buffer (Qualigens) and centrifuged at 7000 rpm for 10 min at 4°C. The O.D was measured at 370 nm using UV-Visible spectrophotometer (UV-2450, Shimadzu, Singapore). Protein oxidation was measured as protein carbonyl using the calculated average (CA) = (S) - (C) and extinction coefficient of $0.022 \mu\text{M}^{-1} \text{cm}^{-1}$.

Protein carbonyl (nmol/ ml) = Calculated average (CA)/ $0.022 \mu\text{M}^{-1} \text{cm}^{-1}$ (a/b)

Where, Extinction coefficient = $0.022 \mu\text{M}^{-1} \text{cm}^{-1}$

a= volume of sample used (μl)

b= volume of Guanidine HCl (μl)

2.8.3. Estimation of Proline content

Proline accumulation in fresh leaves was determined according to the method of Bates et al. (1973). Plant tissue (0.2 g) was ground in 5 ml of 3% Sulfosalisilic acid and centrifuged at 5000 rpm for 5 min. The supernatant, 1 ml each was taken fresh test tubes (in triplicates). To each sample, 1 ml of Acid Ninhydrin (1.25 g Ninhydrin, 30 ml GAA, 20 ml 6M Phosphoric acid) and 1 ml of Glacial Acetic Acid was added. The mixture was then kept in dry bath (WiseTherm HB-48P) at 95°C for 1 h followed by cooling to room temperature. After the tubes were cooled, 10 ml of toluene was added to each tube and mixed vigorously. This mixture was allowed to settle and O.D was taken at 520 nm using UV-Visible spectrophotometer (UV-2450, Shimadzu, Singapore). L-Proline was used as a standard for quantification by plotting a standard graph against concentration.

2.8.4. Ascorbic acid assay

Ascorbate (ASA) was estimated according to the method of Kampfenkel et al. (1995). Fresh leaf tissue (0.1 g) was ground with 1 ml of extraction buffer (0.1 M HCl + 0.1 mM

EDTA). The extract was centrifuged at 12000 rpm for 2 min in an eppendorf tube and the supernatant was used for the ascorbate assay. The reaction mixture contained, 20 μ l of sample, 20 μ l of 0.4 M phosphate buffer (pH 7.4), 80 μ l of color reagent (containing two solutions [A]. TCA (4.6%), H₃PO₄ (15.3%), FeCl₃ (0.6%) and [B] 2, 2 dipyridyl (4%) in 70 % ethanol, in the ratio of 2.75:1) and 10 μ l of 0.5% N-ethylmaleimide. The mixture was incubated at 42°C for 45 min and absorbance was measured at 520 nm. Ascorbic acid was used as standard.

2.8.5. Superoxide dismutase (SOD) enzyme activity assay

The activity of SOD was assayed according to Boveris (1984). Leaf tissue (0.2 g) was homogenized in 1.5 ml of 50 mM sodium phosphate buffer (pH 7.8) and centrifuged at 4°C for 1 min. The supernatant used to carry out the SOD assay at 480 nm. Blank or Reaction (1) contained 2.5 ml of 10 mM Na₂CO₃; 0.1 ml of 10 mM sodium phosphate buffer; 0.1 ml of 6 mM disodium EDTA and 0.3 ml of deionised water. Reaction (2) contained 2.5 ml of 10 mM Na₂CO₃; 0.1 ml of 10 mM sodium phosphate buffer; 0.1 ml of 6 mM disodium EDTA and 0.3 ml of 4.5 mM epinephrine. Reaction (3) contained 2.5 ml of 10 mM Na₂CO₃; 0.1 ml of supernatant; 0.1 ml of 6 mM disodium EDTA and 0.3 ml of 4.5 mM epinephrine. Protein concentration of enzyme extract was measured using Bradford method at an absorbance of 595 nm and the SOD activity was expressed as SOD activity (ΔA) min⁻¹ mg⁻¹ protein.

2.8.6. Extraction and quantification of polyamines

Preparation of perchloric extract was done according to Flores and Gatson (1982). Plant tissue (0.1g) was ground in a pre-chilled mortar and pestle with 2 ml of 5% cold (v/v) perchloric acid and incubated at 5°C for 1 h. The extract was then centrifuged at 12000 rpm for 30 min. Supernatant was collected and used for the extraction of soluble-conjugated polyamines-benzoylation using High Performance Liquid Chromatography

(HPLC) according to Redmong and Tseng (1979). To 1 ml of 2N NaOH, 500 μ l of perchloric extract and 10 μ l of benzoyl chloride was added and vortexed for 10 sec and incubated at room temperature for 20 min. 2 ml of saturated NaCl and 2 ml of diethyl ether was then added and centrifuged at 5000 rpm for 5 min. 1ml of ether phase was collected and evaporated to dryness and dissolved in 500 μ l of 60% methanol. The extract was filtered through 0.2 μ m Ultipor®N66®Nylon 6, 6 membrane filter and 10 μ l of sample was analyzed in a Waters HPLC system, using an isocratic system (methanol: water, 6:4). The mobile flow rate was 1 ml min⁻¹ for a run time of 20 min. Polyamines were separated using a C18 -5 μ m Column (Waters spherisorb ODS2- 250 mm x 4.6 mm). The polyamine peaks were determined at 254 nm with a Waters 2996 photodiode array detector based on RT, spectral characteristics. Spermine and spermidine standards (25 mM) were used as external standards and the results were calculated based on the peak area.

2.9. Gene expression studies

RNA Extraction and quantification: Leaf tissue (0.1 g) was ground using liquid nitrogen and extracted following the protocol mentioned in the RNA purification reagent (Invitrogen). The samples were ground in 0.6 ml of RNA extraction buffer (Invitrogen) and placed in eppendorf tubes. The tubes were gently flicked and contents mixed and incubated at room temperature (RT) for 10 min and centrifuged at 12000 rpm for 4 min. The supernatant was carefully taken and 125 μ l of 5M NaCl and 350 μ l of chloroform was added and mixed by inversion. The mixture was then centrifuged at 12000 rpm for 10 min at 4°C. The top aqueous phase was taken and equal volume of isopropanol was added, mixed and incubated at RT for 10 min followed by centrifugation at 12000 rpm for 15 min at 4°C. 1 ml of 70% ethanol was added to the pellet and centrifuged at 12000 rpm for 2-3 min at RT. The pellet was then dissolved in 50 μ l of sterile distilled water. The RNA was quantified using spectrophotometer at 260 and 280 nm.

cDNA preparation and Real time analysis Real time PCR: cDNA synthesis was done using PCR kit (Invitrogen Superscript III Reverse Transcriptase, Cat no: 18080/093/044/085) following the given protocol (Fig 2.9 A). 5 µg equivalent RNA, 1 µl random primer and sterile water was added to make up the volume of 12 µl in PCR vials. The mixture was heated at 70 °C for 5 min, cooled and spun. 5 µl of 5 X reaction buffer, 1.5 µl of dNTPs (10 mM) and 1 µl superscript III RT was added making the volume to 25 µl using sterile water. The following PCR reaction was carried out using Corbett research PCR thermocycler at three different consecutive temperatures of 25°C for 10 min, 42°C for 1 h, and 75°C for 15 min. The samples were kept at -20 °C. Expression of genes for anti-oxidant enzymes (APX, SOD, PCS, GR) was studied using Bio-Rad, MJ Miniopticon Real time PCR Detection system (Fig 2.9 B). The Primers (oligonucleotides, Table 2.10) were procured from Pharmads and Equipments Pvt. Ltd. Reaction was followed in 25 µl total volume using the protocol given with the Bio-Rad kit (SsoAdvanced SYBR Green Supermix, Cat no: 172-5260). 5 µl of cDNA prepared in the above step, 2 µl of primer, 12.5 µl of 2X master mix and 5.5 µl of sterile water was added in optically flat capped white PCR tubes. Amplification was carried out for 40 cycles. Data was analyzed using Bio-Rad CFX manager software.

2.10. Statistical analysis

The data shown corresponds to the mean values \pm standard deviation (SD). One-way analysis of variance (ANOVA) and Duncan's multiple range test by using Microsoft Excel XLSTAT (version 2015.2.01.17315) were performed to confirm the variability of the results and the determination of significant ($P \leq 0.05$) difference between treatment groups, respectively.

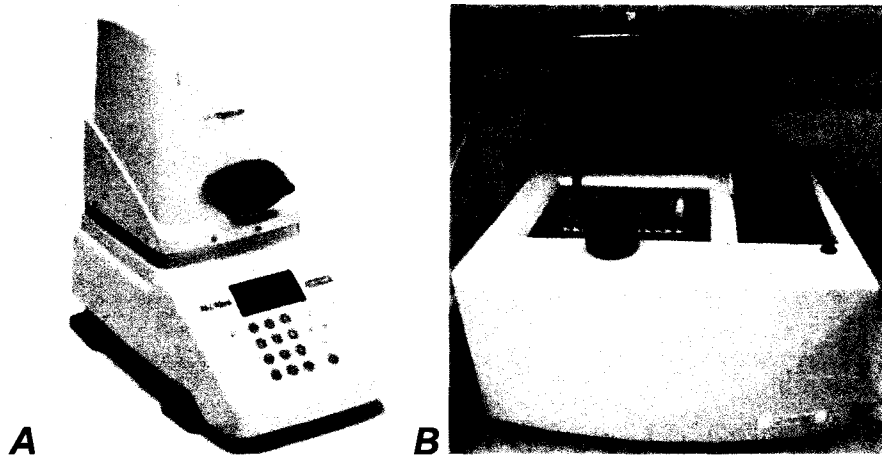


Fig 2.9. Real time PCR, BioRad, MJ Mini Opticon (A), PCR Corbett Research, Gradient Palm Cycler (B).

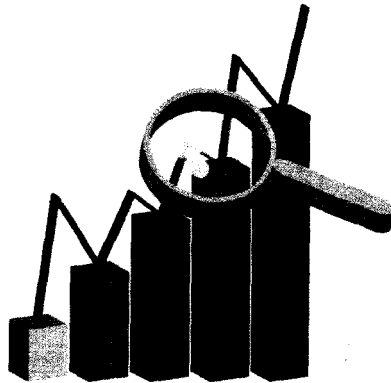
Table 2.9. List of anti-oxidant primers (Reverse and Forward) used to study gene expression by real time analysis procured from Pharmaids and Equipments Pvt. Ltd. Here APX= Ascorbate peroxidase of thylakoid, SOD= Superoxide dismutase, GR= Glutathione reductase and PCS= Phyto-chelatin synthase.

Primer name	Oligo Number	Sequence
APX	91211B3-1255C12 17/44	APX-Thy-L 5'- GCT AAA CTG AGC GAC CTT GG -3'
	91211B3-1255D12 18/44	APX-Thy-R 5'- GCT GCT CCT ACC GTT ACT GG -3'
SOD	30121B3-9644D10 5/32	SOD-F 5'-CGT CGA TCT CCC ATC ATT TT-3'
	30121B3-9644E10 6/32	SOD-R 5'-CTT GTT CCG TTT TGT GTG GA-3'
GR	30121B3-9644F10 7/32	GR- F 5'- TGA GGA GGT CAG GGA TTT TG -3'
	30121B3-9644G10 8/32	GR- R 5'- GCA TGG TGC TAT TGT GGT TG- 3'
PCS	30121B3-9644H09 1/32	PC-F 5'- CGA AGA TTC CAT TTC CCA GA -3'
	30121B3-9644A10 2/32	PC-R 5'- GCT TTC ACC GAT ATC CTC GA -3'

CHAPTER

3

RESULTS



*Learn from yesterday, live for today, hope for tomorrow.
The important thing is not to stop questioning.*

-----**Albert Einstein**

RESULTS

TABLE OF CONTENTS

Sr. No	Title of the topic	Page no
3.1	Nanoparticle size determination	72
3.2	Release of ions from metallo-NPs and its bulk counterparts	74
3.3	Seed Germination, External and Internal Morphological Changes	76
3.4	Translocation of Nanoparticles within rice roots and leaves	83
3.4.1	Atomic Absorption Spectroscopy	83
3.4.2	Transmission Electron Microscopy	90
3.5	Carbon dioxide fixation studies using Infrared gas analyser (IRGA)	92
3.6	Effect of MNPs on light reactions of photosynthesis (Chlorophyll Fluorescence measurements)	95
3.7	Changes in the photosynthetic pigment content upon MNP exposure	97
3.8	Effect of MNPs on oxidative damage	108
3.8.1.	Lipid peroxidation	108
3.8.2	Protein oxidation	108
3.8.3	Proline assay	108
3.9	Assay of enzymatic and non-enzymatic antioxidants	112
3.9.1	Ascorbate assay and Superoxide dismutase (SOD) activity	112
3.9.2	Polyamines (spermine, spermidine) content	112
3.10	Gene expression studies of antioxidant enzymes (SOD, APX, GR) and metal chelating enzyme Phytochelatin synthase (PC) by Real Time-PCR	115
3.11	Effect of bulk metals in comparison to MNPs on the morphological, physiological and biochemical processes in <i>O. sativa</i> .	118
3.12	Summary of Results	127

The influence of Copper (II) Oxide (50 nm), Zinc Oxide (<50 and 100 nm) NPs and bulk CuSO_4 and ZnSO_4 on the morphological, physiological, biochemical and molecular processes in *Oryza sativa* was individually investigated. The results are presented individually and as a comparative account of CuO and ZnO NPs as well as two different sizes of ZnO NPs. The study also compares the effect of MNPs vis-a-vis Cu and Zn bulk metals in hydroponically grown *O. sativa* plants. This study also focusses on the release of ions from both metallo-nanoparticles and bulk metals (CuSO_4 and ZnSO_4) in Hoagland's nutrient solution, to elucidate the difference in mechanism of damage to *O. sativa* plants under NP and bulk metal stress.

3.1. Nanoparticle Size Determination

The Copper (II) Oxide and Zinc Oxide NPs were characterized using the scanning electron microscope (SEM). The shape of CuO NPs was observed to be spherical (Fig 3.1 A) and ZnO NP (<50 nm and <100 nm) was found to be non-spherical (Fig 3.1 B, C). SEM data of MNPs obtained were in accordance to the specifications mentioned by the suppliers. The particle size was also determined using X-ray diffractometer and the size of commercially obtained CuO NP (Sigma-Aldrich; <50 nm) was experimentally found to be 50 ± 2 nm (Fig 3.1 A). Also, the particle size of ZnO NP of <50 nm size (Sigma-Aldrich, India) and <100 nm size (Sigma-Aldrich, India) was found to be 35 ± 2 nm and 100 ± 2 nm respectively (Fig 3.1 B, C).

The behavior, size and interaction of MNP with media in Hoagland's solution, was also studied using dynamic light scattering (DLS) analyzer. It was observed that CuO, ZnO (50 nm) and ZnO (100 nm) NPs showed a diameter of 278.4 ± 31 nm, 112.6 ± 40 nm and 168 ± 50 nm in Hoagland's solution respectively.

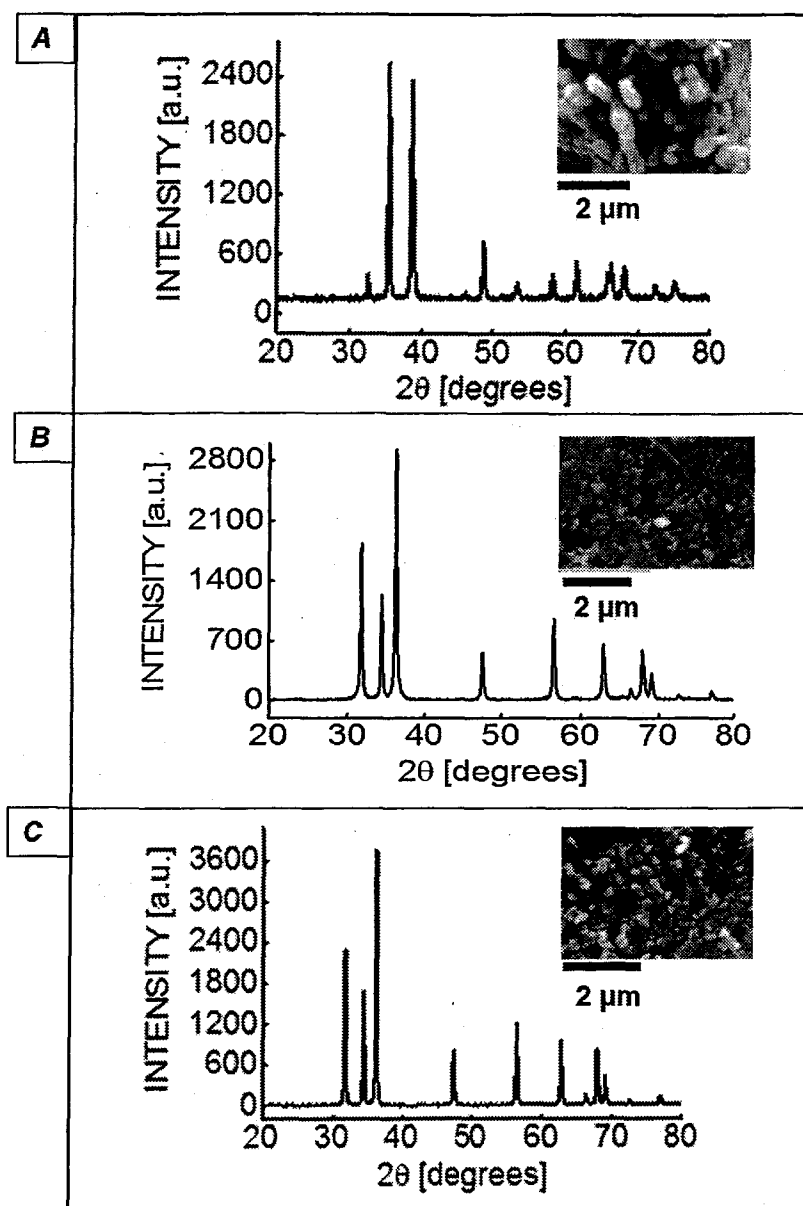


Fig 3.1. Scanning electron microscope images (30,000 X) and X-ray Diffractometer (Rigaku, Japan) pattern taken at room temperature in the range $2\theta=20^{\circ}$ - 80° with a step of 0.02° and a speed= $2^{\circ}/\text{min}$ using Cu $k\alpha$ radiation ($\lambda=0.15406$ nm) to determine the size and shape of MNPs. X-ray diffraction pattern of CuO NPs showing spherical shape and size of <50 nm size (A), X-ray diffraction pattern of ZnO <50 nm showing non-spherical shape and <50 nm size (B), X-ray diffraction pattern of ZnO <100 nm showing non-spherical shape and size of 100 nm (C).

3.2. Release of Ions from Metallo-NPs and its Bulk Counterparts

The release of metal ions from metallo-NPs (CuO and ZnO NP) and bulk metals (CuSO₄, ZnSO₄), in both water and Hoagland's nutrient solution was measured (Table 3.2 A). Dissolution of metallo-NPs in Hoagland's solution increased with increase in MNP concentration compared to control, however, the ions released from MNPs were far less than the ions released from its bulk counterparts. It was observed that 1000 mg L⁻¹ of CuO NPs released 1.16 ± 0.090 mg L⁻¹ of Cu ions in Hoagland's solution as compared to its control, whereas, ZnO NPs of 100 nm size released 12.06 ± 0.05 mg L⁻¹ of Zn ions at the same concentration (Table 3.2 A). Also, ZnO NPs of <50 nm size at 1000 mg L⁻¹ released 6.638 ± 0.37 mg L⁻¹ of Zn ions in Hoagland's solution. This indicated that larger sized ZnO NPs (100 nm) released 55% more ions compared to smaller sized ZnO NPs (50 nm) at 1000 mg L⁻¹. The result also shows that there was a much greater release of ions from bulk metals than MNPs (Table 3.2 A). It was observed that bulk Cu at 1000 mg L⁻¹, released 70-fold (80.76 ± 2.56 mg L⁻¹) more Cu ions than CuO NPs (1.16 ± 0.090 mg L⁻¹), whereas, bulk Zn released 19-fold (230.3 ± 0.07 mg L⁻¹) more Zn ions than ZnO NPs of 100 nm size (12.06 ± 0.05 mg L⁻¹) and 35-fold more ions than ZnO NP of <50 nm size (6.638 ± 0.37 mg L⁻¹) at the same concentration.

When data was seen in terms of percent ions released with respect to amount of MNPs as well as bulk metals, it was observed that with increase in the amount of MNPs, the amount of ions released was relatively less in Hoagland's solution (Table 3.2 B). It was seen that 100 mg of CuO NPs released 0.37% of Cu ions whereas 1000 mg of CuO NPs resulted in a release of 0.12% Cu ions. In case of ZnO NPs, 100 and 1000 mg of ZnO NPs of <50 nm size released 3.33% and 0.66% Zn ions respectively. Similarly, 100 mg of 100 nm sized ZnO NPs released 9% of Zn ions whereas 1000 mg of ZnO NPs released only 1.2% of Zn

Table 3.2. Amount of ions released from MNP and its bulk counterpart in water and Hoagland's solution (A) and percent ions released from MNPs and bulk metals at 100 and 1000 mg L⁻¹ weight bases (B). Data represent mean values ± SD (n=3). Means in the column followed by the *same letter* indicate insignificant differences at p≤0.05.

A	MNP / Bulk (mg L ⁻¹)	Cu ²⁺ ion released (mg L ⁻¹)				Zn ²⁺ ion released (mg L ⁻¹)					
		CuO NP (50 nm)		Bulk Cu		ZnO NP (100 nm)		ZnO NP (<50 nm)		Bulk Zn	
		Water	Hoagland's solution	Water	Hoagland's solution	Water	Hoagland's solution	Water	Hoagland's solution	Water	Hoagland's solution
	0	0.012 ± 0.001 ^e	0.015 ± 0.001 ^c	0.012 ± 0.001 ^f	0.015 ± 0.001 ^f	0.231 ± 0.05 ^e	0.052 ± 0.05 ^f	0.231 ± 0.03 ^c	0.052 ± 0.05 ^e	0.231 ± 0.05 ^e	0.052 ± 0.05 ^f
	2.5	0.01 ± 0.001 ^e	0.06 ± 0.010 ^d	0.19 ± 0.001 ^e	0.21 ± 0.002 ^e	0.899 ± 0.001 ^d	1.266 ± 0.02 ^e	0.510 ± 0.06 ^b	0.701 ± 0.81 ^d	0.51 ± 0.05 ^e	0.55 ± 0.001 ^e
	10	0.02 ± 0.001 ^d	0.05 ± 0.012 ^d	0.78 ± 0.050 ^d	0.79 ± 0.044 ^d	5.03 ± 0.02 ^c	1.329 ± 0.02 ^d	5.119 ± 0.09 ^a	2.070 ± 2.35 ^e	2.09 ± 0.02 ^d	2.2 ± 0.001 ^d
	50	0.06 ± 0.01 ^c	0.14 ± 0.009 ^c	4.02 ± 0.388 ^c	4.04 ± 0.480 ^c	9.814 ± 0.01 ^b	2.102 ± 0.01 ^c	4.764 ± 0.09 ^a	2.730 ± 0.86 ^c	10.23 ± 0.05 ^c	10.2 ± 0.02 ^c
	100	5.06 ± 0.48 ^b	0.37 ± 0.015 ^b	8.23 ± 0.557 ^b	8.63 ± 0.667 ^b	8.133 ± 1.70 ^b	8.951 ± 0.03 ^b	4.964 ± 0.58 ^a	3.330 ± 0.93 ^b	19.04 ± 0.04 ^b	21.0 ± 0.01 ^b
	1000	6.26 ± 0.59 ^a	1.16 ± 0.090 ^a	77.88 ± 1.19 ^a	80.76 ± 2.56 ^a	12.97 ± 0.02 ^a	12.06 ± 0.05 ^a	4.547 ± 1.09 ^a	6.638 ± 0.37 ^a	229.6 ± 1.45 ^a	230.3 ± 0.07 ^a
Ions released on weight bases (%) = ions released /weight of MNP or bulk metals x 100 (in Hoagland's solution only)											
B	MNP/ Bulk (mg L ⁻¹)	CuO NP		Bulk Cu		ZnO NP (100 nm)		ZnO NP (50 nm)		Bulk Zn	
		Ions released	%	Ions released	%	Ions released	%	Ions released	%	Ions released	%
		Weight									
	100	0.37 ± 0.015	0.37	8.63 ± 0.667	8.6	8.951 ± 0.03	9	3.330 ± 0.93	3.33	21.0 ± 0.01	21
	1000	1.16 ± 0.090	0.12	80.76 ± 2.560	8.1	12.06 ± 0.05	1.2	6.638 ± 0.37 ^a	0.66	230.3 ± 0.07	23.03

ions (Table 3.2 B). However, both bulk Cu and Zn did not show this (Table 3.2 B). In case of bulk metals, the percent release of Cu and Zn ions with respect to amount of CuSO₄ and ZnSO₄ respectively remained more or less constant (Table 3.2 B).

3.3. Seed Germination, External and Internal Morphological Changes

The germination rate, shoot and root length and biomass was manually measured for each set of plants exposed to CuO and ZnO NPs ($n=5$). Mean and standard deviation from different treatments was analysed using ANOVA and Duncan's post hoc test. On treatment with low concentrations of CuO NPs (2.5-50 mg L⁻¹), the germination rate remained unaffected compared to control, however, at higher concentrations, (100-1000 mg L⁻¹) of CuO NPs a decrease of approximately 7% was observed (Table 3.3.1), whereas on treatment with both sizes (<50 and 100 nm) of ZnO NPs, the germination rate was unaffected at all concentrations (0-1000 mg L⁻¹) compared to control (Table 3.3.2 & 3).

The shoot and root length of *O. sativa* plants treated with 0-1000 mg L⁻¹ of MNPs was measured after 6 d of growth. At 2.5- 50 mg L⁻¹ of CuO NPs, the shoot length was not different from control; however, at 100 and 1000 mg L⁻¹, a significant decrease by 27% and 31% was observed respectively (Table 3.3.1). Similarly, on exposure to 2.5- 50 mg L⁻¹ of ZnO NPs of <50 nm size, slight change in shoot length was observed, but a significant decrease by 10% and 20% in shoot length was observed at 100 and 1000 mg L⁻¹ respectively (Table 3.3.2). ZnO NP of 100 nm size also resulted in decreased shoot length by 7% and 31% at 100 and 1000 mg L⁻¹ respectively. The root length of MNP treated plants was similar to control up to 100 mg L⁻¹, however, further increase in concentration to 1000 mg L⁻¹ of CuO and ZnO (<50 and 100 nm) NPs resulted in root length reduction by 23%, 42% and 25% respectively (Table 3.3.1- 3). The decrease in shoot and root length observed after 30 d of CuO (Fig 3.3.1 B) and ZnO (Fig 3.3.2 B, D) NP was comparable to

Table 3.3.1. Percent germination, shoot, root length (6 d old plants) and biomass (30 d old plants) of *Oryza sativa* var. Jyoti grown at different concentrations of CuO NPs. SFM=shoot fresh mass; SDM=shoot dry mass; RFM=root fresh mass; RDM=root dry mass. Data represent mean values \pm SD ($n=5$). Means in the column followed by the *same letter* indicate insignificant differences at $p \leq 0.05$.

CuO NPs (mg L ⁻¹)	Percent Germination (%)	Shoot length (mm)	Root length (mm)	Biomass (g)			
				SFM	SDM	RFM	RDM
Control (0)	96.0 \pm 3.97 ^a	35.2 \pm 6.3 ^{ab}	48.4 \pm 6.3 ^a	0.64 \pm 0.01 ^a	0.087 \pm 0.05 ^b	0.192 \pm 0.02 ^c	0.025 \pm 0.01 ^a
2.5	94.7 \pm 3.10 ^{ab}	31.0 \pm 1.2 ^{bc}	45.8 \pm 5.9 ^a	0.64 \pm 0.02 ^a	0.092 \pm 0.03 ^a	0.193 \pm 0.03 ^c	0.021 \pm 0.02 ^e
10	90.1 \pm 1.86 ^{bc}	27.8 \pm 1.6 ^{cd}	43.8 \pm 6.8 ^{ab}	0.63 \pm 0.02 ^a	0.087 \pm 0.02 ^b	0.205 \pm 0.02 ^b	0.021 \pm 0.01 ^e
50	89.7 \pm 6.61 ^c	39.0 \pm 3.36 ^a	48.5 \pm 2.8 ^a	0.61 \pm 0.02 ^a	0.078 \pm 0.01 ^c	0.188 \pm 0.02 ^d	0.023 \pm 0.01 ^c
100	89.2 \pm 4.53 ^c	25.7 \pm 3.4 ^d	42.2 \pm 3.5 ^{ab}	0.43 \pm 0.01 ^b	0.071 \pm 0.03 ^e	0.180 \pm 0.02 ^e	0.024 \pm 0.01 ^b
1000	88.7 \pm 4.82 ^c	24.3 \pm 3.1 ^d	37.2 \pm 4.3 ^b	0.44 \pm 0.05 ^b	0.075 \pm 0.02 ^d	0.209 \pm 0.01 ^a	0.021 \pm 0.01 ^d

Table 3.3.2. Percent germination, shoot, root length (6 d old plants) and biomass (30 d old plants) of *Oryza sativa* var. Jyoti grown at different concentrations of ZnO (<50 nm) NPs. SFM=shoot fresh mass; SDM=shoot dry mass; RFM=root fresh mass; RDM=root dry mass. Data represent mean values \pm SD ($n=5$). Means in the column followed by the same letter indicate insignificant differences at $p \leq 0.05$.

ZnO (<50 nm) NPs (mg L ⁻¹)	Percent Germination (%G)	Shoot length (mm)	Root length (mm)	Biomass (g)			
				SFM	SDM	RFM	RDM
Control (0)	90.5 \pm 4.5 ^a	29.0 \pm 1.9 ^a	47.9 \pm 3.1 ^a	0.647 \pm 0.05 ^a	0.082 \pm 0.002 ^a	0.250 \pm 0.11 ^b	0.022 \pm 0.007 ^b
2.5	91.4 \pm 5.9 ^a	27.7 \pm 3.3 ^b	46.9 \pm 6.9 ^a	0.588 \pm 0.01 ^a	0.074 \pm 0.003 ^b	0.263 \pm 0.11 ^{ab}	0.018 \pm 0.001 ^b
10	90.3 \pm 7.3 ^a	29.1 \pm 2.9 ^{ab}	46.5 \pm 3.9 ^a	0.562 \pm 0.08 ^a	0.072 \pm 0.004 ^b	0.258 \pm 0.11 ^{ab}	0.023 \pm 0.007 ^b
50	89.4 \pm 7.6 ^a	27.0 \pm 1.1 ^{ab}	41.0 \pm 3.7 ^{ab}	0.426 \pm 0.02 ^c	0.064 \pm 0.001 ^b	0.245 \pm 0.09 ^b	0.026 \pm 0.005 ^b
100	91.3 \pm 5.3 ^a	26.1 \pm 3.4 ^b	38.8 \pm 4.7 ^b	0.497 \pm 0.02 ^b	0.070 \pm 0.002 ^b	0.200 \pm 0.06 ^b	0.024 \pm 0.004 ^b
1000	88.6 \pm 8.5 ^a	23.2 \pm 4.6 ^c	27.7 \pm 3.5 ^c	0.423 \pm 0.03 ^c	0.066 \pm 0.006 ^b	0.242 \pm 0.01 ^b	0.021 \pm 0.006 ^b

Table 3.3.3. Percent germination, shoot, root length (6 d old plants) and biomass (30 d old plants) of *Oryza sativa* var. Jyoti grown at different concentrations of ZnO (100 nm) NPs. SFM=shoot fresh mass; SDM=shoot dry mass; RFM=root fresh mass; RDM=root dry mass. Data represent mean values \pm SD ($n=5$). Means in the column followed by the *same letter* indicate insignificant differences at $p \leq 0.05$.

ZnO (100 nm) NPs (mg L ⁻¹)	Percent Germination (%G)	Shoot length (mm)	Root length (mm)	Biomass (g)			
				SFM	SDM	RFM	RDM
Control (0)	94.4 \pm 1.7 ^{ab}	23.6 \pm 4.2 ^{ab}	38.4 \pm 7.5 ^a	0.63 \pm 0.03 ^a	0.085 \pm 0.001 ^a	0.194 \pm 0.002 ^b	0.023 \pm 0.001 ^b
2.5	95.8 \pm 1.3 ^a	22.9 \pm 2.9 ^{ab}	37.3 \pm 9.2 ^a	0.618 \pm 0.04 ^a	0.086 \pm 0.008 ^a	0.24 \pm 0.07 ^a	0.022 \pm 0.002 ^b
10	94.8 \pm 1.9 ^{ab}	24.3 \pm 3.4 ^a	39.5 \pm 5.3 ^a	0.56 \pm 0.09 ^a	0.077 \pm 0.008 ^b	0.23 \pm 0.03 ^{ab}	0.021 \pm 0.001 ^b
50	93.3 \pm 3.5 ^{ab}	25.0 \pm 3.01 ^a	41.0 \pm 4.2 ^a	0.42 \pm 0.01 ^b	0.073 \pm 0.013 ^c	0.207 \pm 0.01 ^{ab}	0.022 \pm 0.002 ^b
100	95.5 \pm 2.6 ^a	21.9 \pm 2.64 ^b	35.4 \pm 7.5 ^a	0.43 \pm 0.02 ^b	0.070 \pm 0.002 ^b	0.19 \pm 0.02 ^b	0.023 \pm 0.003 ^b
1000	92.3 \pm 4.1 ^b	16.4 \pm 1.54 ^c	29.0 \pm 5.3 ^b	0.45 \pm 0.02 ^b	0.070 \pm 0.006 ^b	0.22 \pm 0.009 ^{ab}	0.027 \pm 0.005 ^b

the decline seen after 6 d (Fig 3.3.1 A, Fig 3.3.2 A & C) of plant growth respectively. It was also observed that older plants showed no phenotypic changes up to 50 mg L⁻¹ of CuO NPs but higher concentration (100 and 1000 mg L⁻¹) of the NP resulted in leaf chlorosis and leaf tip necrosis of plants (Fig 3.3.1). ZnO NPs of both sizes higher than 10 mg L⁻¹ concentration resulted in similar phenotypical changes (Fig 3.3.2). The results show that onset of phenotypic damage in *O. sativa* plants was caused at high concentrations (50 mg L⁻¹ and above) by both sizes of ZnO NPs and at very high concentrations (100-1000 mg L⁻¹) of CuO NPs.

Shoot biomass, on fresh mass basis (SFM), was unaffected up to 50 mg L⁻¹ of CuO NP but decreased by 34% and 31% at concentrations of 100 and 1000 mg L⁻¹ respectively. However, on dry mass basis (SDM), the shoot biomass showed a slight increase (6%) at low concentration (2.5 mg L⁻¹) and subsequent decrease at higher concentration of CuO NP (Table 3.3.1).

In case of plants exposed to 1000 mg L⁻¹ of ZnO NP, it was seen that SFM decreased by 35% with <50 nm sized ZnO and 29% with 100 nm sized ZnO NP compared to control, whereas, decrease in the SDM was more or less same \approx 18% at 1000 mg L⁻¹ concentration for plants grown with both sizes of the nanoparticles (Table 3.3.2 & 3).

The root fresh biomass (RFM) remained unchanged at 2.5 mg L⁻¹ of CuO NPs, followed by an increase in the RFM by 9% at 1000 mg L⁻¹, whereas root dry biomass (RDM) decreased due to the treatment as compared to control (Table 3.3.1). In case of ZnO NPs, root biomass both RFM and RDM was unaffected with both sizes (<50 & 100 nm) of NPs (Table 3.3.2 & 3).

The effect of CuO and ZnO NPs on trichomes, stomata and root surface was studied at 0 (control), 10 and 1000 mg L⁻¹ using scanning electron microscope (SEM). The leaves treated with both MNPs showed an increase in the number and size of trichomes as well as

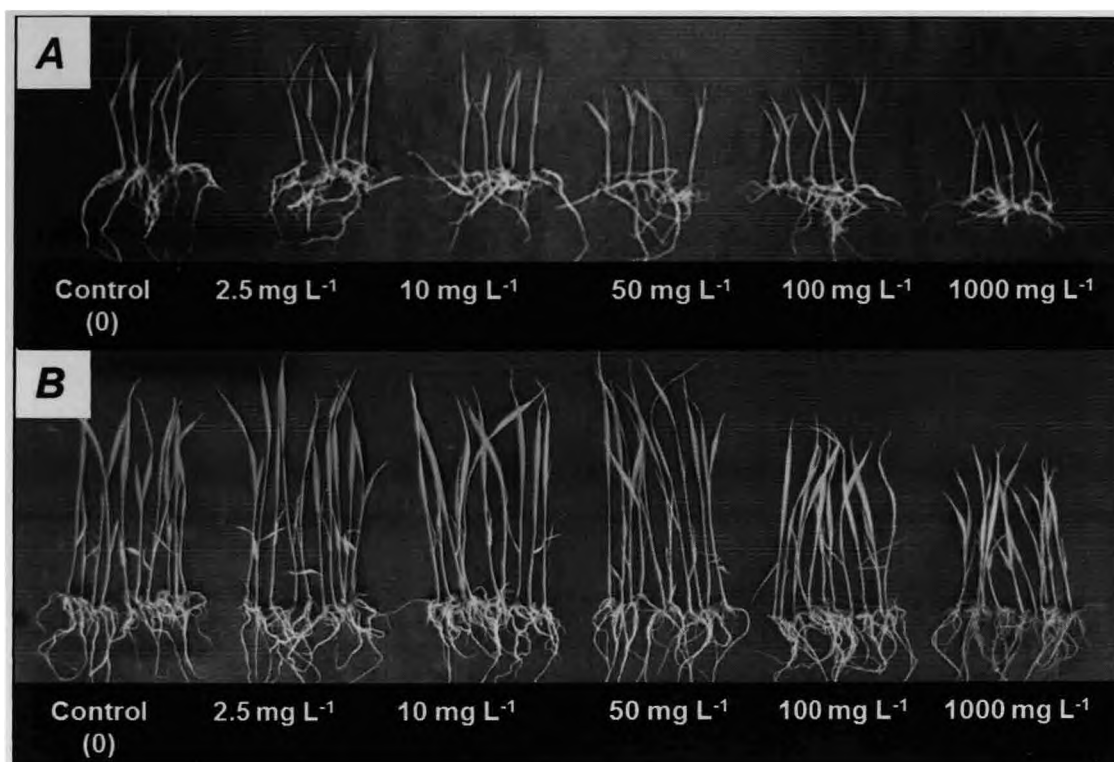


Fig 3.3.1. Pictorial diagram showing shoot and root length in 6 d (A) and 30 d (B) old rice seedlings treated with CuO NPs grown in a hydroponic culture system.

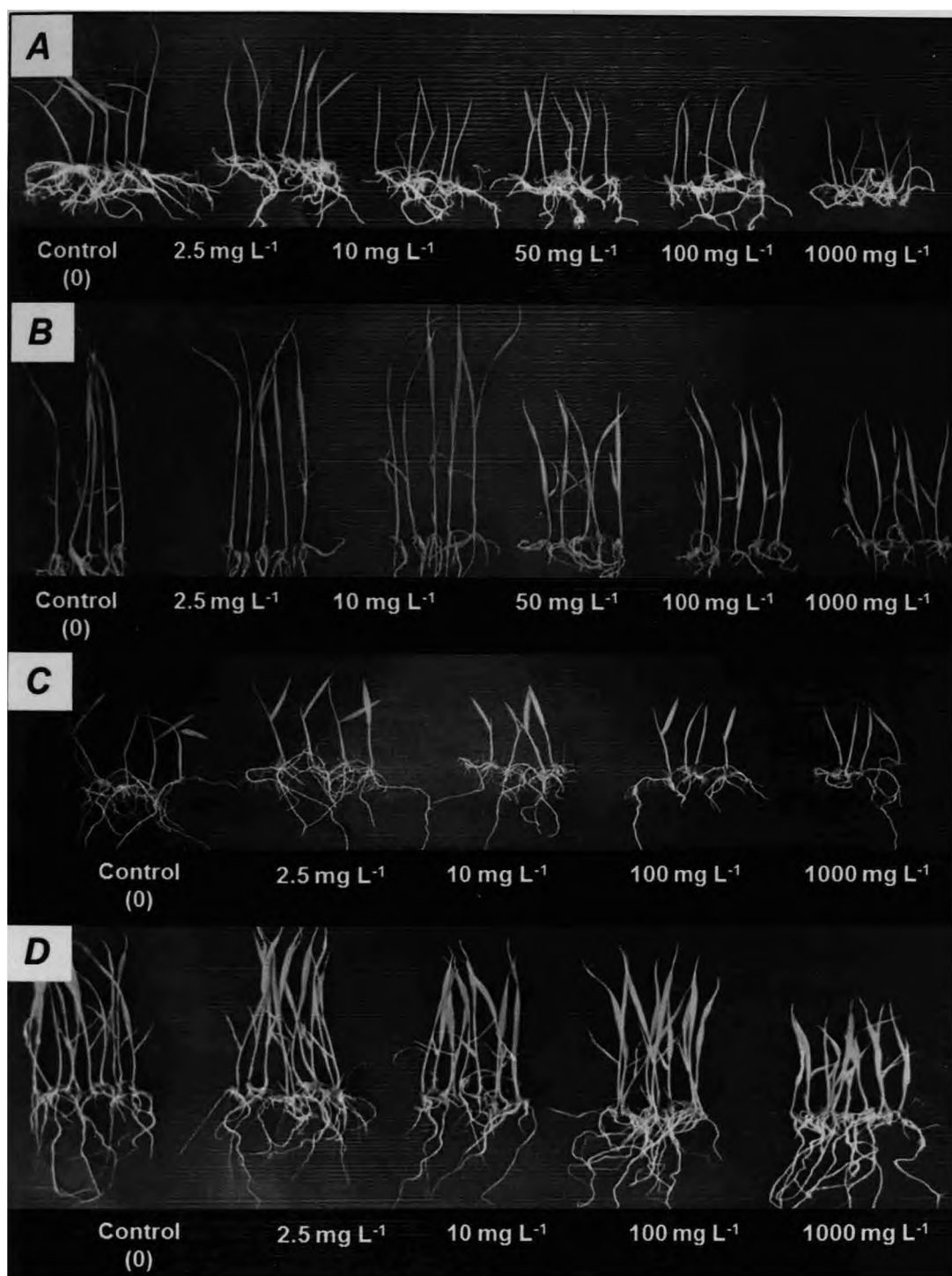


Fig 3.3.2. Pictorial diagram showing shoot and root length in 6 d (A, C) and 30 d (B, D) old rice seedlings treated with ZnO NPs of size < 50 nm (A, B) and 100 nm (C, D) grown in a hydroponic culture system.

a decline in the number of stomata compared to control (Fig 3.3.3 & 4). The SEM images also revealed reduction in the opening of the stomata and thickness of small cuticular papillae (or small papillae; SP), nipple-like structures, on the leaf surface of plants treated with 10 and 1000 mg L⁻¹ of CuO (Fig 3.3.3) and ZnO (Fig 3.3.4) NPs compared to control. Figure 3.3.3 G-I showed damage to root surface at 1000 mg L⁻¹ with CuO and figure 3.3.4 G-I showed damage caused by ZnO NPs treatment. Similar results were obtained with < 50 nm sized ZnO NPs (data not shown).

The cross section of leaves and roots of *O. sativa* treated with CuO and ZnO (100 nm) NPs was studied using light microscope (LM) as well as transmission electron microscope (TEM). Few changes in the internal leaf morphology upon exposure to MNPs using LM were observed. Cross sections of leaf revealed that upon treatment with MNPs, an increase in the chloroplast number and size in the mesophyll cells was observed at 2.5 mg L⁻¹ of both CuO (Fig 3.3.5 B) and ZnO (Fig 3.3.5 H) NPs, however, at 1000 mg L⁻¹, a reduction in the number of chloroplasts with a decrease in the leaf thickness and larger vascular bundles (LV) were observed compared to control (Fig 3.3.5 F, L). Transverse sections of roots, showed no significant changes in the cell structure when treated with CuO (Fig 3.3.6 F-O) and ZnO NPs (Fig 3.3.6 f-o), however, an increase in the root hairs with CuO (Fig 3.3.6 E) and ZnO (Fig 3.3.6 e) NP treatment at 1000 mg L⁻¹ was observed.

3.4. Translocation of Nanoparticles within Rice Roots and Leaves

3.4.1. Atomic Absorption Spectroscopy

Copper content in whole leaf and leaf segments (apex, mid and basal) increased with increase in CuO NPs concentration (Table 3.4.1.1). No significant increase in Cu accumulation in apical, mid and basal parts of leaf up to 10 mg L⁻¹ treatment was observed, however, further increase in the CuO NP concentration resulted in a significant increase in

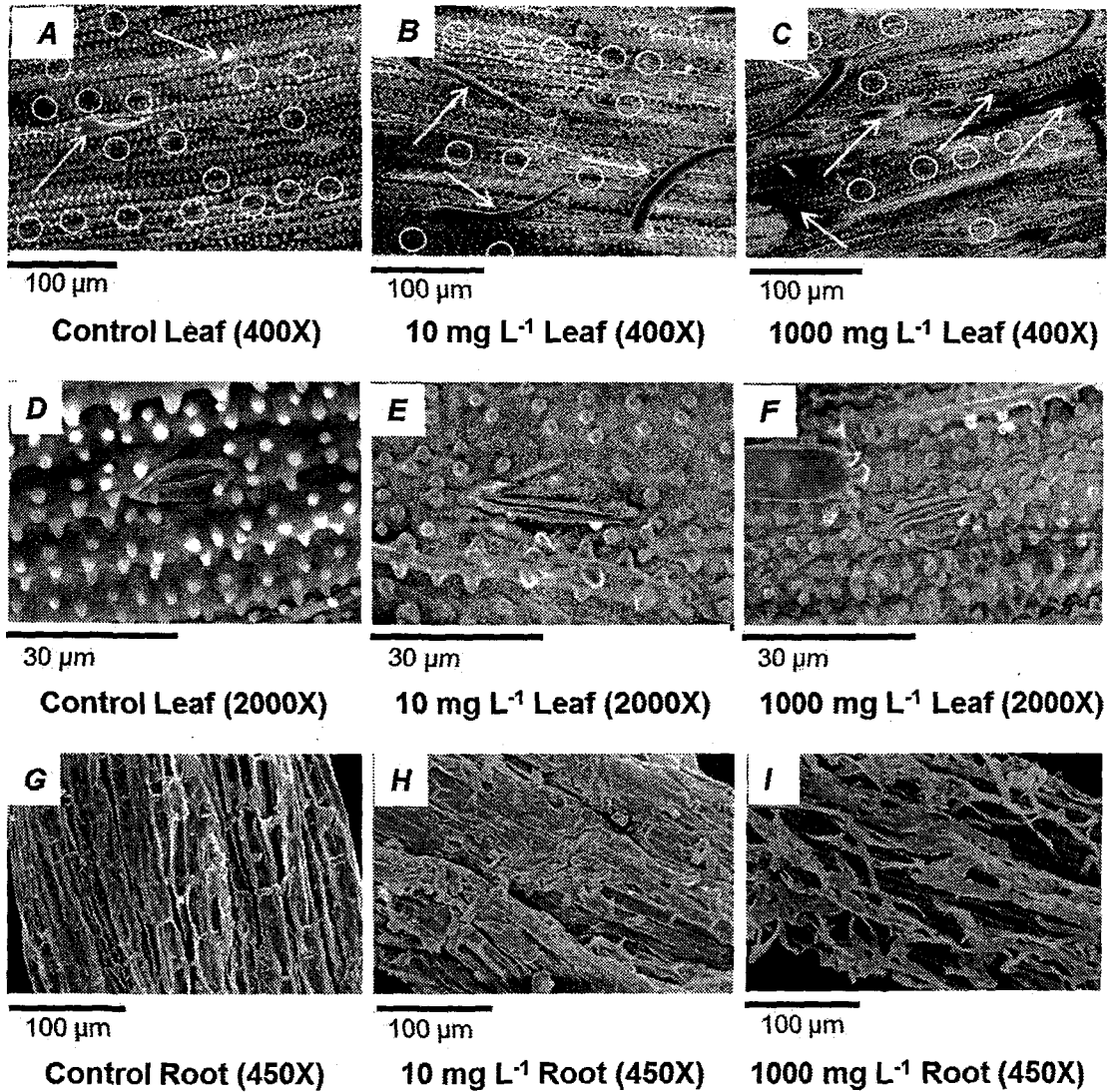


Fig 3.3.3. SEM images of leaf (adaxial) surface showing number and size of stomata and trichomes (A-C), size of stomata (D-F) and external morphology of roots (G-I) of plants treated with CuO NP for 30 d. The arrows indicate trichomes and the circles represent stomata.

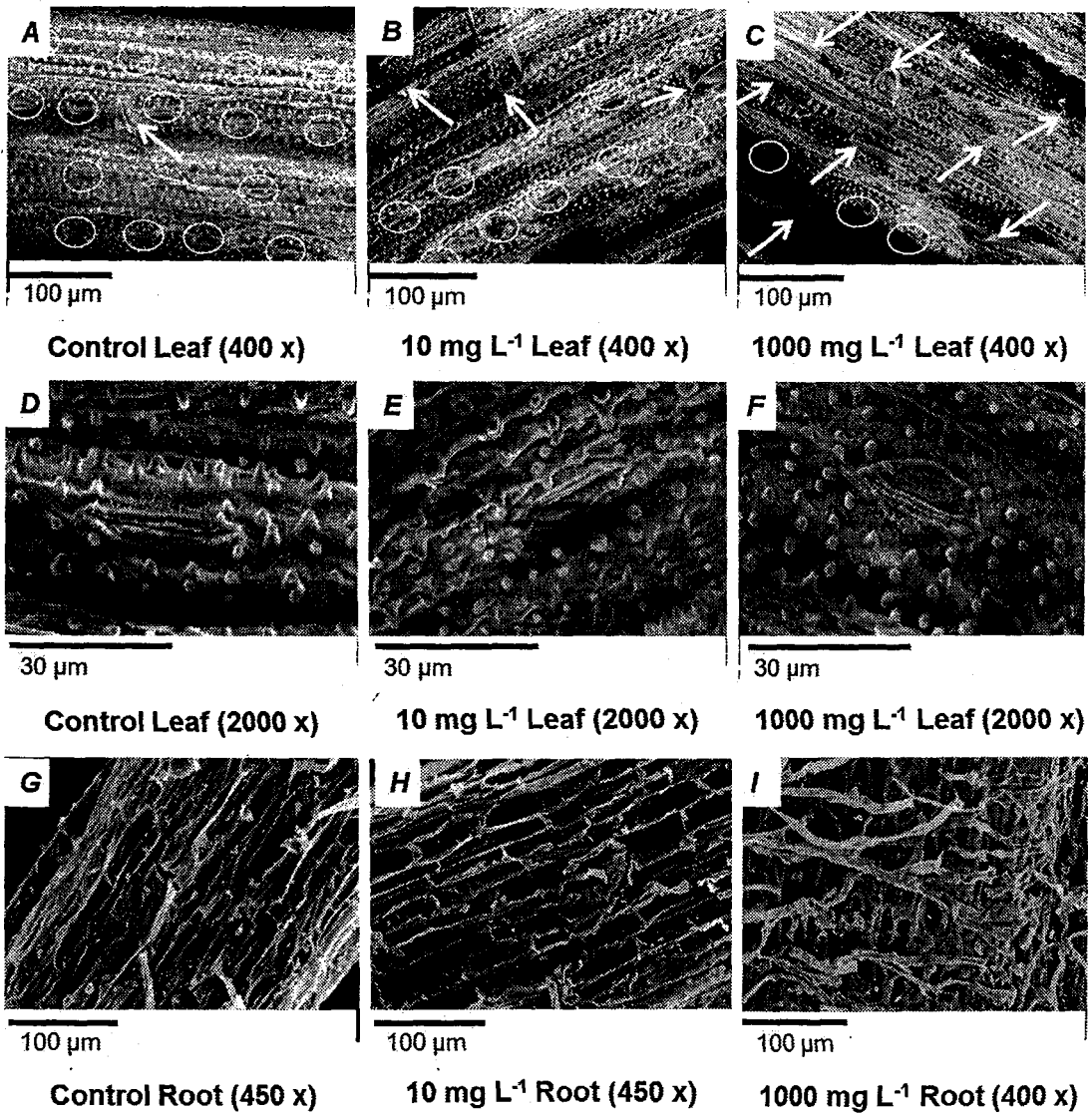


Fig 3.3.4. SEM images of leaf (adaxial) surface showing number and size of stomata and trichomes (A-C), size of stomata (D-F) and external morphology of roots (G-I) of plants treated with ZnO NP for 30 d. The arrows indicate trichomes and the circles represent stomata.

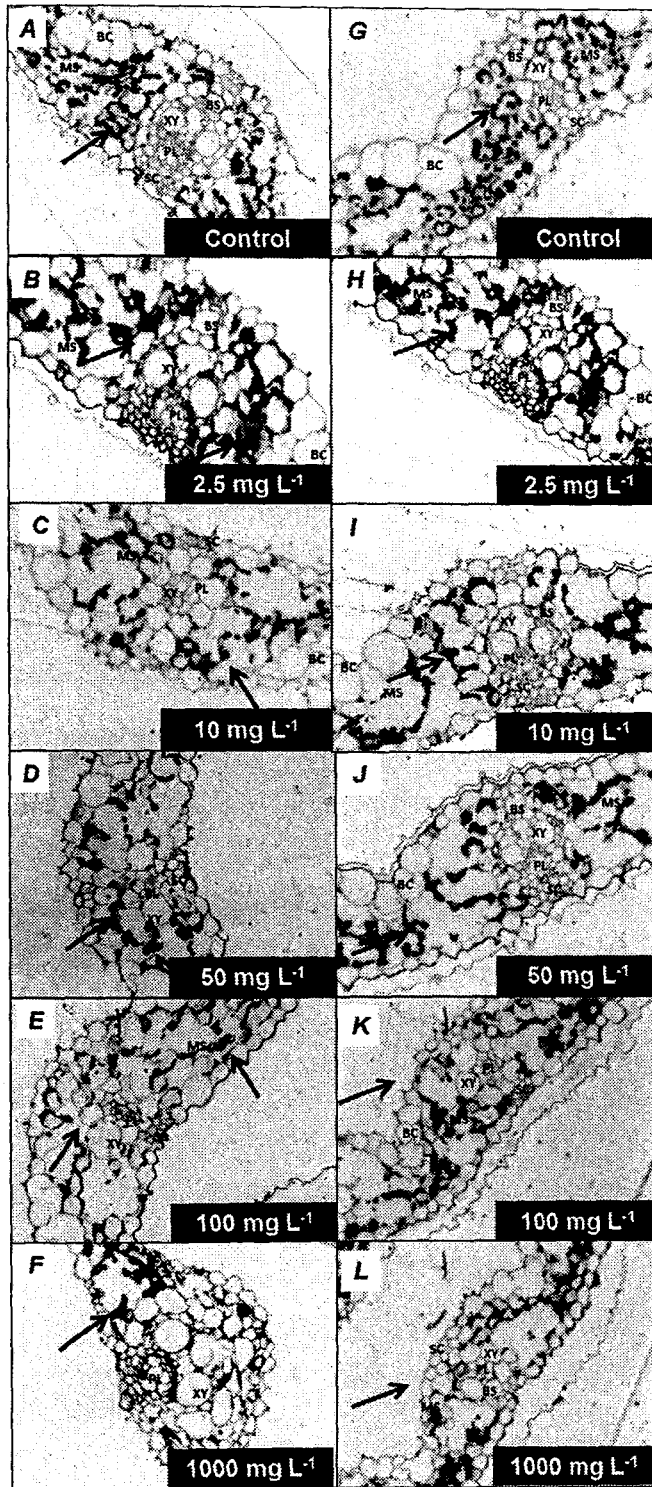


Fig 3.3.5. Cross section (40 X) of mature rice leaf treated with CuO (A-F) and ZnO (G-K) NPs at different concentrations after 30 d of growth. SC, sclerenchymatous cell; MS, Mesophyll layer; PL, phloem; XY, xylem; BS, bundle sheath cell; BC, bulliform cell.

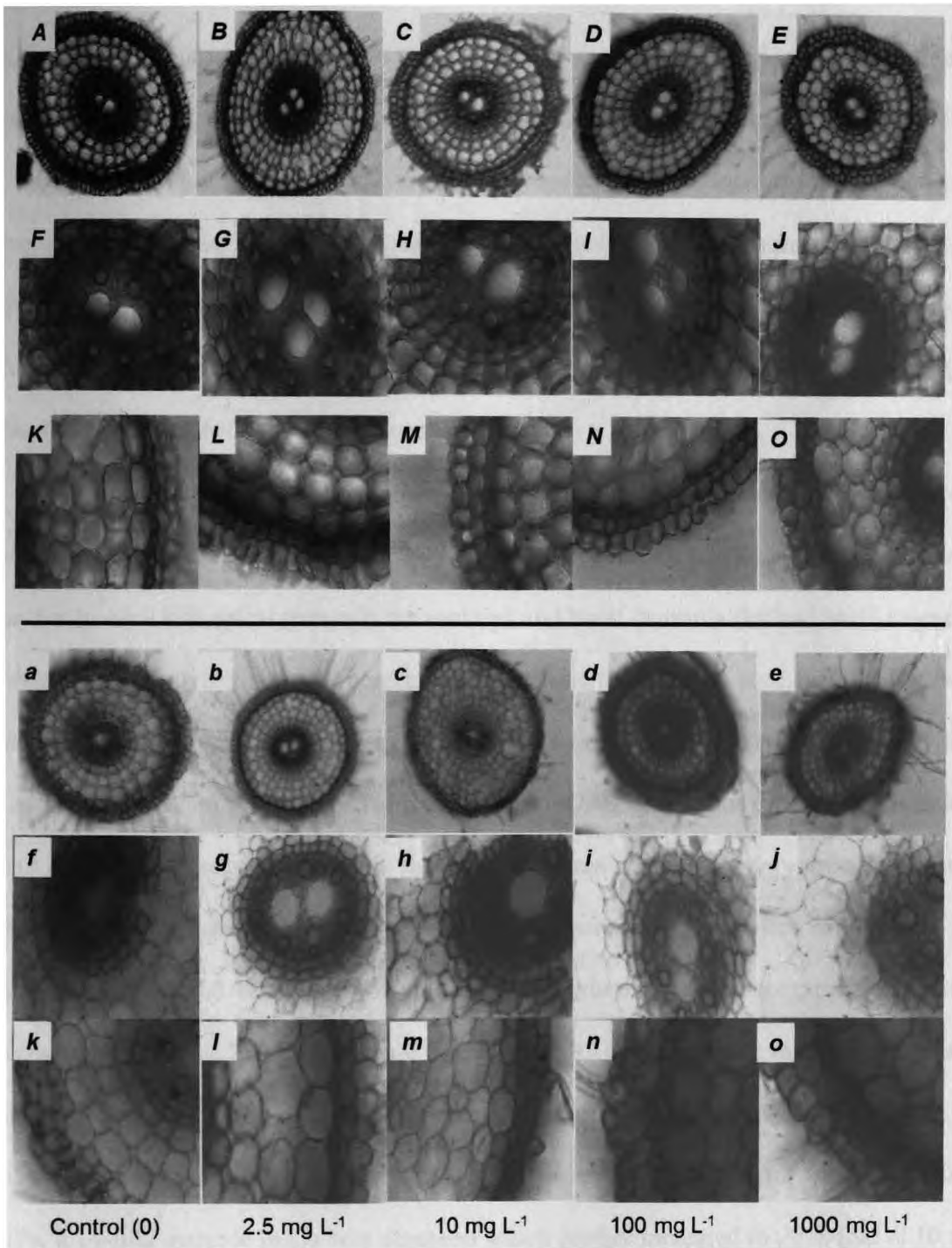


Fig 3.3.6. Cross section (40 X) of mature rice leaf treated with CuO (A-O) and ZnO (a-o) NPs at different concentrations [10 x magnification (A-E; a-e) and 40 x magnifications (F-O; f-o)].

Cu content. No specific pattern of accumulation was seen in apex, mid and basal segments of leaves as concentration of Cu was more or less same in these segments (Table 3.4.1.1). The whole leaf tissue analysed for Cu content revealed a gradual increase in Cu content in leaves with increase in CuO NP treatment. The analysis of Cu content in whole leaf showed a 71% increase in plants treated with 10 mg L⁻¹ concentration of CuO NPs which further increased to 113% (2-fold) in plants treated with 100 mg L⁻¹ and 453% (5.5-fold) in plants treated with 1000 mg L⁻¹ concentration.

Copper accumulation in roots was also analyzed by examining the primary and secondary roots independently (Table 3.4.1.1). The primary and secondary roots were further divided into apical (towards the root tip) and basal (towards the leaf base) segments which were analyzed for Cu content. Accumulation of Cu in root indicated greater accumulation of Cu in apical root tip area than the basal area. Furthermore, secondary root had a greater accumulation than the primary root. Also, apical root tip area of secondary root had a greater accumulation than the basal root area of the secondary root. It was seen that apical root tip area of primary root had 38-fold increase in Cu content compared to 20-fold increase in the basal area of primary root, whereas, apical root tip area of the secondary root had a 218-fold increase compared to 85.6-fold increase in basal root area at the highest concentration of CuO NP treatment as compared to control (Table 3.4.1.1). In whole roots, uptake of Cu also increased with increase in CuO NPs. At 2.5 mg L⁻¹ of CuO NPs, a 14-fold increase in Cu was observed which further increased to 27.7-fold at 10 mg L⁻¹, 37-fold at 50 mg L⁻¹ and 76-fold at 100 mg L⁻¹, however, at the highest concentration an increase of only 9.4-fold was observed compared to control (Table 3.4.1.1). On the other hand, the atomic absorption spectrophotometer analysis of rice plants treated with ZnO NPs (<50 and 100 nm) revealed that Zn content increased with increase in ZnO NPs in both leaf and root as a result of the treatment (Table 3.4.1.2). It was also seen that

Table 3.4.1.1. Cu content in leaf and root of *O. sativa* plants treated with CuO NPs at 0–1,000 mg L⁻¹ concentrations for 30 d. Data represent mean values ± SD (n=5). Means in the column followed by the *same letter* indicate insignificant differences at p≤0.05.

MNPs [mg L ⁻¹]	Cu content in Leaf [mg kg ⁻¹ DM]				Cu content in Root [mg kg ⁻¹ DM]				
	Apical	Mid	Basal	Whole leaf tissue	Primary root			Secondary root	
					Apical root tip area	Basal root area	Apical root tip area	Basal root area	Whole root tissue
0	3.44 ± 0.3 ^d	5.15 ± 0.15 ^c	4.50 ± 0.4b ^c	3.12 ± 0.14 ^d	26.19 ± 15.0 ^d	36.09 ± 5.9 ^f	14.58 ± 5.9 ^e	18.96 ± 10.2 ^e	20.21 ± 2.0 ^e
2.5	3.64 ± 0.1 ^d	3.42 ± 0.3 ^c	3.21 ± 1.4 ^c	5.0 ± 0.21 ^c	221.41 ± 18.5 ^d	135.68 ± 16.2 ^e	140.90 ± 4.9 ^e	109.19 ± 24.3 ^e	289.0 ± 10.2 ^d
10	3.57 ± 0.26 ^d	3.70 ± 0.3 ^c	3.49 ± 0.9 ^c	5.36 ± 0.32 ^c	689.06 ± 20.8 ^c	417.45 ± 19.6 ^d	868.24 ± 20.9 ^d	628.01 ± 15.2 ^d	559.9 ± 14.9 ^c
50	6.20 ± 0.6 ^c	5.45 ± 0.26 ^c	6.43 ± 0.1 ^b	5.9 ± 0.36 ^c	843.26 ± 31.9 ^b	462.17 ± 20.9 ^c	1308.70 ± 40.6 ^c	834.08 ± 20.1 ^c	753.2 ± 11.7 ^b
100	8.50 ± 0.45 ^b	8.27 ± 1.22 ^b	6.97 ± 0.1 ^b	6.65 ± 0.50 ^b	989.70 ± 50.2 ^a	603.71 ± 26.7 ^b	1710.16 ± 60.2 ^b	1165.00 ± 30.3 ^b	1544.1 ± 18.9
1000	14.11 ± 0.9 ^a	14.36 ± 3.3 ^a	21.30 ± 3.3 ^a	17.27 ± 1.45 ^a	989.47 ± 48.3 ^a	737.50 ± 21.2 ^a	3182.26 ± 62.3 ^a	1624.09 ± 40.2 ^a	190.14 ± 10.9

accumulation of Zn at all concentrations in root tissue was many fold higher than seen in shoot with both sizes of ZnO NPs. Moreover, plants grown with <50 nm size NP, showed relatively less accumulation of Zn in both root as well as in shoot tissue compared to plants grown with 100 nm size ZnO NPs (Table 3.4.1.2). Plants grown at 2.5 mg L⁻¹ concentration of ZnO NPs of <50 nm size showed an accumulation of 18% (1.2-fold) Zn in shoot tissue which increased further to 121.5% (2.2-fold) at 10 mg L⁻¹, 579% (6.8-fold) at 50 mg L⁻¹, 462% (5.6-fold) at 100 mg L⁻¹ and 962% (10.6-fold) at 1000 mg L⁻¹ compared to control. Zn content of roots also increased with increase in concentration of ZnO NPs of <50 nm size. At 2.5 mg L⁻¹ of ZnO NPs of <50 nm size an increase of 33.9% (1.3-fold) was observed which increased to 125.9% (2.25-fold) at 10 mg L⁻¹, 183% (2.8-fold) at 100 mg L⁻¹ and 81.3% (1.8-fold) at 1000 mg L⁻¹ concentration. In case of ZnO NPs of 100 nm size the Zn content of whole leaf tissue increased from 211% (3-fold) at 2.5 mg L⁻¹ to 447.6% (5.4-fold) at 50 mg L⁻¹ compared to control. At higher concentrations, the Zn content in leaf increased by 1030% (11-fold) at 100 mg L⁻¹ and by 1314% (14-fold) at 1000 mg L⁻¹. Similarly, the Zn content of whole root tissue treated with ZnO NPs of 100 nm size also increased as the NP concentration was increased. At 2.5 and 10 mg L⁻¹, an increase in Zn content by approximately 240% (3.4-fold) was observed which increased further to 3076% (38-fold) at 100 mg L⁻¹ and 5876% (60-fold) at 1000 mg L⁻¹ respectively.

3.4.2. Transmission Electron Microscopy

Internalization of CuO and ZnO NPs in *O. sativa* and changes in the morphology of leaf and root organelles was further studied using transmission electron microscope (TEM) at All India Institute of Medical Sciences (AIIMS), New Delhi. Variations in mesophyll cell structures such as decrease in the number of chloroplasts and increase in the number of mitochondria were observed in case of CuO (Fig 3.4.2.1 B) and ZnO (Fig 3.4.2.2 E, F) NP

Table 3.4.1.2. Zn content in *O. sativa* treated with ZnO NPs at 0–1000 mg L⁻¹ concentrations for 30 d. Data represent mean values ± SD (*n*=5). Means in the column followed by the *same letter* indicate insignificant differences at *p*≤0.05.

Conc. of ZnO NPs	Zn content (mg L ⁻¹)			
	ZnO NPs <50 nm		ZnO NPs 100 nm	
	Whole Leaf	Whole Root	Whole leaf	Whole root
0	16.7 ± 1.9 ^c	97.7 ± 6.6 ^c	21.00 ± 3.0 ^c	118.06 ± 1.94 ^c
2.5	19.8 ± 2.5 ^d	130.9 ± 9.9 ^d	65.51 ± 1.5 ^d	402.34 ± 0.89 ^d
10	37.0 ± 5.6 ^c	220.8 ± 8.9 ^b	110.03 ± 5.0 ^c	400.34 ± 1.8 ^d
50	113.4 ± 10.3 ^b	267.2 ± 11.2 ^a	115.0 ± 6.3 ^c	453.44 ± 10.9 ^c
100	93.9 ± 10.2 ^b	276.5 ± 10.2 ^a	237.45 ± 6.5 ^b	4494.02 ± 11.86 ^b
1000	177.4 ± 11.2 ^a	177.2 ± 10.9 ^c	297.10 ± 3.7 ^a	7055.89 ± 9.86 ^a

stress. Increase in number of chloroplast was observed at 2.5 mg L⁻¹ of CuO (Fig not shown) and ZnO NPs (Fig 3.4.2.2 B). Presence of starch granules were observed at 50 mg L⁻¹ of ZnO NPs (Fig 3.4.2.2 D) but not seen in case of CuO NPs. The bundle sheath cells however, were not visibly affected upon both CuO (Fig 3.4.2.1 C) and ZnO (Fig 3.4.2.2 C) NP exposure. TEM micrographs showed non-localised accumulation of CuO and ZnO NPs inside the leaf and root compared to control. Accumulation of CuO NPs occurred in the intercellular spaces and cytosol of leaves (Fig 3.4.2.1 D-F) and roots (Fig 3.4.2.1 J-L) in the form of aggregates or clusters at 1000 mg L⁻¹ (Fig 3.4.2.1 L). ZnO NPs also accumulated in the leaf (Fig 3.4.2.2 I) and root cells (Fig 3.4.2.2 J-L). Accumulation of NP in the leaf was especially observed in the chloroplasts resulting in decreased number of thylakoids per granum at higher than 50 mg L⁻¹ concentration of both CuO (Fig 3.4.2.1 G-I) and ZnO (Fig 3.4.2.2 G-I) NPs, and distortion (wavy arrangement) of the thylakoid membrane as well as swelling of the intra-thylakoidal space at highest concentration of CuO NPs treatment (Fig 3.4.2.1 I).

3.5. Carbon Dioxide Fixation Studies Using Infrared Gas Analyser (IRGA)

The photosynthetic rate (P_N), transpiration rate (E) and stomatal conductance (g_s) was measured using the Infra-red gas analyzer at different concentrations (0- 1000 mg L⁻¹) of CuO and ZnO (<50 and 100 nm) NPs after 30 d of growth (Fig 3.5). The plants grown with CuO NPs showed a gradual decrease in P_N , E and in g_s with increasing concentration of the NP (Fig 3.5 A). The photosynthetic rate (P_N) and transpiration rate did not change significantly at low concentration (up to 10 mg L⁻¹), but decreased by ~68% at 100 mg L⁻¹ and ~86% at 1000 mg L⁻¹ of CuO NPs (Fig 3.5 A). Stomatal conductance showed no changes up to 50 mg L⁻¹ concentration of the CuO NPs but decreased by 72% and 90% at

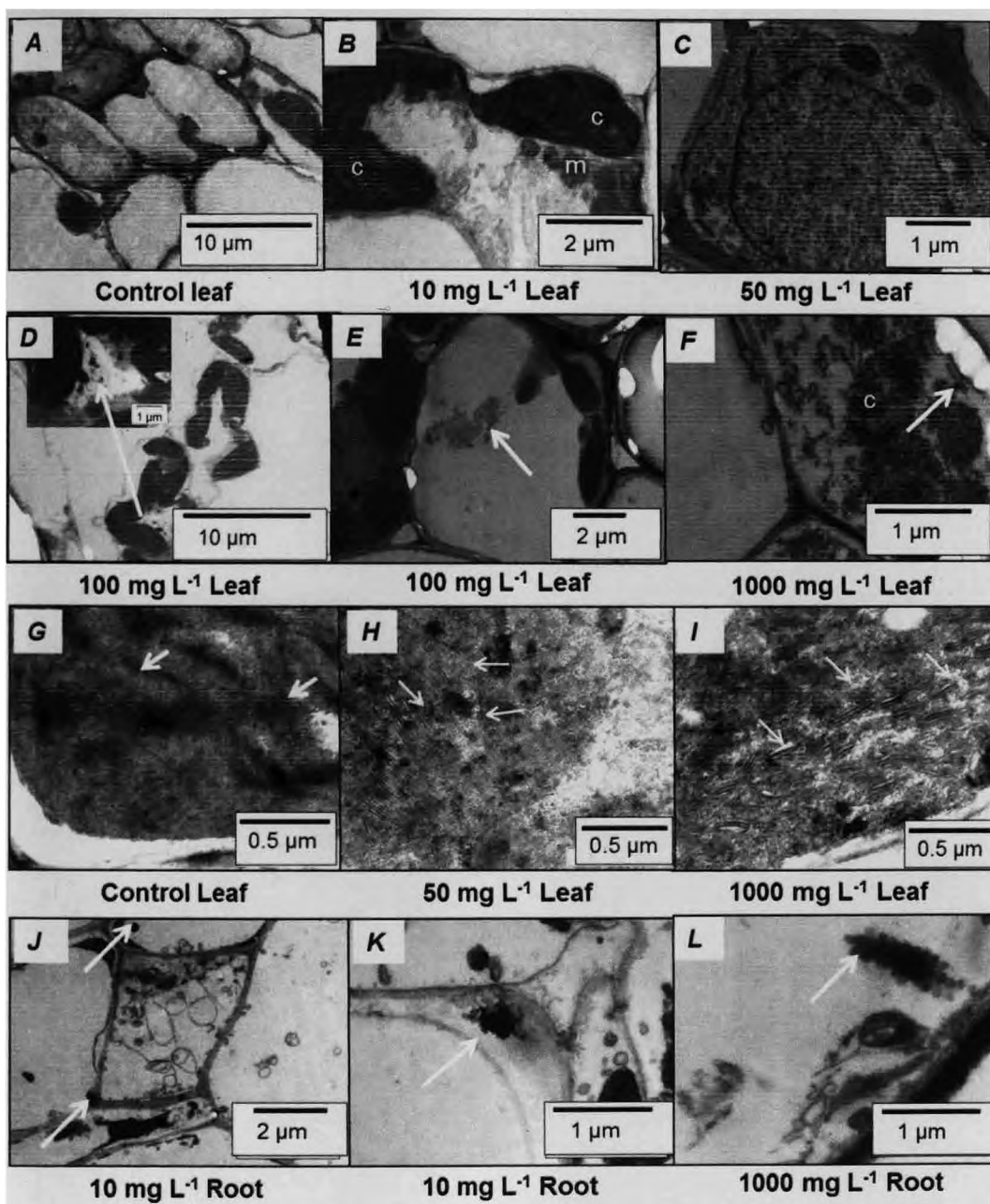


Fig 3.4.1. Electron photomicrographs of leaf (A-I) and roots (J-L) of *O. sativa* showing changes in organelles and accumulation of CuO NPs. Whole cell of untreated leaf (A); treated leaf showing number of chloroplast, c and mitochondria, m (B); intact bundle sheath cells (C); accumulation of CuO NPs in cytosol (D -F); fully stacked thylakoids (G), partially stacked and accumulation of CuO NPs (H), destacked (2-3 thylakoids per granum) and distorted arrangement of thylakoids (I), images of root showing CuO NP aggregation and cluster formation (J-L) in roots.

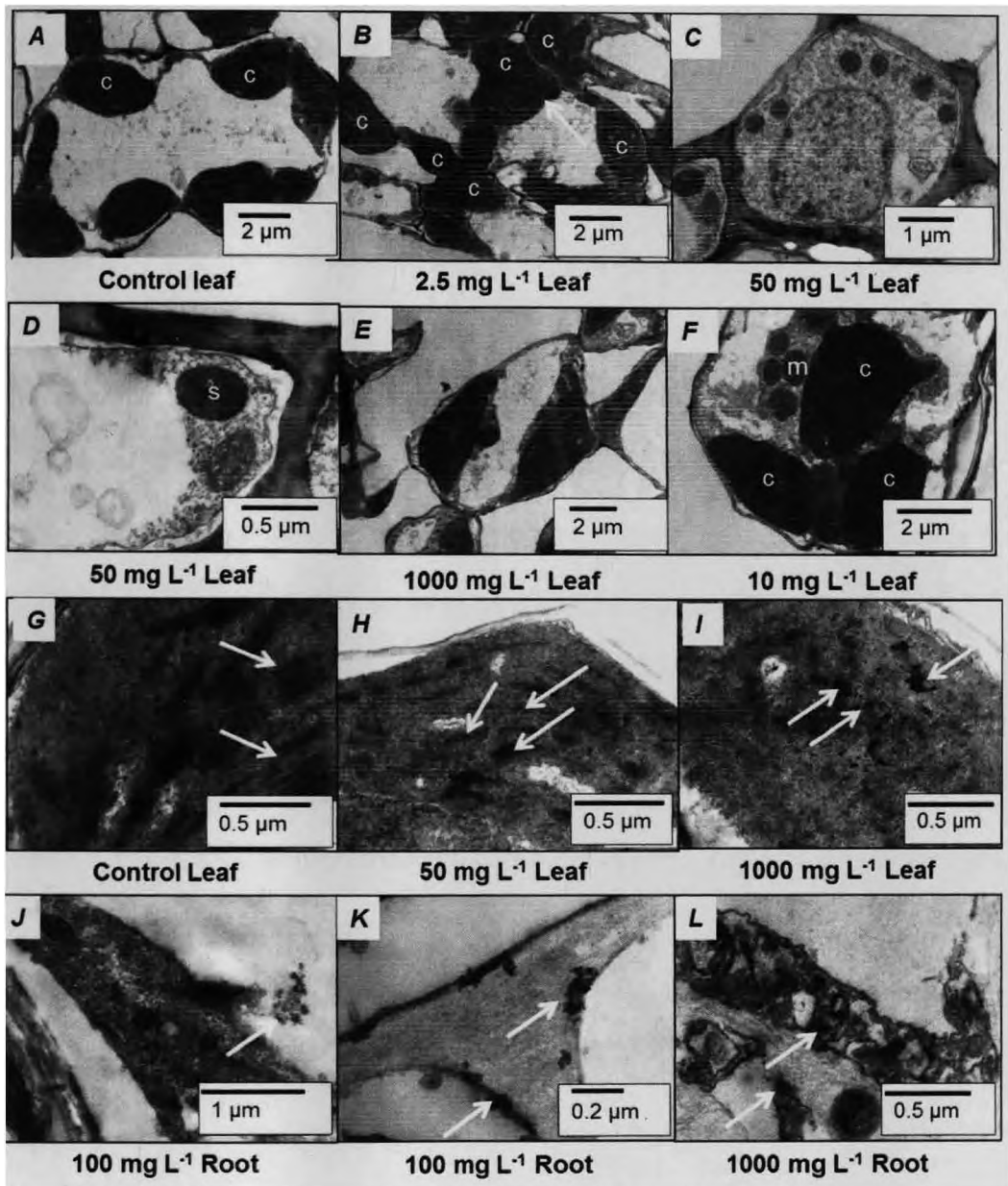


Fig 3.4.2. Electron photomicrographs of leaf (A-I) and roots (J-L) of *O. sativa* showing changes in organelles and accumulation of ZnO NPs in leaf and root. Whole cell of untreated leaf (A); number of chloroplast at low concentration (B); intact bundle sheath cells (C); presence of starch granules, s (D); chloroplast number, c (E); number of mitochondria, m (F); fully stacked thylakoids (G), partially stacked (H-I) and accumulation of ZnO NPs in roots (J-L).

100 and 1000 mg L⁻¹ concentration respectively (Fig 3.5 A).

Both sizes of ZnO NPs also resulted in a gradual decrease in P_N , E and g_s with increasing concentration (Fig 3.5 B, C). It was seen that, a decrease of up to 95% in CO₂ assimilation, 77% in transpiration rate and 57% in stomatal conductance was observed at 1000 mg L⁻¹ concentration of <50 nm sized ZnO NPs (Fig 3.5 B). In case of ZnO NP of 100 nm size, the net CO₂ assimilation rate (P_N) declined by 94%, while transpiration rate (E) and stomatal conductance decreased by 65% and 83% respectively at 1000 mg L⁻¹ concentration of 100 nm size ZnO NPs. P_N showed greater decrease in plants treated with ZnO NP than seen with CuO NPs at the highest concentration.

3.6. Effect of MNPs on light reactions of photosynthesis (Chlorophyll Fluorescence measurements)

The maximum quantum efficiency of PSII measured as F_v/F_m ratio did not change up to 50 mg L⁻¹ of CuO NP but decreased by 46% at 1000 mg L⁻¹ compared to control (Fig 3.6.1 A). The photochemical quenching (q_p) was not affected up to 100 mg L⁻¹ treatment but completely diminished at 1000 mg L⁻¹ of CuO NPs. The non-photochemical quenching (q_N) was also not significantly different from control up to 100 mg L⁻¹ of CuO NPs, however, at 1000 mg L⁻¹ q_N increased by 10% compared to control (Fig 3.6.1 A). The quantum efficiency of PSII measured when all the PSII reaction are closed, denoted by Φ_{PSII} was found similar to control up to 10 mg L⁻¹ decreasing on an average of 35% at 50 and 100 mg L⁻¹, declining further to 84% at 1000 mg L⁻¹ CuO NPs compared to control (Fig 3.6.1 B). Likewise, ZnO NPs showed similar effect on Chl fluorescence measurements. The maximum quantum efficiency of PSII (F_v/F_m ratio) and q_p decreased in plants grown with <50 nm (Fig 3.6.2 A) and 100 nm (Fig 3.6.3 A) size ZnO NPs. The decrease in both parameters was greater in plants grown with 100 nm size ZnO NPs than seen in plants grown with <50 nm size ZnO NPs. It was observed that the F_v/F_m ratio and q_p decreased by

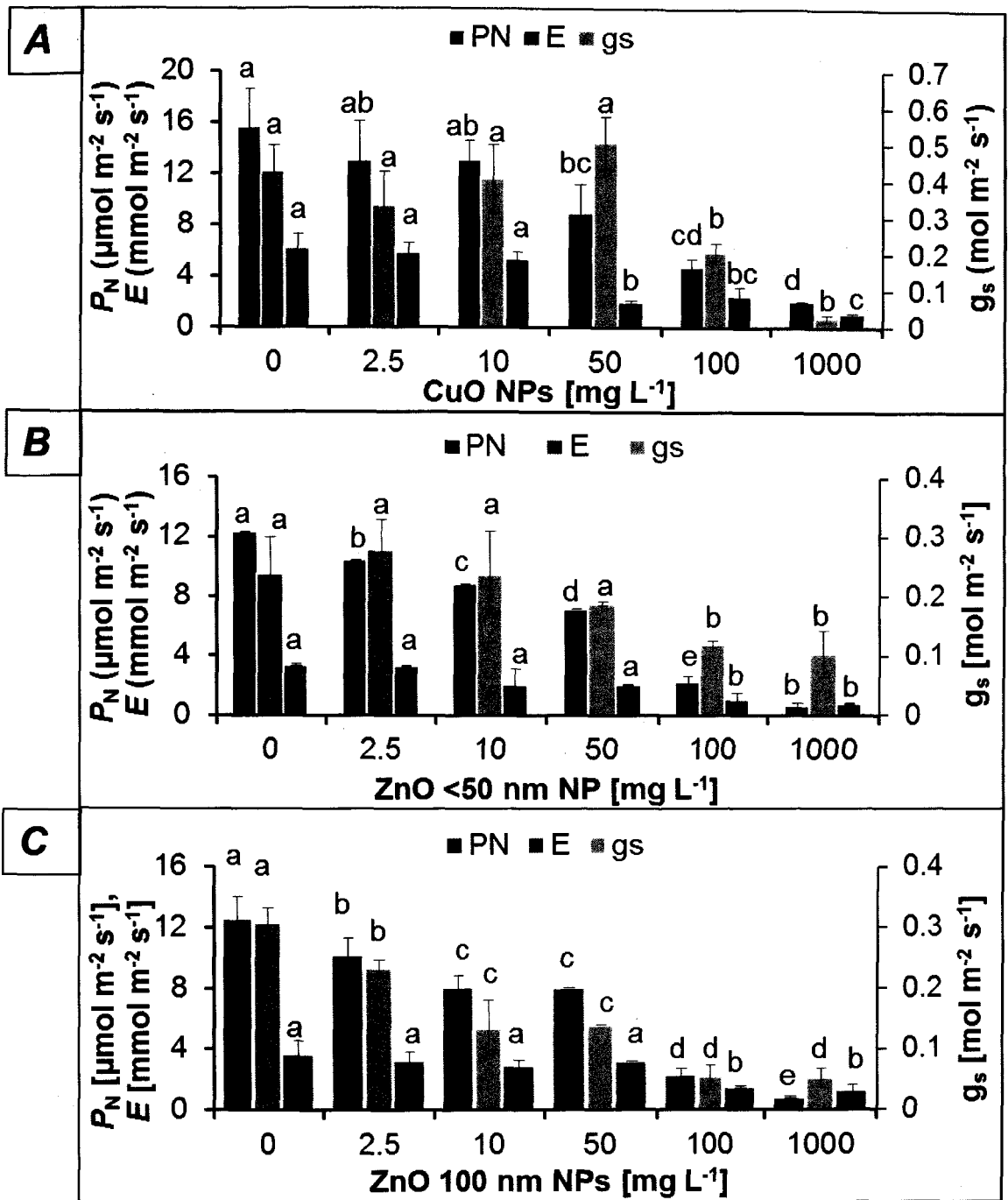


Fig. 3.5. Photosynthetic rate (P_N), stomatal conductance (g_s), and transpiration rate (E) of rice plants treated with CuO (A) and ZnO of <50 nm size (B) and ZnO of 100 nm size (C) NPs after 30 d. Bars represent mean values \pm SD ($n=5$). Bars denoted by the same letter indicate insignificant difference at $p \leq 0.05$.

39% and 73% in plants grown at 1000 mg L⁻¹ of <50 nm size NPs, however, q_N remained unaffected (Fig 3.6.2 A). The quantum efficiency of PSII (Φ_{PSII}) was found similar to control up to 2.5 mg L⁻¹ of <50 nm sized ZnO NP. Further increase in ZnO NPs of <50 nm size resulted in a decline of PSII quantum efficiency up to 86% at 1000 mg L⁻¹ compared to control (Fig 3.6.2 B). The plants grown with 100 nm sized ZnO NP showed that F_v/F_m ratio and q_p decreased by 53% and 93% respectively at 1000 mg L⁻¹ (Fig 3.6.3 A). Also, the non-photochemical quenching (q_N) decreased (21%) at 1000 mg L⁻¹ of 100 nm ZnO NPs (Fig 3.6.3 A). The quantum efficiency of PSII (Φ_{PSII}) was found similar to control up to 10 mg L⁻¹ of 100 nm sized ZnO NPs. Further increase in ZnO NPs of 100 nm size resulted in a decline of Φ_{PSII} up to 84% at 1000 mg L⁻¹ compared to control (Fig 3.6.3 B).

3.7. Changes in the photosynthetic pigment content upon MNP exposure

The qualitative and quantitative profile of photosynthetic pigment were analysed using High Performance Liquid Chromatography (HPLC) in response to the treatment with CuO and ZnO NPs. On treatment with CuO and ZnO NPs, no qualitative changes were observed in the pigment content (Fig 3.7.1- 3), however, quantitative changes in chlorophyll and carotenoid contents were observed (Table 3.7.1- 3). Chlorophyll and carotenoid content, except for β -carotene showed a significant increase at 2.5 mg L⁻¹ treatment of CuO and ZnO NPs. Neoxanthin content increased by 87% at 2.5 mg L⁻¹ as compared to control followed by a decrease of 28% and 41% at 100 and 1000 mg L⁻¹ of CuO NPs respectively. Other Car such as violaxanthin increased by 95% at 2.5 mg L⁻¹ treatment followed by decrease of 73% and 58% at 100 and 1000 mg L⁻¹ of CuO NPs. Lutein content increased by 67% at 2.5 mg L⁻¹ and decreased gradually to 70% at 1,000 mg L⁻¹ concentration of the NP. β -carotene content showed no change up to 10 mg L⁻¹, but decreased by 70% and 90% at 100 and 1,000 mg L⁻¹ of CuO NPs respectively.

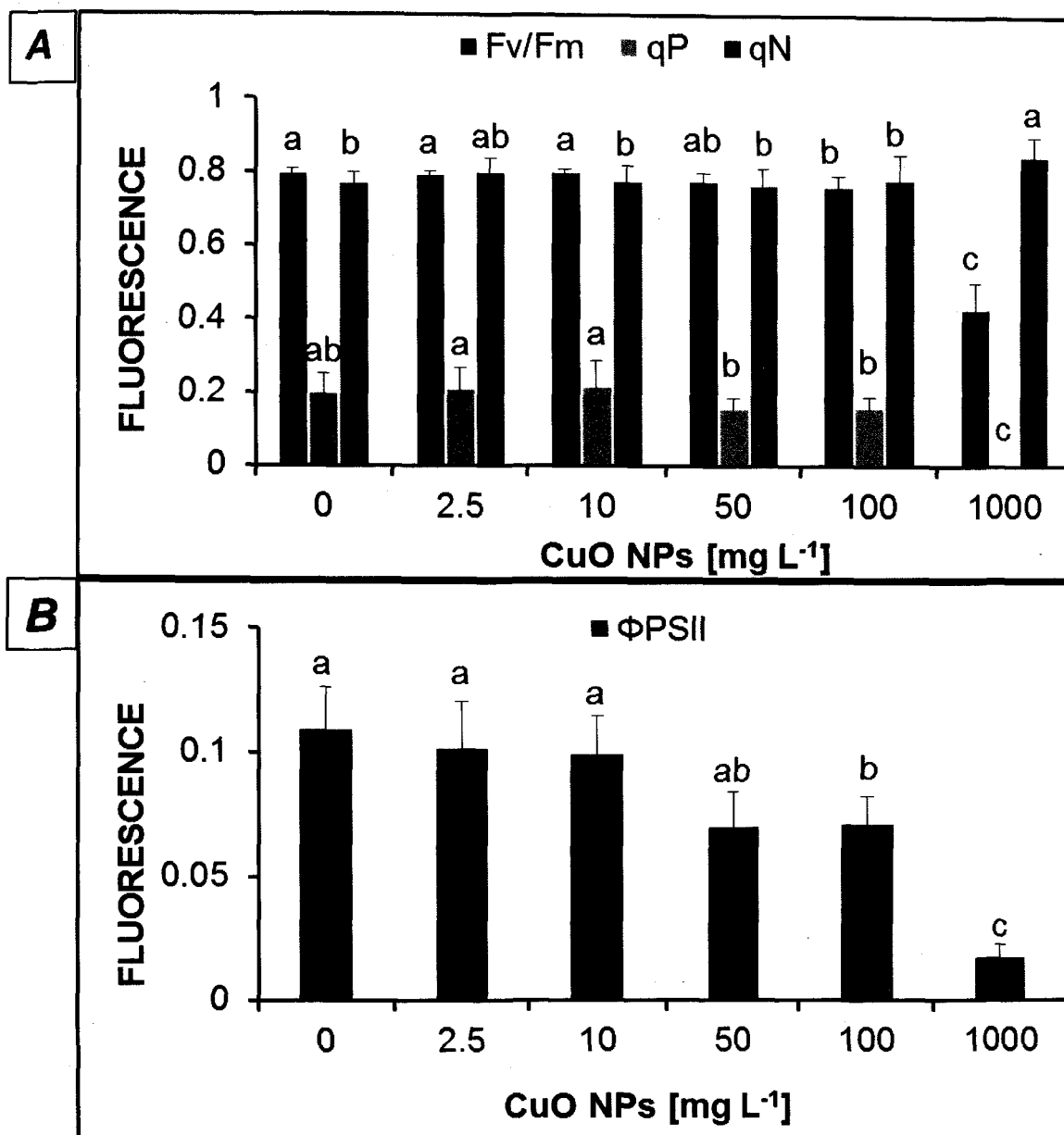


Fig 3.6.1. Maximum quantum efficiency of PSII (F_v/F_m), photochemical quenching (q_p) and non-photochemical quenching (q_N ; *A*); quantum efficiency of PSII (*B*) of rice plants treated with CuO NPs for 30 d. Bars represent mean values \pm SD ($n=5$). Bars denoted by the *same letter* indicate insignificant difference at $p \leq 0.05$.

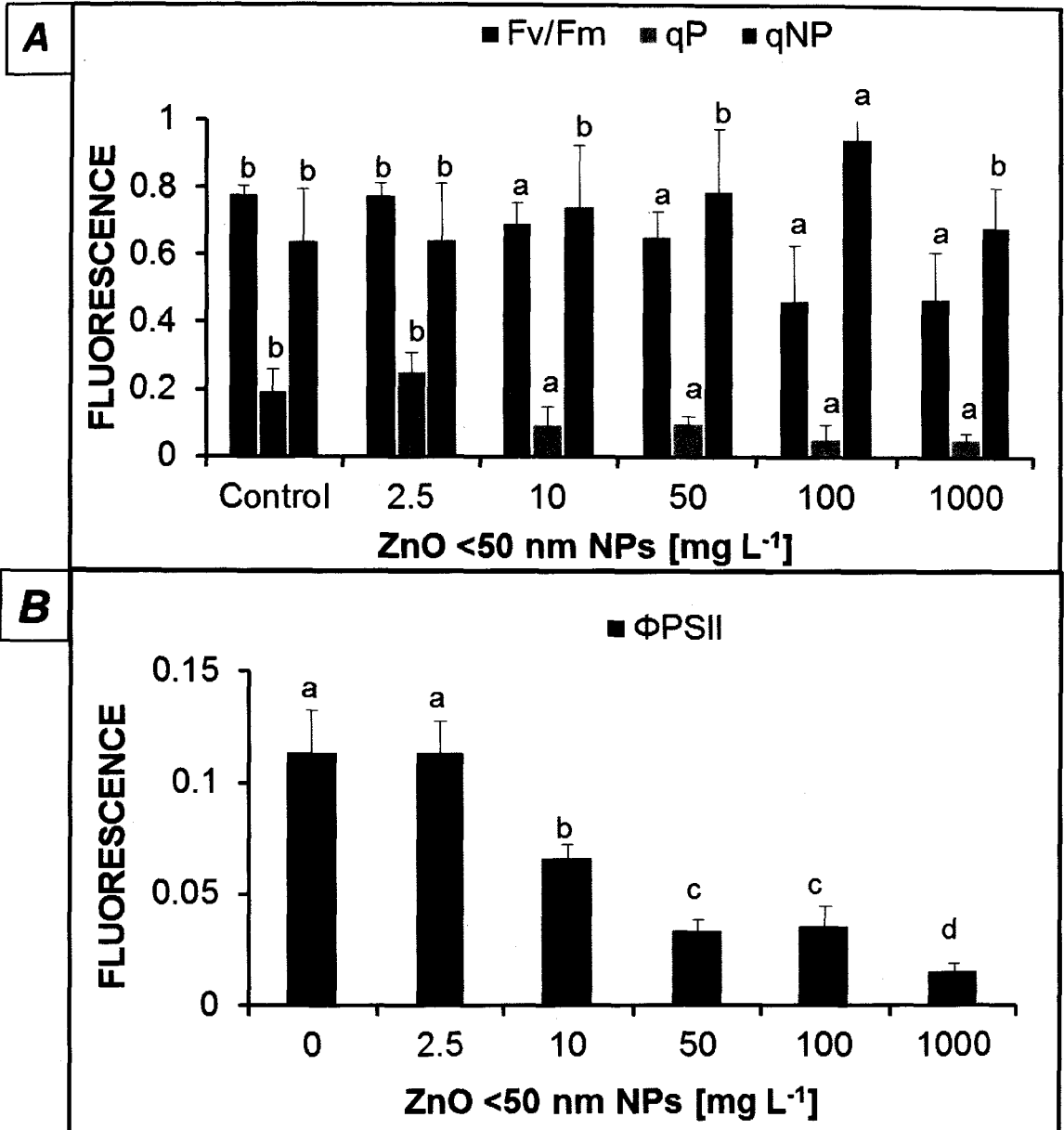


Fig 3.6.2. Maximum quantum efficiency of PSII (F_v/F_m), photochemical quenching (q_p), non-photochemical quenching (q_N ; *A*) and quantum efficiency of PSII (*B*) of rice plants treated with ZnO (<50 nm) NPs for 30 d. Bars represent mean values \pm SD ($n=5$). Bars denoted by the *same letter* indicate insignificant difference at $p \leq 0.05$.

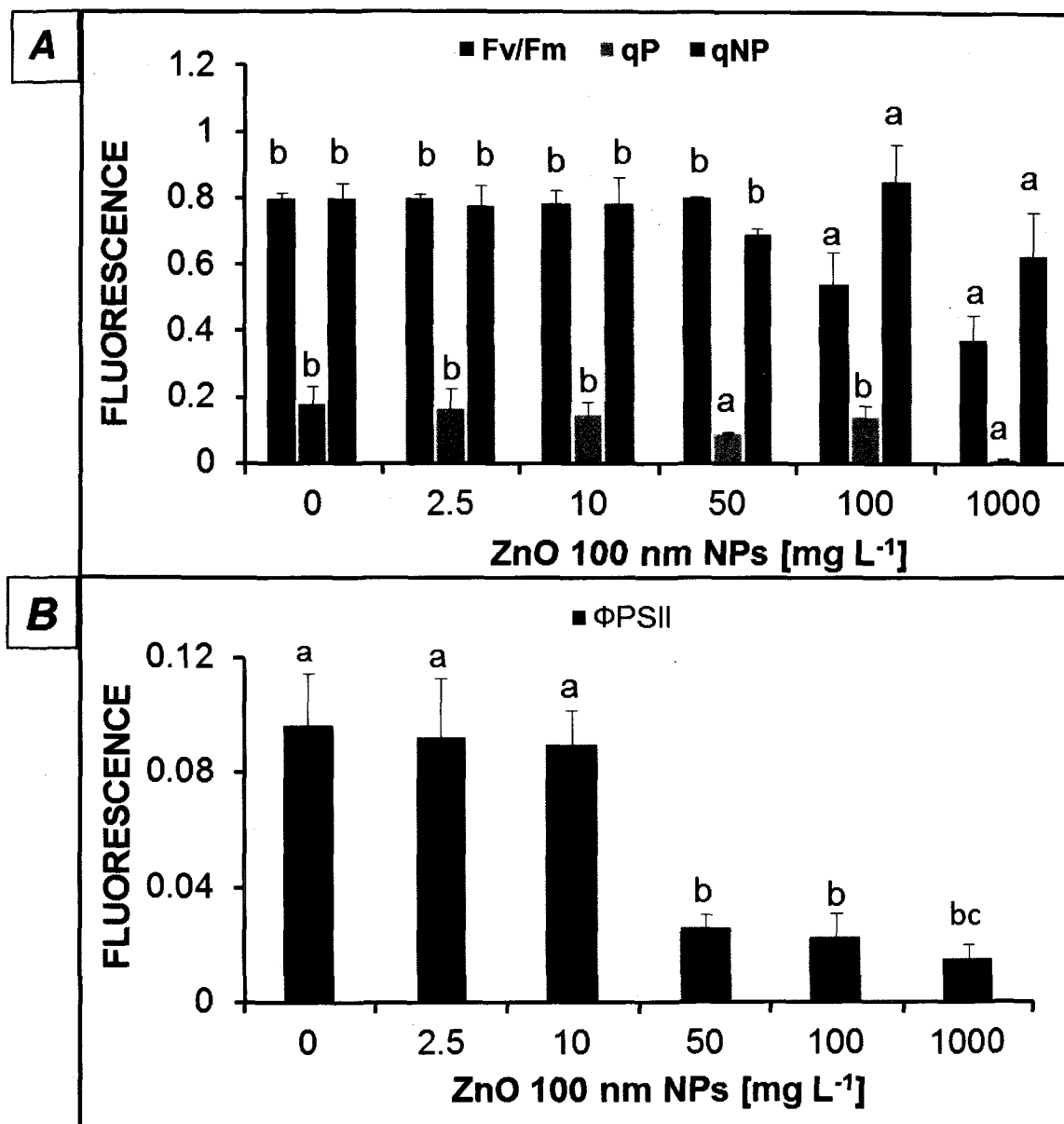


Fig 3.6.3. Maximum quantum efficiency of PSII (Fv/Fm), photochemical quenching (qp), non-photochemical quenching (q_N; A) and quantum efficiency of PSII (B) of rice plants treated with ZnO (100 nm) NPs for 30 d. Bars represent mean values ± SD (n=5). Bars denoted by the *same letter* indicate insignificant difference at p≤0.05.

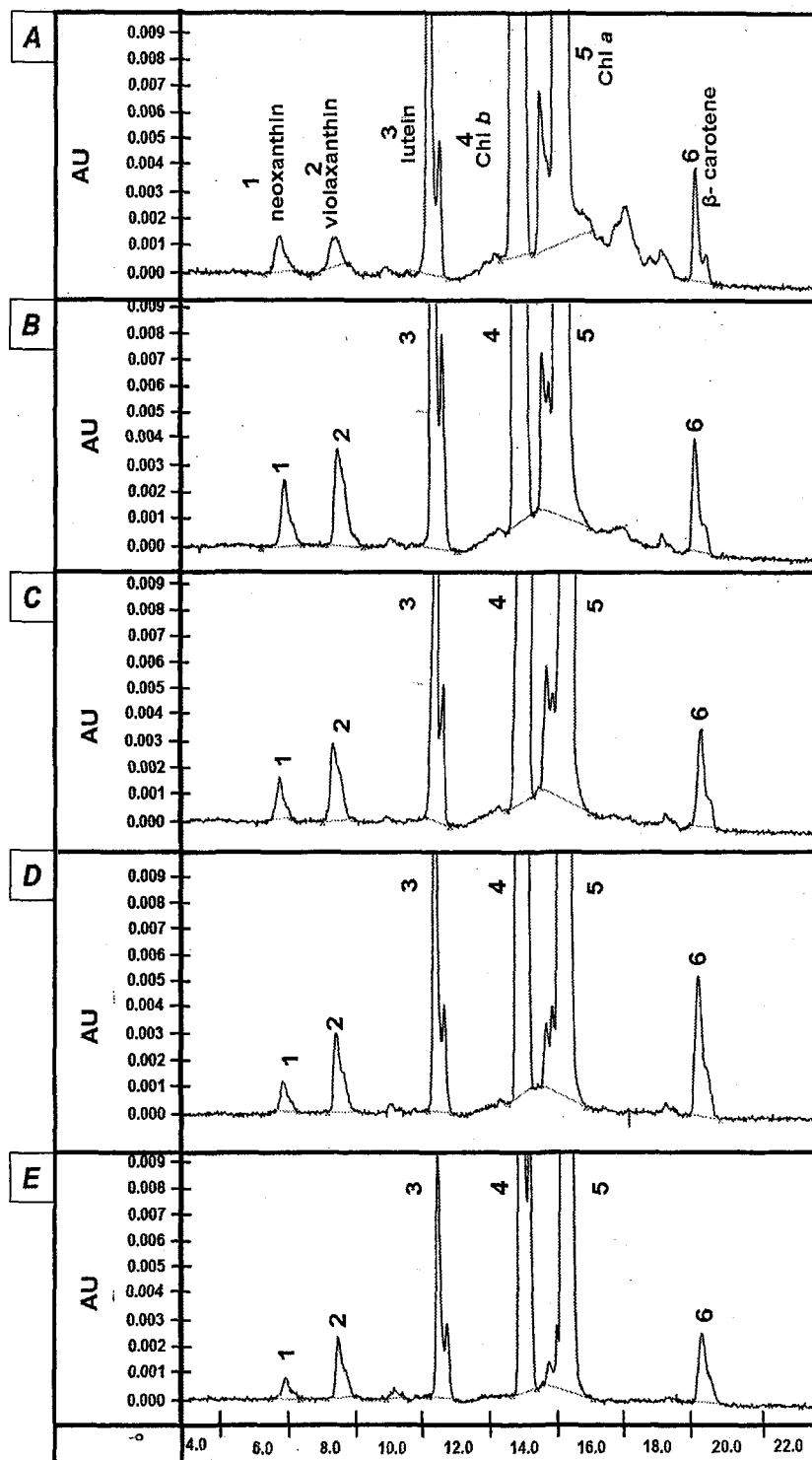


Fig 3.7.1. HPLC Profile extracted at 445 nm of photosynthetic pigments in rice plants after 30 d of CuO NP treatment [*A*= control, *B*=2.5 mg L⁻¹, *C*= 10 mg L⁻¹, *D*=100 mg L⁻¹ and *E*= 1000 mg L⁻¹].

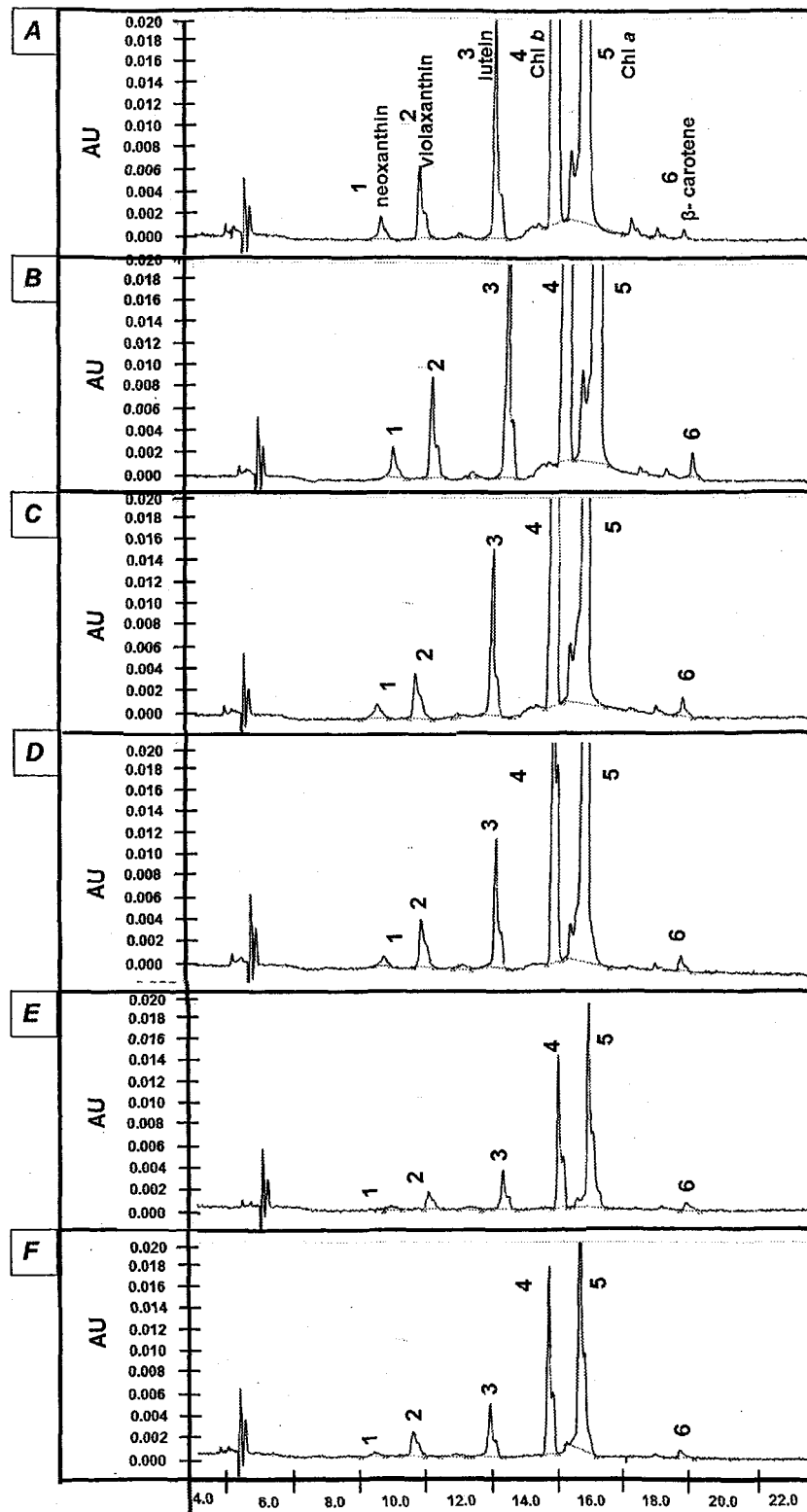


Fig 3.7.2. HPLC Profile extracted at 445 nm of photosynthetic pigments in rice plants after 30 d of ZnO (<50 nm) NP treatment [A= control, B=2.5 mg L⁻¹, C= 10 mg L⁻¹, D= 50 mg L⁻¹, E=100 mg L⁻¹ and F= 1000 mg L⁻¹].

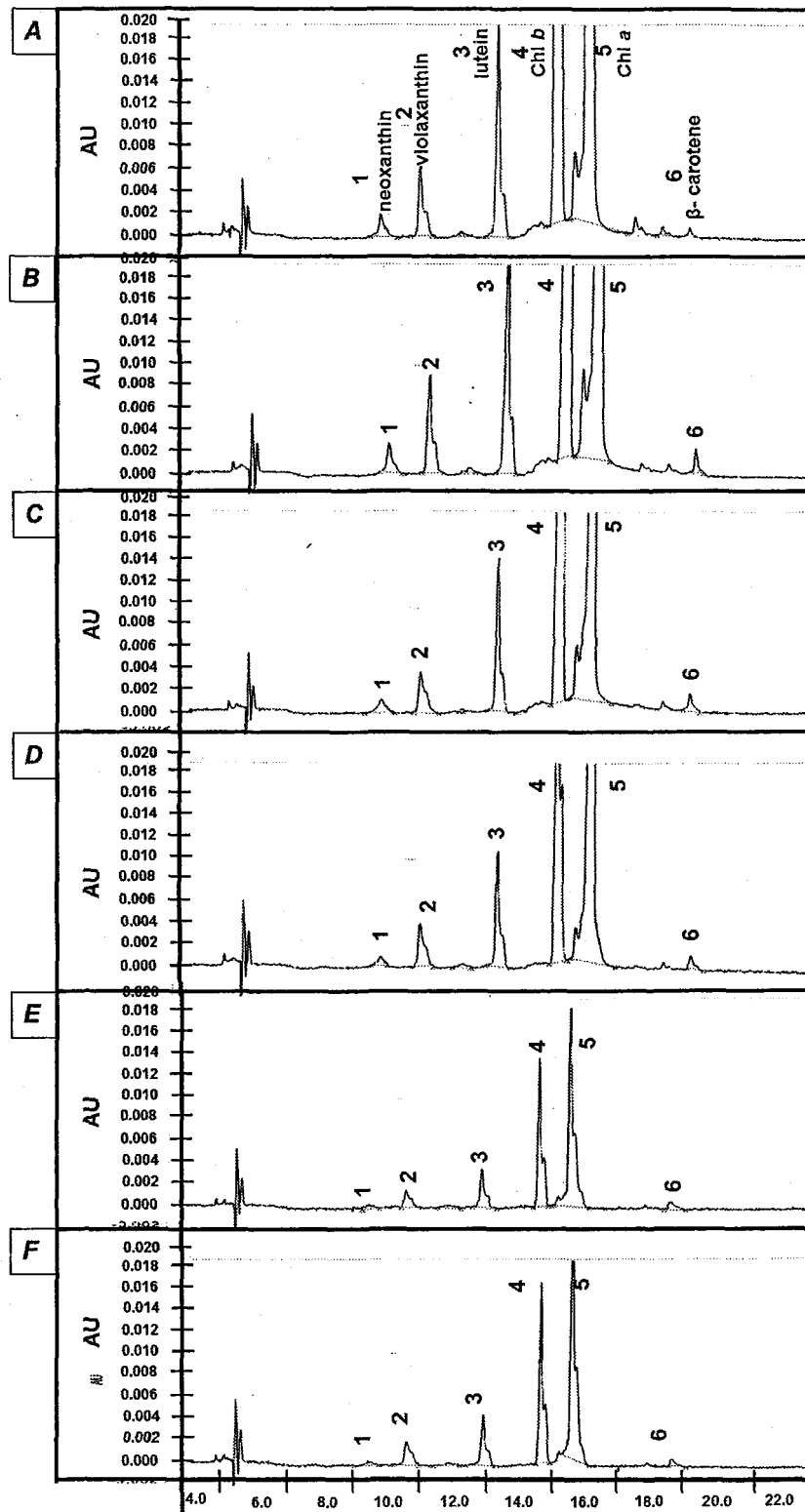


Fig 3.7.3. HPLC Profile extracted at 445 nm of photosynthetic pigments in rice plants after 30 d of ZnO (100 nm) NP treatment [A= control, B=2.5 mg L⁻¹, C= 10 mg L⁻¹, D= 50 mg L⁻¹, E=100 mg L⁻¹ and F= 1000 mg L⁻¹].

An increase in Chl *a* and *b* content by 56% and 54% was observed at 2.5 mg L⁻¹ CuO NP. Further increase in CuO NP concentration led to a decrease in Chl *a* and *b* content by 60% and 66% at 100 mg L⁻¹ and 84% and 89% at 1000 mg L⁻¹ respectively. The ratio of Chl *a/b* showed no change up to 10 mg L⁻¹ but increased by 41% at 1,000 mg L⁻¹ of CuO NPs. The ratio of total chlorophyll and carotenoids decreased with increasing concentration of CuO NPs (Table 3.7.1). Plants treated with low concentration of ZnO NP of both the sizes showed a slight increase in Chl and Car concentration (Table 3.7.2 & 3). Greater than 10 mg L⁻¹ concentration of ZnO NPs resulted in a gradual decrease in chlorophyll and Car content except for β -carotene which increased with increasing concentration of ZnO NPs (Table 3.7.2 & 3). The increase in the photosynthetic pigments at low concentration was higher in plants grown in 100 nm sized ZnO NPs compared to plants grown at <50 nm sized ZnO NPs (Table 3.7.2 & 3). Chl/ Car ratio at highest concentration of ZnO NP decreased by 36% and 71% for particle size of <50 nm and 100 nm respectively. However, the ratio of Chl *a/b* increased with increasing concentration of ZnO NPs of both sizes (Table 3.7.2 & 3).

Cars such as neoxanthin, violaxanthin and lutein increased by 19%, 37% and 27% at 2.5 mg L⁻¹ and decreased by 79%, 55% and 71% at concentrations up to 1000 mg L⁻¹ of ZnO NP of <50 nm size respectively (Table 3.7.2). β -carotene content increased up to a maximum of 4.5-fold (347%) at 10 mg L⁻¹ and only by 1.8-fold (77%) at 1000 mg L⁻¹ of <50 nm size compared to control. Chl *a* and *b* content increased by 27% at 2.5 mg L⁻¹ ZnO NP (<50 nm) concentration, gradually decreasing by 74% and 83% respectively as compared to control (Table 3.7.2). Similar pattern of changes in pigments (Chl and Car) was seen in plants grown with 100 nm sized ZnO NPs (Table 3.7.3).

Table 3.7.1. The Car content and relative Chl content of *O. sativa* leaves treated with CuO NPs at 0–1,000 mg L⁻¹ concentrations for 30 d. β -carotene was used as standard. Data represent mean values \pm SD ($n=5$). Means in the column followed by the *same letter* indicate insignificant differences at $p \leq 0.05$. The ratios were calculated taking mean values of the respective pigments.

Pigment content [$\mu\text{g g}^{-1}$ FM]	CuO NPs [mg L^{-1}]				
	0	2.5	10	100	1000
Neoxanthin	3.5 ± 0.01^b	6.5 ± 0.02^a	3.2 ± 0.02^b	2.5 ± 0.01^c	2.0 ± 0.01^d
Violaxanthin	1.3 ± 0.001^b	2.4 ± 0.06^a	1.0 ± 0.009^b	0.3 ± 0.001^c	0.5 ± 0.009^d
Lutein	2.3 ± 0.003^b	3.9 ± 0.07^a	2.1 ± 0.009^b	1.1 ± 0.007^c	0.7 ± 0.07^d
β-carotene	4.9 ± 0.30^a	5.3 ± 0.05^a	5.2 ± 0.09^a	1.47 ± 0.07^b	0.5 ± 0.02^c
Chl <i>a</i>	37.7 ± 0.03^b	60.3 ± 0.05^a	35.0 ± 0.22^b	15 ± 0.01^c	6.0 ± 0.02^d
Chl <i>b</i>	25.8 ± 0.01^b	39.9 ± 0.04^a	23.2 ± 0.28^b	8.8 ± 0.001^c	2.9 ± 0.001^d
Chl <i>a/b</i> ratio	1.46	1.51	1.50	1.7	2.06
Total Chl/ Car ratio	5.29	5.5	5.06	4.4	2.4
Chl <i>a (b)</i>/ (N+V+L+ β-car) ratio					

Table 3.7.2. The Car content and relative Chl content of *O. sativa* leaves treated with ZnO (<50 nm) NP at 0-1000 mg L⁻¹ concentration after 30 d of growth. Data represent mean values ± SD (n=5). Means in the column followed by the *same letter* indicate insignificant differences at p≤0.05. The ratios were calculated taking mean values of the respective pigments.

Pigment content [μg g ⁻¹ FM]	ZnO (<50 nm) NPs [mg L ⁻¹]					
	0	2.5	10	50	100	1000
Neoxanthin	1.15 ± 0.004 ^b	1.36 ± 0.004 ^a	1 ± 0.04 ^b	0.46 ± 0.04 ^c	0.34 ± 0.01 ^d	0.24 ± 0.01 ^e
Violaxanthin	3.11 ± 0.002 ^b	4.3 ± 0.005 ^a	2.5 ± 0.05 ^c	2.4 ± 0.03 ^c	0.87 ± 0.03 ^e	1.41 ± 0.09 ^d
Lutein	7.7 ± 0.004 ^b	9.8 ± 0.003 ^a	5.77 ± 0.03 ^c	4.5 ± 0.01 ^d	1.66 ± 0.01 ^f	2.20 ± 0.07 ^e
β-carotene	1.7 ± 0.01 ^f	6.6 ± 0.02 ^b	7.6 ± 0.07 ^a	5 ± 0.07 ^c	4.7 ± 0.07 ^d	3 ± 0.01 ^e
Chl <i>a</i>	42.44 ± 0.001 ^b	53.98 ± 0.02 ^a	30.9 ± 0.03 ^c	28 ± 0.044 ^c	8.9 ± 0.034 ^d	10.9 ± 0.02 ^e
Chl <i>b</i>	37.24 ± 0.02 ^b	47.22 ± 0.03 ^a	27.90 ± 0.033 ^c	19.64 ± 0.045 ^d	5.19 ± 0.063 ^f	6.4 ± 0.001 ^e
Chl <i>a/b</i> ratio	1.13	1.14	1.10	1.42	1.7	1.7
Total Chl/ Car ratio	6.57	6.29	5.89	6.09	4.2	4.18
[Chl <i>a (b)</i> / (V+L+ β-car) ratio]						

Table 3.7.3. The Car content and relative Chl content of *O. sativa* leaves treated with ZnO (100 nm) NP treated rice plants at 0-1000 mg L⁻¹ concentration after 30 d of growth. Data represent mean values \pm SD ($n=5$). Means in the column followed by the *same letter* indicate insignificant differences at $p \leq 0.05$. The ratios were calculated taking mean values of the respective pigments.

Pigment content [$\mu\text{g g}^{-1}$ FM]	ZnO (100 nm) NPs [mg L^{-1}]					
	0	2.5	10	50	100	1000
Neoxanthin	2.3 ± 0.004^c	3.3 ± 0.004^a	3.1 ± 0.04^b	1.9 ± 0.04^d	0.6 ± 0.01^f	0.8 ± 0.01^e
Violaxanthin	7.3 ± 0.002^c	12.0 ± 0.005^a	11.3 ± 0.05^b	5.8 ± 0.03^d	4.6 ± 0.03^e	3.8 ± 0.09^f
Lutein	18.9 ± 0.004^c	34.5 ± 0.003^a	27.2 ± 0.03^b	13.7 ± 0.01^d	7.2 ± 0.01^e	7.1 ± 0.07^e
β -carotene	0.8 ± 0.01^c	4.10 ± 0.02^b	3.7 ± 0.07^c	3.9 ± 0.07^c	5.5 ± 0.07^a	5.5 ± 0.01^a
Chl <i>a</i>	95.2 ± 0.001^c	161.6 ± 0.02^a	144.3 ± 0.03^b	77.7 ± 0.044^d	21.5 ± 0.034^e	32.2 ± 0.02^f
Chl <i>b</i>	101.8 ± 0.02^c	155.8 ± 0.03^a	117.1 ± 0.033^b	46.9 ± 0.045^d	16.7 ± 0.063^e	1.48 ± 0.001^f
Chl <i>a/b</i> ratio	0.93	1.04	1.23	1.66	1.28	2.16
Total Car/Chl ratio [Chl <i>a</i> (<i>b</i>)/ (V+L+ β -car) ratio]	6.72	5.88	5.7	4.9	2.13	1.95

3.8. Effect of MNPs on oxidative damage

3.8.1. Lipid Peroxidation

In this study, we observed no lipid peroxidation at all concentrations (0- 1000 mg L⁻¹) of CuO and ZnO NPs (<50 nm and 100 nm) indicating absence of oxidative damage even at high MNP exposure. The malondialdehyde content, indicator of lipid peroxidation in plants was not significantly different from control (untreated) plants at all concentration (2.5- 1000 mg L⁻¹; Fig 3.8.1).

3.8.2. Protein Oxidation

The protein carbonyl content of plants treated with both CuO and ZnO NPs (<50 nm and 100 nm size) also did not show any variation from untreated plants (control) indicating absence of protein oxidation by the treatment (Fig 3.8.2).

3.8.3. Proline Assay

A significant increase in proline content indicating osmotic stress was observed with increased concentration of CuO and ZnO NPs (Fig 3.8.3). Proline content of leaf was not significantly different from control up to 100 mg L⁻¹ of CuO NP, however, the content increased by 2.5-fold at 1000 mg L⁻¹ concentration compared to control (Fig 3.8.3). Treatment with ZnO NP also showed more or less same effect. It was seen that at low concentration of 2.5 mg L⁻¹, the proline content did not change with both sizes of ZnO NPs upon 30 d exposure (Fig 3.8.3 B, C). However, increasing concentration of ZnO NPs of <50 nm size, the proline content increased to 76% (1.8-fold) at 50 mg L⁻¹ and 166% (2.6-fold) at 1000 mg L⁻¹ as compared to control (Fig 3.8.3 B, C). Whereas, ZnO NPs of 100 nm size resulted in higher accumulation of proline content to 30% (1.3-fold) at 50 mg L⁻¹ and 117% (2-fold) increase at 1000 mg L⁻¹ concentration as compared to control.

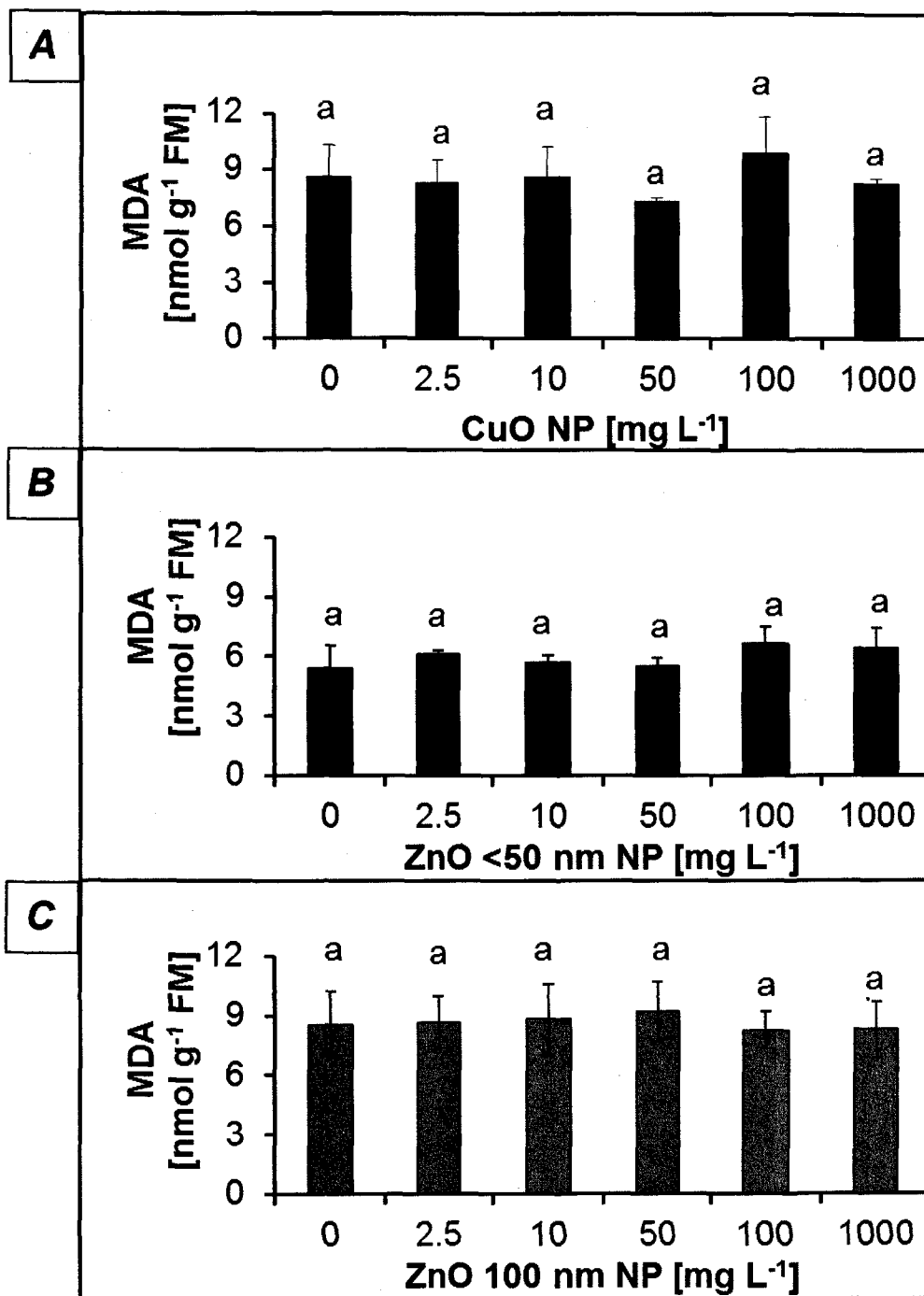


Fig 3.8.1. Malondialdehyde (MDA) content in rice plants treated with CuO (A) and ZnO of <50 nm size (B) and ZnO of 100 nm size (C) NPs after 30 d. Bars represent mean values \pm SD ($n=5$). Bars denoted by the *same letter* indicate insignificant difference at $p \leq 0.05$.

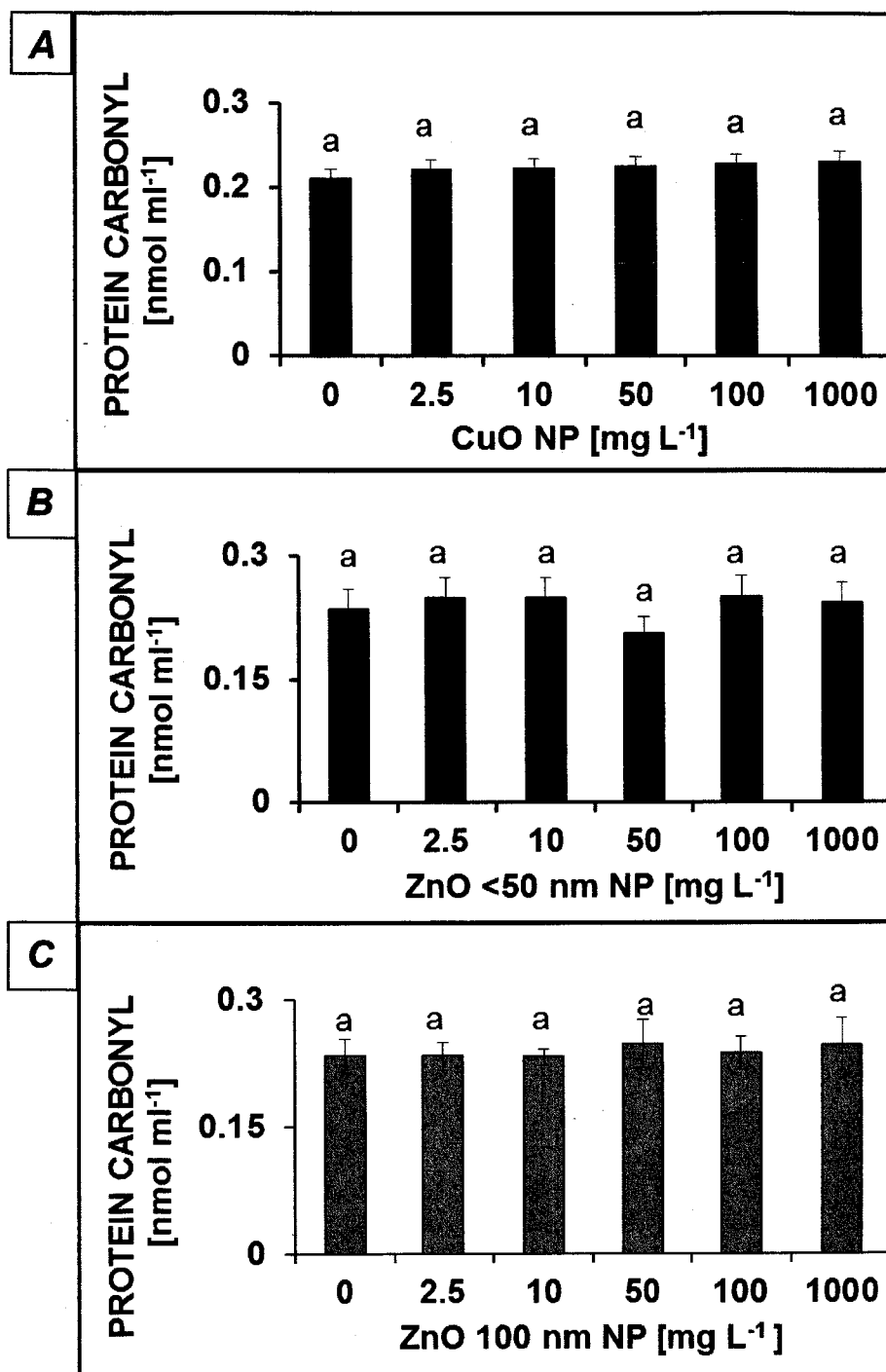


Fig 3.8.2. Protein carbonyl content in rice plants treated with CuO (A) and ZnO of <50 nm size (B) and ZnO of 100 nm size (C) NPs after 30 d. Bars represent mean values \pm SD ($n=5$). Bars denoted by the *same letter* indicate insignificant difference at $p \leq 0.05$.

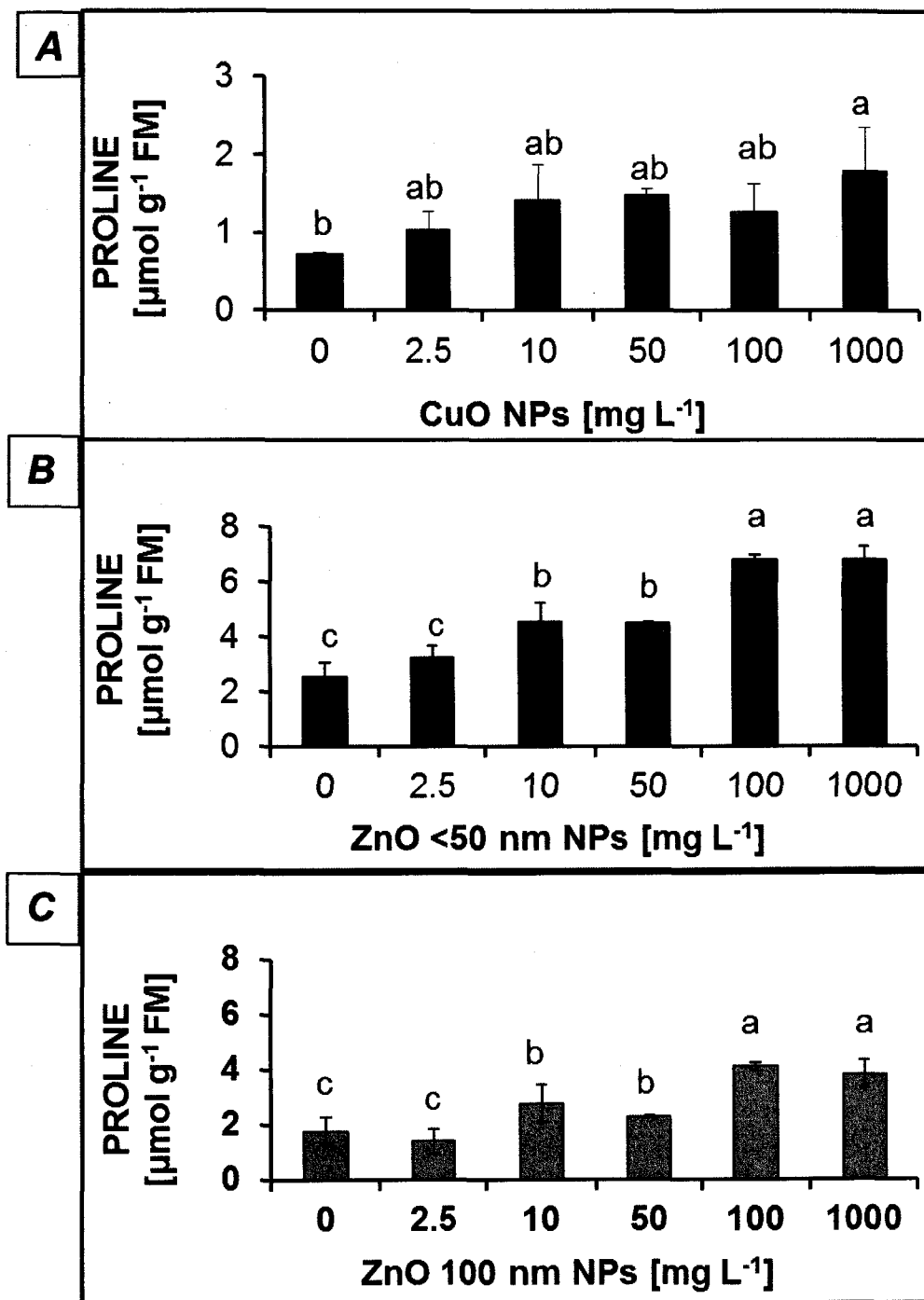


Fig 3.8.3. Proline content in rice plants treated with CuO (A) and ZnO of <50 nm size (B) and ZnO of 100 nm size (C) NPs after 30 d. Bars represent mean values \pm SD ($n=5$). Bars denoted by the *same letter* indicate insignificant difference at $p \leq 0.05$.

3.9. Assay of enzymatic and non-enzymatic antioxidants

3.9.1. Ascorbate assay and Superoxide dismutase (SOD) activity

The ascorbate content of leaf tissue increased upon treatment with MNPs (Fig 3.9.1 A). In case of CuO NPs, an increased by 2.4-fold (147%) compared to control at low concentration (2.5 mg L^{-1}) of CuO NPs was observed. When the concentration of CuO NPs was increased to 10 mg L^{-1} , the ascorbate content increased by 3.3 fold, which further increased by 3.5 fold and 2.8-fold at 50 and 100 mg L^{-1} respectively. At 1000 mg L^{-1} of CuO an increase in leaf ascorbate content by 5.2-fold compared to control was observed (Fig 3.9.1 A). ZnO (100 nm) NP treatment showed no significant change up to 100 mg L^{-1} , however, at 1000 mg L^{-1} , the ascorbate content in leaf tissue was increased by 19% (1.2-fold) compared to control (Fig 3.9.1 A). Superoxide dismutase (SOD), an intracellular enzymatic antioxidant which is ubiquitous and provides the first line of defence against the toxic effects of elevated levels of ROS showed no change in activity at all treatment concentrations of CuO NPs. However, a decrease of 24% in SOD activity was observed at 1000 mg L^{-1} of ZnO (100 nm) NP concentration (Fig 3.9.1 B).

3.9.2. Polyamines (spermine, spermidine) Content

In this study, spermine (spm) content of leaves progressively increased while spermidine (spd) content gradually decreased in plants exposed to CuO NPs (Fig 3.9.2 A). An initial increase in spm content by 71% at 2.5 mg L^{-1} was observed, which increased up to 170% at 1000 mg L^{-1} of CuO NPs compared to control. Spd content decreased by 66% at 2.5 mg L^{-1} of CuO NPs, however, at the highest concentration (1000 mg L^{-1}), a decline of 80% was observed compared to control (Fig 3.9.2 B). Contrary to the results obtained with CuO NPs, plants treated with ZnO (100 nm) NPs showed decreased spm content. Spermine decreased by 36% at 2.5 mg L^{-1} , and 97% at 1000 mg L^{-1} of ZnO NP compared to control

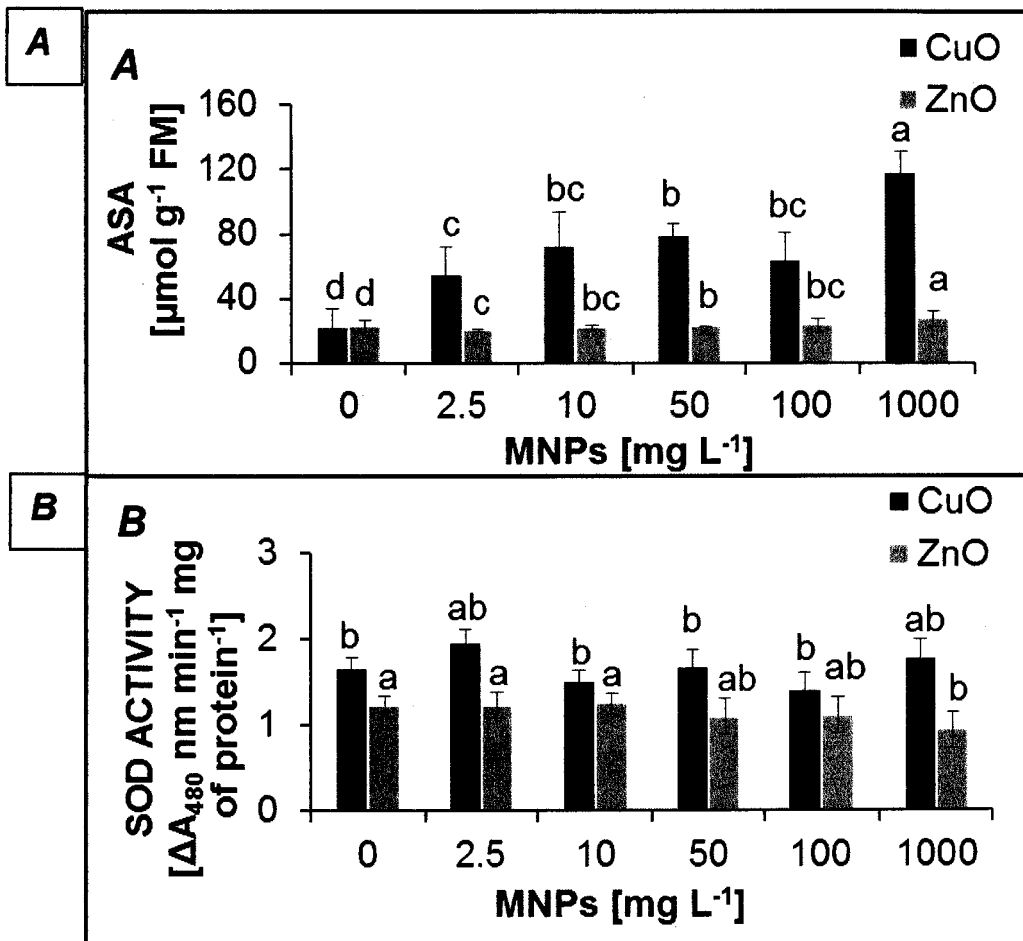


Fig 3.9.1. Ascorbate content (A) and Superoxide dismutase (SOD) activity (B) of rice plants treated with CuO and ZnO (100 nm) nanoparticles for 30 d. Bars represent mean values \pm SD ($n=5$). Bars denoted by the *same letter* indicate insignificant difference at $p \leq 0.05$.

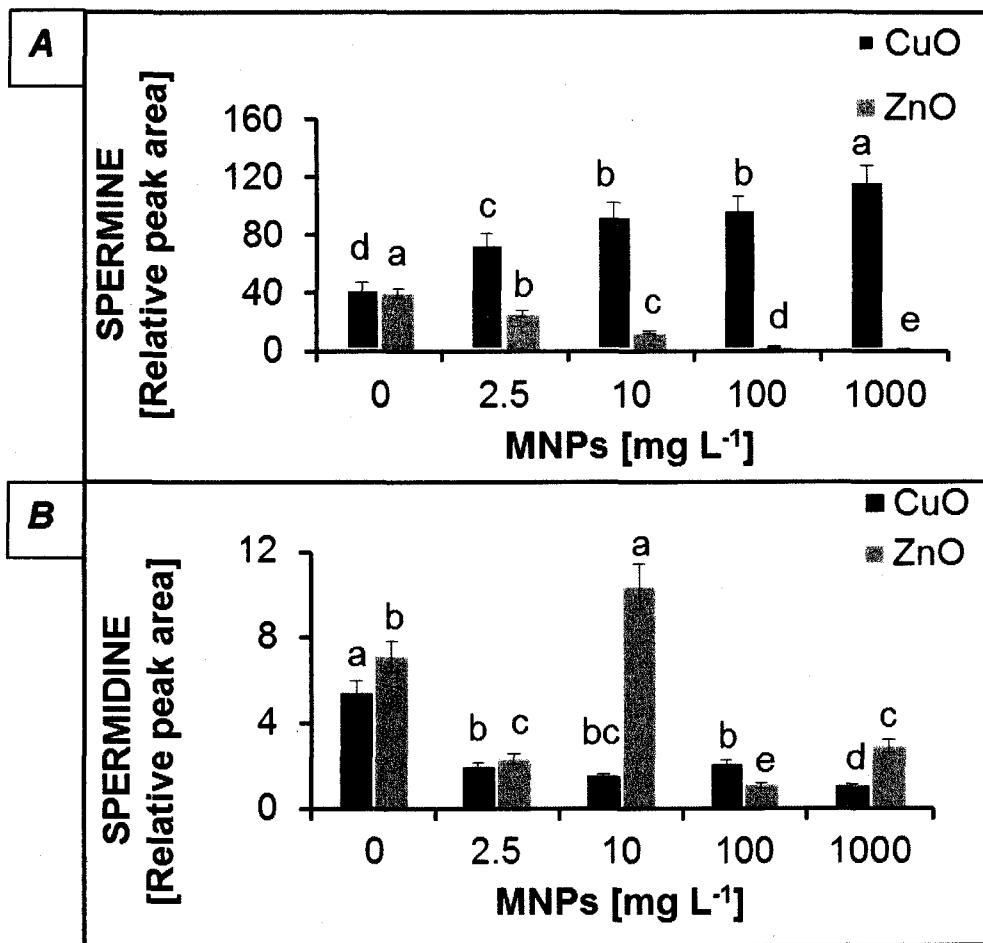


Fig 3.9.2. Spermine (A) and spermidine (B) content of rice plants treated with CuO and ZnO (100 nm) nanoparticles for 30 d. Bars represent mean values \pm SD ($n=2$). Bars denoted by the *same letter* indicate insignificant difference at $p \leq 0.05$.

(Fig 3.9.2 A). Spd content also decreased by 67% at 2.5 mg L⁻¹ and by 85% and 59% at 100 and 1000 mg L⁻¹ of ZnO NPs respectively (Fig 3.9.2 B).

3.10. Gene expression studies of antioxidant enzymes (SOD, APX, GR) and metal chelating enzyme Phytochelatin synthase (PC) by Real Time-PCR

Gene expression of enzymatic antioxidants such as superoxide dismutase (SOD), ascorbate peroxidase (APX), Glutathione reductase (GR) and phyto-chelatin synthase (PC) was investigated with CuO and ZnO NPs grown plants (Fig 3.10). On treatment with CuO NP, the relative fold expression level of SOD at 2.5 mg L⁻¹ was similar to control, however, SOD expression level increased to 1.5-fold at 50 mg L⁻¹ and doubled at 100 mg L⁻¹ compared to control. At the highest concentration of CuO NP a significant decrease (64%; 2.8-fold) in the level of SOD expression was observed compared to control (Fig 3.10 A). Gene expression of APX upon CuO NP stress increased by 215% (3-fold) at 10 mg L⁻¹, however, at higher concentration of 50, 100 and 1000 mg L⁻¹ of CuO NP treatment gene expression of APX was similar to that of control (Fig 3.10 B). GR expression decreased gradually with increasing concentration of CuO NP treatment and was found to be reduced to 45-fold at 1000 mg L⁻¹ of CuO NPs (Fig 3.10 C).

In case of ZnO (100 nm) NPs, the relative fold expression level of SOD at 2.5-10 mg L⁻¹ was similar to control, however, increase in ZnO NP concentration led to an increase of SOD gene expression by 1.5-fold and 2-fold at 100 and 1000 mg L⁻¹ respectively (Fig 3.10 A). A gradual decrease of 73% in APX expression up to 50 mg L⁻¹ and a maximum decrease of 92% (12-fold) at 1000 mg L⁻¹ of ZnO (100 nm) NP were observed (Fig 3.10 B). However, a 157% (2.56-fold) increase in APX expression was observed at 100 mg L⁻¹ compared to control. GR expression showed an increase of 2-fold

and 1.7-fold at 10 and 1000 mg L⁻¹ concentration respectively as compared to control (Fig 3.10 C).

Phyto-chelatin synthase (PC) gene expression showed insignificant change compared to control up to 100 mg L⁻¹ of CuO and ZnO (100 nm) NP exposure, however, at 1000 mg L⁻¹ of both MNPs, an increase in the PC gene expression by 130-fold was observed (Fig 3.10 D).

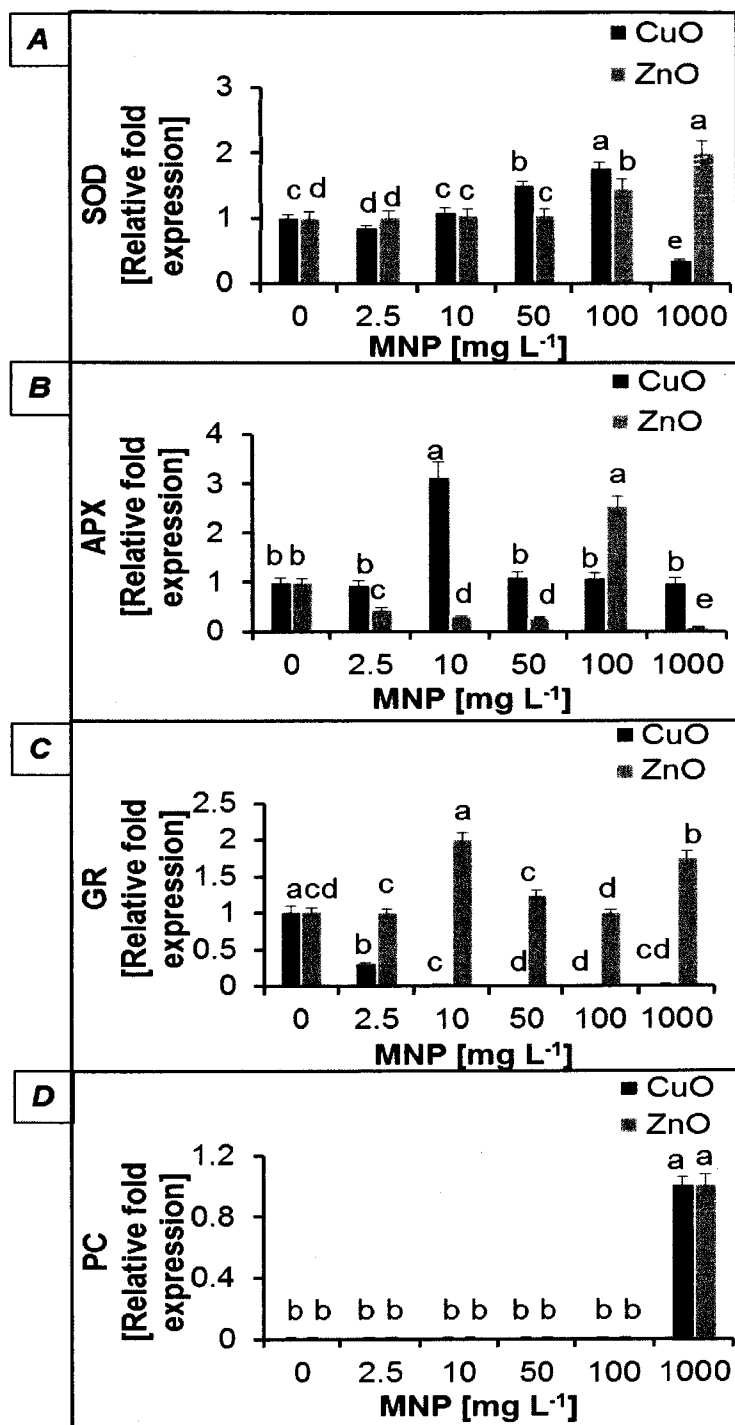


Fig 3.10. Gene expression of Superoxide dismutase (A), Ascorbate peroxidase (B), Glutathione reductase (C) and Phytochelatin synthase (D) in rice plants treated with CuO and ZnO (100 nm) nanoparticles for 30 d. Bars represent mean values \pm SD ($n=5$). Bars denoted by the *same letter* indicate insignificant difference at $p \leq 0.05$.

3.11. Effect of Bulk Metals in Comparison to MNPS on the Morphological, Physiological and Biochemical Processes in *O. Sativa*.

Data was also obtained by treating plants with bulk metals to compare the effect with MNPs. Though both resulted in inhibition to photosynthesis, it was seen that bulk metals caused greater inhibition to plant growth and photosynthesis due to oxidative damage to lipids and proteins, whereas, no such oxidative damage was observed with MNPs. This study was mainly done to understand if the mechanism of toxicity of MNPs in *O. sativa* was similar to bulk metals or whether MNPs exhibited a different mechanism of action.

Bulk metal vs MNPs:

Both CuO NPs and bulk Cu decreased germination by 7% at 1000 mg L⁻¹ compared to their respective controls (Table 3.3.1; Table 3.11.1). Bulk Zn also reduced seed germination by 6% whereas ZnO NPs of both sizes showed no change in percent germination compared to their respective controls (Table 3.3.2 & 3; Table 3.11.2). A greater decline in shoot was observed on treatment with bulk Cu and bulk Zn then seen with CuO (Table 3.3.1; Table 3.11.1) and ZnO (Table 3.3.2 & 3; Table 3.11.2) NPs respectively. The plantlets treated with highest concentration (1000 mg L⁻¹) of bulk metals showed reduction in shoot length by 74% compared to 31% seen at the same concentration with CuO NP (Table 3.3.1; Table 3.11.1). Similar results were obtained with bulk Zn in comparison to the ZnO NPs of both sizes (Table 3.3.2 & 3; Table 3.11.2). The root length on treatment with 1000 mg L⁻¹ CuO NPs and ZnO NPs showed a decrease of 23% and 42% compared to control respectively (Table 3.3.1-3), whereas bulk Cu treatment led to complete root length inhibition and bulk Zn showed no change in root length at the same concentration (Table 3.11.1& 2).

The shoot fresh biomass (SFM) at 1000 mg L⁻¹ of bulk Cu reduced by 63% compared to 31% observed with CuO NPs at the same concentration (Table 3.3.1; Table 3.11.1). Furthermore, the root fresh biomass (RFM) and root dry biomass (RDM) upon treatment with bulk Cu decreased by 76% and 79% at 100 mg L⁻¹ respectively while completely inhibiting root growth at 1000 mg L⁻¹ whereas plants treated with CuO NPs showed an increase in RFM by 9% and a decrease in RDM by only 12% at 1000 mg L⁻¹ (Table 3.3.1; Table 3.11.1). On the other hand, on treatment with bulk Zn, the shoot and root fresh biomass decreased by 40% and 19% respectively with a similar decrease in its corresponding dry mass (Table 3.11.2). Surprisingly, a similar decline in SFM and RFM was observed in case of ZnO NPs of both sizes with no significant difference from control in dry mass (SDM and RDM), however, this decline was observed after 15 d in case of bulk Zn and after 30 d with ZnO NPs of both sizes (Table 3.3.2 & 3; Table 3.11.2).

Scanning electron microscopic images showed that 1000 mg L⁻¹ of both CuO and ZnO NPs and bulk Cu and Zn resulted in increased number and size of trichomes as well as decreased size of stomata upon treatment. Furthermore, damage to the roots was observed in both cases, however, bulk Cu further led to absence of root hairs at 100 mg L⁻¹ and complete inhibition of root growth at 1000 mg L⁻¹. Plants treated with bulk Cu accumulated a maximum of up to 4.6-fold (362%) Cu in leaves at 50 mg L⁻¹ while CuO NPs resulted in a maximum of up to 454% (5.5 fold) at 1000 mg L⁻¹. In roots, however, massive accumulation of Cu was seen in plants treated with bulk Cu compared to CuO NPs (Table 3.11.1). The highest accumulation of Cu in leaf and root tissue was on treatment with bulk Cu at 50 (i.e. 18.03 ± 1.9 mg L⁻¹) and 100 mg L⁻¹ (i.e. 3738.7 ± 30.8 mg L⁻¹) respectively (Table 3.11.1). Plants treated with CuO NPs showed a maximum of Cu accumulation in leaf at 1000 mg L⁻¹ (17.27 ± 1.45 mg L⁻¹) and root at 100 mg L⁻¹ (1544.1 ± 18.9 mg L⁻¹) respectively.

Table 3.11.1. Percent germination, shoot, root length (6 d), biomass (30 d), content of copper (Cu) in leaf and root tissue and the Chl ratio, Chl/ Car ratio of *O. sativa* treated with bulk Cu at different concentrations. SFM=shoot fresh mass; SDM=shoot dry mass; RFM=root fresh mass; RDM=root dry mass. Data represent mean values \pm SD ($n=5$). Means in the column followed by the *same letter* indicate insignificant differences at $p \leq 0.05$.

Bulk Cu (mg L ⁻¹)	Percent germination (%)	Shoot length (mm)	Root length (mm)	Shoot biomass (g)		Root biomass (g)		Cu content (mg L ⁻¹)		Chl <i>a/b</i> ratio	Chl/ Car ratio
				SFM	SDM	RFM	RDM	In leaf	In root		
0	94.0 \pm 2.90 ^a	40.7 \pm 3.08 ^a	53.0 \pm 2.36 ^a	0.553 \pm 0.02 ^a	0.0846 \pm 0.001 ^a	0.208 \pm 0.01 ^a	0.025 \pm 0.001 ^a	3.9 \pm 0.8 ^d	27.18 \pm 2.61 ^c	0.77	2.58
2.5	95.0 \pm 3.52 ^a	43.7 \pm 3.07 ^a	50.4 \pm 0.55 ^a	0.508 \pm 0.03 ^a	0.0843 \pm 0.002 ^a	0.206 \pm 0.01 ^a	0.024 \pm 0.001 ^a	12.66 \pm 2.2 ^c	273.7 \pm 15.9 ^d	1.33	2.98
10	93.5 \pm 2.74 ^a	40.8 \pm 1.12 ^a	53.4 \pm 0.91 ^a	0.465 \pm 0.07 ^a	0.0725 \pm 0.01 ^a	0.217 \pm 0.01 ^a	0.024 \pm 0.002 ^a	15.91 \pm 1.3 ^b	592.2 \pm 20.6 ^c	1.46	2.59
50	90.3 \pm 2.42 ^a	25.7 \pm 0.72 ^b	11.2 \pm 0.90 ^b	0.467 \pm 0.03 ^a	0.0744 \pm 0.012 ^a	0.068 \pm 0.009 ^b	0.008 \pm 0.001 ^b	18.03 \pm 1.9 ^a	1608.5 \pm 53.7 ^b	1.08	1.91
100	93.0 \pm 3.79 ^a	23.2 \pm 0.35 ^c	7.8 \pm 3.15 ^c	0.457 \pm 0.01 ^a	0.0794 \pm 0.009 ^a	0.05 \pm 0.008 ^c	0.005 \pm 0.002 ^c	13.34 \pm 2.3 ^c	3738.69 \pm 30 ^a	1.66	1.85
1000	87.6 \pm 7.39 ^b	10.6 \pm 0.30 ^d	--	0.202 \pm 0.01 ^b	0.0402 \pm 0.008 ^b	--	--	11.41 \pm 1.2 ^c	--	--	--

Table 3.11.2. Percent germination, shoot, root length (6 d) and biomass (30 d) of *O. sativa* treated with bulk Zn at different concentrations. SFM=shoot fresh mass; SDM=shoot dry mass; RFM=root fresh mass; RDM=root dry mass. Data represent mean values \pm SD ($n=5$). Means in the column followed by the *same letter* indicate insignificant differences at $p \leq 0.05$.

Conc. Of Bulk Zn	% Germination	Shoot length	Root length	Shoot biomass		Root biomass	
				SFM	SDM	RFM	RDM
0	93.8 \pm 1.0 ^a	25.8 \pm 0.3 ^a	40.5 \pm 0.6 ^a	0.544 \pm 0.03 ^a	0.0745 \pm 0.01 ^a	0.13 \pm 0.009 ^a	0.0234 \pm 0.001 ^a
2.5	95.6 \pm 2.5 ^a	25.3 \pm 1.1 ^a	40.6 \pm 1.6 ^a	0.537 \pm 0.02 ^a	0.0779 \pm 0.02 ^a	0.145 \pm 0.017 ^a	0.0221 \pm 0.002 ^a
10	93.1 \pm 1.3 ^a	26.6 \pm 0.6 ^a	38.3 \pm 1.5 ^a	0.512 \pm 0.01 ^a	0.0781 \pm 0.01 ^a	0.145 \pm 0.014 ^a	0.024 \pm 0.004 ^a
50	91.1 \pm 1.0 ^a	24.3 \pm 0.7 ^a	34.3 \pm 0.9 ^b	0.348 \pm 0.02 ^b	0.0632 \pm 0.015 ^b	0.14 \pm 0.018 ^a	0.0245 \pm 0.003 ^a
100	88.6 \pm 1.7 ^a	24.7 \pm 0.3 ^a	30.7 \pm 1.5 ^c	0.368 \pm 0.02 ^b	0.0624 \pm 0.011 ^b	0.136 \pm 0.009 ^a	0.0246 \pm 0.003 ^a
1000	88.1 \pm 3.4 ^a	16.0 \pm 1.0 ^b	23.2 \pm 1.2 ^d	0.325 \pm 0.03 ^b	0.060 \pm 0.018 ^b	0.105 \pm 0.004 ^b	0.021 \pm 0.005 ^b

Both bulk Cu and CuO NPs resulted in an increase of Chl *a/b* ratio and a decrease of Chl/ Car ratio at higher concentrations (Table 3.11.1). The plants exposed to 1000 mg L⁻¹ of bulk Cu showed an increase in the Chl *a/b* ratio by 115% compared to the 41% increase seen with CuO NPs. However, the Chl/ Car ratio decreased by 28% at 1000 mg L⁻¹ on treatment with bulk Cu compared to the 55% decline seen with CuO NPs at the same concentration. The quantum efficiency of photosystem II measured as F_v/F_m ratio decreased by 59% and 46% at 1000 mg L⁻¹ of bulk Cu and CuO NPs respectively (Fig 3.11.1 A). Photochemical quenching (q_p) decreased by up to 86% at 1000 mg L⁻¹ of bulk Cu while CuO NPs completely inhibited q_p at the same concentration (Fig 3.11.1 B). The non- photochemical quenching (q_N) indicative of photochemical energy that is dissipated in the form of heat increased and was more or less same with CuO NPs and bulk Cu at 1000 mg L⁻¹ (Fig 3.11.1 C). Net CO₂ assimilation rate (P_N), transpiration rate (E) and stomatal conductance (g_s) declined on treatment with CuO NPs and bulk Cu with increasing concentration (Fig 3.11.1 D-F). Measurements of plants treated with 1000 mg L⁻¹ of bulk Cu could not be taken as the leaves appeared stunted, not suitable for gas exchange analysis. Comparative analysis of bulk Cu and CuO NPs at 100 mg L⁻¹, showed greater decrease in P_N , E and g_s of plants treated with bulk Cu. It was observed that bulk Cu showed a reduction in P_N , E and g_s by 86%, 79% and 80% at 100 mg L⁻¹ respectively as compared to CuO NPs by 68%, 60% and 72% in P_N , E and g_s respectively (Fig 3.11.1 D-F). A similar decrease was seen in rice plants treated with bulk Zn and ZnO NPs (<50 nm and 100 nm) in this study (Fig 3.11.2).

The decline in transpiration rate of bulk Zn and ZnO NPs of <50 nm size was similar (71-77%) whereas ZnO NPs of larger size decreased E by 65%. The stomatal conductance of bulk Zn was similar to larger sized ZnO NPs (83-97%) and reduced by 57% with ZnO NPs of

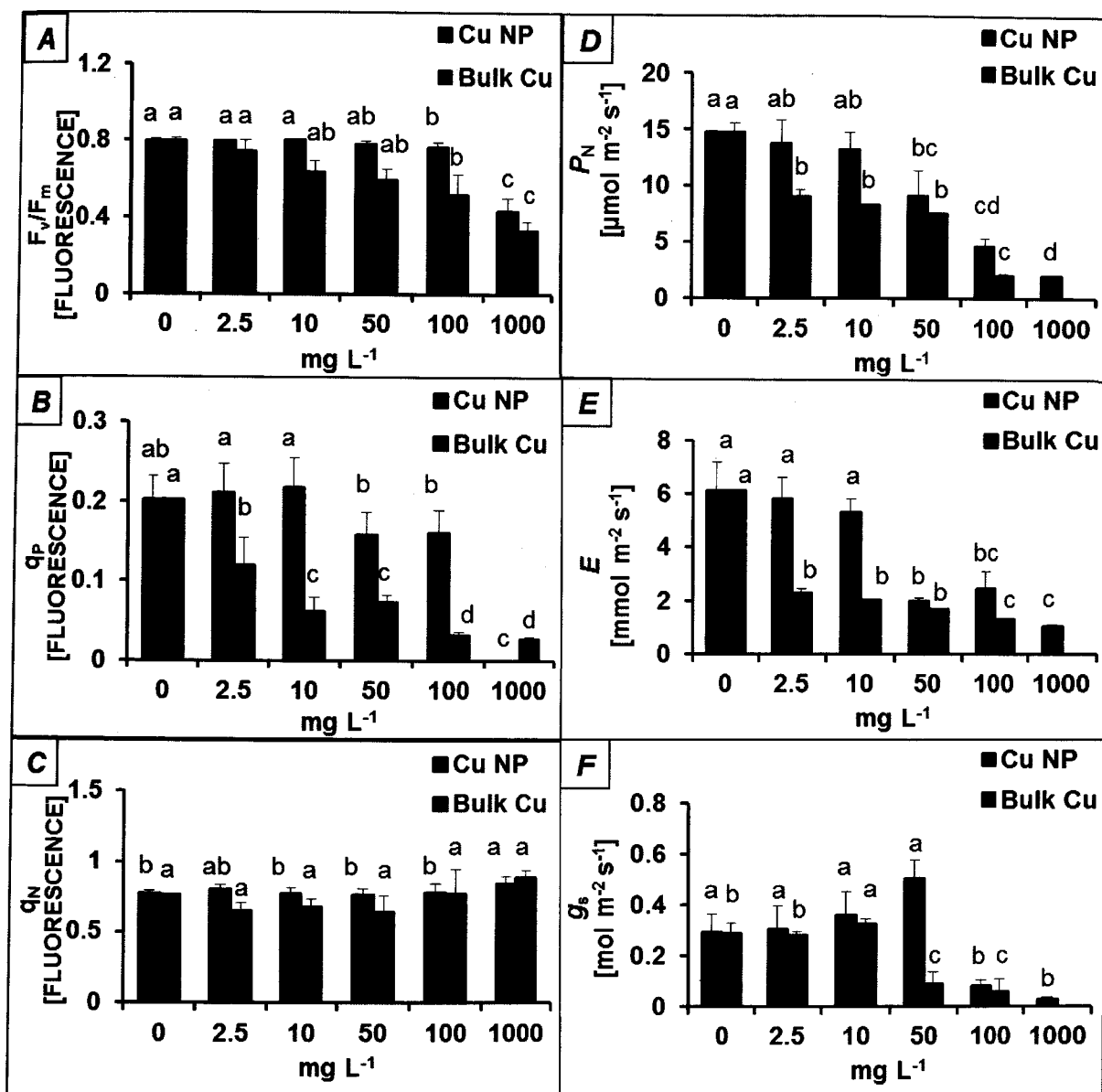


Fig 3.11.1. The maximum quantum efficiency of PSII (F_v/F_m ; A), photochemical quenching (q_p ; B), non-photochemical quenching (q_N ; C), photosynthesis rate (P_N ; D), transpiration rate (E ; E) and stomatal conductance (g_s ; F) of rice plants treated with bulk Cu and CuO NPs. Bars represent mean values \pm SD ($n=5$). Bars denoted by the same letter indicate insignificant difference at $p \leq 0.05$.

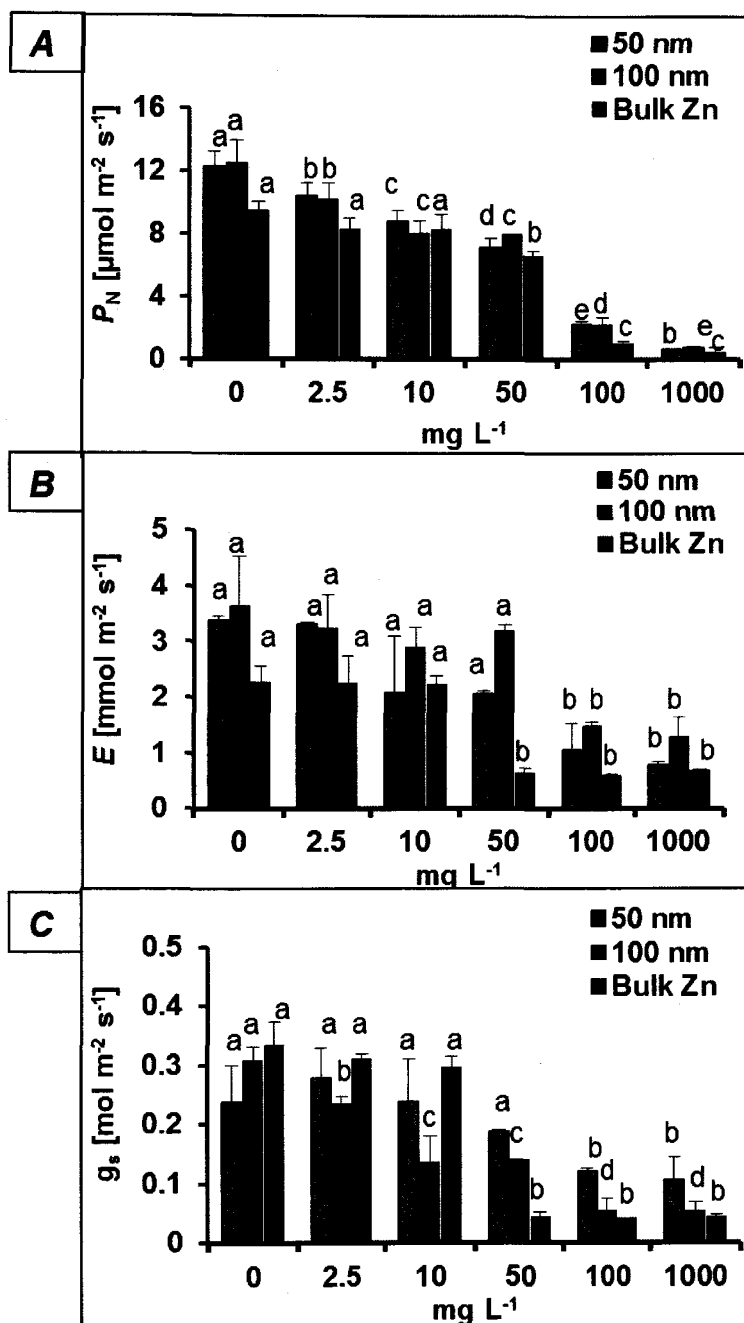


Fig 3.11.2. Photosynthetic rate (P_N ; A), transpiration rate (E ; B), and stomatal conductance (g_s ; C) of rice plants treated with ZnO (<50, 100 nm) NP and bulk Zn. Bars represent mean values \pm SD ($n=5$). Bars denoted by the *same letter* indicate insignificant difference at $p \leq 0.05$.

<50 nm size. The results show that photosynthesis was greatly affected in plants treated with bulk Cu and Zn as compared to CuO and ZnO NPs.

Most importantly, lipid peroxidation, indicative of oxidative damage was observed only on treatment with bulk Cu with no significant increase in lipid or protein oxidation with CuO NPs (Fig 3.11.3 A). Bulk Cu exposure led to an increase of MDA content by 27% at 1000 mg L⁻¹ but no change on treatment with CuO NPs (Fig 3.11.3 A). Likewise, bulk Zn, increased MDA content (25%) at high concentration while ZnO NPs of both sizes did not show any change in MDA content at all concentrations (Fig 3.11.3 E).

Proline, an osmolyte and osmo-protectant, increased gradually by 3.4-fold up to 100 mg L⁻¹ of bulk Cu treatment compared to a maximum increase of 2.5-fold seen at 1000 mg L⁻¹ of CuO NPs (Fig 3.11.3 B). Bulk Zn and ZnO NPs of both sizes showed an increase in proline content with increase in the respective concentrations (Fig 3.11.3 F). Bulk Zn increased by 4.3-fold (433%) at 1000 mg L⁻¹, while ZnO NPs of <50 nm and 100 nm size resulted in an increase of 2.65-fold (266%) and 2.1-fold (217%) respectively (Fig 3.11.3 F). Ascorbic acid, a non-enzymatic anti-oxidant showed an increase of 20% at 100 mg L⁻¹ of bulk Cu treatment while CuO NP exposure led to an increase of only 10% at 1000 mg L⁻¹ (Fig 3.11.3 C). On the other hand, ZnO (100 nm) NPs resulted in increased ascorbate content at 1000 mg L⁻¹ by 24% compared to control. Superoxide dismutase (SOD) activity increased by 34% at 1000 mg L⁻¹ of bulk Cu but SOD activity did not show any change upon CuO and ZnO NP treatment (Fig 3.11.3 D). The results show that bulk metals resulted in far greater oxidative damage in rice indicated via increased lipid peroxidation and SOD activity in case of CuO NPs and ZnO NPs. Higher osmotic stress as a result of bulk metals indicated by increased proline content was observed compared to MNPs (Fig 3.11.3 B, F).

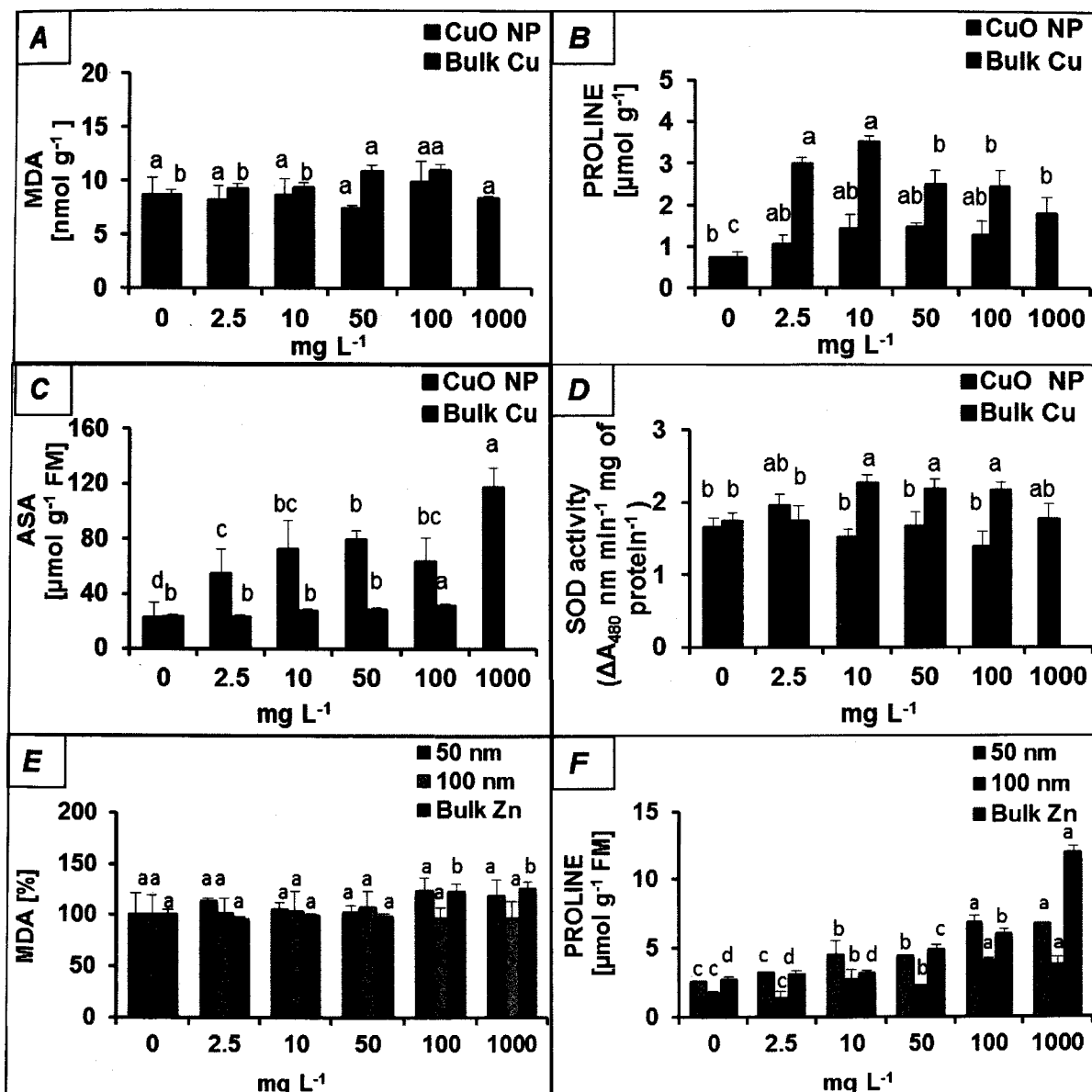


Fig 3.11.3. Malondialdehyde (A), proline (B), ascorbate (C) content and superoxide dismutase activity (D) of rice plants treated with CuO NPs and bulk Cu; Percent MDA content (E) and proline content (F) of rice treated with ZnO NPs and bulk Zn. Bars represent mean values \pm SD ($n=5$). Bars denoted by the same letter indicate insignificant difference at $p \leq 0.05$.

3.12. Summary of Results

This research work has highlighted findings that have gained insight into the phytotoxic effects of metallo-NPs. In this study, it was seen that MNPs did not significantly affect seed germination rate but decreased shoot, root length and biomass. Chlorosis of leaf and necrosis at the tip was observed at higher concentration. An increase in the number of trichomes and decrease in the number and size of stomata was observed due to MNP treatment. The treatment resulted in increased accumulation of Cu and Zn in leaves and root observed in a dose-dependent manner. The accumulation of MNPs was several folds higher in roots than seen in leaves. CuO and ZnO NPs were found to accumulate inside the cell, in cytosol and organelles of both leaf and root in the form of clusters. Accumulation of MNPs in the leaves was observed in chloroplasts and resulted in destacking of thylakoid membranes (decreased number of thylakoids per granum) and distortion of thylakoid membranes (wavy arrangement).

The MNPs were found to exhibit toxic effects on photosynthesis by affecting the light reaction and the carbon dioxide assimilation process. MNP treatment resulted in a decrease in the maximum quantum efficiency of PSII (F_v/F_m ratio), photochemical quenching (q_p) and photosynthetic pigment content with an increase in the non-photochemical quenching (q_n). However, MNPs at concentration of 2.5 mg L^{-1} were found to be beneficial to photosynthesis and photosynthetic pigments.

In the present study, plants did not show any oxidative damage to lipids and protein due to MNP treatment but experienced osmotic damage with both MNPs as indicated by increased proline content in treated plants. This observation of no oxidative damage due to the treatment is also substantiated by insignificant increase in the activity of superoxide dismutase (SOD)

and only slight increase in ascorbate content, a non-enzymatic antioxidant at higher CuO NP concentration. However, an increase in the expression level of superoxide dismutase (SOD), ascorbate peroxidase (APX) and Glutathione reductase (GR) was observed with both CuO and ZnO (100 nm) NP but in a dose independent manner. Expression level of phytochelatin (PC) was also studied and was found to be significantly higher at the highest concentration of MNPs. Likewise, polyamines (PA), spermine also increased as a result of CuO NP treatment but decreased in plants treated with ZnO NPs.

Comparative study of MNPs and its bulk counterparts revealed that bulk metals released large amounts of metal ions, compared to the minute quantity released by MNPs, which resulted in generation of ROS causing greater oxidative and osmotic stress and relatively higher negative effect on plant growth processes than observed with MNPs.

CHAPTER

4

DISCUSSION



To raise new questions, new possibilities, to regard old problems from a new angle, require creative imagination and marks real advance in science.

-----**Albert Einstein**

DISCUSSION

TABLE OF CONTENTS

Sr.No	Title of the topic	Page No.
4.1	Dissolution of MNPs in aqueous medium	129
4.2	Plant growth and Biomass	132
4.3	External leaf and root morphology	135
4.4	Internalization and uptake of MNPs	136
4.5	Photosynthesis	140
4.6	Oxidative damage	144
4.7	Conclusion	150

Nanotechnology is one of the rapidly developing industries, owing to their wide applications and unique properties. Over exploitation of metal oxide nanoparticles results in their subsequent release into the environment entering the food chain through plants into humans with consequences unknown, hence it is quintessential to elucidate the impact of the NP size and concentration on plants. The present investigation was conducted in order to assess the effect of CuO and ZnO NP and their threshold level on various physiological, biochemical and molecular parameters in *Oryza sativa* var. Jyoti as studies have shown that behaviour of nanoparticles varies among plant species. Limited information is available on the phytotoxic effect of NPs and their threshold level in crop plants in general and rice in particular.

4.1. Characterization and Dissolution of MNPs in Aqueous Medium

Size of the MNP in powdered form was found to be more or less same as given by the supplier's specification. However, their size in nutrient solution was found to be larger probably due to formation of agglomerates. The greater hydrodynamic diameter (size) of MNPs observed using DLS revealed that MNPs on interaction with the components of the nutrient medium were able to form larger sized nanoparticles either by agglomeration or aggregation depending on the elemental form. The nanoparticles used in this study had distinguishable grain boundaries as observed in the SEM images (Fig 3.1). Agglomerates are a group of primary particles gathered by weak Van der Waals forces and aggregates are referred to as a lump of nano sized particles held by the strong chemical bonds and nanoparticle in nutrient solution can form both agglomerate as well as aggregates (Kim et al., 2012b). They also reported that NPs could deagglomerate upon interaction with the biological system (root) and that the nanoparticles retain its physicochemical properties upon such an interaction. In our study, we had a clear solution up to 50 mg L⁻¹ concentration, however, concentration at

100 mg L⁻¹ showed slight turbidity and solution at 1000 mg L⁻¹ showed deposition of MNPs on surface of root and vessel probably indicating agglomeration formation of MNPs up to 100 mg L⁻¹ concentration and aggregation formation at the highest concentration.

Dissolution refers to the release of ions from metal oxide nanoparticles (MNPs) in aqueous solution as MNPs are known to exhibit toxic effect either as a consequence of metal ion released from MNPs or as MNPs itself or both. The actual reason of phytotoxicity to plants based on the literature currently available is rather unpredictable, therefore, in order to answer the question, MNP dissolution study was carried out to confirm whether the negative effect was due to MNP per se or due to their ions or both. Our results showed (Table 3.2) that CuO NP dissolution in Hoagland's solution at highest concentrations were very small on percent (0.12%) as well as on weight basis (1.16 ± 0.09 mg L⁻¹) in comparison to its bulk counterpart (8% and 80.76 ± 2.56 mg L⁻¹ respectively). There was no much difference in ionization value at low and high concentration of CuO NP as was seen with ZnO NP which at low concentrations (below 10 mg L⁻¹) released more or less same amount of ions on percent (13% and 20% respectively) and weight basis (1.3 ± 0.02 mg L⁻¹ and 2.0 ± 0.001 mg L⁻¹). However, at highest concentration the dissolution of ZnO NP was considerably less in percent basis (1.2%) and weight basis (12.1 ± 0.05 mg L⁻¹) as compared to the much higher dissolution value for the bulk metal (23% and 230 ± 0.07 mg L⁻¹; Table 3.2). Our data also indicates that MNP size may play a role in dissolution as 50 nm size ZnO NPs showed relatively lesser ionization at all concentrations as compared to 100 nm size ZnO NPs (Table 3.2). Low level of dissolution of MNP is also supported by our results with lipid peroxidation and protein oxidation as ions released by the NPs were insufficient to cause oxidative damage (Fig 3.8.1 & 2). On the other hand, bulk metal (CuSO₄) caused significant amount of peroxidation of lipids (Fig 3.11.3 A) and oxidation of protein (data not shown). Our results suggest that the

no changes as it is mentioned.

physiological, biochemical and molecular changes observed in this study was predominantly due to metal oxide nanoparticle and not due to the ions (Table 3.2). Our data with higher concentration of Zn bulk metal showed lesser peroxidation of lipids which could be due to zinc divalent ions being in stable state without undergoing redox reactions thereby preventing oxidative damage as well as ion leakage (Tavallali et al., 2010). The observed insignificant release of ions from MNPs as compared to its bulk counterpart could be due to the physicochemical characteristics of NPs such as shape, size and surface charge (Thul and Sarangi 2015). pH and ionic strength of the nutrient medium could also influence increased agglomeration and aggregation of MNPs consequently lowering MNP dissolution (Thul and Sarangi 2015).

It has been reported that MNPs on their own without dissociating into its ion can affect growth in several plants (Lee et al., 2008; Lee et al., 2013; Lin and Xing 2008). Lee et al. (2008) reported that phytotoxicity observed in *Triticum aestivum* (wheat) and *Phaseolus radiates* (mung bean) was due to Cu NPs and not due to solubilized cupric (Cu^{2+}) ions. In another study with buckwheat Lee et al. (2013) showed that CuO and ZnO NPs solely reduced root length and biomass of seedlings as they measured the concentration of metal ions released from ZnO and CuO NP suspension of 4000 mg L^{-1} concentration and observed the ion concentration to be only 1.5 mg L^{-1} and 4.6 mg L^{-1} respectively. Report by Lin and Xing (2008) also showed that phytotoxicity in ryegrass was due to Zn nanoparticles and not by solubilized Zn^{2+} ions as the ions ($< 8 \text{ mg L}^{-1}$) were not sufficient to cause the negative effect on growth. In a similar study with ZnO NPs, Ghodake et al. (2011) also showed that phytotoxicity to growth in *A. cepa* was attributed to ZnO NP accumulation. However, there are reports which suggest that the effect on growth and germination is due to dissolution of ions from MNP. Perreault et al., (2010) in a study with CuO NPs reported that the cause of

toxicity in *Lemna gibba* was due to release of Cu^{2+} . Lalau et al. (2015) in *Landoltia punctata* and Saison et al. (2010) in *C. reinhardtii* also reported phytotoxicity of CuO NPs due to their ions. Likewise, Lee and An (2013) also attributed toxicity to green algae *Pseudokirchneriella subcapitata* due to free dissolved zinc ions. In another study Navarro et al. (2008b) reported that AgNPs produced solubilized Ag^+ that affected the photosynthetic yield of *C. reinhardtii*.

Our study with CuO and ZnO NPs on various physiological and biochemical parameters showed a dose dependent toxicity and the effect was due to the metal particle itself and not due to its ions. However, work by Lin and Xing, (2008) suggests that whether the phytotoxicity of NPs is due to NP or its ions is largely dependent upon the metal involved as well as the physical and chemical properties of NPs.

4.2. Plant growth and Biomass

Negligible effect of CuO and ZnO NPs on seed germination observed in this study (Table 3.3.1-3) may be due to non-permeation of MNPs through the seed coat as seed coat exhibits selective permeability that protects the embryo from MNP toxicity by restricting the entry of NPs during germination and allows the entry of MNPs through the emerging radicles in the growth medium. A slight decrease (6-7%) in seed germination at the highest concentration of CuO NPs observed in this study may be due to the physical adsorption of NPs to the seed coat surface restricting the uptake of water and nutrients thus causing inhibition of germination. The physical adsorption of NPs to the seed coat surface could be due to its rough surface or due to electrostatic or hydrophobic interactions between NP and seed coat as a result of variations in the lipid content and cutinisation of the seed coat. Insignificant change in seed germination due to MNP has been reported by others. Stampoulis et al. (2009) in *Cucurbita pepo* reported that Cu NPs and ZnO NPs at 1000 mg L^{-1} did not affect seed

germination. Lee et al., (2010), using 400- 4000 mg L⁻¹ of aluminium oxide (~150 nm size), silicon dioxide (42.8 nm size) and magnetite (<50 nm size) NPs in *Arabidopsis thaliana* also observed no inhibition of seed germination. Boonyanitipong et al., (2011) in rice at 10-1000 mg L⁻¹ and Lin and Xing (2007) in radish, rape, lettuce, and cucumber at 2000 mg L⁻¹ also showed no inhibition of seed germination due to ZnO NPs treatment. A few reports, however, observed inhibition of seed germination. Shi et al. (2011) using as little as 1 mg L⁻¹ concentration of CuO NPs in duckweeds (*Landoltia punctata*) and Lee et al. (2013) using 4000 mg L⁻¹ of CuO NP in buckwheat (*Fagopyrum esculentum*) showed inhibition to seed germination. The result indicates that seed size and plant species and its sensitivity along with factors such as elemental composition, particle size and concentration of MNPs may be a reason for the variation in seed germination.

The reduction in shoot, root length and shoot biomass observed in our study (Table 3.3.1- 3) indicate that the MNP treatment resulted in growth restriction. The decrease in root, shoot length and biomass is due to the negative effect on photosynthesis as we observed considerable decrease in quantum efficiency of photosynthesis (Fig 3.6.1- 3) as well as CO₂ fixation (Fig 3.5) as a result of the MNP treatment. Uptake of metallo nanoparticles can cause damage to the roots by inhibiting its elongation due to its accumulation in cytosol as well as nucleus as reported by Ghodake et al. (2011). The accumulation of MNP is also reported to cause membrane damage affecting physiological processes associated with the membrane such as photosynthesis and ion transport, leading to inhibition in root length and biomass followed by cell death (Shen et al., 2010). Slight increase observed in root fresh mass (RFM) at highest concentration of CuO NP (Table 3.3.1) could be due to CuO NP forming agglomerates or aggregates at 1000 mg L⁻¹ concentration adhering to roots adding to RFM despite roots being washed thoroughly in running water prior to weighing. The greater RFM at 1000 mg L⁻¹ CuO

NP treatment is associated with comparatively low accumulation of Cu NP at 1000 mg L⁻¹ than seen at 100 mg L⁻¹ as CuO NP seems to aggregate at 1000 mg L⁻¹ concentration and thereby prevent their intake by the plants resulting in low toxicity and better growth seen as higher RFM at 1000 mg L⁻¹ concentration of CuO NP. Considerably less aggregation was observed with ZnO NPs therefore there was a gradual increase in accumulation of Zn NP in roots and no change in the RFM/RDM upon ZnO NP treatment.

Others have also shown decrease in shoot, root length and biomass due to various MNPs. Lidon and Henriques (1998) showed reduction in rice shoot and root length upon much lesser concentration (1.25 mg L⁻¹) of Cu NPs. Lin and Xing (2007; 2008) reported significant decrease in root and shoot length in *Brassica napus* (rape), *Lolium perenne* (ryegrass), *Lactuca sativa* (lettuce), *Raphants sativus* (radish), and *Cucumis sativus* (cucumber) due to ZnO NP at a range of 20-2000 mg L⁻¹ concentration. Stampoulis et al. (2009) showed that CuO NPs decreased root length and biomass in *C. pepo* at 1,000 mg L⁻¹ concentration whereas López-Moreno et al. (2010) observed decreased root length in *Glycine max* at 4000 mg L⁻¹ of ZnO NPs. Manzo et al. (2011) showed that plants such as *Lepidium sativum* and *Vicia faba* grown in ZnO NP contaminated soil sample containing 230 mg Zn kg soil⁻¹ also resulted in reduced root length. Boonyanitipong et al. (2011) also showed decline in root elongation of *Oryza sativa* grown with 100-1000 mg L⁻¹ ZnO NPs. Lee et al. (2008) showed that Cu NP also caused a reduction in the growth and biomass of *P. radiatus* and *T. aestivum* by 65% and 75% at 1000 mg L⁻¹ respectively. Musante and White (2012) also reported a reduction in *C. pepo* growth and transpiration by 60–70% due to the CuO NPs. Wang et al. (2015) reported an 80% reduction in plant biomass and photosynthesis of *Arabidopsis* seedlings when exposed to ZnO NPs at 300 mg L⁻¹. Zhao et al. (2013) also showed a decline in the root and shoot biomass of corn (*Zea mays*) exposed to ZnO NPs at 400 and 800 mg kg⁻¹ concentration. The changes in

root biomass observed were different for both MNPs (CuO and ZnO NPs), irrespective of size, indicated that the impact was mainly due to the elemental form of MNPs.

4.3. External Leaf and Root Morphology

The decrease in the number and size of stomata and increase in the number and size of trichomes as a result of MNP exposure (Fig 3.3.3 & 4) reveals that MNP treatment were able to cause morphological changes which are similar to changes generally seen under drought conditions. We also show, for the first time, variation in the size of cuticular papillae (CP, a specialized cell structure composed of lignin that densely cover adaxial and abaxial surfaces of leaves; Golam and Arshad 2002; Fig 3.3.3-4 *E-F*) due to the MNP treatment which may be an adaptive process of rice plants against biotic and abiotic stresses to prevent water losses (Yoji et al., 1983).

The external morphological damage to the roots (Fig 3.3.3 & 4 G-I) upon exposure to CuO and ZnO NPs may be due to NP adherence to the root surface, forming agglomerates or aggregates, blocking root pores resulting in limited water uptake and nutrients. Limitation of water absorption is also supported by plants experiencing osmotic stress during the treatment as seen by greater accumulation of proline (Fig 3.8.3). This may lead to development of lateral root and greater root hair density (Fig 3.3.6 *E & e*), simultaneously causing reduction in root elongation in order to compensate for water and nutrient uptake to some extent (Table 3.3.1-3). The importance of root hairs in water and nutrient uptake has been documented during osmotic and metal stress; however, studies on the changes in external morphological structures in response to MNP stress are limited. García-Sánchez et al. (2015) showed that *A. thaliana* exposure to Ag-NPs, TiO₂ anatase-NPs and COOH-functionalized, multi-walled PELCO® Carbon Nanotubes affected the root epidermal cells leading to increased root hair formation

while repressing root-hair-specific genes using transcriptome analysis. Wang et al. (2013) reported that when second generation plants were grown from seeds of CeO₂ NPs (10 mg L⁻¹) treated plants, it developed extensive root hairs compared to control. Others have shown decrease in root structure by interference with root development. For instance, Lee et al. (2013) showed that CuO and ZnO NPs altered the root tip morphological features resulting in shorter and fewer hairs at concentrations of 2000- 4000 mg L⁻¹ in buckwheat, *Fagopyrum Esculentum* and suggested that intracellular localization of MNPs could be associated with NP induced structural alterations of the cellular cytoskeletal network, thereby translating local signalling events for root initiation and maintenance of root tip growth. Yin et al. (2011) also showed that seedlings of *Lolium multiflorum* treated with gum Arabic-coated AgNPs at 40 mg L⁻¹ caused complete inhibition of root hair development reducing gravitropism in roots inducing cell apoptosis and disruption of auxin transport which is essential for root growth. Pokhrel and Dubey (2013) showed that corn (*Zea mays*) roots exposed to ZnO NPs at 1000 mg L⁻¹ did not affect the root hair density but resulted in root damage by pocket formation (called “tunnelling-like effect”) at the primary root tip as a result of cell dissolution.

4.4. Internalization and uptake of MNPs

The increased accumulation of Cu and Zn observed in whole leaves and root tissue upon exposure to CuO and ZnO NP in this study indicates a dose-dependent uptake of MNPs by the plant (Table 3.4.1 & 2) Entry of NPs through plant roots can occur via several plausible routes like admission through intercellular plasmodesmata or via the symplastic route due to capillary forces, osmotic pressure and through diameter (5- 20 nm) of cell wall pores (Navarro et al. 2008a). Metallo-nanoparticles could also enter roots through apical meristematic tissue more effectively due to greater flexibility of pore size, a mechanism found to be dominant in the

translocation process of metal complexes (Nowack et al., 2006). Navarro et al. (2008a) have also reported that association of NP with root can also influence size of pores to facilitate their uptake. Accumulation may also occur due to large amount of mucilage secreted by the root tips and hairs contributing to the adsorption of NPs (Zhang et al. 2011). Formation of lateral roots also creates new absorbing surfaces and even provides an additional pathway for MNPs to enter the stele (Zhang et al., 2015) as differentiation of these roots allows penetration of NPs into the root epidermis reaching the vascular cylinder (Peret et al., 2009). Less accumulation of Cu observed in this study at 1000 mg L⁻¹ concentration of CuO NPs compared to 100 mg L⁻¹ could be due to a portion of NPs forming agglomerates/ aggregates due to high concentration or due to greater damage to the roots by “tunnelling-like effect” at the root tips reported by Pokhrel and Dubey (2013). However, relatively greater accumulation of Cu observed at 1000 mg L⁻¹ concentration, despite greater damage to root, than in control could be explained by development of lateral roots and higher density of root hairs in the roots observed at highest concentration grown plants (Fig 3.3.6 E, e). Decreased translocation of MNPs from roots to leaves was observed as can be seen by much lesser accumulation of MNP in shoot than in root (Table 3.4.1 & 2). This dichotomy in accumulation at root and leaves indicates an exclusion mechanism adapted by the rice plant to prevent translocation of MNP from root to more sensitive parts such as leaves where physiological processes take place. Our data suggests that transport of MNPs from the roots to the shoots is greatly minimized by major accumulation of MNPs in root organelles such as cytosol, intracellular space and cell wall (Fig 3.4.1 J, K L & Fig 3.4.2 J, K L) thereby allowing only a small portion of absorbed NPs to be transported to the shoots. Our data also shows cluster formation of CuO and ZnO NPs in root cell thereby accumulating most of the MNPs in the cell (Fig 3.4.1 J, K L & Fig 3.4.2 J, K L) rendering them immobile for further transportation to the shoot. It is reported that

metal may precipitate in root cell due to formation of metallo-complex as a result of ligands with organic molecules such pectin in the cell wall and with citrate, malate, in addition to, high affinity chelating compounds derived from nicotinamide, phytosiderophores and peptides such as metallothioneins (Alvarez- Fernandez et al., 2014; Vaculik et al. 2012). Once absorbed by the roots or bound to organic compounds, all NPs may not be available for transportation to shoots as they may be stored in root cell itself by sub-cellular compartmentalization and sequestration (Rico et al., 2011) which explains relative higher MNPs in roots than in leaves. Likewise, the metal transporters such as Metal Transporter 3 (MTP3), Zinc-Induced Facilitator 1 (ZIF1), Vacuolar Iron Transporter 2 (VIT 2), Cation Exchanger 4 (CAX 4) and Copper Transporters 5 (COPT 5) are present on the xylem parenchyma cells or phloem companion cells, may also help in MNP unloading from xylem and phloem redistributing it back to the root (Peng and Gong 2014), however, we have not studied this aspect.

Based on the level of MNP uptake in this study we may suggest an order of accumulation as ZnO (100 nm) > CuO NP (50 nm) > ZnO NP (50 nm). This may be due to the difference in colloidal stability, surface area and aggregation state of larger sized MNPs compared to smaller sized MNPs, increasing cell wall permeability by creating “holes” through enlargement of pore size to a greater extent than small sized MNPs which could then easily diffuse through these holes via interaction with cell-wall proteins and polysaccharides (Fleischer et al., 1999). There are limited studies on accumulation and translocation of MNP in plants. Lin and Xing (2008) reported absorption and aggregation of ZnO NPs on the root surface of *Lolium perenne* (ryegrass) leading to its subsequent internalization. Hernandez-Viezcas et al. (2011) showed that ZnO NP accumulated in the vascular system of roots and

leaves of *Prosopis juliflora-velutina* (velvet mesquite) using K-edge μ XANES and μ XRF as a result of ZnO NP adsorption on the root surface.

Uptake and accumulation of MNPs in leaves and roots confirmed using AAS were than further investigated to study the accumulation of MNPs on the internal morphology of rice plants. Decrease in cell size and number of chloroplasts and increase in number of mitochondria observed at high concentration (50 mg L^{-1} and above) of MNP in our study suggest decreased photosynthetic activity and increased cost of cell maintenance under the treatment. The accumulation of CuO and ZnO NPs was observed in chloroplasts which caused decrease in number of thylakoids per granum and distortion (wavy arrangement) of the thylakoid membrane as well as swelling of the intra-thylakoidal space upon MNPs exposure (Fig 3.4.1 I). This is first time observation of such distortion and swelling of thylakoids in rice chloroplast as a result of the NP treatment. The decline in the number of thylakoids per grana is considered to be a result of reduced amount in PSII-LHCII complexes which play a crucial role in light-harvesting as well as ultrastructural organization of thylakoids. Decreased LHC molecules might have prevented over-energization (over reduction) lowering the chances of ROS formation and thereby preventing oxidative damage to plants. Absence of ROS formation in this study is also suggested by absence of lipid peroxidation (Fig 3.8.1) and protein oxidation (Fig 3.8.2). However, at concentration of 2.5 mg L^{-1} of MNPs, the effect was slightly beneficial as number of chloroplast in mesophyll cells increased and this was also supported by significant increase in photosynthetic pigments observed at the same concentration of the NP treatment. The negligible effect of MNPs to bundle sheath cells as compared to mesophyll cells revealed that the mesophyll cells were highly susceptible to MNP attack as compared to bundle sheath cells (Fig 3.4.1 & 2). This may be due to the presence of thylakoid membrane in mesophyll cells which is then structurally and functionally affected

no changes as it is explained.

due to the accumulation of MNPs. It was also observed that CuO NPs resulted in greater damaging effect on the chloroplast as compared to ZnO NPs, although, accumulation of ZnO NPs was higher than CuO NPs in leaves. This may be because Cu acts as a cofactor in many photosynthetic enzymes and can substitute the central Mg ion of chlorophyll as a damage mechanism leading to inhibition of photosynthesis, in addition to, playing an important role in the ultrastructural organisation of the thylakoid membranes (Yruela 2009).

There are only a few studies on the effect of MNP on internal morphology. Nhan et al. (2015) reported alterations to chloroplast due to the accumulation of aggregated CeO₂ NPs (100 and 500 mg L⁻¹) in the cytosol of leaf cells and on the outer membrane of the chloroplasts which appeared to be swollen and ruptured in case of conventional and Bt-transgenic cotton. Some report show accumulation of MNP in the internal organelles without any structural alteration. Lee et al. (2013) showed the presence of CuO and ZnO NPs in root cells of buckwheat, *Fagopyrum Esculentum* at 500 mg L⁻¹. Lee et al. (2008) also showed significant uptake of Cu NPs in the cytoplasm and cell wall of the root cell of *P. radiatus* and *T. aestivum* at 1,000 mg L⁻¹. Similarly, Lin and Xing (2008) reported the presence of ZnO NPs using EM in the nuclei, apoplast and cytoplasm of endodermal cells in *Lolium perenne* (ryegrass) at 1,000 mg L⁻¹. Also, Lidon and Henriques (1998) showed accumulated Cu in vacuoles of rice leaves at concentrations of 0.01 and 1.25 mg L⁻¹ Cu NP in plants treated with 0.002- 1.25 mg L⁻¹. However, there are enough reports of the effect of heavy metals on changes in internal morphology of plants. A review by Solymosi and Bertrand (2012) described the structural alteration in the chloroplast due to heavy metals such as Cd, Cu, Hg, Mn, Ni, Pb and Zn. Todeschini et al. (2011) also showed that Zn altered the ultrastructure of leaves of *Populus alba* at 300 mg Kg⁻¹ by reducing the number of chloroplasts per cell in palisade tissue, increasing starch granules and showing presence of autophagic vacuoles and

mitochondria with cristae. Likewise, Izaguirre-Mayoral and Sinclair (2005) observed severe ultrastructural damage to chloroplast of soybean upon Mn exposure causing destacking and enlargement of non-appressed lamellae increasing the lipid bodies while simultaneously causing depletion of starch grains in the cells. Swollen pro-thylakoids in the plastids with criss-crossing stromal strands in newly formed thylakoids was also shown by Abdelkader et al. (2007) in leaves of *Triticum aestivum* upon treatment with NaCl (600 mM).

4.5. Photosynthesis

The decline observed in the net photosynthetic rate (P_N) at the highest concentration of MNPs (Fig 3.5) may be due to the damage caused to thylakoid membrane as a result of the greater accumulation of the MNPs. The decrease in stacking of thylakoid membrane resulted in reduction in the photosynthetic pigments (Table 3.5.1- 3) thereby, decreasing photosynthesis. The decline in photosynthetic rate (P_N) could also be due to parallel decrease observed in transpiration (E) and stomatal conductance (g_s ; Fig 3.5). Reduction observed in net CO₂ fixation could also be associated with low frequency of number and size of stomata and stomatal closure (Fig 3.3.3- 4) which may limit carbon dioxide to chloroplast thus limiting photosynthesis and simultaneously leading to prevention of water losses. The MNP treatment may be causing osmotic stress which is indicated by increased proline levels observed in this study (Fig 3.8.3). Suppression of net photosynthesis and transpiration by MNPs has been reported by a few researchers. Nekrasova et al. (2011) showed that CuO NPs reduced net photosynthesis through loss of Chl and Car in *Elodea densa* at concentration of 0.5- 5 mg L⁻¹. Likewise, Shi et al. (2011) reported a decrease in photosynthesis due to reduction in content of photosynthetic pigments in *Landoltia punctate*, duckweeds upon exposure to 1 mg L⁻¹ CuO NPs. Musante and White (2012) documented a decline in biomass and transpiration of yellow

squash (*C. pepo*) upon treatment with Cu NP (<50 nm) and Ag NPs. Reduced photosynthesis has also been reported with heavy metals. For instance, Alaoui-Sosse et al. (2004) reported a decrease in net photosynthesis and stomatal conductance in cucumber upon 20 mg Kg⁻¹ bulk copper exposure. In a similar study, Pietrini et al. (2003) showed a decrease in the net CO₂ assimilation rate and transpiration in *Phragmites australis* treated with 50 -100 µM Cd.

The decrease observed in quantum efficiency of light reaction of photosynthesis indicated by the reduction in F_v/F_m ratio, photochemical quenching (q_p) and non-photochemical quenching (q_N ; Fig 3.6.1- 3) may also be largely due to the reduction in the number of thylakoids per grana (Fig 3.4.1 & 2) which may lead to alteration in size of LHC and thereby decline in the photosynthetic pigments upon accumulation of Cu and Zn in leaf tissue (Table 3.5.1- 3). Increased Chl *a/b* ratio observed in this study reveals that Chl *b* is more sensitive to MNP exposure than Chl *a*, resulting in compromised light absorbing efficiency of PSII thus reducing F_v/F_m ratio as seen in this study (Fig 3.6.1-3). In addition to decrease in photosynthetic pigments, the decrease in photochemical efficiency of photosynthesis (q_p) could also be due to the functional replacing of Mg²⁺ with Cu and Zn ions (Vinit-Dunand et al., 2002). Decreased F_v/F_m ratio was largely due to decreased F_m as F_o remain constant, indicating no significant change in the arrangement and orientation of pigments in LHC but overall decrease in the pigment content. The decrease in F_m may also indicate low efficiency of energy transfer to the reaction centre due to effect on PS II apparatus itself (32 kDa protein; Kumar and Prasad 2015). Study of light reaction of photosynthesis in plants upon MNP treatment is still in its infancy. Saison et al. (2010) in *Chlamydomonas reinhardtii* showed that core-shell CuO NPs at 4- 20 mg L⁻¹ had a deteriorative effect on the Chl content which resulted in decrease in F_v/F_m and q_p and increase in q_N . Our data also indicate that the MNP treatment resulted in destacking of thylakoid membrane which may lead to smaller LHC and

low pigments resulting in low F_v/F_m and q_p . Perreault et al. (2010) also reported that *Lemna gibba* on exposure to 100- 400 mg L⁻¹ of CuO NPs showed inhibition of maximal PSII fluorescence yield (F_v /F_m), maximum fluorescence yield of PSII at steady-state of fluorescence (F'_v /F'_m) and photochemical quenching (q_p) with increase in the non-photochemical quenching (q_N). Decline in PSII activity due to heavy metal stress has also been reported. Cambrollé et al. (2011) showed that bulk Cu reduced quantum efficiency of PSII thereby limiting net photosynthesis rate in yellow horned poppy, *Glaucium flavium* Crantz and suggested that decreased photochemical quenching (q_p) as a result of metal toxicity was due to chronic photo-inhibition, damaging the photosynthetic apparatus by indirectly interfering with the Ca²⁺ ions. Todeschini et al. (2011) showed that *Populus alba* exposed to Zn heavy metal decreased the PSII activity and suggested that the decline was mainly due to reduction of D1 and D2 protein expression. Chugh and Sawhney (1999) showed that Cd treatment to peas decreased expression level of genes required for carbon assimilation (ribulose-1, 5-bisphosphate carboxylase, NADP-glyceraldehyde-3-phosphate dehydrogenase, fructose-1, 6-bisphosphatase and NADP-malate dehydrogenase) processes. In contrast to decrease in photosynthetic pigments at high concentration of MNP in our study we also observed an increase in pigment contents at low concentrations of MNPs (Table 3.5.1- 3). The increase in photosynthetic pigments at low concentration may be explained due to Cu and Zn being essential micro nutrient required for many physiological processes such as photosynthetic electron transport, mitochondrial respiration, oxidative stress responses, cell wall metabolism, hormone signalling (Yruela, 2005) and biosynthesis of plant pigments by Zn (Aravind and Prasad 2004b).

Reports on decline in photosynthetic pigments due to MNPs are limited but enough work on effect of heavy metals on pigments has been done. Dimpka et al. (2012) showed that

chlorophyll content of wheat was significantly reduced with 500 mg Kg⁻¹ of both CuO and ZnO NPs exposure. Likewise, chlorophyll content in *Scenedesmus obliquus* was reported to be reduced due to SiO₂ NPs (10-20 nm) by Wei et al. (2010). In contrary to our results at high concentration of the MNP, Prasad et al. (2012) using ZnO NPs at a concentration of 400-2000 mg L⁻¹ and Sharma et al. (2012) using Ag NPs at a concentration of 100 mg L⁻¹ showed an increase in the pigment content in peanut and *Brassica juncea* respectively. Work on effect of heavy metals on pigments has been documented in a review on the subject by Solymosi and Bertrand (2012). They reported that excess heavy metals including Cu and Zn directly interact with pigment biosynthesis leading to pigment degradation and could also result in replacement of Mg in Chl. They also reported that heavy metal may damage chloroplast membrane structure, alterations in grana stacking as well as inactivation or loss of function of essential enzymes, and uptake of other essential elements such as Fe and Mg, thereby negatively affecting photosynthesis.

4.6. Oxidative damage

In addition to Mehler reaction, ionic form of metals are known to cause oxidative stress in plants through generation of ROS via Haber–Weiss reaction or Fenton’s reaction affecting cellular processes by causing lipid peroxidation (LPO), oxidizing proteins and damaging nucleic acids (Gill and Tuteja 2010). However, in the present study uptake and accumulation of CuO and ZnO NPs did not cause any oxidative damage indicated by the absence of lipid peroxidation (Fig 3.8.1) and protein oxidation (Fig 3.8.2). Also, decrease in the pigment content (Table 3.5.1- 3) and significant destacking of thylakoid membrane (Fig 3.4.1 & 2) seen in our study is a direct indication of smaller light harvesting complex which may also prevent over-energization of the PSII system and generation of free radicals through

Mehler reaction and which may be reason for observing no oxidative damage to lipids and protein in this study. Insignificant lipid peroxidation observed in our study could be due to the existence of MNPs as biological inert forms that do not initiate a response or interact with biomolecules or non-redox forms of MNPs that cannot undergo oxidation-reduction reactions due to its lack of electron transfer abilities, unsuitable for the generation of excess metabolic ROS to cause oxidative damage. Similar observation of no oxidative damage to plants by NP was also reported by Foltete et al. (2011) working with TiO₂ nanocomposites (ATN) in *V. faba*. Ma et al. (2010) showed that In₂O₃ NPs (0–1,000 mg L⁻¹) also did not induce lipid peroxidation due to low dissolution of NPs in *A. thaliana*. Also, Liu et al. (2013) showed a significant reduction in ROS and absence of lipid peroxidation with neither cell wall damage nor membrane damage with 0.01 mg mL⁻¹ water-soluble fullerene malonic acid derivative (FMAD) in root tips of *A. thaliana* seedlings and suggested that lack of lipid peroxidation may be due to disruption of auxin, abnormal cell division, and disorganization of microtubule resulted in reduced mitochondrial activity and lower ROS generation. Wang et al. (2011) also reported no peroxidation of lipids in shoots of ryegrass and pumpkin treated with Fe₃O₄ NPs (30 and 100 mg L⁻¹), however, they reported lipid peroxidation in roots and suggested that peroxidation of lipids in root may be due to blockage of aquaporins and alteration in the root respiration rate. Other studies by Song et al. (2012) also showed absence of lipid peroxidation upon treatment with nTiO₂ (200–2,000 mg L⁻¹) in duckweeds (*Lemna minor*) suspensions. Contrary to this Liu et al. (2013) with carbon nanotubes in tobacco plant cells and Faisal et al. (2013) with NiO (23.34 nm) in tomato cell suspension reported oxidative damage to the cell.

Lack of oxidative damage in our study is also supported by unaltered SOD activity observed upon MNP treatment (Fig 3.9.1 B). Significant increase in ascorbate content at the highest concentration of the MNP in this study (Fig 3.9.1 A), as well as, increased gene

expression of SOD, APX and GR at certain concentrations observed in this study (Fig 3.10 A-C) indicates protection against oxidative stress in the plants in response to MNP treatment and therefore no oxidation of lipids and proteins (Table 3.4.1 & 2). Baxter et al. (2014) suggested that ascorbate content in plants upon metal stress could increase due to the cross-talk between co-activated pathways mediated at different levels such as cross-talk mediated by ethylene, jasmonic acid and abscisic acid or the integration between diverse networks of mitogen-activated protein kinase (MAPK) and transcription factors cascades and cross-talk between different receptors and signalling complexes.

Plants antioxidant defense system include enzymatic (SOD, CAT, APX, and GR) and non-enzymatic (ASA and carotenoids) antioxidants to prevent damage due to metal stress (Gill and Tuteja 2010). SOD is a key enzyme providing the first line of defense against elevated levels of ROS and catalyses the dismutation of O_2^- into H_2O_2 maintaining intracellular O_2^- concentrations, while APX, which is present largely in the chloroplast, readily scavenges the hydrogen peroxide produced by SOD into water molecules. APX is regenerated by dehydroascorbate reductase (DHAR) through the utilization of reduced glutathione that is generated by GR (two main enzymes of the ascorbate-glutathione cycle) thus effectively reducing ROS (Rico et al., 2015).

It is generally believed that the variations in enzyme activities in exposed plants are responses to modulations in ROS concentration, however, the role of NPs on the regulation of antioxidant defense system in plants is still not clear. Reports have showed irregular and unpredictable effects of NPs on antioxidant enzyme activities with lack of information on their gene expression studies (Rico et al., 2015). Shaw and Hossain (2013) reported enhanced SOD, APX and GR activity as well increased ascorbate content in rice seedlings as a result of the CuO NPs (1.0 and 1.5 mM) upon 7d and 14d exposure. Lei et al. (2008) reported an increase

in the activities of SOD, CAT and APX in spinach upon TiO₂ NPs exposure. Similarly, Song et al. (2012) showed increased SOD and CAT in *L. minor* upon TiO₂ NPs treatment. Likewise, Foltete et al. (2011) reported decreased GR and APX activities in *V. faba* upon TiO₂ NPs exposure. Kumar et al. (2013) also showed that gold NPs increased the activity of APX, CAT, GR, and SOD in *Arabidopsis thaliana*. Morales et al. (2013) also reported elevated CAT activity in shoots and APX in roots upon CeO₂ NPs accumulation in *Coriandrum sativum* L.

Significant increase in proline content observed in this study (Fig 3.8.3) indicates osmotic stress induced by MNPs. The osmotic stress under our study is also revealed by changes in the external rice leaf morphology such as increased trichomes, decreased number and size of stomata and stomata being closed (Fig 3.3.3- 4 A-F) all being sign of osmotic stress. Reduction in the transpiration rate and stomatal conductance observed in our measurements (Fig 3.5) also suggest that the treatment signalled osmotic stress to plants. The osmotic stress may also be due to blocking of pores (Wang et al., 2012) by aggregation of MNPs specifically at higher concentrations resulting in altered plant-water potential that may limit water uptake. Small increase in proline, as a possible result of osmotic stress was probably due to hydroponic growth conditions which produce relatively less osmolyte compared to plants grown in soil (Tada et al., 2014; Claussen 2002). Proline is an osmo-protectant and a widely distributed compatible solute and osmolyte that is reported to accumulate in plants during biotic and abiotic stress. In addition to being an osmolyte proline can also act as a non-enzymatic antioxidant and is reported to effectively quench free radicals stabilizing proteins, DNA and membranes by forming stable nitroxyl radicals in the presence of hydroxyl radicals ($\cdot\text{OH}$) as well as reversible charge-transfer complexes that react directly with singlet oxygen due to its low ionization potential (Siripornadulsil et al., 2002). They also showed that high proline levels also produce increased GSH levels in a reduced environment

which facilitates sequestration of heavy metal phytochelatin conjugates in the cell inhibiting damage to lipids and proteins. The role of proline during heavy metal stress is well documented; however, there are limited reports on its significance upon MNP stress. Proline accumulation in plants due to NP has been reported by a few authors. Shaw and Hussain (2013) has reported proline accumulation in rice upon Cu NPs exposure and in faba bean (*Vicia faba* L.) seedlings upon exposure of graphene oxide (GO; size: 0.5–5 μm) nano sheets. Gunjan et al. (2014) in *B. juncea* reported a 2.9 fold increase in proline content due to 400 mg L^{-1} concentration of gold NPs. Zarafshar et al. (2015), however, showed no significant change in proline content in the two-year old wild pear (*P. biosseriana*) seedlings upon treatment with nano-SiO₂ (10-15 nm). Increased proline accumulation in response to heavy metals has been reported by several researchers (Emamverdian et al., 2015; Sun et al., 2007; Alia and Saradhi 1991).

Spermine (spm) synthesis was observed to be induced by CuO NPs but not by ZnO NPs and spermine and spermidine decreased upon treatment with both the MNP in this study reveals selective synthesis of high molecular weight polyamines (PAs) upon treatment with MNP (Fig 3.9.2). Increased spermine content observed in this study may have role as an antioxidant, however the same was not observed in case of ZnO NPs (Fig 3.8.1) which may suggest that PAs such as Spm and Spd are independent of each other with non-specific mode of actions which can vary based on the metal involved as well as plant species (Fig 3.9.2). Spm role as a free radical scavenger with singlet oxygen quenching ability, protecting DNA from ROS as decreased TBARS formation in diverse systems is reported (Ha et al., 1998 and Groppa et al., 2001). Literature revealed no published data on influence of MNP on the polyamine; however, role of polyamines as an antioxidant with metal stress has been reported with variable result. Weinstein et al. (1986) reported that Cd-treated oat seedlings showed up

to 10-fold increment in Put with a marginal rise in Spd and Spm content, whereas PAs in Cd-treated bean (*Phaseolus vulgaris*) seedlings was organ-specific, with increased Put in root, hypocotyl, and epicotyl, decreased Spm in all seedling parts and decreased Spd in leaves with no change in the roots. Jacobsen et al. (1992) also observed that chromium exposed leaves of barley and rape did not affect spm or spd contents at all but increased putrescine content depending on concentration and duration of exposure. Tadolini et al. (1984) reported that polyamines prevented lipid peroxidation of liposomes vesicles. Lin and Kao (1999) showed that copper reduced spm concentration in rice leaves with no changes in spd levels. Gong et al. (2016) reported that exogenously supplied Spd reduced oxidative stress in *Boehmeria nivea* (L.) Gaudich.

Increased levels of phytochelatin gene expression (PC) observed upon exposure to MNPs at the highest concentration (Fig 3.10 D) may be a result of plants defense mechanism to actively chelate the metal particles in leaves by compartmentalization of metal-PC complexes preventing MNP induced damage and may have bound to MNPs forming complexes in roots limiting the translocation of MNPs to the productive leaf tissue as seen with greater accumulation of MNPs in the root tissue (Table 3.4.1 & 2). PCs play an important role in heavy metal detoxification and homeostasis, sulphur metabolism and as antioxidants (Hall 2002). The defense strategies in plants particularly counteracting metal stress include specific low and moderately large sized molecules such as phytochelatins (Cobbett and Goldsbrough 2002), metallothionins (Guo et al., 2008), and other thiol rich compounds which behave as chaperons to maintain the cellular homeostasis (Nelson 1999). PC responses to MNPs are recently being investigated; however, the mechanism of detoxification though well studied with Cd, still remains unclear with MNPs. A few studies with effect of MNPs on PC has been done, however, most of the work has been done with bulk metals. In a recent study

with MNPs, Polak et al. (2014) exposed *Caenorhabditis elegans* wild-type and a metal sensitive triple knockout mutants (*mtl-1;mtl-2;pcs-1*) to ZnO NPs (0–50 mg L⁻¹) and reported that ZnO NPs were able to transcriptionally activate metallothioneins (*mtl-1* and *mtl-2*) and phytochelatin synthase (*pcs-1*) in an attempt to minimize ZnO NP toxicity. Krystofova et al. (2013) also showed significant variations in protein content, phytochelatin levels and GST activity in tobacco BY-2 cells treated with Fe₂O₃-OH and Fe₂O₃-NH₂ MNPs. Heiss et al. (2003) reported an increase in phytochelatin protein accumulation in leaves but not in roots of *Brassica juncea* they also showed that, PCs are not produced in all plants. Role of PC with heavy metal stress has been reported by various groups (Cobbett 2000; Kowshik et al., 2002; Landberg and Greger 2004).

4.7. Conclusion

In this study, the morphological, physiological and biochemical response of rice to CuO, ZnO (50 and 100 nm) NPs were investigated. The threshold of toxicity of rice plant (*O. sativa* var. Jyoti) grown hydroponically in MNPs for 30 d was studied and it was found that concentrations of 100 mg L⁻¹ and above for CuO MNPs and 50 mg L⁻¹ and above for ZnO MNPs were toxic to the plants. Size effect of ZnO (50 and 100 nm) in rice was also studied and it was observed that plants treated with ZnO NPs of 100 nm size accumulated greater amounts of Zn in leaves and roots as compared to ZnO NPs of 50 nm size and the phytotoxicity observed at high concentrations was independent of NP size. Our dissolution studies revealed that MNPs released only small amounts of ions in Hoagland's solution as compared to their respective bulk metals which suggests that the physiological, biochemical and molecular changes observed in this study was predominantly due to metal oxide nanoparticle and not as a result of ions released by MNPs. Rice was found to be a hyper-

accumulator of both CuO and ZnO NPs as they could accumulate large amounts of MNPs. Accumulation of MNPs in roots was many fold greater than in leaves. In leaves, MNPs accumulated in the chloroplast causing damage to the thylakoid structure by decreasing thylakoid stacking (number of thylakoids per granum) and causing distortion (wavy arrangement) of thylakoids and swelling of inter-thylakoidal space negatively affecting photosynthesis. The decrease in rice growth and biomass upon MNP treatment was associated with decrease in F_v/F_m ratio, q_p , P_N , E and g_s as well as reduction of photosynthetic pigments. MNPs could form aggregates at highest concentration which may block root pores resulting in limited uptake of water and nutrients inducing osmotic stress indicated by increased proline content. Morphological changes such as increased number and size of trichomes, decreased number and size of stomata, variations in cuticular papillae also suggest osmotic stress due to MNPs in this study. Absence of lipid peroxidation and protein oxidation in this study indicate no oxidative stress which may suggest absence of ROS upon MNP treatment. In addition, increase observed in the antioxidant processes (ascorbate, carotenoids, spermine, SOD, APX, GR and PC) also prevented oxidative stress by effectively inhibiting ROS generation. Increased PC gene expression at the highest concentration also shows plants defense mechanism to actively chelate the metal particles in leaves by compartmentalization of metal-PC complexes preventing further damage. Here we suggest a different mechanism of phytotoxicity and loss of plant productivity by MNPs than by bulk metal. It is suggested that MNPs affect plant productivity mainly by causing accumulation of NPs in organelles especially chloroplasts resulting in destacking and distortions in thylakoids membranes and not due to metal ions as no oxidative damage was observed. On the other hand, Bulk metal treatment released large amounts of ions as compared to MNPs resulting in ROS generation causing oxidative stress leading to loss of plant productivity.

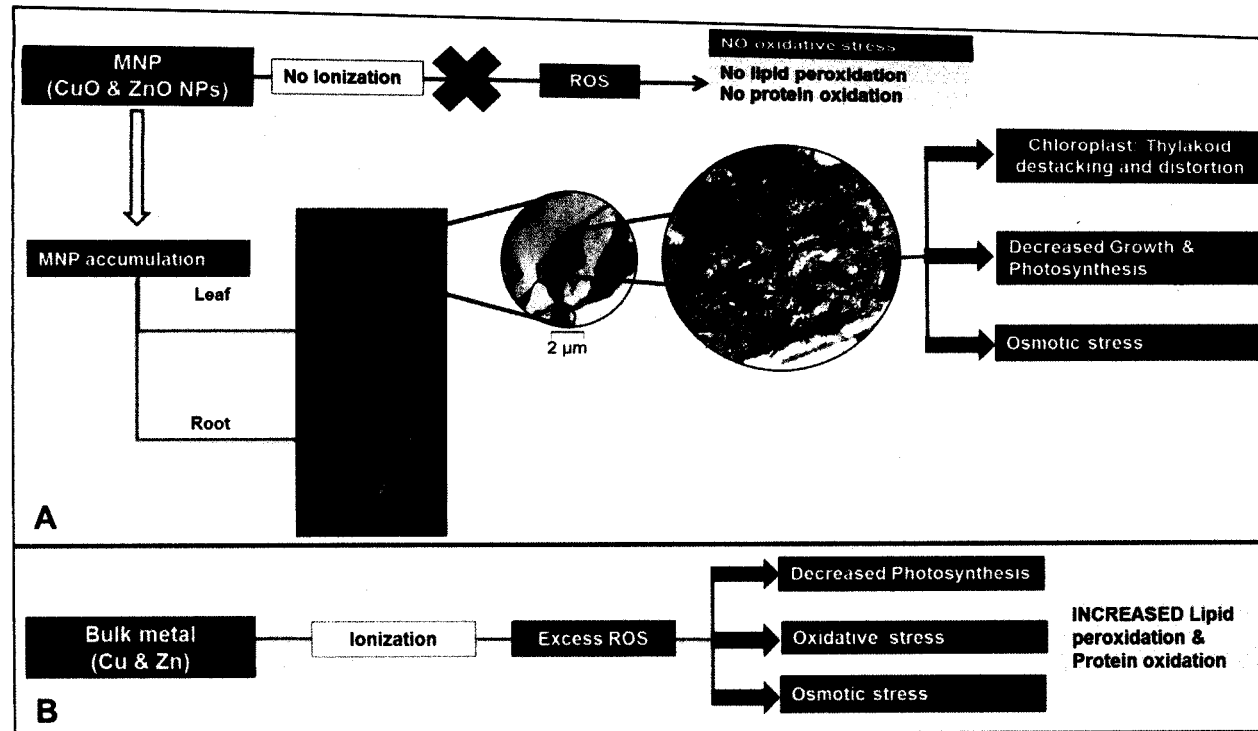
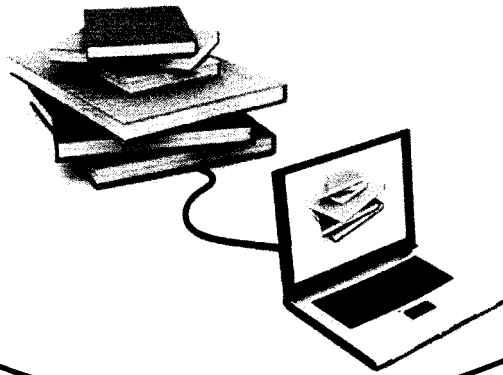


Fig 4.7. Mechanism of Metallo-nanoparticle (MNP) effect (A) and Bulk metal (Cu & Zn) effect (B) in *Oryza sativa* grown hydroponically. MNPs did not result in excess ROS generation, therefore, no oxidative stress in rice, instead MNPs accumulated in rice chloroplast and altered the ultrastructure of the organelle, hampering growth, photosynthesis and simultaneously causing osmotic stress. Bulk metals, unlike MNPs, resulted in ionization, producing excess ROS thereby affecting growth and photosynthesis, consequently, causing oxidative and osmotic stress in rice upon treatment.

REFERENCES



“Research is to see what everybody else has seen, and to think what nobody else has thought”

Albert Szent-Gyorgyi

- Abbasi, E., Aval, S. F., Akbarzadeh, A., Milani, M., Nasrabadi, H. T., Joo, S. W., Hanifehpour, Y., Nejati-Koshki, K., & Pashaei-Asl, R. (2014). Dendrimers: synthesis, applications, and properties. *Nanoscale Research Letters*, 9(1), 247. doi:10.1186/1556-276X-9-247
- Abdelkader, A. F., Aronsson, H., Solymosi, K., Böddi, B., & Sundqvist, C. (2007). High salt stress induces swollen prothylakoids in dark-grown wheat and alters both prolamellar body transformation and reformation after irradiation. *Journal of Experimental Botany*, 58(10), 2553–2564. doi:10.1093/jxb/erm085
- Alaoui-Sossé, B., Genet, P., Vinit-Dunand, F., Toussaint, M.-L., Epron, D., & Badot, P.-M. (2004). Effect of copper on growth in cucumber plants (*Cucumis sativus*) and its relationships with carbohydrate accumulation and changes in ion contents. *Plant Science*, 166(5), 1213–1218. doi:10.1016/j.plantsci.2003.12.032
- Alia & Pardha Saradhi, P. (1991). Proline accumulation under heavy metal stress. *Journal of Plant Physiology*, 138(5), 554–558. doi:10.1016/S0176-1617(11)80240-3
- Álvarez-Fernández, A., Díaz-Benito, P., Abadía, A., López-Millán, A.-F., & Abadía, J. (2014). Metal species involved in long distance metal transport in plants. *Frontiers in Plant Science*, 5, 105. <http://doi.org/10.3389/fpls.2014.00105>
- Anderson, J. M. (1986). Photoregulation of the composition, function, and structure of thylakoid membranes. *Annual Review of Plant Biology*, 37, 93–136. doi:10.1146/annurev.pp.37.060186.000521
- Aravind, P., & Prasad, M. N. V. (2003). Zinc alleviates cadmium-induced oxidative stress in *Ceratophyllum demersum* L.: a free floating freshwater macrophyte. *Plant Physiology and Biochemistry*, 41, 391–397. doi:10.1016/S0981-9428(03)00035-4
- Aravind, P., & Prasad, M. N. V. (2004a). Zinc protects chloroplasts and associated photochemical functions in cadmium exposed *Ceratophyllum demersum* L., a freshwater macrophyte. *Plant Science*, 166, 1321–1327. doi:10.1016/j.plantsci.2004.01.011
- Aravind, P., & Prasad, M. N. V. (2004b). Carbonic anhydrase impairment in cadmium-treated *Ceratophyllum demersum* L. (free floating freshwater macrophyte): toxicity reversal by zinc. *Journal of Analytical Atomic Spectrometry*, 19, 52. doi:10.1039/b307282g

- Aravind, P., & Prasad, M. N. V. (2005a). Modulation of cadmium-induced oxidative stress in zinc involves ascorbate-glutathione cycle and glutathione metabolism. *Plant Physiology and Biochemistry*, 43, 107–116. doi:10.1016/j.plaphy.2005.01.002
- Aravind, P., & Prasad, M. N. V. (2005b). Cadmium-induced toxicity reversal by zinc in *Ceratophyllum demersum* L. (a free floating aquatic macrophyte) together with exogenous supplements of amino- and organic acids. *Chemosphere*, 61, 1720–1733. doi:10.1016/j.chemosphere.2005.03.088
- Asada, K. (2006). Production and scavenging of reactive oxygen species in chloroplasts and their functions. *Plant Physiology*, 141, 391–396. doi:10.1104/pp.106.082040
- Ashraf, M., & Foolad, M. R. (2007). Roles of glycine betaine and proline in improving plant abiotic stress resistance. *Environmental and Experimental Botany*, 59(2), 206–216. doi:10.1016/j.envexpbot.2005.12.006
- Atha, D. H., Wang, H., Petersen, E. J., Cleveland, D., Holbrook, R. D., Jaruga, P., Dizdaroglu, M., Xing, B., & Nelson, B. C. (2012). Copper oxide nanoparticle mediated DNA damage in terrestrial plant models. *Environmental Science and Technology*, 46(3), 1819–1827. doi:10.1021/es202660k
- Auffan, M., Rose, J., Bottero, J. -Y., Lowry, G. V., Jolivet, J. -P., & Wiesner, M. R., (2009). Towards a definition of inorganic nanoparticles from an environmental, health and safety perspective. *Nature Nanotechnology*, 4, 634–641. doi:10.1038/nnano.2009.242
- Baer, D. R., Gaspar, D. J., Nachimuthu, P., Techane, S. D., & Castner, D. G. (2010). Application of surface chemical analysis tools for characterization of nanoparticles. *Analytical and Bioanalytical Chemistry*, 396, 983–1002. doi:10.1007/s00216-009-3360-1
- Bali, R., Siegele, R., & Harris, A. T. (2010). Biogenic Pt uptake and nanoparticle formation in *Medicago sativa* and *Brassica juncea*. *Journal of Nanoparticle Research*, 12, 3087–3095. doi:10.1007/s11051-010-9904-7
- Barceló, J., & Poschenrieder, C. (1990). Plant water relations as affected by heavy metal stress: A review. *Journal of Plant Nutrition*, 13, 1–37. doi:10.1080/01904169009364057
- Barnes, R. J., Riba, O., Gardner, M. N., Scott, T. B., Jackman, S. A., & Thompson, I. P. (2010). Optimization of nano-scale nickel/iron particles for the reduction of high

- concentration chlorinated aliphatic hydrocarbon solutions. *Chemosphere*, 79, 448–454. doi:10.1016/j.chemosphere.2010.01.044
- Barr, R. & Crane, F. L. (1973). A study of chloroplast membrane polypeptides from mineral-deficient maize in relation to photosynthetic activity. In *Proceedings of the Indiana Academy of Science*, 83, pp. 95-104.
- Bates, L. S., Waldren, R. P., & Teare, I. D. (1973). Rapid determination of free proline for water-stress studies. *Plant and Soil*, 39, 205–207.
- Battke, F., Leopold, K., Maier, M., Schmidhalter, U., & Schuster, M. (2008). Palladium exposure of barley: uptake and effects. *Plant Biology*, 10, 272–276. doi:10.1111/j.1438-8677.2007.00017.x
- Baxter, A., Mittler, R., & Suzuki, N. (2014). ROS as key players in plant stress signalling. *Journal of Experimental Botany*, 65(5), 1229–1240. doi:10.1093/jxb/ert375
- Becheri, A., Durr, M., Lo Nostro, P., & Baglioni, P. (2008). Synthesis and characterization of zinc oxide nanoparticles: application to textiles as UV-absorbers. *Journal of Nanoparticle Research*, 10, 679–689. doi:10.1007/s11051-007-9318-3
- Begum, P., & Fugetsu, B. (2012). Phytotoxicity of multi-walled carbon nanotubes on red spinach (*Amaranthus tricolor* L.) and the role of ascorbic acid as an antioxidant. *Journal of Hazardous Materials*, 243, 212–222. doi:10.1016/j.jhazmat.2012.10.025
- Biswas, P., & Wu, C. Y. (2005). Critical review: nanoparticles and the environment. *Journal of the Air & Waste Management Association*, 55, 708–746.
- Bohnert, H. J., Nelson, D. E., & Jensen, R. G. (1995). Adaptations to Environmental Stresses. *The Plant Cell*, 7(7), 1099–1111. doi:10.1105/tpc.7.7.1099
- Boonyanitipong, P., Kositsup, B., Kumar, P., Baruah, S., & Dutta, J. (2011). Toxicity of ZnO and TiO₂ nanoparticles on germinating rice seed *Oryza sativa* L. *International Journal of Bioscience, Biochemistry and Bioinformatics*, 1, 282–285. doi:10.7763/IJBBB.2011.V1.53
- Boveris, A. (1984). Determination of the production of superoxide radicals and hydrogen peroxide in mitochondria. In: *Methods in Enzymology*, 105, 429–435.
- Brayner, R., Dahoumane, S.A., Yéprémian, C., Djediat, C., Meyer, M., Couté, A., & Fiévet, F. (2010). ZnO nanoparticles: synthesis, characterization, and ecotoxicological studies. *Langmuir* 26, 6522–6528. doi:10.1021/la100293s

- Brüggemann, L. I., Pottosin, I. I., & Schonknecht, G. (1998). Cytoplasmic polyamines block the fast-activating vacuolar cation channel. *The Plant Journal*, 16(1), 101–105. doi:10.1046/j.1365-313x.1998.00274.x
- Cambrollé, J., Mateos-Naranjo, E., Redondo-Gómez, S., Luque, T., & Figueroa, M. E. (2011). Growth, reproductive and photosynthetic responses to copper in the yellow-horned poppy, *Glaucium flavum* Crantz. *Environmental and Experimental Botany*, 71(1), 57–64. doi:10.1016/j.envexpbot.2010.10.017
- Cherif, J., Derbel, N., Nakkach, M., Bergmann, H. von., Jemal, F., & Lakhdar, Z. B. (2010). Analysis of in vivo chlorophyll fluorescence spectra to monitor physiological state of tomato plants growing under zinc stress. *Journal of Photochemistry and Photobiology B: Biology*, 101, 332–339. doi:10.1016/j.jphotobiol.2010.08.005
- Christian, P., Von der Kammer, F., Baalousha, M., & Hofmann, T. (2008). Nanoparticles: structure, properties, preparation and behaviour in environmental media. *Ecotoxicology*, 17, 326–343. doi:10.1007/s10646-008-0213-1
- Chugh, L. K., & Sawhney, S. K. (1999). Photosynthetic activities of *Pisum sativum* seedlings grown in presence of cadmium. *Plant Physiology and Biochemistry*, 37(4), 297–303. doi:10.1016/S0981-9428(99)80028-X
- Claussen, W. (2002). Growth, water use efficiency, and proline content of hydroponically grown tomato plants as affected by nitrogen source and nutrient concentration. *Plant and Soil*, 247(2), 199-209.
- Cobbett, C. S. (2000). Phytochelatin biosynthesis and function in heavy-metal detoxification. *Current Opinion in Plant Biology*, 3(3), 211–216.
- Cobbett, C., & Goldsbrough, P. (2002). Phytochelatins and metallothioneins: roles in heavy metal detoxification and homeostasis. *Annual Review of Plant Biology*, 53, 159–182. doi:10.1146/annurev.arplant.53.100301.135154
- Creissen, G., Edwards, E. A., & Mullineaux, P. M. (1994). Glutathione reductase and ascorbate peroxidase. In *Causes of Photooxidative Stress and Amelioration of Defense Systems in Plants*, C. H. Foyer and P. M. Mullineaux, eds (Boca Raton, FL: CRC Press), pp. 343–364

- Da Costa, M. V. J., & Sharma, P. K. (2016). Effect of copper oxide nanoparticles on growth, morphology, photosynthesis, and antioxidant response in *Oryza sativa*. *Photosynthetica*, 54(1), 110–119. doi:10.1007/s11099-015-0167-5
- Dalin, P., Ågren, J., Björkman, C., Huttunen, P., & Kärkkäinen, K. (2008). Leaf trichome formation and plant resistance to herbivory. In *Induced plant resistance to herbivory* (Springer Netherlands), pp. 89–105.
- Damoiseaux, R., George, S., Li, M., Pokhrel, S., Ji, Z., France, B., Xia, T., E., Rallo, R., Mädler, L., Cohen, Y., Hoek, E. M. V., & Nel, A. (2011). No time to lose -high throughput screening to assess nanomaterial safety. *Nanoscale*, 3(4), 1345–1360. <http://doi.org/10.1039/c0nr00618a>.
- Dekker, J. P., & Boekema, E. J. (2005). Supramolecular organization of thylakoid membrane proteins in green plants. *Biochimica et Biophysica Acta*, 1706, 12–39. doi:10.1016/j.bbabi.2004.09.009
- Dhobale, S., Thite, T., Laware, S. L., Rode, C. V., Koppikar, S. J., Ghanekar, R. -K., & Kale, S. N. (2008). Zinc oxide nanoparticles as novel alpha-amylase inhibitors. *Journal of Applied Physics*, 104, 094907. doi:10.1063/1.3009317
- Dimkpa, C. O., McLean, J. E., Latta, D. E., Manangón, E., Britt, D. W., Johnson, W. P., Boyanov, M. I., & Anderson, A. J. (2012). CuO and ZnO nanoparticles: phytotoxicity, metal speciation, and induction of oxidative stress in sand-grown wheat. *Journal of Nanoparticle Research*, 14, 1125. doi:10.1007/s11051-012-1125-9
- Du, W., Sun, Y., Ji, R., Zhu, J., Wu, J., & Guo, H. (2011). TiO₂ and ZnO nanoparticles negatively affect wheat growth and soil enzyme activities in agricultural soil. *Journal of Environmental Monitoring*, 13, 822–828. doi:10.1039/c0em00611d
- Emamverdian, A., Ding, Y., Mokhberdoran, F., & Xie, Y. (2015). Heavy Metal Stress and Some Mechanisms of Plant Defense Response. *The Scientific World Journal*, 2015, 1–18. doi:10.1155/2015/756120
- Englbrecht, C.C., Schoof, H., & Böhm, S. (2004). Conservation, diversification and expansion of C₂H₂ zinc finger proteins in the *Arabidopsis thaliana* genome. *BMC Genomics* 5, 39. doi:10.1186/1471-2164-5-39
- EPA 2003, <https://www.epa.gov/dwstandardsregulations/secondary-drinking-water-standards-guidance-nuisance-chemicals>

EPA 2007, <https://cfpub.epa.gov/ncea/risk/recordisplay.cfm?deid=140917>

Evans, P. T. (1989). Review: do polyamines have roles in plant development? *Annual Review of Plant Physiology and Plant Molecular Biology*, 2(1), 1–19. doi:10.1603/EN13078

Faisal, M., Saquib, Q., Alatar, A. A., Al-Khedhairi, A. A., Hegazy, A. K., & Musarrat, J. (2013). Phytotoxic hazards of NiO-nanoparticles in tomato: A study on mechanism of cell death. *Journal of Hazardous Materials*, 250–251, 318–332. doi:10.1016/j.jhazmat.2013.01.063

Figure 1.7.2 A, Non-cyclic photophosphorylation (Z scheme) of photosynthesis in plants, <http://biol100.class.uic.edu/lectures/ps01.htm>.

Figure 1.7.2 B, Carbon dioxide fixation of photosynthesis in plants, <http://chemistry.about.com/od/lecturenoteslab1/ss/Calvin-Cycle.htm>

Fleischer, M. A., O'Neill, R., & Ehwald, R. (1999). The pore size of non-graminaceous plant cell wall is rapidly decreased by borate ester cross-linking of the pectic polysaccharide rhamnogalacturon II. *Plant Physiology*, 121, 829–828.

Flores, H. E., & Galston, A. W. (1982). Analysis of polyamines in higher plants by high performance liquid chromatography. *Plant Physiology*, 69, 701–706.

Foltête, A. -S., Masfaraud, J. -F., Bigorgne, E., Nahmani, J., Chaurand, P., Botta, C., Labille, J., Rose, J., Féraud, J. F., & Cotelle, S. (2011). Environmental impact of sunscreen nanomaterials: ecotoxicity and genotoxicity of altered TiO₂ nanocomposites on *Vicia faba*. *Environmental Pollution*, 159(10), 2515–2522. doi:10.1016/j.envpol.2011.06.020

Franklin, N. M., Rogers, N. J., Apte, S. C., Batley, G. E., Gadd, G. E., & Casey, P. S. (2007). Comparative toxicity of nanoparticulate ZnO, bulk ZnO, and ZnCl₂ to a freshwater microalga (*Pseudokirchneriella subcapitata*): The importance of particle solubility. *Environmental Science and Technology*, 41(24), 8484–8490. doi:10.1021/es071445r

Frazier, T. P., Burklew, C. E., & Zhang, B. (2014). Titanium dioxide nanoparticles affect the growth and microRNA expression of tobacco (*Nicotiana tabacum*). *Functional & Integrative Genomics*, 14(1), 75–83. doi:10.1007/s10142-013-0341-4

Gajewska, E., & Skłodowska, M. (2005). Antioxidative responses and proline level in leaves and roots of pea plants subjected to nickel stress. *Acta Physiologiae Plantarum*, 27(3), 329–340. doi:10.1007/s11738-005-0009-3

- Galston, A. W., & Sawhney, R. K. (1990). Polyamines in plant physiology. *Plant Physiology*, 94(2), 406–410. doi:10.1104/pp.94.2.406
- Gao, F., Hong, F., Liu, C., Zheng, L., Su, M., Wu, X., Yang, F., Wu, C., & Yang, P. (2006). Mechanism of nano-anatase TiO₂ on promoting photosynthetic carbon reaction of spinach: inducing complex of rubisco-rubisco activase. *Biological Trace Element Research*, 111, 239–253. doi:10.1385/BTER:111:1:239
- García-Sánchez, S., Bernal, I., & Cristobal, S. (2015). Early response to nanoparticles in the *Arabidopsis* transcriptome compromises plant defence and root-hair development through salicylic acid signalling. *BMC Genomics*, 16, 341. doi:10.1186/s12864-015-1530-4
- Gardea-Torresdey, J.L., Gomez, E., Peralta-Videa, J.R., Parsons, J.G., Troiani, H., & Jose-Yacamán, M. (2003). Alfalfa Sprouts: A Natural Source for the Synthesis of Silver Nanoparticles. *Langmuir*, 19, 1357–1361. doi:10.1021/la020835i
- Garg, N., & Manchanda, G. (2009). ROS generation in plants: Boon or bane? *Plant Biosystems - An International Journal Dealing with All Aspects of Plant Biology*, 143(1), 81–96. doi:10.1080/11263500802633626
- Gemperlová, L., Nováková, M., Vaňková, R., Eder, J., & Cvikrová, M. (2006). Diurnal changes in polyamine content, arginine and ornithine decarboxylase, and diamine oxidase in tobacco leaves. *Journal of Experimental Botany*, 57(6), 1413–1421. doi:10.1093/jxb/erj121
- Geranio, L., Heuberger, M., & Nowack, B. (2009). The behavior of silver nanotextiles during washing. *Environmental Science and Technology*, 43, 8113–8118. doi:10.1021/es9018332
- Ghafariyan, M.H., Malakouti, M.J., Dadpour, M.R., Stroeve, P., & Mahmoudi, M. (2013). Effects of magnetite nanoparticles on soybean chlorophyll. *Environmental Science and Technology*, 47, 10645–10652. doi:10.1021/es402249b
- Ghodake, G., Seo, Y. D., & Lee, D. S. (2011). Hazardous phytotoxic nature of cobalt and zinc oxide nanoparticles assessed using *Allium cepa*. *Journal of Hazardous Materials*, 186(1), 952–955. doi:10.1016/j.jhazmat.2010.11.018

- Giammar, D.E., Maus, C.J., & Xie, L. (2007). Effects of Particle Size and Crystalline Phase on Lead Adsorption to Titanium Dioxide Nanoparticles. *Environmental Engineering Science*, 24, 85–95. doi:10.1089/ees.2007.24.85
- Gill, S. S., & Tuteja, N. (2010). Reactive oxygen species and antioxidant machinery in abiotic stress tolerance in crop plants. *Plant Physiology and Biochemistry*, 48, 909–930. doi:10.1016/j.plaphy.2010.08.016
- Giraldo, J. P., Landry, M. P., Faltermeier, S. M., McNicholas, T. P., Iverson, N. M., Boghossian, A. A., Reuel, N. F., Hilmer, A. J., Sen, F., Brew, J. A., & Strano, M. S. (2014). Plant nanobionics approach to augment photosynthesis and biochemical sensing. *Nature Materials*, 13(4), 400–408. doi:10.1038/nmat3890
- Glińska, S., Gapińska, M., Michlewska, S., Skiba, E., & Kubicki, J. (2016). Analysis of *Triticum aestivum* seedling response to the excess of zinc. *Protoplasma*, 253(2), 367–377. doi:10.1007/s00709-015-0816-3
- Golam, S. A. K. M., & Arshad, A. M. (2002). Studies on the leaf epidermis of rice (*Oryza sativa* L.). *Indian Journal of Agricultural Research*, 36, 24–28.
- Gomes, M.P., Marques, T.C.L.L.S.M., Carneiro, M.M.L.C. & Soares, Â.M. (2012). Anatomical characteristics and nutrient uptake and distribution associated with the Cd-phytoremediation capacity of *Eucalyptus camaldulenses* Dehnh. *Journal Of Soil Science and Plant Nutrition*, 12 (3), 481-495.
- Gong, X., Liu, Y., Huang, D., Zeng, G., Liu, S., Tang, H., Zhou, L., Hu, X., Zhou, Y., & Tan, X. (2016). Effects of exogenous calcium and spermidine on cadmium stress moderation and metal accumulation in *Boehmeria nivea* (L.) Gaudich. *Environmental Science and Pollution Research*, 2016. [Epub ahead of print] PubMed PMID: 26801927.
- Gong, Z., Tang, M. M., Wu, X., Phillips, N., Galkowski, D., Jarvis, G. A., & Fan, H. (2016). Arginine- and Polyamine-Induced Lactic Acid Resistance in *Neisseria gonorrhoeae*. *PLoS One*, 11(1), e0147637. doi:10.1371/journal.pone.0147637
- González-Melendi, P., Fernández-Pacheco, R., Coronado, M. J., Corredor, E., Testillano, P. S., Risueño, M. C., Marquina, C., Ibarra, M. R., Rubiales, D., & Pérez-de-Luque, A. (2008). Nanoparticles as smart treatment-delivery systems in plants: assessment of different techniques of microscopy for their visualization in plant tissues. *Annals of Botany*, 101, 187–195. doi:10.1093/aob/mcm283

- Gottschalk, F., & Nowack, B. (2011). The release of engineered nanomaterials to the environment. *Journal of Environmental Monitoring*, 13, 1145–1155. doi:10.1039/c0em00547a
- Gottschalk, F., Sonderer, T., Scholz, R. W., & Nowack, B. (2009). Modeled environmental concentrations of engineered nanomaterials (TiO₂, ZnO, Ag, CNT, fullerenes) for different regions. *Environmental Science and Technology*, 43, 9216–9222. doi:10.1021/es9015553
- Grill, E., Winnacker, E. L., & Zenk, M. H. (1987). Phytochelatins, a class of heavy-metal-binding peptides from plants, are functionally analogous to metallothioneins. *Proceedings of the National Academy of Sciences of the United States of America*, 84(2), 439–443.
- Groppa, M. D., Tomaro, M. L., & Benavides, M. P. (2001). Polyamines as protectors against cadmium or copper-induced oxidative damage in sunflower leaf discs. *Plant Science*, 161(3), 481–488. doi:10.1016/S0168-9452(01)00432-0
- Groß, F., Durner, J., & Gaupels, F. (2013). Nitric oxide, antioxidants and prooxidants in plant defence responses. *Frontiers in Plant Science*, 4, 419. doi:10.3389/fpls.2013.00419
- Gunjan, B., Zaidi, M., & Sandeep, A. (2014). Impact of Gold Nanoparticles on Physiological and Biochemical Characteristics of *Brassica juncea*. *Journal of Plant Biochemistry and Physiology*, 02, 133. doi:10.4172/2329-9029.1000133
- Guo, W. -J., Meenam, M. & Goldsbrough, P. B. (2008). Examining the specific contributions of individual *Arabidopsis* metallothioneins to copper distribution and metal tolerance. *Plant Physiology*, 146, 1697–1706. doi:10.1104/pp.108.115782
- Gutschick, V. P. (1999). Biotic and abiotic consequences of differences in leaf structure. *New Phytologist*, 143(1), 3–18. doi:10.1046/j.1469-8137.1999.00423.x
- Guzman, K. A. D., Finnegan, M. P., & Banfield, J. F. (2006). Influence of surface potential on aggregation and transport of titania nanoparticles. *Environmental Science and Technology*. 40(24), 7688–7693.
- Ha, H. C., Sirisoma, N. S., Kuppusamy, P., Zweier, J. L., Woster, P. M., & Casero, R. A. (1998). The natural polyamine spermine functions directly as a free radical scavenger. *Proceedings of the National Academy of Sciences, USA*, 95, 11140–11145.

- Hall, J. L. (2002). Cellular mechanisms for heavy metal detoxification and tolerance. *Journal of Experimental Botany*, 53(366), 1–11. doi:10.1093/jexbot/53.366.1
- Hasegawa, P. M., Bressan, R. A., Zhu, J. -K., & Bohnert, H. J. (2000). Plant cellular and molecular responses to high salinity. *Annual Review of Plant Physiology and Plant Molecular Biology*, 51(1), 463–499. doi:doi:10.1146/annurev.arplant.51.1.463
- Haverkamp, R. G., & Marshall, A. T. (2009). The mechanism of metal nanoparticle formation in plants: Limits on accumulation. *Journal of Nanoparticle Research*, 11, 1453–1463. doi:10.1007/s11051-008-9533-6
- He, L., Liu, Y., Mustapha, A., & Lin, M. (2011). Antifungal activity of zinc oxide nanoparticles against *Botrytis cinerea* and *Penicillium expansum*. *Microbiological Research*, 166, 207–215. doi:10.1016/j.micres.2010.03.003
- Heiss, S., Wachter, A., Bogs, J., Cobbett, C., & Rausch, T. (2003). Phytochelatin synthase (PCS) protein is induced in *Brassica juncea* leaves after prolonged Cd exposure. *Journal of Experimental Botany*, 54, 1833–1839. doi:10.1093/jxb/erg205
- Hermle, S., Vollenweider, P., Günthardt-Goerg, M. S., McQuattie, C. J. & Matyssek, R. (2007). Leaf responsiveness of *Populus tremula* and *Salix viminalis* to soil contaminated with heavy metals and acidic rainwater. *Tree Physiology*. 27, 1517–1531.
- Hernandez-Viezcas, J. A., Castillo-Michel, H., Servin, A. D., Peralta-Videa, J. R., & Gardea-Torresdey, J. L. (2011) Spectroscopic verification of zinc absorption and distribution in the desert plant *Prosopis juliflora-velutina* (velvet mesquite) treated with ZnO nanoparticles. *Chemical Engineering Journal*, 170, 346–352.
- Hewakuruppu, Y. L., Dombrovsky, L. A., Chen, C., Timchenko, V., Jiang, X., Baek, S., & Taylor, R. A. (2013). Plasmonic “pump-probe” method to study semi-transparent nanofluids. *Applied Optics*, 52(24), 6041–6050. doi: 10.1364/AO.52.006041.
- Hoagland, D. R., & Arnon, D. I. (1950). The water-culture method for growing plants without soil. *California Agricultural Experiment Station Circular*, 347(347), 1–32. doi:citeulike-article-id:9455435
- Hong, F., Yang, F., Liu, C., Gao, Q., Wan, Z., Gu, F., Wu, C., Ma, Z., Zhou, J., & Yang, P. (2005). Influences of nano-TiO₂ on the chloroplast aging of spinach under light. *Biological Trace Element Research*, 104(3), 249–260. doi:10.1385/BTER:104:3:249

- Horikoshi, S., & Serpone, N. (2013). Introduction to Nanoparticles, in *Microwaves in Nanoparticle Synthesis: Fundamentals and Applications* (eds S. Horikoshi and N. Serpone), Wiley-VCH Verlag GmbH & Co. KGaA, Weinheim, Germany. doi: 10.1002/9783527648122.ch1
- Horton, P., 1999. Hypothesis: Are grana necessary for regulation of light harvesting? *Australian Journal of Plant Physiology*, 26(7), 659–669. doi:10.1071/PP99095
- Hoshino, A., Fujioka, K., Oku, T., Suga, M., Sasaki, Y. F., Ohta, T., Yasuhara, M., Suzuki, K., & Yamamoto, K. (2004). Physicochemical properties and cellular toxicity of nanocrystal quantum dots depend on their surface modification. *Nano Letters*, 4(11), 2163–2169. doi:10.1021/nl048715d
- https://web.stanford.edu/dept/EHS/prod/researchlab/IH/nano/what_are_nanomaterials.html
- <https://www.sciencedaily.com/terms/nanoparticle.htm>
- Izaguirre-Mayoral, M. L., & Sinclair, T. R. (2005). Soybean genotypic difference in growth, nutrient accumulation and ultrastructure in response to manganese and iron supply in solution culture. *Annals of Botany*, 96, 149–158. doi:10.1093/aob/mci160
- Jacobsen, S., Hauschild, M. Z., & Rasmussen, U. (1992). Induction by chromium ions of chitinases and polyamines in barley (*Hordeum vulgare* L.) and rape (*Brassica napus* L. ssp. oleifera). *Plant Science*, 84(2), 119–128. doi:10.1016/0168-9452(92)90125-6
- Jimenez, A. (1998). Role of the Ascorbate-Glutathione Cycle of Mitochondria and Peroxisomes in the Senescence of Pea Leaves. *Plant Physiology*, 118(4), 1327–1335. doi:10.1104/pp.118.4.1327
- Johnson, A. C., Bowes, M. J., Crossley, A., Jarvie, H. P., Jurkschat, K., Jürgens, M. D., Lawlor, A. J., Park, B., Rowland, P., Spurgeon, D., Svendsen, C., Thompson, I. P., Barnes, R. J., Williams, R. J., & Xu, N. (2011). An assessment of the fate, behaviour and environmental risk associated with sunscreen TiO₂ nanoparticles in UK field scenarios. *Science of the Total Environment*, 409(13), 2503–2510. doi:10.1016/j.scitotenv.2011.03.040.
- Judy, J. D., Unrine, J. M., & Bertsch, P. M. (2011). Evidence for biomagnification of gold nanoparticles within a terrestrial food chain. *Environmental Science and Technology*, 45(2), 776–781. doi:10.1021/es103031a

- Kaegi, R., Ulrich, A., Sinnet, B., Vonbank, R., Wichser, A., Zuleeg, S., Simmler, H., Brunner, S., Vonmont, H., Burkhardt, M., & Boller, M. (2008). Synthetic TiO₂ nanoparticle emission from exterior facades into the aquatic environment. *Environmental Pollution*, 156, 233–239. doi:10.1016/j.envpol.2008.08.004.
- Kahru, A., Ivask, A., Kasemets, A., Põllumaa, L., Kurvet, I., Francois, M., Dubourguier, H. C. (2005). Biotests and biosensors in ecotoxicological risk assessment of field soils polluted with zinc, lead and cadmium. *Environmental Toxicology and Chemistry*, 24(11), 2973–2982.
- Kampfenkel, K., Vanmontagu, M., & Inze, D. (1995). Extraction and determination of ascorbate and dehydroascorbate from plant tissue. *Analytical Biochemistry*, 225, 165–167.
- Karuppanapandian, T., Moon, J., Kim, C., & Manoharan, K. (2011). Reactive oxygen species in plants: their generation, signal transduction, and scavenging mechanisms. *Australian Journal of Crop Science*, 5(6), 709–725.
- Kasukabe, Y., He, L. X., Nada, K., Misawa, S., Ihara, I., & Tachibana, S. (2004). Overexpression of spermidine synthase enhances tolerance to multiple environmental stresses and up-regulates the expression of various stress regulated genes in transgenic *Arabidopsis thaliana*. *Plant and Cell Physiology*, 45(6), 712–722. doi:10.1093/pcp/pch083
- Kehrer, J.P. (2000). The Haber-Weiss reaction and mechanisms of toxicity. *Toxicology*, 149, 43–50.
- Keller, A. A., McFerran, S., Lazareva, A., & Suh, S. (2013). Global life cycle releases of engineered nanomaterials. *Journal of Nanoparticle Research*, 15, 1692. doi:10.1007/s11051-013-1692-4
- Kim, K.-M., Kim, T.-H., Kim, H.-M., Kim, H.-J., Gwak, G.-H., Paek, S.-M., & Oh, J.-M. (2012b). Colloidal behaviors of ZnO nanoparticles in various aqueous media. *Toxicology and Environmental Health Sciences*, 4(2), 121–131. doi:10.1007/s13530-012-0126-5
- Kim, S. D., Ma, H., Allen, H. E., & Cha, D. K. (1999). Influence of dissolved organic matter on the toxicity of copper to *Ceriodaphnia dubia*: effect of complexation kinetics. *Environmental Toxicology and Chemistry*, 11, 2433–2437

- Kim, S., Lee, S., & Lee, I. (2012a). Alteration of phytotoxicity and oxidant stress potential by metal oxide nanoparticles in *Cucumis sativus*. *Water, Air and Soil Pollution*, 223(5), 2799–2806. doi:10.1007/s11270-011-1067-3
- Kishor, P., Hong, Z., Miao, G. H., Hu, C., & Verma, D. (1995). Overexpression of [δ]-pyrroline-5-carboxylate synthetase increases proline production and confers osmotolerance in transgenic plants. *Plant Physiology*, 108(4), 1387–1394. doi:10.1104/PP.108.4.1387
- Kowshik, M., Deshmukh, N., Vogel, W., Urban, J., Kulkarni, S.K., & Paknikar, K.M. (2002). Microbial synthesis of semiconductor CdS nanoparticles, their characterization, and their use in the fabrication of an ideal diode. *Biotechnology and Bioengineering*, 78, 583–588. doi:10.1002/bit.10233
- Krystofova, O., Sochor, J., Zitka, O., Babula, P., Kudrle, V., Adam, V., & Kizek, R. (2013). Effect of magnetic nanoparticles on tobacco BY-2 cell suspension culture. *International Journal of Environmental Research and Public Health*, 10, 47–71. doi:10.3390/ijerph10010047
- Kumar, A., & Prasad, M. N. V. (2015). Lead-induced toxicity and interference in chlorophyll fluorescence in *Talinum triangulare* grown hydroponically. *Photosynthetica*, 53, 66–71. doi:10.1007/s11099-015-0091-8
- Kumar, V., Guleria, P., Kumar, V., & Yadav, S.K. (2013). Gold nanoparticle exposure induces growth and yield enhancement in *Arabidopsis thaliana*. *Science of the Total Environment*, 461–462, 462–8. doi:10.1016/j.scitotenv.2013.05.018
- Kumari, A., Yadav, S. K., & Yadav, S. C. (2010). Biodegradable polymeric nanoparticles based drug delivery systems. *Colloids and Surfaces B: Biointerfaces*, 75(1), 1–18. doi:10.1016/j.colsurfb.2009.09.001
- Kumari, M., Khan, S. S., Pakrashi, S., Mukherjee, A., & Chandrasekaran, N. (2011). Cytogenetic and genotoxic effects of zinc oxide nanoparticles on root cells of *Allium cepa*. *Journal of Hazardous Materials*, 190(1-3), 613–621. doi:10.1016/j.jhazmat.2011.03.095
- Kumari, M., Mukherjee, A., & Chandrasekaran, N. (2009). Genotoxicity of silver nanoparticles in *Allium cepa*. *Science of the Total Environment*, 407(19), 5243–5246. doi:10.1016/j.scitotenv.2009.06.024

- Lalau, C. M., Mohedano, R. de A., Schmidt, É. C., Bouzon, Z. L., Ouriques, L. C., dos Santos, R. W., da Costa, C. H., & Matias, W. G. (2015). Toxicological effects of copper oxide nanoparticles on the growth rate, photosynthetic pigment content, and cell morphology of the duckweed *Landoltia punctata*. *Protoplasma*, 252(1), 221–229. doi:10.1007/s00709-014-0671-7
- Landberg, T., & Greger, M. (2004). No phytochelatin (PC2 and PC3) detected in *Salix viminalis*. *Physiologia Plantarum*, 121, 481–487. doi:10.1111/j.0031-9317.2004.00347.x
- Lee, C. W., Mahendra, S., Zodrow, K., Li, D., Tsai, Y.-C., Braam, J., & Alvarez, P. J. J. (2010). Developmental phytotoxicity of metal oxide nanoparticles to *Arabidopsis thaliana*. *Environmental Toxicology and Chemistry / SETAC*, 29(3), 669–675. doi:10.1002/etc.58
- Lee, S., Chung, H., Kim, S., & Lee, I. (2013). The Genotoxic Effect of ZnO and CuO Nanoparticles on Early Growth of Buckwheat, *Fagopyrum Esculentum*. *Water, Air, Soil Pollution*, 224, 1668. doi:10.1007/s11270-013-1668-0.
- Lee, W. M., & An, Y. J. (2013). Effects of zinc oxide and titanium dioxide nanoparticles on green algae under visible, UVA, and UVB irradiations: no evidence of enhanced algal toxicity under UV pre-irradiation. *Chemosphere*, 91, 536–544.
- Lee, W.-M., An, Y.-J., Yoon, H., & Kweon, H.-S. (2008). Toxicity and bioavailability of copper nanoparticles to the terrestrial plants mung bean (*Phaseolus radiatus*) and wheat (*Triticum aestivum*): plant agar test for water-insoluble nanoparticles. *Environmental Toxicology and Chemistry / SETAC*, 27(9), 1915–1921.
- Lei Z., Mingyu S., Xiao, W., Chao, L., Chunxiang, Q., Liang, C., Hao, H., Xiaoqing., & Fashui, H. (2008). Antioxidant stress is promoted by nano-anatase in spinach chloroplasts under UV-B radiation. *Biological Trace Element Research*, 121, 69–79.
- Lidon, F. C., & Henriques, F. S. (1998). Role of rice shoot vacuoles in copper toxicity regulation. *Environmental and Experimental Botany*, 39(3), 197–202. doi:10.1016/S0098-8472(97)00025-7
- Lin, C. C., & Kao, C. H. (1999). Excess copper induces an accumulation of putrescine in rice leaves. *Botanical Bulletin- Academia Sinica*, 40, 213–18.

- Lin, D., & Xing, B. (2007). Phytotoxicity of nanoparticles: Inhibition of seed germination and root growth. *Environmental Pollution*, 150(2), 243–250. doi:10.1016/j.envpol.2007.01.016
- Lin, D., & Xing, B. (2008). Root Uptake and Phytotoxicity of ZnO Nanoparticles. *Environmental Science and Technology*, 42(15), 5580–5585. doi:10.1021/es800422x
- Lin, S., Reppert, J., Hu, Q., Hudson, J. S., Reid, M. L., Ratnikova, T. A., Rao, A. M., Luo, H. & Ke, P. C. (2009). Uptake, translocation, and transmission of carbon nanomaterials in rice plants. *Small*, 5: 1128–1132. doi:10.1002/smll.200801556
- Liu, H. P., Dong, B. H., Zhang, Y. Y., Liu, Z. P., & Liu, Y. L. (2004). Relationship between osmotic stress and the levels of free, conjugated and bound polyamines in leaves of wheat seedlings. *Plant Science*, 166(5), 1261–1267. doi:10.1016/j.plantsci.2003.12.039
- Liu, Q., Chen, B., Wang, Q., Shi, X., Xiao, Z., Lin, J., & Fang, X. (2009). Carbon nanotubes as molecular transporters for walled plant cells. *Nano Letters*, 9, 1007–1010. doi:10.1021/nl803083u
- Liu, Q., Zhang, X., Zhao, Y., Lin, J., Shu, C., Wang, C., & Fang, X. (2013). Fullerene-induced increase of glycosyl residue on living plant cell wall. *Environmental Science And Technology*, 47(13), 7490–7498.
- Liu, X-M., Zhang, F-D., Feng, Z-B., Zhang, S. Q., He, X. S., Wang, R-F., & Wang, Y-J. (2005). Effects of nano-ferric oxide on the growth and nutrients absorption of peanut. *Plant Nutrition and Fertilizer Science*, 11:14–18.
- Long, K. E., Van Genderen, E. J., & Klaine, S. J. (2004). The effects of low hardness and pH on copper toxicity to *Daphnia magna*. *Environmental Toxicology and Chemistry*, 23, 72–75.
- López-Moreno, M. L., de la Rosa, G., Hernández-Viezcas, J. A., Castillo-Michel, H., Botez, C. E., Peralta-Videa, J. R., & Gardea-Torresdey, J. L. (2010). Evidence of the differential biotransformation and genotoxicity of ZnO and CeO₂ nanoparticles on soybean (*Glycine max*) plants. *Environmental Science and Technology*, 44(19), 7315–7320. doi:10.1021/es903891g
- Luther, G. W., & Rickard, D. T. (2005). Metal sulfide cluster complexes and their biogeochemical importance in the environment. *Journal of Nanoparticle Research*, 7(6), 389–407. doi:10.1007/s11051-005-4272-4

- Lynch, I., Dawson, K. A., & Linse, S. (2006). Detecting cryptic epitopes created by nanoparticles. *Science's STKE: Signal Transduction Knowledge Environment*, 2006(327), 14. doi:10.1126/stke.3272006pe14
- Ma, R., Zhang, M., Li, B., Du, G., Wang, J., & Chen, J. (2005). The effects of exogenous Ca²⁺ on endogenous polyamine levels and drought-resistant traits of spring wheat grown under arid conditions. *Journal of Arid Environments*, 63(1), 177–190. doi:10.1016/j.jaridenv.2005.01.021
- Ma, X. L., Wang, Y. J., Xie, S. L., Wang, C., & Wang, W. (2007). Glycine betaine application ameliorates negative effects of drought stress in tobacco. *Russian Journal of Plant Physiology*, 54(4), 472–479. doi:10.1134/S1021443707040061
- Ma, Y., Kuang, L., He, X., Bai, W., Ding, Y., Zhang, Z., Zhao, Y., & Chai, Z. (2010). Effects of rare earth oxide nanoparticles on root elongation of plants. *Chemosphere*, 78, 273–279. doi:10.1016/j.chemosphere.2009.10.050
- Maiale, S., Sánchez, D. H., Guirado, A., Vidal, A., & Ruiz, O. A. (2004). Spermine accumulation under salt stress. *Journal of Plant Physiology*, 161(1), 35–42. doi:10.1078/0176-1617-01167
- Majid, M., Ali, A., & Essia, B. (2012). Effect of salinity on sodium and chloride uptake, proline and soluble carbohydrate contents in three alfalfa varieties. *Journal of Agriculture and Veterinary Science*, 1(6), 01–06.
- Makino, A., Miyake, C., & Yokota, A. (2002). Physiological functions of the water-water cycle (Mehler reaction) and the cyclic electron flow around PSI in rice leaves. *Plant Cell Physiology*, 43(9), 1017–1026.
- Maksymiec, W., Russa, R., Urbanik-Sypniewska, T., & Baszynski, T. (1994). Effect of excess Cu on the photosynthetic apparatus of runner bean leaves treated at two different growth stages. *Physiologia Plantarum*, 91, 715–721. doi:10.1111/j.1399-3054.1994.tb03010.x
- Manceau, A., Nagy, K. L., Marcus, M. A., Lanson, M., Geoffroy, N., Jacquet, T., & Kirpichtchikova, T. (2008). Formation of metallic copper nanoparticles at the soil–root interface. *Environmental Science and Technology*, 42(5), 1766–1772. doi:10.1021/es072017o

- Manzo, S., Rocco, A., & Carotenuto, R. (2011). Investigation of ZnO nanoparticles' ecotoxicological effects towards different soil organisms. *Environmental Science and Pollution Research*, 18, 756–763.
- Marschner, H., 1995. Mineral nutrition of higher plants, Academic press, second edition, San Diego.
- Maynard, A. D., Aitken, R. J., Butz, T., Colvin, V., Donaldson, K., Oberdörster, G., Philbert, M. A., Ryan, J., Seaton, A., Stone, V., Tinkle, S. S., Tran, L., Walker, N. J., & Warheit, D. B. (2006). Safe handling of nanotechnology. *Nature*, 444, 267–269. doi:10.1038/444267a
- Mingyu, S., Wu, X., Chao, L., Chunxiang, Q., Xiaoqing, L., Liang, C., Hao, H., & Fashui, H. (2007). Promotion of energy transfer and oxygen evolution in spinach photosystem II by nano-anatase TiO₂. *Biological Trace Element Research*, 119, 183–192. doi:10.1007/s12011-007-0065-1
- Mittler, R. (2002). Oxidative stress, antioxidants and stress tolerance. *Trends in Plant Science*, 7(9), 405–410. doi:10.1016/S1360-1385(02)02312-9
- Mittler, R., Vanderauwera, S., Gollery, M., & Van Breusegem, F. (2004). Reactive oxygen gene network of plants. *Trends in Plant Science*, 9(10), 490–498. doi:10.1016/j.tplants.2004.08.009
- Mocquot, B., Vangronsveld, J., Clijsters, H., & Mench, M. (1996). Copper toxicity in young maize (*Zea mays* L.) plants: effects on growth, mineral and chlorophyll contents and enzyme activities. *Plant and Soil*, 182, 287–300. doi:10.1007/BF00029060
- Mody, V. V., Siwale, R., Singh, A., & Mody, H. R. (2010). Introduction to metallic nanoparticles. *Journal of Pharmacy and Bioallied Sciences*, 2(4), 282–289. <http://doi.org/10.4103/0975-7406.72127>
- Møller, I. M., Jensen, P. E., & Hansson, A. (2007). Oxidative modifications to cellular components in plants. *Annual Review of Plant Biology*, 58(1), 459–481. doi:10.1146/annurev.arplant.58.032806.103946
- Morales, M. I., Rico, C. M., Hernandez-Viezcas, J. A., Nunez, J. E., Barrios, A. C., Tafoya, A., Flores-Marges, J. P., Peralta-Videa, J. R., & Gardea-Torresdey, J. L. (2013). Toxicity assessment of cerium oxide nanoparticles in cilantro (*Coriandrum sativum* L.)

- plants grown in organic soil. *Journal of Agricultural and Food Chemistry*, 61(26), 6224–6230. doi:10.1021/jf401628v
- Mueller, N.C., & Nowack, B. (2008). Exposure modeling of engineered nanoparticles in the environment. *Environmental Science and Technology*, 42(12), 4447–4453. doi:10.1021/es7029637
- Musante, C., & White, J. C. (2012). Toxicity of silver and copper to *Cucurbita pepo*: Differential effects of nano and bulk-size particles. *Environmental Toxicology*, 27(9), 510–517. doi:10.1002/tox.20667
- Nagajyoti, P. C., Lee, K. D., & Sreekanth, T. V. M. (2010). Heavy metals, occurrence and toxicity for plants: a review. *Environmental Chemistry Letters*, 8, 199–216. doi:10.1007/s10311-010-0297-8
- Navarro, E., Baun, A., Behra, R., Hartmann, N. B., Filser, J., Miao, A.-J., Quigg, A., Santschi, P. H., & Sigg, L. (2008a). Environmental behaviour and ecotoxicity of engineered nanoparticles to algae, plants, and fungi. *Ecotoxicology*, 17, 372–386. doi:10.1007/s10646-008-0214-0.
- Navarro, E., Wagner, B., Marconi, F., Kaegi, R., Odzak, N., Box, P. O., Navarro, E., Piccapietra, F., Wagner, B., Marconi, F., Kaegi, R., Odzak, N., Sigg, L., & Behra, R. (2008b). Toxicity of silver nanoparticles to *Chlamydomonas reinhardtii*. *Environmental Science and Technology*, 42(23), 8959–8964. doi:10.1021/es801785m
- Nekrasova, G. F., Ushakova, O. S., Ermakov, A. E., Uimin, M. A., & Byzov, I. V. (2011). Effects of copper (II) ions and copper oxide nanoparticles on *Elodea densa* Planch. *Russian Journal of Ecology*, 42, 458–463. doi:10.1134/S1067413611060117
- Nelson, N. (1999). Metal ion transporters and homeostasis. *EMBO Journal*, 18, 4361–4371. doi:10.1093/emboj/18.16.4361
- Nhan, L. Van, Ma, C., Rui, Y., Liu, S., Li, X., Xing, B., & Liu, L. (2015). Phytotoxic Mechanism of Nanoparticles: Destruction of Chloroplasts and Vascular Bundles and Alteration of Nutrient Absorption. *Scientific Reports*, 5(1), 11618. doi:10.1038/srep11618
- Noctor, G., & Foyer, C. H. (1998). Ascorbate and glutathione: Keeping Active Oxygen under Control. *Annual Review of Plant Physiology and Plant Molecular Biology*, 49(1), 249–279. doi:10.1146/annurev.arplant.49.1.249

- Noji, T., Kamidaki, C., Kawakami, K., Shen, J. R., Kajino, T., Fukushima, Y., Sekitoh, T., & Itoh, S. (2011). Photosynthetic oxygen evolution in mesoporous silica material: Adsorption of photosystem II reaction center complex into 23 nm nanopores in SBA. *Langmuir*, 27, 705–713. doi:10.1021/la1032916
- Nowack, B., Schulin, R., & Robinson, B. H. (2006). Critical assessment of chelant-enhanced metal phytoextraction. *Environmental Science and Technology*, 40(17), 5225-5232. doi:10.1021/es0604919
- Ojamäe, L., Aulin, C., Pedersen, H., & Käll, P.-O. (2006). IR and quantum-chemical studies of carboxylic acid and glycine adsorption on rutile TiO₂ nanoparticles. *Journal of Colloid and Interface Science*, 296, 71–78. doi:10.1016/j.jcis.2005.08.037
- OJEC (Official Journal of the European Communities) 1998. Council Directive 98/83/EEC of 3 November 1998, concerning water quality for human consumption. OJEC of 5 December 1998, pp.32-54.
- Oukarroum, A., Bras, S., Perreault, F., & Popovic, R. (2012). Inhibitory effects of silver nanoparticles in two green algae, *Chlorella vulgaris* and *Dunaliella tertiolecta*. *Ecotoxicology and Environmental Safety*, 78, 80–85. doi:10.1016/j.ecoenv.2011.11.012
- Ouzounidou, G., Moustakas, M., & Strasser, R. J. (1997). Sites of action of copper in the photosynthetic apparatus of maize leaves: kinetic analysis of chlorophyll fluorescence, oxygen evolution, absorption changes and thermal dissipation as monitored by photoacoustic signals. *Functional Plant Biology*, 24(1), 81-90. doi:10.1071/PP96028
- Pakrashi, S., Jain, N., Dalai, S., Jayakumar, J., Chandrasekaran, P. T., Raichur, A. M., Chandrasekaran, N., & Mukherjee, A. (2014). In vivo genotoxicity assessment of titanium dioxide nanoparticles by *Allium cepa* root tip assay at high exposure concentrations. *PLoS ONE*, 9(2). doi:10.1371/journal.pone.0087789
- Parsons, J. G., Lopez, M. L., Gonzalez, C. M., Peralta-Videa, J. R., & Gardea-Torresdey, J. L. (2010). Toxicity and biotransformation of uncoated and coated nickel hydroxide nanoparticles on mesquite plants. *Environmental Toxicology and Chemistry*, 29(5), 1146-1154. doi:10.1002/etc.146
- Peng, J. & Gong, J. (2014). Vacuolar sequestration capacity and long-distance metal transport in plants. *Frontiers in Plant Science*, 5, 19. doi: 10.3389/fpls.2014.00019

- Péret, B., Larrieu, A., & Bennett, M. J. (2009). Lateral root emergence: A difficult birth. *Journal of Experimental Botany*, 60(13), 3637–3643. doi: 10.1093/jxb/erp232.
- Perreault, F., Oukarroum, A., Melegari, S. P., Matias, W. G. & Popovic, R. (2012). Polymer coating of copper oxide nanoparticles increases nanoparticles uptake and toxicity in the green alga *Chlamydomonas reinhardtii*. *Chemosphere*, 87(11), 1388-1394.
- Perreault, F., Oukarroum, A., Pirastru, L., Sirois, L., Gerson Matias, W., & Popovic, R. (2010). Evaluation of copper oxide nanoparticles toxicity using chlorophyll fluorescence imaging in *Lemna gibba*. *Journal of Botany*, 2010, Article ID 763142, 1–9. doi:10.1155/2010/763142
- Pietrini, F., Iannelli, M. A, Pasqualini, S., & Massacci, A. (2003). Interaction of cadmium with glutathione and photosynthesis in developing leaves and chloroplasts of *Phragmites australis* (Cav.) Trin. ex Steudel. *Plant Physiology*, 133(2), 829–837. doi:10.1104/pp.103.026518
- Poborilova, Z., Opatrilova, R., & Babula, P. (2013). Toxicity of aluminium oxide nanoparticles demonstrated using a BY-2 plant cell suspension culture model. *Environmental and Experimental Botany*, 91, 1–11. doi:10.1016/j.envexpbot.2013.03.002
- Pokhrel, L. R., & Dubey, B. (2013). Evaluation of developmental responses of two crop plants exposed to silver and zinc oxide nanoparticles. *Science of the Total Environment*, 452–453, 321–332. doi:10.1016/j.scitotenv.2013.02.059
- Polak, N., Read, D. S., Jurkschat, K., Matzke, M., Kelly, F. J., Spurgeon, D. J., & Stürzenbaum, S. R. (2014). Metalloproteins and phytochelatin synthase may confer protection against zinc oxide nanoparticle induced toxicity in *Caenorhabditis elegans*. *Comparative Biochemistry and Physiology - C Toxicology and Pharmacology*, 160(1), 75–85. doi:10.1016/j.cbpc.2013.12.001
- Prasad, M. N. V., & Hagemeyer, J. (1999). *Heavy Metal Stress in Plants*. Berlin, Heidelberg: Springer Berlin Heidelberg. doi:10.1007/978-3-662-07745-0
- Prasad, M. N. V., & Strzalka, K. (1999). Impact of heavy metals on photosynthesis. In: Prasad, M. N. V., Hagemeyer, J., (eds), *Heavy Metal Stress in Plants*, pp.117-138. Springer Publishers, Berlin. doi:10.1007/978-3-662-07745-0

- Prasad, T. N. V. K. V., Sudhakar, P., Sreenivasulu, Y., Latha, P., Munaswamy, V., Reddy, K. R., Sreepasad, T.S., Sajanalal, P.R., & Pradeep, T. (2012). Effect of nanoscale zinc oxide particles on the germination, growth and yield of peanut. *Journal of Plant Nutrition*, 35(6), 905–927. doi:10.1080/01904167.2012.663443
- Premanathan, M., Karthikeyan, K., Jeyasubramanian, K. & Manivannan, G. (2011). Selective toxicity of ZnO nanoparticles toward Gram-positive bacteria and cancer cells by apoptosis through lipid peroxidation. *Nanomedicine: Nanotechnology, Biology and Medicine*, 7(2), 184-192.
- Rahming, V. R., & Fazal, M. A. (2014). Effects of Oxidation on Protein-Nanoparticle Interactions. *British Journal of Pharmaceutical Research*, 4(2), 172.
- Rao, A. S. V. C., & Reddy, A. R. (2008). Glutathione reductase: a putative redox regulatory system in plant cells. In: Khan NA, Singh S, Umar S, Editors, sulfur assimilation and abiotic stresses in plants, Springer, The Netherlands, pp 111–147
- Rausser, W. E. (1999). Structure and function of metal chelators produced by plants: the case for organic acids, amino acids, phytin, and metallothioneins. *Cell Biochemistry and Biophysics*, 31(1), 19–48. doi:10.1007/BF02738153
- Raven, J.A., Evans, M.C., & Korb, R.E. (1999). The role of trace metals in photosynthetic electron transport in O₂-evolving organisms. *Photosynthesis Research*, 60, 111–150.
- Redmond, J. W., & Tseng, A. (1979). High-pressure liquid chromatographic determination of putrescine, cadaverine, spermidine and spermine. *Journal of Chromatography A*, 170(2), 479–81. doi:10.1016/S0021-9673(00)95481-5
- Ren, G., Hu, D., Cheng, E. W. C., Vargas-Reus, M. A., Reip, P., & Allaker, R. P. (2009). Characterisation of copper oxide nanoparticles for antimicrobial applications. *International Journal of Antimicrobial Agents*, 33, 587–590. doi:10.1016/j.ijantimicag.2008.12.004
- Reznick, A. Z., & Packer, L. (1994). Oxidative damage to proteins: spectrophotometric method for carbonyl assay. In: *Methods in Enzymology* (ed) Vol. 233, Academic press Inc, pp 357–363.
- Rico C. M., Peralta-Videa J. R., & Gardea-Torresdey J. L. (2015). “Chemistry, biochemistry of nanoparticles, and their role in antioxidant defense system in plants,” in

- Nanotechnology and Plant Sciences, eds Siddiqui M. H., Al-Wahaibi M. H., Mohammad F., editors. (Cham: Springer International Publishing), 1–18.
- Rico, C. M., Hong, J., Morales, M. I., Zhao, L., Barrios, A. C., Zhang, J. -Y., Peralta-Videa, J. R., & Gardea-Torresdey, J. L. (2013). Effect of cerium oxide nanoparticles on rice: a study involving the antioxidant defense system and in vivo fluorescence imaging. *Environmental Science and Technology*, 47, 5635–5642. doi:10.1021/es401032m
- Rico, C. M., Majumdar, S., Duarte-Gardea, M., Peralta-Videa, J. R., & Gardea-Torresdey, J. L. (2011). Interaction of nanoparticles with edible plants and their possible implications in the food chain. *Journal of Agricultural and Food Chemistry*, 59(8), 3485-3498. doi:10.1021/jf104517j
- Ridley, M. K., Hackley, V. A., & Machesky, M. L. (2006). Characterization and surface-reactivity of nanocrystalline anatase in aqueous solutions. *Langmuir*, 22, 10972–10982.
- Roco, M.C. (2003). Broader societal issues of nanotechnology. *Journal of Nano Research*, 5, 181–189.
- Roco, M.C. (2005). Environmentally responsible development of nanotechnology. *Environmental Science and Technology*, 39,107A– 112A.
- Roh, J., Sim, S. J., Yi, J., Park, K., Chung, K. H., Ryu, D., & Choi, J. (2009). Ecotoxicity of silver nanoparticles on the soil nematode *Caenorhabditis elegans* using functional ecotoxicogenomics. *Environmental Science and Technology*, 43(10), 3933–3940. doi:10.1021/es803477u
- Romero-Puertas, M. C., Corpas, F. J., Sandalio, L. M., Leterrier, M., Rodriguez-Serrano, M., Del Rio, L. A., & Palma, J. M. (2006). Glutathione reductase from pea leaves: Response to abiotic stress and characterization of the peroxisomal isozyme. *New Phytologist*, 170(1), 43–52. doi:10.1111/j.1469-8137.2006.01643.x
- Romero-Puertas, M. C., Palma, J. M., Gomez, M., Del Rio, L. A., & Sandalio, L. M. (2002). Cadmium causes the oxidative modification of proteins in pea plants. *Plant, Cell and Environment*, 25(5), 677–686. doi:10.1046/j.1365-3040.2002.00850.x
- Saison, C., Perreault, F., Daigle, J. C., Fortin, C., Claverie, J., Morin, M., & Popovic, R. (2010). Effect of core-shell copper oxide nanoparticles on cell culture morphology and photosynthesis (photosystem II energy distribution) in the green alga, *Chlamydomonas reinhardtii*. *Aquatic Toxicology*, 96(2), 109–114. doi:10.1016/j.aquatox.2009.10.002

- Salt, D. E., & Rauser, W. E. (1995). MgATP-Dependent transport of phytochelatins across the tonoplast of oat roots. *Plant Physiology*, 107(4), 1293–1301. doi:10.1104/pp.107.4.1293.
- Sankhalkar, S., & Sharma, P. K. (2002). Protection against photo oxidative damage provided by enzymatic and non-enzymatic antioxidant system in sorghum seedlings. *Indian Journal of Experimental Biology*, 40, 1260-1268.
- Savouré, A., Jaoua, S., Hua, X. J., Ardiles, W., Van Montagu, M., & Verbruggen, N. (1995). Isolation, characterization, and chromosomal location of a gene encoding the delta 1-pyrroline-5-carboxylate synthetase in *Arabidopsis thaliana*. *FEBS Letters*, 372(1), 13–19.
- Schwab, F., Zhai, G., Kern, M., Turner, A., Schnoor, J. L., & Wiesner, M. R. (2015). Barriers, pathways and processes for uptake, translocation and accumulation of nanomaterials in plants- Critical review. *Nanotoxicology*, 1–22. doi:10.3109/17435390.2015.1048326
- Schwacke, R., Grallath, S., Breitzkreuz, K. E., Stransky, E., Stransky, H., Frommer, W. B., & Rentsch, D. (1999). LeProT1, a transporter for proline, glycine betaine, and gamma-amino butyric acid in tomato pollen. *The Plant Cell*, 11(3), 377–392.
- Semisch, A., Ohle, J., Witt, B., & Hartwig, A. (2014). Cytotoxicity and genotoxicity of nano- and microparticulate copper oxide: role of solubility and intracellular bioavailability. *Particle and Fibre Toxicology*, 11, 10.
- Servin, A. D., Castillo-Michel, H., Hernandez-Viezcas, J. A., Diaz, B. C., Peralta-Videa, J. R., & Gardea-Torresdey, J. L. (2012). Synchrotron Micro-XRF and Micro-XANES confirmation of the uptake and translocation of TiO₂ nanoparticles in cucumber (*Cucumis sativus*) Plants. *Environmental Science and Technology*, 46, 7637–7643. doi:10.1021/es300955b
- Sharma, P. K., & Hall, D. O. (1996). Effect of photo inhibition and temperature on carotenoids in sorghum leaves. *Indian Journal of Biochemistry and Biophysics*, 33, 471–477.
- Sharma, P. K., Shetye, R., & Bhonsle, S. (1997). Effect of supplementary ultraviolet-B radiation on young wheat seedlings. *Current Science*, 72, 400-405
- Sharma, P., Bhatt, D., Zaidi, M. G. H., Saradhi, P. P., Khanna, P. K., & Arora, S. (2012). Silver nanoparticle-mediated enhancement in growth and Antioxidant Status of *Brassica juncea*. *Applied Biochemistry and Biotechnology*, 167(8), 2225–2233. doi:10.1007/s12010-012-9759-8

- Shaw, A. K., & Hossain, Z. (2013). Impact of nano-CuO stress on rice (*Oryza sativa* L.) seedlings. *Chemosphere*, 93(6), 906–915. doi:10.1016/j.chemosphere.2013.05.044
- Shaymurat, T., Gu, J., Xu, C., Yang, Z., Zhao, Q., Liu, Y., & Liu, Y. (2012). Phytotoxic and genotoxic effects of ZnO nanoparticles on garlic (*Allium sativum* L.): a morphological study. *Nanotoxicology*, 6, 241–248. doi:10.3109/17435390.2011.570462
- Shen, C. X., Zhang, Q. F., Li, J., Bi, F. C., & Yao, N. (2010). Induction of programmed cell death in Arabidopsis and rice by single-wall carbon nanotubes. *American Journal of Botany*, 97, 1602–1609. doi:10.3732/ajb.1000073
- Sheykhabglou, R., Sedghi, M., Tajbakhsh Shishevan, M., & Sharifi, R. S. (2010). Effects of nano-iron oxide particles on agronomic traits of soybean. *Notulae Scientia Biologicae*, 2(2), 112–113.
- Shi, J., Abid, A. D., Kennedy, I. M., Hristova, K. R., & Silk, W. K. (2011). To duckweeds (*Landoltia punctata*), nanoparticulate copper oxide is more inhibitory than the soluble copper in the bulk solution. *Environmental Pollution*, 159(5), 1277–1282. doi:10.1016/j.envpol.2011.01.028
- Siddiqui, M. H., Al-Wahaibi, M. H., Faisal, M., & Al Sahli, A. A. (2014). Nano-silicon dioxide mitigates the adverse effects of salt stress on *Cucurbita pepo* L. *Environmental Toxicology and Chemistry*, 33, 2429–2437. doi:10.1002/etc.2697
- Sioutas, C., Delfino, R. J., & Singh, M. (2005). Exposure assessment for atmospheric ultrafine particles (UFPs) and implications in epidemiologic research. *Environmental Health Perspectives*, 113:947–955.
- Siripornadulsil, S., Traina, S., Verma, D. P. S., & Sayre, R. T. (2002). Molecular mechanisms of proline-mediated tolerance to toxic heavy metals in transgenic microalgae. *The Plant Cell*, 14(11), 2837–2847. doi:10.1105/tpc.004853
- Sleator, R. D., & Hill, C. (2002). Bacterial osmoadaptation: the role of osmolytes in bacterial stress and virulence. *FEMS Microbiology Reviews*, 26(1), 49–71. doi:10.1111/j.1574-6976.2002.tb00598.x
- Smirnoff, N. (2000). Ascorbic acid: Metabolism and functions of a multi-faceted molecule. *Current Opinion in Plant Biology*, 3(3), 229–235. doi:10.1016/S1369-5266(00)00069-8
- Solymosi, K., & Bertrand, M. (2012). Soil metals, chloroplasts, and secure crop production: a review. *Agronomy for sustainable development*, 32(1), 245–272.

- Sommer, A. L., & Lipman, C. B. (1926). Evidence on the indispensable nature of zinc and boron for higher green plants. *Plant Physiology*, 1(3), 231–249.
- Song, G., Gao, Y., Wu, H., Hou, W., Zhang, C., & Ma, H. (2012). Physiological effect of anatase TiO₂ nanoparticles on *Lemna minor*. *Environmental Toxicology and Chemistry*, 31(9), 2147–2152. doi:10.1002/etc.1933
- Song, U., Jun, H., Waldman, B., Roh, J., Kim, Y., Yi, J., & Lee, E. J. (2013b). Functional analyses of nanoparticle toxicity: A comparative study of the effects of TiO₂ and Ag on tomatoes (*Lycopersicon esculentum*). *Ecotoxicology and Environmental Safety*, 93, 60–67. doi:10.1016/j.ecoenv.2013.03.033
- Song, U., Shin, M., Lee, G., Roh, J., Kim, Y., & Lee, E. J. (2013a). Functional analysis of TiO₂ nanoparticle toxicity in three plant species. *Biological Trace Element Research*, 155(1), 93–103. doi:10.1007/s12011-013-9765-x
- Srikanth, K., Mahajan, A., Pereira, E., Duarte, A. C., & Venkateswara Rao, J. (2015). Aluminium oxide nanoparticles induced morphological changes, cytotoxicity and oxidative stress in Chinook salmon (CHSE-214) cells. *Journal of Applied Toxicology*, 35(10), 1133–1140. doi:10.1002/jat.3142
- Srivalli, B., Sharma, G., & Khanna-Chopra, R. (2003). Antioxidative defense system in an upland rice cultivar subjected to increasing intensity of water stress followed by recovery. *Plant Physiology*, 119, 503–512.
- Stampoulis, D., Sinha, S. K., & White, J. C. (2009). Assay-dependent phytotoxicity of nanoparticles to plants. *Environmental Science and Technology*, 43(24), 9473–9479. doi:10.1021/es901695c
- Stone, V., Nowack, B., Baun, A., van den Brink, N., Kammer, Fv., Dusinska, M., Handy, R., Hankin, S., Hassellöv, M., Joner, E., & Fernandes, T.F. (2010). Nanomaterials for environmental studies: Classification, reference material issues, and strategies for physico-chemical characterisation. *Science of the Total Environment*, 408, 1745–1754. doi:10.1016/j.scitotenv.2009.10.035
- Sun, R. L., Zhou, Q. X., Sun, F. H., & Jin, C. X. (2007). Antioxidative defense and proline/phytochelatin accumulation in a newly discovered Cd-hyperaccumulator, *Solanum nigrum* L. *Environmental and Experimental Botany*, 60(3), 468–476. doi:10.1016/j.envexpbot.2007.01.004

- Sun, W., Luna-Velasco, A., Sierra-Alvarez, R., & Field, J. A. (2013). Assessing protein oxidation by inorganic nanoparticles with enzyme-linked immunosorbent assay (ELISA). *Biotechnology and Bioengineering*, 110(3), 694–701. doi:10.1002/bit.24754
- Tada Y., Komatsubara S., Kurusu T. (2014). Growth and physiological adaptation of whole plants and cultured cells from a halophyte turf grass under salt stress. *AoB Plants* 6:plu041 10.1093/aobpla/plu041
- Tadolini, B., Cabrini, L., Landi, L., Varani, E., & Pasquali, P. (1984). Polyamine binding to phospholipid vesicles and inhibition of lipid peroxidation. *Biochemical and Biophysical Research Communications*, 122(2), 550–555. doi:10.1016/S0006-291X(84)80068-6
- Taiz, L., & Zeiger, E. (2010). *Plant Physiology* (5th ed.). Sinauer Associates.
- Tapiero, H., & Tew, K. D. (2003). Trace elements in human physiology and pathology: zinc and metallothioneins. *Biomedicine & Pharmacotherapy*, 57(9), 399–411.
- Tavallali, V., Rahemi, M., Eshghi, S., Kholdebarin, B., & Ramezani, A. (2010). Zinc alleviates salt stress and increases antioxidant enzyme activity in the leaves of pistachio (*Pistacia vera* L. “Badami”) seedlings. *Turkish Journal of Agriculture and Forestry*, 34(4), 349–359. doi:10.3906/tar-0905-10
- Thul, S. T. & Sarangi, B. K. (2015). Nanotechnology and Plant Sciences: Nanoparticles and Their Impact on Plants. In H. M. Siddiqui, H. M. Al-Wahaibi, & F. Mohammad, eds. Cham: Springer International Publishing, pp. 37–53.
- Todeschini, V., Lingua, G., D’Agostino, G., Carniato, F., Roccotiello, E., & Berta, G. (2011). Effects of high zinc concentration on poplar leaves: A morphological and biochemical study. *Environmental and Experimental Botany*, 71(1), 50–56. doi:10.1016/j.envexpbot.2010.10.018
- Tourinho, P. S., van Gestel, C. A. M., Lofts, S., Svendsen, C., Soares, A. M. V. M., & Loureiro, S. (2012). Metal-based nanoparticles in soil: fate, behavior, and effects on soil invertebrates. *Environmental Toxicology and Chemistry*, 31, 1679–1692. doi:10.1002/etc.1880
- Tsonev, T., & Lidon, F. J. C. (2012). Zinc in plants - An overview. *Emirates Journal of Food and Agriculture*, 24(4), 322–333. doi:10.1016/B978-0-12-077125-7.50013-X
- Tsuzuki, T. (2009). Commercial scale production of inorganic nanoparticles, *International Journal of Nanoscience*, 6, 567–578.

- Ursache-Oprisan, Manuela, E. F., Creanga, D., & Caltun, O. (2011). Sunflower chlorophyll levels after magnetic nanoparticle supply. *African Journal of Biotechnology*, 10, 7092.
- Vaculík, M., Landberg, T., Greger, M., Luxová, M., Stoláriková, M., & Lux, A. (2012). Silicon modifies root anatomy, and uptake and subcellular distribution of cadmium in young maize plants. *Annals of Botany*, 110 (2), 433–443.
- Vallee, B. L., & Auld, D. S (1990). Zinc coordination, function, and structure of zinc enzymes and other proteins. *Biochemistry*, 29, 5647–5659.
- Vaseem, M., Umar, A & Hahn, Y. B. (2010). ZnO nanoparticles: growth, properties, and applications. *Metal Oxide Nanostructures and Their Applications*, 5, 1-36.
- Verbruggen, N., Hua, X. J., May, M., & Van Montagu, M. (1996). Environmental and developmental signals modulate proline homeostasis: evidence for a negative transcriptional regulator. *Proceedings of the National Academy of Sciences of the United States of America*, 93(16), 8787–8791.
- Vinit-Dunand, F., Epron, D., Alaoui-Sossé, B., & Badot, P. -M. (2002). Effects of copper on growth and on photosynthesis of mature and expanding leaves in cucumber plants. *Plant Science*, 163(1), 53–58. doi:10.1016/S0168-9452(02)00060-2
- Wang, H., Kou, X., Pei, Z., Xiao, J. Q., Shan, X., & Xing, B. (2011). Physiological effects of magnetite (Fe₃O₄) nanoparticles on perennial ryegrass (*Lolium perenne* L.) and pumpkin (*Cucurbita mixta*) plants. *Nanotoxicology*, 5(1), 30–42. doi:10.3109/17435390.2010.489206
- Wang, Q., Ebbs, S. D., Chen, Y., & Ma, X. (2013). Trans-generational impact of cerium oxide nanoparticles on tomato plants. *Metallomics: Integrated Biometal Science*, 5(6), 753–759. doi:10.1039/c3mt00033h
- Wang, S. -H., Yang, Z. -M., Yang, H., Lu, B., Li, S. -Q., & Lu, Y. -P. (2004). Copper-induced stress and antioxidative responses in roots of *Brassica juncea* L. *Botanical Bulletin-Academia Sinica*, 45, 203–212.
- Wang, X., Yang, X., Chen, S., Li, Q., Wang, W., Hou, C., Gao, X., Wang, L., & Wang, S. (2015). Zinc Oxide Nanoparticles Affect Biomass Accumulation and Photosynthesis in *Arabidopsis*. *Frontiers in Plant Science*, 6, 1243. doi:10.3389/fpls.2015.01243

- Wang, Y., Noguchi, K., & Terashima, I. (2008). Distinct light responses of the adaxial and abaxial stomata in intact leaves of *Helianthus annuus* L. *Plant, Cell and Environment*, 31(9), 1307–1316. doi:10.1111/j.1365-3040.2008.01843.x
- Wang, Z., Xie, X., Zhao, J., Liu, X., Feng, W., White, J. C., & Xing, B. (2012). Xylem- and phloem-based transport of CuO nanoparticles in maize (*Zea mays* L.). *Environmental Science and Technology*, 46(8), 4434–4441. doi:10.1021/es204212z
- Wei, C., Zhang, Y., Guo, J., Han, B., Yang, X., & Yuan, J. (2010). Effects of silica nanoparticles on growth and photosynthetic pigment contents of *Scenedesmus obliquus*. *Journal of Environmental Sciences*, 22(1), 155–160. doi:10.1016/S1001-0742(09)600875
- Weinstein, L. H., Kaur-Sawhney, R., Rajam, M. V., Wettlaufer, S. H., & Galston, A. W. (1986). Cadmium-Induced Accumulation of Putrescine in Oat and Bean Leaves. *Plant Physiology*, 82(3), 641–645. doi:10.1104/pp.82.3.641
- Werker, E. (2000). Trichome diversity and development. *Advances in Botanical Research*, 31, 1–35
- Wiesner, M. R., Lowry, G. V., Alvarez, P., Dionysiou, D., & Biswas, P. (2006). Assessing the Risks of Manufactured Nanomaterials. *Environmental Science & Technology*, 40, 4336–4345. doi:10.1021/es062726m.
- Wigginton, N. S., Haus, K. L., & Hochella, M. F. (2007). Aquatic environmental nanoparticles. *Journal of Environmental Monitoring*, 9(12), 1306–1316. doi:10.1039/b712709j
- Witters, H. E. (1998). Chemical speciation dynamics and toxicity assessment in aquatic systems. *Ecotoxicology and Environmental Safety*, 41, 90–95.
- Wu, S. G., Huang, L., Head, J., Chen, D., Kong, I. C., & Tang, Y. J. (2012). Phytotoxicity of metal oxide nanoparticles is related to both dissolved metals ions and adsorption of particles on seed surfaces. *Journal of Petroleum and Environmental Biotechnology*, 03(04). doi:10.4172/2157-7463.1000126
- Xuming, W., Fengqing, G., Linglan, M., Jie, L., Sitao, Y., Ping, Y., Fashui, H. (2008). Effects of nano-anatase on ribulose-1, 5-bisphosphate carboxylase/oxygenase mRNA expression in spinach. *Biological Trace Element Research*, 126, 280–289. doi:10.1007/s12011-008-8203-y

- Yang, F., Liu, C., Gao, F., Su, M., Wu, X., Zheng, L., Hong, F., & Yang, P. (2007a). The improvement of spinach growth by nano-anatase TiO₂ treatment is related to nitrogen photoreduction. *Biological Trace Element Research*, 119, 77–88. doi:10.1007/s12011-007-0046-4
- Yang, J., Zhang, J., Liu, K., Wang, Z., & Liu, L. (2007b). Involvement of polyamines in the drought resistance of rice. *Journal of Experimental Botany*, 58(6), 1545–1555. doi:10.1093/jxb/erm032
- Yin, L., Cheng, Y., Espinasse, B., Colman, B. P., Auffan, M., Wiesner, M., Rose, J., Liu, J., Bernhardt, E. S. (2011). More than the ions: The effects of silver nanoparticles on *lolium multiflorum*. *Environmental Science and Technology*, 45(6), 2360–2367. doi:10.1021/es103995x
- Yoji, T., Kiyotaka, K., & Peter, B. K. (1983). Leaf surface fine-structures in rice plants cultured under shaded and non-shaded conditions. *Japanese Journal of Crop Science*, 52, 534–543.
- You, J., Zhang, Y., & Hu, Z. (2011). Bacteria and bacteriophage inactivation by silver and zinc oxide nanoparticles. *Colloids Surfaces B Biointerfaces*, 85, 161–167. doi:10.1016/j.colsurfb.2011.02.023
- Yruela, I. (2005). Copper in plants. *Brazilian Journal of Plant Physiology*, 17, 145–156. doi:10.1590/S1677-04202005000100012
- Yruela, I. (2009). Copper in plants: Acquisition, transport and interactions. *Functional Plant Biology*, 36, 409–430. doi:10.1071/FP08288
- Zarafshar, M., Akbarinia, M., Askari, H., Hosseini, S. M., Rahaie, M., & Struve, D. (2015). Toxicity assessment of SiO₂ nanoparticles to pear seedlings. *International Journal of Nanoscience and Nanotechnology*, 11(1), 13–22.
- Zhang, P., Ma, Y. & Zhang, Z. (2015). Nanotechnology and Plant Sciences: Nanoparticles and Their Impact on Plants. In H. M. Siddiqui, H. M. Al-Whaibi, & F. Mohammad, eds. Cham: Springer International Publishing, pp. 77–99.
- Zhang, X., Yan, S., Tyagi, R. D., & Surampalli, R. Y. (2011). Synthesis of nanoparticles by microorganisms and their application in enhancing microbiological reaction rates. *Chemosphere*, 82(4), 489–494. doi:10.1016/j.chemosphere.2010.10.023

Zhao, L., Hernandez-Viezcas, J. A., Peralta-Videa, J. R., Bandyopadhyay, S., Peng, B., Munoz, B., Keller, A. A., & Gardea-Torresdey, J. L. (2013). ZnO nanoparticle fate in soil and zinc bioaccumulation in corn plants (*Zea mays*) influenced by alginate. *Environmental Science: Processes and Impacts*, 15, 260–266. doi:10.1039/C2EM30610G.

Zolla, L., & Rinalducci, S. (2002). Involvement of active oxygen species in degradation of light-harvesting proteins under light stresses. *Biochemistry*, 41, 14391–14402.



Vera da costa <veradacosta5@gmail.com>

Fwd: [Urkund] 0% similarity - librarian@unigoa.ac.in

1 message

Asst. Registrar(PG) <arpg@unigoa.ac.in>
To: Vera da costa <veradacosta5@gmail.com>

Thu, Jul 21, 2016 at 12:02 PM

----- Forwarded message -----

From: **Satish Shetye** <shetye@unigoa.ac.in>
Date: Fri, Jul 15, 2016 at 2:30 PM
Subject: Fwd: [Urkund] 0% similarity - librarian@unigoa.ac.in
To: "Asst. Registrar(PG)" <arpg@unigoa.ac.in>, Donald Rodrigues <dracad@unigoa.ac.in>
Cc: Gopakumar V <librarian@unigoa.ac.in>

Please process the thesis.....srs

----- Forwarded message -----

From: **Gopakumar V** <librarian@unigoa.ac.in>
Date: 15 July 2016 at 12:54
Subject: Fwd: [Urkund] 0% similarity - librarian@unigoa.ac.in
To: Satish Shetye <shetye@unigoa.ac.in>

Dear sir

The thesis submitted by Ms. Maria Vera Jesus Da Costa, Department of Botany shows 0% Of similarity with external sources.

Report available below.

Student message: Morphological, Physiological, Biochemical and Molecular Response of Rice Seedlings to Metallo-Nanoparticles

Document : Thesis in Botany_MVJDC_July 2016.pdf [D21104597]

IMPORTANT! The analysis contains 1 warning(s).

About 0% of this document consists of text similar to text found in 29 sources. The largest marking is 9 words long and is 100% similar to its primary source.

PLEASE NOTE that the above figures do not automatically mean that there is plagiarism in the document. There may be good reasons as to why parts of a text also appear in other sources. For a reasonable suspicion of academic dishonesty to present itself, the analysis, possibly found sources and the original document need to be examined closely.

Click here to open the analysis:

<https://secure.urdund.com/view/20793487-813603-671818>

Click here to download the document:

<https://secure.urdund.com/archive/download/21104597-302255-114065>

--

Dr. Satish R. Shetye
Goa University
Taleigao Plateau
Goa, India, 403206
Phone: +91 832 651 9001 (O)
+91 832 246 1660 (R)
Fax: +91 832 245 1184
e-mail: shetye@unigoa.ac.in

LIST OF PUBLICATIONS

- ❖ **Maria Vera Da Costa and Prabhat Sharma (2016)** Effect of copper oxide nanoparticles on the structure, photosynthesis and anti-oxidant response in *Oryza sativa*. **PHOTOSYNTHETICA 54 (1): 110-119**. doi:10.1007/s11099-015-0167-5
(Impact Factor: 1.558)
- ❖ **Maria Vera Da Costa and Prabhat Sharma (2015)** Influence of TiO₂ nanoparticle on photosynthesis and biochemical processes in *Oryza sativa*. **Int. J. Rec. Sci. Res. 6 (1): 2445-2451 (ISSN: 0976-3031). SJIF 2015: 5.971; ICV: 5.72.**

Effect of copper oxide nanoparticles on growth, morphology, photosynthesis, and antioxidant response in *Oryza sativa*

M.V.J. DA COSTA and P.K. SHARMA[†]

Department of Botany, Goa University, Goa, India 403 206

Abstract

The physiological and biochemical behaviour of rice (*Oryza sativa*, var. Jyoti) treated with copper (II) oxide nanoparticles (CuO NPs) was studied. Germination rate, root and shoot length, and biomass decreased, while uptake of Cu in the roots and shoots increased at high concentrations of CuO NPs. The accumulation of CuO NPs was observed in the cells, especially, in the chloroplasts, and was accompanied by a lower number of thylakoids per granum. Photosynthetic rate, transpiration rate, stomatal conductance, maximal quantum yield of PSII photochemistry, and photosynthetic pigment contents declined, with a complete loss of PSII photochemical quenching at 1,000 mg(CuO NP) L⁻¹. Oxidative and osmotic stress was evidenced by increased malondialdehyde and proline contents. Elevated expression of ascorbate peroxidase and superoxide dismutase were also observed. Our work clearly demonstrated the toxic effect of Cu accumulation in roots and shoots that resulted in loss of photosynthesis.

Additional key words: ascorbate; nanoparticle; proline; superoxide dismutase; thylakoid.

Introduction

Development of new nanomaterials and their application in various industrial uses results in greater pollution of the environment by nanoparticles (NPs) (Corredor *et al.* 2009). In recent years, NPs with sizes typically below 100 nm have been applied in an increasing number of commercial applications (Corredor *et al.* 2009), such as electronics, optics, textiles, medicine, catalysts, water treatment, and environmental remediation (Zhang and Elliot 2006). In 2005, the total global investment in nanotechnology was \$10 billion and is set to reach \$1 trillion by 2015 (Harrison 2007), leading to further increase of engineered NPs released into our environment. Manufactured NPs enter the environment unintentionally through atmospheric emissions, domestic waste water, agriculture, and accidental release during manufacture and transport (Klaine *et al.* 2008). This

ultimately leads to NPs entry into soil and water bodies thereby affecting plants and animals. Due to their physical and chemical properties, NPs also interact with living systems. Studies on the interaction of NPs with the environment are being carried out in order to shed light on questions regarding size, structure, and reactivity in aquatic and sedimentary systems, their association with other colloids and behaviour in comparison to bulk counterparts (Klaine *et al.* 2008). However, the toxic potential of NPs to plants and their bioavailability are yet to be investigated (Klaine *et al.* 2008).

Metallo-NPs differ from bulk counterparts in surface characteristics, such as copious reactive sites and mobility regulated by deposition or aggregation (Maynard *et al.* 2006) which is in turn dependent on pH, temperature, particle size, ionic strength, and concentration (Wiesner

Received 8 February 2015, accepted 29 June 2015, published as online-first 10 August 2015.

[†]Corresponding author; phone: 0832 6519346, fax: 0832 2451184, e-mail: prabhat_k_sharma@rediffmail.com

Abbreviations: AAS – atomic absorption spectrophotometer; APX – ascorbate peroxidase; DM – dry mass; *E* – transpiration rate; FM – fresh mass; *F_m* – maximum fluorescence; *F₀* – initial fluorescence; *F_s* – steady-state fluorescence; *F_v/F_m* – maximal quantum yield of PSII photochemistry; GR – glutathione reductase; *g_s* – stomatal conductance; IRGA – infra red gas analyser; MDA – malondialdehyde; NP(s) – nanoparticle(s); *P_N* – photosynthetic rate; *q_p* – photochemical quenching; ROS – reactive oxygen species; SEM – scanning electron microscope; SOD – superoxide dismutase; TBA – thiobarbituric acid; TEM – transmission electron microscope; XRD – X-ray diffraction.

Acknowledgements: We thank the Department of Science & Technology (DST), New Delhi (SR/SO/PS-63/2009) and UGC–SAP (F. 3–50/2009 (SAP-II)) for funding this work. We would like to thank All India Institute of Medical Sciences, New Delhi for TEM imaging; NIO, Goa for SEM imaging and atomic absorption spectrophotometry; Physics Department, Goa University for NP size determination using X-ray diffractometer. We are grateful to Andrew Willis, Centre for Agroecology, Water and Resilience (CAWR), Coventry University, Coventry, United Kingdom for correcting the English of the manuscript.

Both authors made equal contribution to the work presented in this paper.

et al. 2006). These characteristics lead to electrostatic, hydrogen bonding, and hydrophobic interactions with structural and catalytic proteins in the cell (Ojamäe *et al.* 2006). Literature states that NPs exist as colloids at low concentrations and may form small stable aggregates at moderate concentrations (Klaine *et al.* 2008), while a small amount of metallo-NPs may also dissociate into ions (Navarro *et al.* 2008). The mechanism of NP uptake by plant roots is not clearly understood. Studies have shown that, depending on the size, NPs may enter the plant cell through carrier proteins, aquaporins, ion channels, via fluid phase endocytosis, plasmodesmata transport, or entry may be facilitated through natural organic matter or root exudates and formation of new pores (Rico *et al.* 2011).

Copper is an essential micronutrient required for the normal growth of plants. It is involved in many physiological processes as it exists in multiple oxidative states (Cu^{2+} , Cu^+) *in vivo* (Yruela 2005). It acts as a structural component in regulatory proteins and in those involved in photosynthetic electron transport, mitochondrial respiration, oxidative stress responses, cell wall metabolism, and hormone signalling (Marschner 1995, Raven *et al.* 1999, Solymosi and Bertrand 2012). At the cellular level, Cu plays an important role in signalling of transcription, protein trafficking machinery, oxidative phosphorylation, and iron mobilization as well. The redox property of Cu can also contribute to its toxicity, as free ions catalyse the production of damaging radicals (Manceau *et al.* 2008). No published data are available on the concentration of metallo-NPs including CuO NPs in soil, however, heavy metal Cu is estimated to be in the range of

2–100 mg kg^{-1} (DM) in typical uncontaminated soils (Nagajyoti *et al.* 2010).

In recent years, significant research has been focused on studying CuO NPs effects in plants. The limit of metal NP accumulation, across a range of metals, is proposed to be controlled by the total reducing capacity of the plant (Haverkamp and Marshall 2009). It is reported that the exposure to Cu NP (50 nm) at concentration of 1,000 mg L^{-1} in *Cucurbita pepo* (zucchini) resulted in 90% biomass reduction (Stampoulis *et al.* 2009). Cu NPs were toxic to the growth of *Phaseolus radiatus* (mung bean) and *Triticum aestivum* (wheat) at concentrations up to 1,000 mg L^{-1} (Lee *et al.* 2008). Similarly, reduction in the growth and transpiration of *C. pepo* by 60–70% relative to untreated control was reported by Musante and White (2012) after treatment with CuO NPs. Available published data and the lack of knowledge on the metallo-NPs influence in plants is a major limitation which warrants extensive research on this topic.

Further studies, other than germination, root and shoot length, and biomass need to be carried out with regard to CuO NPs in order to understand better uptake, accumulation, and effects on photosynthesis, and other physiological and biochemical processes in plants. Therefore, this study was conducted to examine the effect of CuO NPs on *Oryza sativa* plants grown hydroponically at concentrations ranging from 0–1,000 mg L^{-1} (w/v) on the growth, accumulation of Cu in leaves and roots, external and internal morphology, photosynthesis, oxidative and osmotic stress, and expression level of antioxidant genes, such as ascorbate peroxidase (APX) and superoxide dismutase (SOD).

Materials and methods

Plant material and treatments: *Oryza sativa* (var. Jyoti), a high yielding rice variety, was obtained from Indian Council of Agricultural Research, Goa and stored in dark at 20°C. CuO NPs (<50 nm size, Sigma-Aldrich) was prepared in Hoagland's solution with concentrations of 0 (control), 2.5, 10, 50, 100, and 1,000 mg L^{-1} (w/v) at pH 6.5. Seeds were surface sterilized using 4% sodium hypochlorite (BDH) solution, washed 5–6 times and soaked in tap water [Cu content < 0.06 mg L^{-1} (w/v)] for 3 d. Germination paper was placed in Petri dishes, rice seeds were sown, and a NP suspension of various concentrations was applied in respective Petri dishes. They were placed in a growth chamber under the temperature of $25 \pm 2^\circ\text{C}$ with 16 h photoperiod and light intensity of 200 $\mu\text{mol}(\text{photon}) \text{m}^{-2} \text{s}^{-1}$. The 6-d-old seedlings were transferred carefully into the hydroponic system and grown for further 24 d. The hydroponic system ensured complete mixing of NPs by use of magnetic stirrers and proper aeration was achieved by air pumps. The solutions were changed with respective NP solutions every third day.

Nanoparticle size determination: Scanning electron microscope (SEM, JSM 5800 LV, JEOL, Japan) operating at a constant acceleration voltage of 10 kV was used to characterize CuO NPs. NPs were ultra-sonicated in 100% ethanol and a drop of this solution was placed onto the stub layered with carbon conductive, double sided adhesive tape (SPI Supplies®, USA). The sample was air-dried and sputter coated with gold for 15 s (SPI-MODULE Gold Sputter Coater) under high vacuum at the National Institute of Oceanography, Goa. Further confirmation of the particle size was done using X-ray diffractometer (XRD ultraX 18HB-300, Rigaku, Japan) with a scintillation counter probe SC-30. CuO NP powder was directly mounted on sample holders and the X-ray diffraction XRD pattern was recorded at room temperature in the range of $2\theta = 20^\circ\text{--}80^\circ$ with a step of 0.02° and 2°min^{-1} speed using Cu α radiation ($\lambda = 0.15406 \text{ nm}$). The data analysis was performed using Traces software (GBC Scientific Instruments, USA) and the particle size was determined using Scherrer's formula considering the first three peaks of the pattern obtained.

Growth, morphology and biomass studies: Percentage of germination, shoot and root length were measured after 6 d. The biomass was measured in 10 randomly selected plants grown in CuO NPs after 30 d. The external leaf and root morphology was studied by visualizing lyophilized segments using SEM (*JSM 5800 LV, JEOL, Japan*). The internal leaf and root morphology was studied using transmission electron microscopy (TEM) at All India Institute of Medical Sciences (AIIMS), New Delhi. The leaf and root tissue was cut into 2×2 mm pieces and fixed in a mixture of 2% paraformaldehyde and 2.5% glutaraldehyde in 0.1 M phosphate buffer for 10:00 h at 4°C. The tissue samples were washed in 0.1 M phosphate buffer at 4°C. Samples were then postfixed at room temperature for 1 h in 1% OsO₄ in 0.1 M phosphate buffer (pH 7.2). Samples were dehydrated in acetone, infiltrated, and embedded in *Araldite CY 212*. Thin, serial sections were cut (70–80 nm thick) using ultramicrotome (*Leica UC6, Leica Microsystems, Germany*), collected on copper grids, stained with uranyl acetate and lead citrate, and examined under a TEM (*Morgagni 268D, Fei Company, The Netherlands*).

Nanoparticle uptake: Uptake of NPs was determined using atomic absorption spectrophotometer (*Flame Furnace system—AAlyst 200, AAS, Perkin Elmer, USA*). The ash was dissolved in 1% HNO₃ (*Merck*) solution and filtered through 0.45 µm Whatman filter paper and then used. The filtered sample was used for AAS analysis in whole root and leaf tissues, as well as in different sections of the leaf (apical, middle, and basal region) at different concentrations of CuO NPs.

Carbon dioxide fixation: Studies were carried out using a portable infrared gas analyser (*ADC Bioscientific, LCI-SD, Hansatech, UK*) using inbuilt software as described by Sharma and Hall (1996). The photosynthetic rate (P_N), transpiration rate (E), and stomatal conductance (g_s) were measured at ambient temperature, CO₂ concentration, and light intensity of 1,200 µmol(photon) m⁻² s⁻¹ using a detachable light source provided by a dichroic lamp (*Hansatech, UK*).

Chlorophyll (Chl) fluorescence measurements were carried out according to Sharma *et al.* (1997) using a fluorescence monitoring system (*FMS-1, Hansatech, UK*). The leaf samples were dark adapted for 10 min to inhibit all light-dependent reactions by completely oxidizing PSII electron acceptor molecules. A weak modulating beam of intensity 3–4 µmol(photon) m⁻² s⁻¹ was focused on the sample to measure initial fluorescence (F_0), followed by exposure to a saturating pulse [approximately 4,000 µmol(photon) m⁻² s⁻¹ for 0.06 s] to measure the maximum fluorescence (F_m). Variable fluorescence (F_v) was determined by subtracting F_0 from F_m as ($F_v = F_m - F_0$) and the maximum quantum yield (F_v/F_m) ratio was calculated. Actinic light was provided at

an intensity of 1,200 µmol(photon) m⁻² s⁻¹ and allowed to reach a steady-state fluorescence yield (F_s) after which far red pulse was given for 5 s. It was then used to calculate the relative contributions for photochemical and nonphotochemical energy dissipation measured as the photochemical quenching (q_p) and nonphotochemical quenching (q_N) using *Modfluor32* software.

Extraction and analysis of photosynthetic pigments: Leaf tissue (0.1 g) was ground in 100% acetone (*Merck, HPLC grade*) making a final volume of 1.5 ml and incubated overnight at 4°C. The homogenate was centrifuged (*Z32HK, HERMLE Labortechnik GmbH, Germany*) at 4°C for 10 min at 4,000 × *g*. One ml of supernatant was collected and filtered through 0.2 µm *Ultipor®N66®Nylon* membrane filter (*PALL Life Sciences, USA*) and 10 µl of sample was analysed in an HPLC system (*Waters, USA*), using two-solvent gradient as a mobile phase (using *Merck HPLC grade chemicals*) composed of solution A (ethyl acetate) and solution B (acetonitrile:water, 9:1). The mobile flow rate was 1.2 ml min⁻¹ for a run time of 30 min. The pigments were separated using a C18 column (*Waters Spherisorb ODS2 – 250 mm × 4.6 mm × 5 µm*). The pigment peaks were determined at 445 nm with a *Waters 2996* photodiode array detector based on RT and spectral characteristics. β-carotene was used as an external standard for quantification of pigments (Sharma and Hall 1996).

Lipid peroxidation was determined by estimation of the malondialdehyde (MDA) content in leaves following Sankhalkar and Sharma (2002). The amount of MDA (extinction coefficient of 155 mM⁻¹ cm⁻¹) was calculated by subtracting nonspecific absorbance at 600 nm from absorbance at 532 nm using UV-Visible spectrophotometer (*UV-2450, Shimadzu, Singapore*).

Proline determination: Proline accumulation in fresh leaves was determined according to the method of Bates *et al.* (1973); the absorbance at 520 nm was measured using UV-Visible spectrophotometer (*UV-2450, Shimadzu, Singapore*). L-proline (*Sigma*) was used as standard.

Ascorbate assay: Estimation of ascorbate (ASA) in fresh leaves was carried out according to the method of Kampfenkel *et al.* (1995); the absorbance at 520 nm was measured using UV-Visible spectrophotometer (*UV-2450, Shimadzu, Singapore*). Ascorbic acid (*Himedia*) was used as standard.

RNA extraction and quantification and gene expression studies: Leaf tissue (0.1 g) was ground using liquid nitrogen and extracted using the protocol mentioned in the RNA extraction kit (*Invitrogen*). The RNA extracted was quantified using a spectrophotometer at 260 and 280 nm (*UV-2450, Shimadzu, Singapore*).

cDNA preparation using RT PCR: cDNA synthesis was done using PCR kit (*Invitrogen Superscript III Reverse Transcriptase*, Cat no: 18080/093/044/085) following the given protocol.

Real time analysis using Real time PCR: Expression of genes for antioxidant enzymes ascorbate peroxidase (APX) and superoxide dismutase (SOD) was studied using *MJ MiniOpticon* real time PCR system, *Bio-Rad*, USA. APX primers (Oligo number: 91211B3–1255C12 17/44) APX–Thy–L 5'– GCT AAA CTG AGC GAC CTT GG –3', (Oligo number: 91211B3–1255D12 18/44) APX–Thy–R 5'–GCT GCT CCT ACC GTT ACT GG –3' and SOD primers (Oligo number: 30121B3–9644D10 5/32) SOD–F 5'–CGT CGA TCT CCC ATC ATT TT–3', (Oligo number: 30121B3–9644E10 6/32) SOD–R 5'–

CTT GTT CCG TTT TGT GTG GA–3' were procured from *Pharmads and Equipments Pvt. Ltd.*, India. Reaction was followed in 50 μ l of total volume using the *Bio-Rad* kit protocol (*SsoAdvanced SYBR Green Supermix*, cat no.: 172–5260). Amplification was carried out for 40 cycles. Data were analysed using *Bio-Rad CFX manager* software.

Statistical analysis: The data shown corresponded to the mean values \pm standard deviation (SD). One-way analysis of variance (ANOVA) and *Duncan's* multiple range test by using *Microsoft Excel XLSTAT* (version 2015.2.01.17315) were performed to confirm the variability of the results and the determination of significant ($P \leq 0.05$) difference between treatment groups, respectively.

Results

The NP characterization studies revealed that the shape of CuO NPs was spherical and the size was estimated as < 50 nm using SEM (Fig. 1A) and applying Scherer's formula to the X-ray diffraction (XRD) data (Fig. 1B).

The germination rate of rice plants was slightly affected (7%) at 1,000 mg L⁻¹ CuO NPs compared with control (Table 1). During the early stage of growth (6 d old), the plantlets showed a decrease in root (23%) and shoot (31%) length compared with the control at higher concentrations (Table 1). The decrease in root and shoot growth was found when the plants were treated with 100 mg L⁻¹ CuO NPs and higher concentrations

(Table 1). Biomass of rice shoots grown at 1,000 mg L⁻¹ CuO NP decreased by 31% on fresh mass (FM) basis and 14% on a dry mass (DM) basis. Root biomass increased by 9% at 1,000 mg L⁻¹ CuO NP when calculated on FM basis but decreased by 16% on DM basis (Table 1) compared with the control.

The effect of CuO NPs on leaf and root surface studied using SEM showed an increase in the number of trichomes (Fig. 2A,B,C) and a decrease in the number (Fig. 2A,B,C) and size of stomata (Fig. 2D,E,F). External damage to the root surface was also observed at 1,000 mg L⁻¹ CuO NPs (Fig. 2G,H,I).

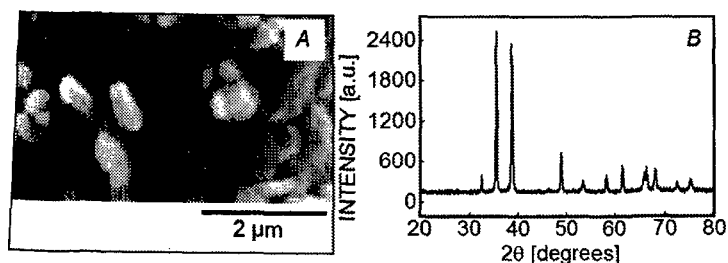


Fig. 1. SEM image of CuO NPs at a magnification of 30,000 \times (A) and X-ray diffraction pattern (B) of CuO NPs recorded at room temperature in the range $2\theta = 20^\circ$ – 80° with a step of 0.02° , speed = 2°min^{-1} using Cu $\text{K}\alpha$ radiation ($\lambda = 0.15406$ nm).

Table 1. Percentage of germination, shoot, root length, and biomass (fresh mass – FM, and dry mass – DM) of *Oryza sativa* treated with CuO nanoparticles (NPs) at different concentrations. Mean values \pm SD ($n = 5$). Means in the column followed by the same letter do not differ significantly at $p < 0.05$.

NPs [mg L ⁻¹]	Germination [%]	Shoot length [mm]	Root length [mm]	Shoot biomass [g]		Root biomass [g]	
				FM	DM	FM	DM
0	96.0 \pm 3.97 ^a	35.2 \pm 6.36 ^{ab}	48.4 \pm 6.33 ^a	0.64 \pm 0.01 ^a	0.087 \pm 0.05 ^c	0.192 \pm 0.02 ^c	0.025 \pm 0.01 ^a
2.5	94.7 \pm 3.10 ^{ab}	31.0 \pm 1.22 ^{bc}	45.8 \pm 5.96 ^a	0.64 \pm 0.02 ^a	0.092 \pm 0.03 ^a	0.193 \pm 0.03 ^c	0.021 \pm 0.02 ^c
10	90.1 \pm 1.86 ^{bc}	27.8 \pm 1.64 ^{cd}	43.8 \pm 6.89 ^{ab}	0.63 \pm 0.02 ^a	0.087 \pm 0.02 ^b	0.205 \pm 0.02 ^b	0.021 \pm 0.01 ^c
50	89.7 \pm 6.61 ^c	39.0 \pm 3.36 ^a	48.5 \pm 2.88 ^a	0.61 \pm 0.02 ^a	0.078 \pm 0.01 ^d	0.188 \pm 0.02 ^d	0.023 \pm 0.01 ^c
100	89.2 \pm 4.53 ^c	25.7 \pm 3.36 ^d	42.2 \pm 3.53 ^{ab}	0.43 \pm 0.01 ^b	0.071 \pm 0.03 ^f	0.180 \pm 0.02 ^e	0.024 \pm 0.01 ^b
1000	88.7 \pm 4.82 ^c	24.3 \pm 3.12 ^d	37.2 \pm 4.35 ^b	0.44 \pm 0.05 ^b	0.075 \pm 0.02 ^e	0.209 \pm 0.01 ^a	0.021 \pm 0.01 ^d

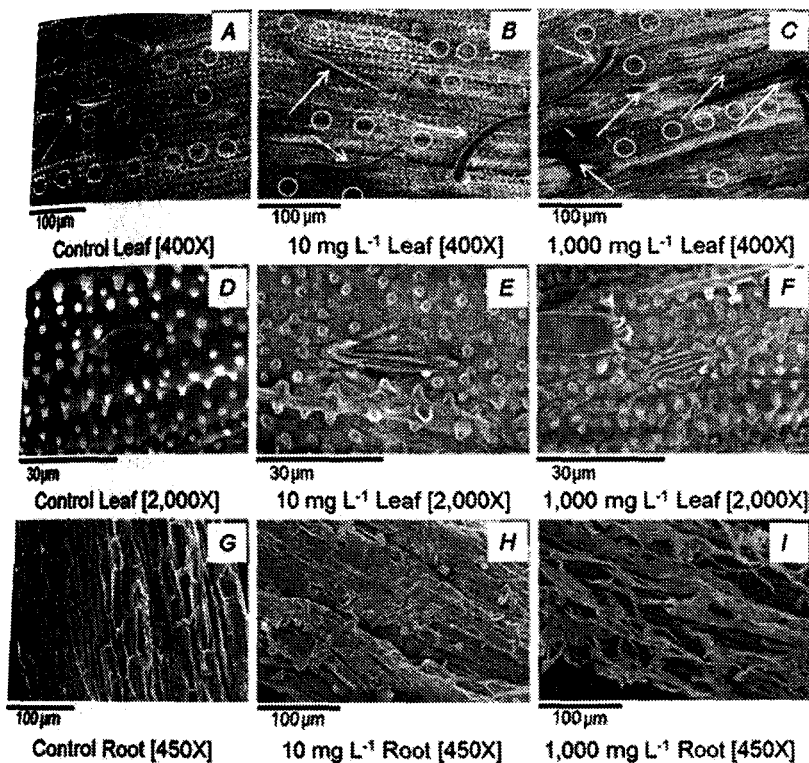


Fig. 2. SEM images of leaf (adaxial) surface showing trichomes (A-C), stomata (D-F), and roots (G-I) of plants treated with CuO nanoparticles for 30 d. The arrows indicate trichomes and the circles represent stomata.

TEM micrographs showed accumulation of CuO NPs inside the leaf and root cells (Fig. 3A-C). Accumulation of NP in the leaf was especially observed in the chloroplasts. The treatments resulted in the reduced number of thylakoids per granum at the concentration higher than 50 mg L⁻¹; a distortion (wavy arrangement) of the thylakoid membranes and swelling of the intrathylakoidal space was observed at 1,000 mg L⁻¹ CuO NPs (Fig. 3D-F).

Cu accumulation in the whole leaf and all leaf

segments increased at the high concentration of CuO NPs (Table 2). The increase of 5.5-fold in the Cu content was observed in the whole leaves treated with 1,000 mg L⁻¹ CuO NP as compared with the control plants. The increase of 76-fold in the Cu content was observed in the whole roots treated with 100 mg L⁻¹. At the highest concentration, however, Cu accumulation in the whole root tissue was only 9.4-fold as compared with the control (Table 2). Leaf segments (apical, middle, and basal region) analysed for the Cu content showed the

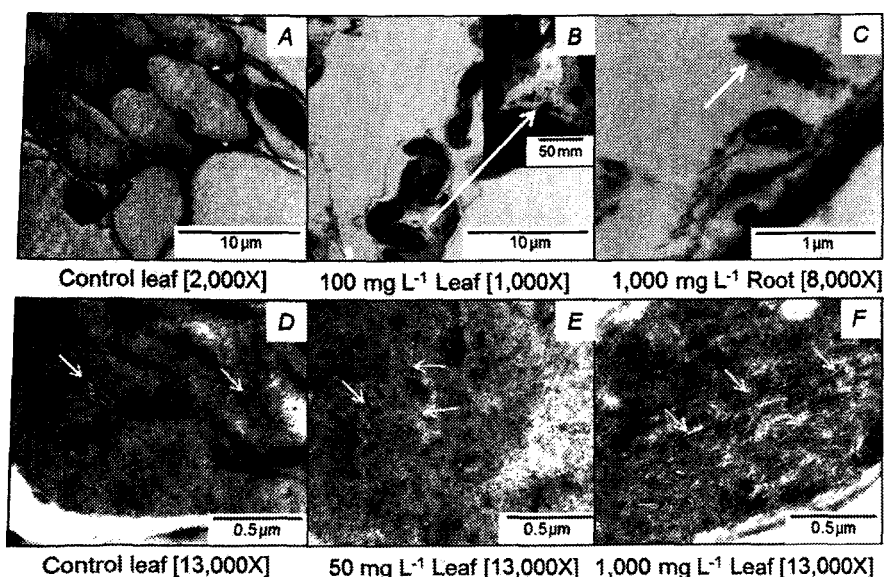


Fig. 3. TEM images of leaf showing the accumulation of CuO nanoparticles in chloroplast (A,B), in root (C), and reduction in chloroplast thylakoid stacking and appearance of the particles in chloroplast (D-F). The arrows indicate CuO nanoparticles (B-C) and changes in thylakoid stacking (D-F).

Table 2. Cu content in leaves and roots of *Oryza sativa* plants treated with CuO nanoparticles (NPs) at concentrations of 0–1,000 mg L⁻¹ for 30 d. Mean values ± SD (n = 3). Means in the column followed by the same letter do not differ significantly at p ≤ 0.05.

CuO NPs [mg L ⁻¹]	Cu in leaf [mg kg ⁻¹ (DM)]				Cu in root [mg kg ⁻¹ (DM)] Whole root tissue
	Whole leaf tissue	Apical region	Middle region	Basal region	
0	3.12 ± 0.14 ^d	3.44 ± 0.3 ^d	5.15 ± 0.15 ^c	4.50 ± 0.4b ^c	20.21 ± 2.0 ^e
2.5	5.0 ± 0.21 ^c	3.64 ± 0.1 ^d	3.42 ± 0.3 ^c	3.21 ± 1.4 ^c	289.0 ± 10.2 ^d
10	5.36 ± 0.32 ^c	3.57 ± 0.26 ^d	3.70 ± 0.3 ^c	3.49 ± 0.9 ^c	559.9 ± 14.9 ^c
50	5.9 ± 0.36 ^{bc}	6.20 ± 0.6 ^c	5.45 ± 0.26 ^c	6.43 ± 0.1 ^b	753.2 ± 11.7 ^b
100	6.65 ± 0.50 ^b	8.50 ± 0.45 ^b	8.27 ± 1.22 ^b	6.97 ± 0.1 ^b	1,544.1 ± 18.9 ^a
1,000	17.27 ± 1.45 ^a	14.11 ± 0.9 ^a	14.36 ± 3.3 ^a	21.30 ± 3.3 ^a	190.14 ± 10.95 ^f

highest accumulation at 1,000 mg L⁻¹. No specific pattern of accumulation was found in apex, middle, and basal segments of leaves (Table 2).

A significant decrease was observed in P_N , E , and g_s at high concentrations of CuO NPs (Fig. 4A). The decrease of 86% in P_N was observed in the plants treated with 1,000 mg L⁻¹ CuO NPs. The similar decrease was also observed in E and g_s (Fig. 4A). The maximum quantum efficiency of PSII measured as F_v/F_m ratio did not significantly differ from control up to 10 mg L⁻¹ of CuO NPs. At 1,000 mg L⁻¹, a decrease of 46% was observed compared with the control (Fig. 4B). The photochemical quenching (q_p) showed no change up to the 100 mg L⁻¹ CuO NPs, but it significantly diminished at 1,000 mg L⁻¹ (Fig. 4B). Nonphotochemical quenching (q_N) showed a slight increase (10%) at 1,000 mg L⁻¹ compared with the control (Fig. 4B).

The Car (violaxanthin, lutein, and β -carotene) content increased by more than 50% at 2.5 mg L⁻¹ CuO NPs, but

higher concentrations of the NPs resulted in a significant decrease in the pigment content (Table 3). Violaxanthin increased by 95% at 2.5 mg L⁻¹ and decreased by more than 58% at concentrations of 100 mg L⁻¹ and above. The lutein content increased by 67% at 2.5 mg L⁻¹, but decreased linearly to 70% at 1,000 mg L⁻¹ compared with the control. The β -carotene content showed no change up to 10 mg L⁻¹, decreasing by 90% at high concentrations (1,000 mg L⁻¹ CuO NPs). Similarly, the Chl a/b ratio showed no change up to 10 mg L⁻¹, but it increased by 41% at 1,000 mg L⁻¹.

We observed a negligible difference in lipid peroxidation, measured as MDA-TBA adducts, up to 1,000 mg L⁻¹ CuO NPs (Fig. 5A). Proline increased up to 2.2 times of the control with 1,000 mg L⁻¹ CuO NPs (Fig. 5B). Similarly, ascorbate, which acts as a nonenzymatic antioxidant, increased by 30% compared with the control in leaves of plants treated with CuO NP at the high concentration (Fig. 5C).

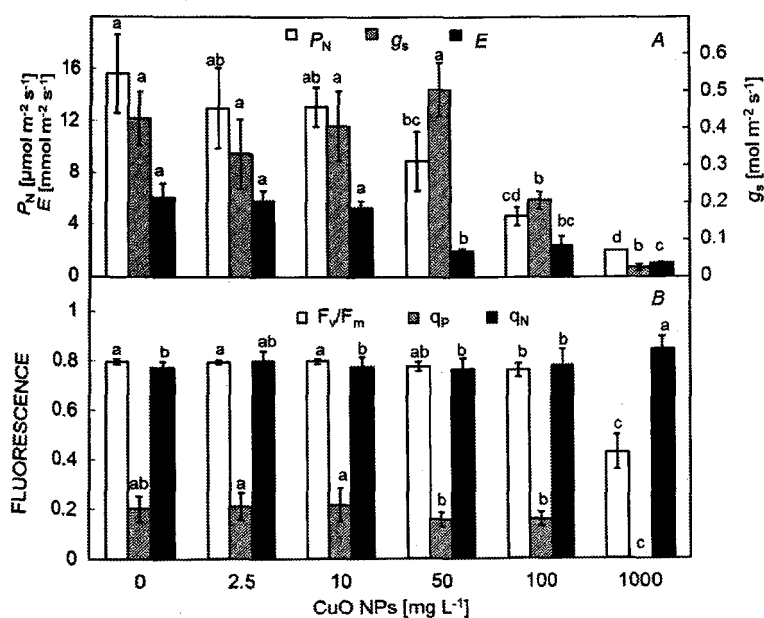


Fig. 4. Photosynthetic rate (P_N), stomatal conductance (g_s), and transpiration rate (E) (A) and photosynthetic efficiency of PSII (F_v/F_m), photochemical quenching (q_p), and nonphotochemical quenching (q_N) (B) of rice plants treated with CuO NPs for 30 d. Mean values ± SD (n = 5). Means in the column followed by the same letter do not differ significantly at p ≤ 0.05.

Table 3. Carotenoid (Car) content and relative chlorophyll (Chl) content of *Oryza sativa* leaves treated with CuO nanoparticles (NPs) at concentrations of 0–1,000 mg L⁻¹ for 30 d. Mean values ± SD (*n* = 3). Means in the row followed by the same letter do not differ significantly at *p* < 0.05. The ratio was calculated taking mean values of the respective pigments.

Pigment content [μg g ⁻¹ (FM)]	CuO NPs [mg L ⁻¹]				
	0	2.5	10	100	1,000
Violaxanthin	1.3 ± 0.001 ^b	2.4 ± 0.06 ^a	1.0 ± 0.009 ^b	0.3 ± 0.001 ^c	0.5 ± 0.009 ^d
Lutein	2.3 ± 0.003 ^b	3.9 ± 0.07 ^a	2.1 ± 0.009 ^b	1.1 ± 0.007 ^c	0.7 ± 0.07 ^d
β-carotene	4.9 ± 0.30 ^a	5.3 ± 0.05 ^a	5.2 ± 0.09 ^a	1.5 ± 0.07 ^b	0.5 ± 0.02 ^c
Chl <i>a/b</i> ratio	1.46	1.51	1.50	1.7	2.06

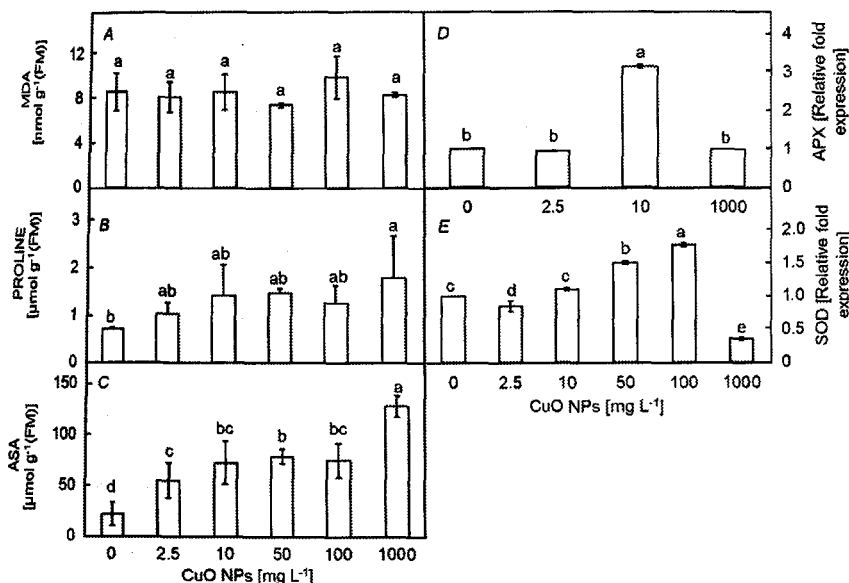


Fig. 5. Malondialdehyde (MDA) (A), proline (B), and ascorbate (ASA) contents (C) and the relative expression of ascorbate peroxidase (APX) (D) and superoxide dismutase (SOD) (E) in rice plants treated with CuO nanoparticles for 30 d. Mean values ± SD (*n* = 5). Means in the column followed by the same letter do not differ significantly at *p* < 0.05.

Gene expression of enzymatic antioxidants, such as ascorbate peroxidase (APX) and superoxide dismutase (SOD), increased with the increasing CuO NP concentration. APX showed a 3-fold increase in its gene expression at 10 mg L⁻¹. At 1,000 mg L⁻¹ of CuO NP, gene expression level of APX was similar to that of

control (Fig. 5D). SOD expression level increased to 1.5-fold at 50 mg L⁻¹ CuO NP and doubled at 100 mg L⁻¹ compared with the control. CuO NP at 1,000 mg L⁻¹ showed a significantly decreased level of SOD expression to that observed in control (Fig. 5E).

Discussion

We observed negligible effect of CuO NPs on seed germination (Table 1); it might be due to a selective permeability that is exhibited by the seed coat. This protects the embryo from CuO NPs toxicity by restricting the entry of NPs until radicles emerge and come into a direct contact with the NPs in the growth medium. Wierzbicka and Obidzińska (1998) reported selective permeability of metallo-NPs. Our results are similar to those reported by Stampoulis *et al.* (2009) in *C. pepo* treated with 1,000 mg L⁻¹ of Cu NPs of 50 nm size, and by Lee *et al.* (2010) with aluminium oxide (~150 nm size), silicon dioxide (42.8 nm size), and magnetite (< 50 nm size) NPs in *Arabidopsis thaliana*. Contrary to our results, CuO NPs are reported being toxic at concentrations as low as 1 mg L⁻¹ in duckweeds

(*Landoltia punctata*; Shi *et al.* 2011) and as high as 4,000 mg L⁻¹ in buckwheat (*Fagopyrum esculentum*; Lee *et al.* 2013), indicating that the elemental composition, particle size, and concentration as well as plant species play an important role in NP toxicity on seed germination.

The reduced shoot and root length values observed in our study (Table 1) might result from accumulation of Cu in root and leaf tissues (Table 2). This was indicated by the massive increase of Cu in roots (76-fold) and leaves (5.5-fold) in comparison with the control (Table 2). Our results were in agreement with earlier work done by Lidon and Henriques (1998) on the effect of Cu on the shoot and root length. They reported that Cu at 0.25 and 1.25 mg L⁻¹ caused a reduction in rice shoot length. Lee *et al.* (2008) showed that Cu NP caused a reduction in the

seedling length of *P. radiatus* and *T. aestivum* by 65% and 75%, respectively. Similarly, CuO NPs decreased root length in *C. pepo* at 1,000 mg L⁻¹ concentration (Stampoulis *et al.* 2009).

Our results of SEM showed external morphological damage to the roots (Fig. 2G–I), reduced number (Fig. 2A–C) and size (Fig. 2D–F) of stomata, and increase of leaf trichomes (Fig. 2A–C). The damage to roots may have affected water uptake, leading to stomatal limitation and thereby limiting net photosynthesis (Fig. 4A). Kennedy and Gonsalves (1987) reported that Cu may adhere to the root surface leading to osmotic stress by decreasing the trans-root potential which is essential for water and ion uptake. Decline in root growth after a treatment with CuO NPs may also result in the reduction of surface area for water uptake, developing a negative water potential leading to osmotic stress (Alia and Pardha Saradhi 1991). The observed increase in the proline content (Fig. 5B), along with the decrease in the number and size of stomata and the increase in trichomes (Fig. 2), clearly indicated the development of osmotic stress due to the treatment. Similarly, the swelling of the intrathylakoidal space (Fig. 3F) is a phenomenon often associated with metal stress (Solymosi and Bertrand 2012) and has been also clearly associated with osmotic stress (Abdelkader *et al.* 2007, Ünneper *et al.* 2014).

Many feasible modes of NP uptake have been suggested but no experimental data are available on the actual mechanism. The AAS analyses revealed that accumulation of NPs in the roots greatly increased when compared to that of leaves (Table 2), indicating that only a small portion of NPs was transported from the roots to the shoots; thus, it led to major toxic effect in the roots. AAS analysis of Cu accumulation in the whole leaves as well as in apical, middle, and basal parts of leaves suggested nonspecific pattern of Cu accumulation. The greater metal content in roots than that in shoots indicates an exclusion mechanism to withstand toxicity; such plants accumulate metals in roots to prevent their transport to shoots (Wang *et al.* 2004). This accumulation may also occur due to large amount of mucilage secreted by the root tips and hairs contributing to the adsorption of NPs (Campbell *et al.* 1990, Zhang *et al.* 2011). Once adsorbed, NPs may not be available for transportation to shoots (Lin and Xing 2008). However, Lidon and Henriques (1998) observed that Cu accumulation in shoots of rice (*Oryza sativa* L. cv. Safari) increased with increasing Cu NP concentration, and accumulation was mainly found in shoot vacuoles. The decline in Cu accumulation in roots at 1,000 mg L⁻¹ observed in this study might occur due to aggregation of CuO NPs at the root–medium interface (Song *et al.* 2015). Lee *et al.* (2008) also showed significant uptake of Cu NPs by *P. radiatus* and *T. aestivum* at 1,000 mg L⁻¹.

We observed the decline in P_N (Fig. 4A) that could result from various factors. The decrease in the number

and size of stomata (Fig. 2D–F) as well as the decline in the photosynthetic pigments (Table 3) might result in the lower rate of photosynthesis (Fig. 4A). The decrease in g_s (Fig. 4A) might also result in the lowering of photosynthesis as well as E (Fig. 4A). The decrease in the thylakoid stacking (Fig. 3E) may also decrease the rate of photosynthesis and is often observed upon metal stress (Solymosi and Bertrand 2012). The decline in the number of thylakoids per grana is considered to be a result of reduced amount in PSII–LHCII complexes which play a crucial role in light-harvesting as well as ultrastructural organization of thylakoids; it may result in decreased Chl *a* fluorescence parameters (Kirchhoff *et al.* 2000). The increase in the Chl *a/b* ratio (Table 3) also indicated the reduced number of thylakoids per granum (A. Telfer, personal communication). The decrease in the number of thylakoids per granum may lower the quantum efficiency of photosynthesis (measured as F_v/F_m ratio) and q_p while increasing q_N (Fig. 4B). Photosynthesis has been reported to be suppressed by CuO NPs in *Elodea densa* (Nekrasova *et al.* 2011) and duckweeds, *Landoltia punctata* (Shi *et al.* 2011). In another report, Saison *et al.* (2010) showed that core–shell CuO NPs had a deteriorative effect on the Chl content of the green alga *Chlamydomonas reinhardtii* causing photoinhibition of PSII that led to dissipation of energy via nonphotochemical pathways. Similarly, Perreault *et al.* (2010) reported that *Lemna gibba*, on exposure to CuO NPs, showed a decrease in q_p with increase in the nonphotochemical quenching. Furthermore, reduction in growth and transpiration of yellow squash (*C. pepo*) was observed after a treatment with nano Cu of size <50 nm (Musante and White 2012). Our results suggest a susceptibility of both light (F_v/F_m) and dark (CO_2 fixation) reactions to CuO NP exposure at high concentrations.

No significant change in the MDA content (Fig. 5A) indicated the absence of lipid peroxidation of cell membrane as a result of CuO NP treatment. The increased accumulation of ascorbate in the leaves (Fig. 5C) suggested the onset of oxidative response to the CuO NP treatment in the plants. The increased expression of enzymatic antioxidants, APX (Fig. 5D) and SOD (Fig. 5E), at 10 and 100 mg L⁻¹ of CuO NPs, respectively, indicated a protective process against development of oxidative stress in the plants. Accumulation of proline (Fig. 5B), an osmoprotectant and a nonenzymatic antioxidant, is an indication of osmotic stress (Alia and Pardha Saradhi 1991) as a result of increasing CuO NP concentration. Osmotic stress in our study was also indicated by morphological changes, such as increase in the size and number of trichomes and the decrease in the number and size of stomata (Fig. 2A, B, C). Proline is one of the widely distributed solutes that is reported to accumulate in plants during adverse stress conditions, such as drought, salinity, high or low temperature (Bohnert *et al.* 1995), or under metal stress (Bassi and Sharma 1993). However, no

accumulation of proline under NP stress has been previously reported. The protective role of proline in mitigating lipid peroxidation upon metal stress was demonstrated in *Chlorella vulgaris* by Mehta and Gaur (1999).

Plant defence mechanisms, such as nonenzymatic (ASA and proline) and enzymatic (APX and SOD) antioxidants, help in mitigating the CuO NP stress. SOD and APX are the key enzymes involved in metabolizing reactive oxygen species (ROS) (Caverzan *et al.* 2012). SOD catalyses the dismutation of $O_2^{\cdot-}$ into H_2O_2 maintaining intracellular $O_2^{\cdot-}$ concentrations (Smirnoff 1993), while APX, which is present mostly in the chloroplast, readily scavenges the hydrogen peroxide produced by SOD into water molecules (Noctor and Foyer 1998). The observed increase in SOD and APX in this study might mitigate an oxidative effect to a certain extent. Studies on the effect of CuO NP on gene expression are few. One such study by Shaw and Hossain (2013) has described enhanced APX and glutathione reductase (GR) activity in rice seedlings as a result of the CuO NP. However, several studies have shown that bulk Cu increases the expression of APX, SOD, and other enzymatic antioxidants in plants (Inzé and van Montagu 1995, Yoshimura *et al.* 2000).

References

- Abdelkader A.F., Aronsson H., Solymosi K. *et al.*: High salt stress induces swollen prothylakoids in dark-grown wheat and alters both prolamellar body transformation and reformation after irradiation. – *J. Exp. Bot.* **58**: 2553-2564, 2007.
- Alia, Pardha Saradhi, P.: Proline accumulation under heavy metal stress. – *J. Plant Physiol.* **138**: 554-558, 1991.
- Bassi R., Sharma S.S.: Changes in proline content accompanying the uptake of zinc and copper by *Lemna minor*. – *Ann. Bot.- London* **72**: 151-154, 1993.
- Bates L.S., Waldren R.P., Teare I.D.: Rapid determination of free proline for water-stress studies. – *Plant Soil* **39**: 205-207, 1973.
- Bohnert H.J., Nelson D.E., Jensen R.G.: Adaptations to environmental stresses. – *Plant Cell* **7**: 1099-1111, 1995.
- Campbell R., Greaves M.P.: Anatomy and community structure of the rhizosphere. – In: Lynch J.M. (ed.): *The Rhizosphere*. Pp. 11-34. John Wiley and Sons Ltd. Publ., London 1990.
- Caverzan A., Passaia G., Rosa S.B. *et al.*: Plant responses to stresses: Role of ascorbate peroxidase in the antioxidant protection. – *Genet. Mol. Biol.* **35**: 1011-1019, 2012.
- Corredor E., Testillano P.S., Coronado M.-J. *et al.*: Nanoparticle penetration and transport in living pumpkin plants: *in situ* subcellular identification. – *BMC Plant Biol.* **9**: 45-45, 2009.
- Harrison P.: Emerging challenges: nanotechnology and the environment. – In: *GEO Year Book 2007*. Pp. 61-68. United Nations Environment Programme (UNEP), Nairobi 2007.
- Haverkamp R.G., Marshall A.T.: The mechanism of metal nanoparticle formation in plants: Limits on accumulation. – *J. Nanoparticle Res.* **11**: 1453-1463, 2009.
- Inzé D., Van Montagu M.: Oxidative stress in plants. – *Curr. Opin. Biotech.* **6**: 153-158, 1995.
- Kampfenkel K., Van Montagu M., Inzé D.: Extraction and determination of ascorbate and dehydroascorbate from plant tissue. – *Anal. Biochem.* **225**: 165-167, 1995.
- Kennedy C.D., Gonsalves F.A.N.: The action of divalent zinc, cadmium, mercury, copper and lead on the trans-root potential and H^+ efflux of excised roots. – *J. Exp. Bot.* **38**: 800-817, 1987.
- Kirchoff H., Horstmann S., Weis E.: Control of the photosynthetic electron transport by PQ diffusion microdomains in thylakoids of higher plants. – *BBA-Bioenergetics* **1459**: 148-168, 2000.
- Klaine S.J., Alvarez P.J.J., Batley G.E. *et al.*: Nanomaterials in the environment: behavior, fate, bioavailability, and effects. – *Environ. Toxicol. Chem.* **27**: 1825-1851, 2008.
- Lee C.W., Mahendra S., Zodrow K. *et al.*: Developmental phytotoxicity of metal oxide nanoparticles to *Arabidopsis thaliana*. – *Environ. Toxicol. Chem.* **29**: 669-675, 2010.
- Lee S., Kim S., Kim S. *et al.*: Assessment of phytotoxicity of ZnO NPs on a medicinal plant, *Fagopyrum esculentum*. – *Environ. Sci. Pollut. Res.* **20**: 848-854, 2013.
- Lee W.M., An Y.J., Yoon H. *et al.*: Toxicity and bioavailability of copper nanoparticles to the terrestrial plants mung bean (*Phaseolus radiatus*) and wheat (*Triticum aestivum*): plant agar test for water-insoluble nanoparticles. – *Environ. Toxicol. Chem.* **27**: 1915-1921, 2008.
- Lidon F.C., Henriques F.S.: Role of rice shoot vacuoles in

- copper toxicity regulation. – *Environ. Exp. Bot.* **39**: 197-202, 1998.
- Lin D., Xing B.: Root uptake and phytotoxicity of ZnO nanoparticles. – *Environ. Sci. Technol.* **42**: 5580-5585, 2008.
- Manceau A., Nagy K.L., Marcus M.A. *et al.*: Formation of metallic copper nanoparticles at the soil-root interface. – *Environ. Sci. Technol.* **42**: 1766-1772, 2008.
- Marschner H.: *Mineral Nutrition of Higher Plants*. Pp. 889. Academic Press, London 1995.
- Maynard A.D., Aitken R.J., Butz T. *et al.*: Safe handling of nanotechnology. – *Nature* **444**: 267-269, 2006.
- Mehta S.K., Gaur J.P.: Heavy metal-induced proline accumulation and its role in ameliorating metal toxicity in *Chlorella vulgaris*. – *New Phytol.* **143**: 253-259, 1999.
- Musante C., White J.C.: Toxicity of silver and copper to *Cucurbita pepo*: Differential effects of nano and bulk-size particles. – *Environ. Toxicol.* **27**: 510-517, 2012.
- Nagajyoti P.C., Lee K.D., Sreekanth T.V.M. *et al.*: Heavy metals, occurrence and toxicity for plants: A review. – *Environ. Chem. Lett.* **8**: 199-216, 2010.
- Navarro E., Baun A., Behra R. *et al.*: Environmental behavior and ecotoxicity of engineered nanoparticles to algae, plants, and fungi. – *Ecotoxicology* **5**: 372-386, 2008.
- Nekrasova G.F., Ushakova O.S., Ermakov A.E. *et al.*: Effects of copper (II) ions and copper oxide nanoparticles on *Elodea densa* Planch. – *Russian J. Ecol.* **42**: 458-463, 2011.
- Noctor G., Foyer C.H.: Ascorbate and glutathione: Keeping active oxygen under control. – *Annu. Rev. Plant Phys.* **49**: 249-279, 1998.
- Ojamiä L., Aulin C., Pedersen H. *et al.*: IR and quantum-chemical studies of carboxylic acid and glycine adsorption on rutile TiO₂ nanoparticles. – *J. Colloid Interface Sci.* **296**: 71-78, 2006.
- Perreault F., Ouakroum A., Pirastru L. *et al.*: Evaluation of copper oxide nanoparticles toxicity using chlorophyll a fluorescence imaging in *Lemna gibba*. – *J. Bot.* **2010**, 1-9, 2010.
- Raven J.A., Evans M.C., Korb R.E.: The role of trace metals in photosynthetic electron transport in O₂ – evolving organisms. – *Photosynth. Res.* **60**: 111-150, 1999.
- Rico C.M., Majumdar S., Duarte-Gardea M. *et al.*: Interaction of nanoparticles with edible plants and their possible implications in the food chain. – *J. Agric. Food Chem.* **59**: 3485-3498, 2011.
- Saison C., Perreault F., Daigle J.C. *et al.*: Effect of core-shell copper oxide nanoparticles on cell culture morphology and photosynthesis (photosystem II energy distribution) in the green alga, *Chlamydomonas reinhardtii*. – *Aquat. Toxicol.* **96**: 109-114, 2010.
- Sankhalkar S., Sharma P.K.: Protection against photooxidative damage provided by enzymatic and non-enzymatic anti-oxidant system in sorghum seedlings. – *Indian J. Exp. Biol.* **40**: 1260-1268, 2002.
- Sharma P.K., Hall D.O.: Effect of photoinhibition and temperature on carotenoids in sorghum leaves. – *Indian J. Biochem. Biophys.* **33**: 471-477, 1996.
- Sharma P.K., Shetye R., Bhonsle S.: Effect of supplementary ultraviolet-B radiation on young wheat seedlings. – *Curr. Sci.* **72**: 400-405, 1997.
- Shaw A.K., Hossain Z.: Impact of nano-CuO stress on rice (*Oryza sativa* L.) seedlings. – *Chemosphere* **93**: 906-915, 2013.
- Shi J., Abid A.D., Kennedy I.M. *et al.*: To duckweeds (*Landoltia punctata*), nanoparticulate copper oxide is more inhibitory than the soluble copper in the bulk solution. – *Environ. Pollut.* **159**: 1277-1282, 2011.
- Smirnoff N.: Tansley Review 52. The role of active oxygen in the response of plants to water-deficit and desiccation. – *New Phytol.* **125**: 27-58, 1993.
- Solymsi K., Bertrand M.: Soil metals, chloroplasts, and secure crop production: a review. – *Agron. Sustain. Dev.* **32**: 245-272, 2012.
- Song, L., Vijver, M. G., Peijnenburg, W. J. G. M.: Comparative toxicity of copper nanoparticles across three Lemnaceae species. – *Sci. Total Environ.* **518-519**: 217-224, 2015.
- Stampoulis D., Sinha S.K., White J.C.: Assay-dependent phytotoxicity of nanoparticles to plants. – *Environ. Sci. Technol.* **43**: 9473-9479, 2009.
- Ünnep R., Zsiros O., Solymsi K. *et al.*: The ultrastructure and flexibility of thylakoid membranes in leaves and isolated chloroplasts as revealed by small-angle neutron scattering. – *BBA- Bioenergetics* **1837**: 1572-1580, 2014.
- Wang S.-H., Yang Z.-M., Yang H. *et al.*: Copper-induced stress and antioxidative responses in roots of *Brassica juncea* L. – *Bot. Bull. Acad. Sin.* **45**: 203-212, 2004.
- Wierzbicka M.S., Obidzińska J.: The effect of lead on seed imbibition and germination in different plant species. – *Plant Sci.* **137**: 155-171, 1998.
- Wiesner M.R., Lowry G.V., Alvarez P. *et al.*: Assessing the risks of manufactured nanomaterials. – *Environ. Sci. Technol.* **40**: 4336-4345, 2006.
- Yoshimura K., Yabuta Y., Ishikawa T. *et al.*: Expression of spinach ascorbate peroxidase isoenzymes in response to oxidative stresses. – *Plant Physiol.* **123**: 223-233, 2000.
- Yruela I.: Copper in plants. – *Brazilian J. Plant Physiol.* **17**: 145-156, 2005.
- Zhang W., Elliott D.W.: Applications of iron nanoparticles for groundwater remediation. – *Remediat. J.* **16**: 7-21, 2006.
- Zhang Z., He X., Zhang H. *et al.*: Uptake and distribution of ceria nanoparticles in cucumber plants. – *Metallomics* **3**: 816-822, 2011.



ISSN: 0976-3031

Available Online at <http://www.recentscientific.com>

International Journal of Recent Scientific Research
Vol. 6, Issue, 1, pp.2445-2451, January, 2015

International Journal
of Recent Scientific
Research

RESEARCH ARTICLE

INFLUENCE OF TITANIUM DIOXIDE NANOPARTICLES ON THE PHOTOSYNTHETIC AND BIOCHEMICAL PROCESSES IN ORYZA SATIVA

Maria Vera J. Da Costa and *Prabhat K. Sharma

Department of Botany, Goa University, Goa

ARTICLE INFO

Article History:

Received 14th, December, 2014

Received in revised form 23th, December, 2014

Accepted 13th, January, 2015

Published online 28th, January, 2015

Key words:

Ascorbic acid, Fv/Fm, Lipid peroxidation, Osmotic stress, Photosynthesis, uptake

ABSTRACT

The phytotoxicity of titanium dioxide nanoparticles (TiO₂ NPs) is a rapidly expanding area of research with a dearth of information regarding its toxicity in plants. We assessed the TiO₂ NP (<25 nm) effect on growth and photosynthesis in *Oryza sativa* var. Jyoti grown in a hydroponic system. Our results show that TiO₂ NPs do not affect germination, however, an overall decrease in seedling growth (root, shoot length and biomass) was observed at high concentration. TiO₂ NP exposure led to greater accumulation of Ti in roots than in shoots, decreasing CO₂ fixation, transpiration rate and stomatal conductance at 1000 ppm with insignificant effect on photosynthetic pigments, quantum efficiency of PSII (Fv/Fm ratio) and photochemical quenching. High treatment caused oxidative and osmotic stress evidenced by increased MDA and proline content. This study thus indicates that Ti accumulation caused phytotoxicity to growth and photosynthesis leading to oxidative and osmotic stress in rice.

© Copy Right, IJRSR, 2014, Academic Journals. All rights reserved.

INTRODUCTION

Metal oxide nanoparticles (NPs) are materials with size range of 1-100 nm (Klaine *et al.*, 2008). Titanium dioxide (TiO₂) NPs are one of the most commonly found particles in the environment as a result of their large scale production and application for commercial purposes such as cosmetics, sunscreens (Mu *et al.*, 2010), semiconductors, pharmaceuticals, energy storage, catalysts, coatings and paints (Kaegi *et al.*, 2008), due to its UV absorption efficiency and transparency to visible light (Franklin *et al.*, 2007). It is also used in the production of textiles (Yuranova *et al.*, 2007) and for solar-driven self-cleaning coatings (Cai *et al.*, 2006). These usages would inevitably lead to increased NP entry into the environment. As far as concentration of NPs in soil or aquatic system is concerned, no direct published data is available (Navarro *et al.*, 2008). Using fate models, Mueller *et al.* (2008), estimated the concentration of TiO₂ NP to be 120 µg/kg³ of agricultural land per year as a result of contaminated sewage sludge. Boxall *et al.* (2007) used simple box models to estimate the amount of Ti in the environment and reported that the expected amounts of Ti and other common NPs (Ce, Zn and Ag) were found to be in the range of 1 to 10 µg/L in natural waters, with total NP concentration scaling up to 100 µg/L approximately in the aquatic system currently which may increase many fold in the near future.

Release of TiO₂ NP in the environment is ameliorating at a very rapid rate contaminating soil and aquatic ecosystems (Farre *et al.*, 2009; Tourinho *et al.*, 2012). TiO₂ NPs are likely to persist and accumulate in the soil and water due to low

dissolution (Baun *et al.*, 2008) forming stable aggregates (French *et al.*, 2009). Agglomeration and aggregation, in the environment are influenced by NP surface characteristics and particle size. These are negatively correlated to soil characteristics such as dissolved organic matter, and positively correlated to pH and ionic strength (Fang *et al.*, 2009).

The mechanism of NP uptake by plant roots is not clearly understood. It is reported that depending on the size nanoparticles, NPs may enter the plant cells through carrier protein, aquaporin, ion channels, fluid phase endocytosis, plasmodesmata transport or entry facilitated through natural organic matter or root exudates and formation of new pores (Rico *et al.*, 2011). Once inside the cell, NPs can bind to the organelles or protein (Rosenbluh *et al.*, 2011) or form aggregates (Guzman *et al.*, 2006). Interaction of NPs in plants not only depends upon the surface characteristics, particle size, temperature, pH and ionic strength (Maynard *et al.*, 2006; Wiesner *et al.*, 2006) but also on the type of interactions with lipids and proteins such as electrostatic, hydrogen bonding, and hydrophobic interactions (Hug and Sulzberger, 1994; Ojamae *et al.*, 2006).

Reports on uptake of TiO₂ NP in plants are limited, especially in food crops (Rico *et al.*, 2011). Uptake, translocation and cell distribution of ultra small TiO₂ NPs (<5 nm) in *Arabidopsis thaliana* was reported to be either facilitated or inhibited by the pectin hydrogel capsule which was released by the roots (Kurepa *et al.*, 2010). Increased accumulation or inactivation of toxic heavy metals by the rhizosphere was also reported to be dependent on plant species (Watanabe *et al.*, 2008). TiO₂

NPs toxicity caused reduction in root cell diameter, hydraulic conductivity, transpiration and leaf growth in maize (Asli and Neumann, 2009) and produced reactive oxygen species (ROS) within organisms due to its photocatalytic activity upon UV exposure (Kahru *et al.*, 2008). TiO₂ NPs are reported to be beneficial to some organisms. For instance, in spinach, TiO₂ NPs increased chlorophyll synthesis, photosynthesis and plant dry weight (Zheng *et al.*, 2005; Hong *et al.*, 2005).

The multidisciplinary application of nanotechnology-products results in the inevitable discharge of NPs into the environment (Navarro *et al.*, 2008). Problems and challenges arise due to phytotoxicity exhibited by the NPs owing to their physicochemical surface characteristics upon interaction with the living system. The lack of knowledge and limited information on the fate and bioavailability of NPs in the environment also augment these problems (Klaine *et al.*, 2008). Our study provides a better understanding of the interaction of TiO₂ NP in *Oryza sativa* var. Jyoti and suggests that light reaction of photosynthesis was uninfluenced on treatment with TiO₂ NPs, while growth (germination, root/ shoot length and biomass) was reduced at highest concentration. We report a decline in the net photosynthesis (A, E and gs), and enhanced oxidative and osmotic stress indicated by increased MDA and proline respectively due to the TiO₂ NP treatment. Results also suggest generation of ascorbate in order to metabolise ROS produced, probably to mitigate the oxidative damage.

MATERIALS AND METHODS

Plant materials and growth conditions

Oryza sativa (var. Jyoti), a high yielding, rice variety was obtained from Indian Council of Agricultural Research (ICAR), Goa and stored in dark at 4°C. TiO₂ NP (<25 nm size, Sigma-Aldrich) solution of 0, 2.5, 10, 50, 100 and 1000 ppm was prepared in Hoagland's solution (pH 6.5). Seeds were surface sterilized using 4% sodium hypochlorite (BDH) solution for 3 min, washed thoroughly with tap water and soaked for 3 days. 100 seeds were sown on germination paper in a Petri plate with respective concentration of TiO₂.

The seeds were germinated in a growth chamber equipped with lamps to provide an irradiance of 200 $\mu\text{mol m}^{-2}\text{s}^{-1}$ with 16 h photoperiod, temperature of $25 \pm 2^\circ\text{C}$ and relative humidity of 70-75%. The 6 day old seedlings were transferred carefully in a hydroponic system containing respective concentration of TiO₂ NPs and were allowed to grow for a further 24 days. The hydroponic system ensured complete mixing of NPs by use of magnetic stirrers and proper aeration achieved by air pumps. The solutions were replenished every third day.

Nanoparticle Characterization Studies

TiO₂ NPs were obtained from Sigma-Aldrich Co. (USA). The physical characteristics as obtained from the supplier were: particle size (<25 nm), surface area (45-55 m^2g^{-1}), mp (1825 °C), and density (3.9 g mL^{-1} at 25 °C), containing 99.7% trace metals basis.

Size characterization using Scanning Electron Microscopy (SEM)

TiO₂ NP was characterized at 30000 X magnification using SEM (JSM 5800 LV, JEOL, Japan) at the National Institute of Oceanography, Goa.

Size characterization using X-ray Diffractometer (XRD)

X-ray Diffractometer (Rigaku) pattern of TiO₂ NPs was recorded at room temperature in the range of $2\theta=20^\circ-80^\circ$ with a step of 0.02° and a speed= 2°/min using Cu α radiation ($\lambda=0.15406$ nm).

Size characterization using dynamic light scattering (DLS) analyzer

DLS measurements in aqueous system were studied using dynamic light scattering ZetaPALS Analyzer (Brookhaven Instruments Corporation, New York, USA). Appropriate amount of TiO₂ NPs was suspended in distilled water as well as Hoagland's nutrient solution and was physically dispersed using an ultrasonicator for 2 min. Each measurement consisting of five replicates were measured with 10 s duration at 25°C and analyzed using BIC Particle Sizing Software Ver.5.23.

Germination, root and shoot length and biomass studies

Percent germination, root, shoot length was manually taken at the early stage (6th day) of growth. The biomass was measured taking 10 plants from each TiO₂ NP treatment group after 30 days of growth. Fresh leaf tissue was dried at 75°C for 72 h noted as dry weight (d.w.).

Nanoparticle uptake

Uptake of TiO₂ NPs was determined using an inductively coupled plasma atomic emission spectrophotometer (Perkin-Elmer Optima 2000 DV ICP-OES) calibrated with single-element calibration standards. The ash was dissolved in 1% HNO₃ (Merck) solution and filtered through 0.45 μm Whatman filter paper. The filtered sample was used for ICP-OES analysis.

Photosynthesis measurements

Photosynthesis measurements were carried out using a portable infra-red gas analyzer (IRGA, ADC Bioscientific, LCi-SD, Hansatech, UK) according to Sharma and Hall (1996). The photosynthesis rate (A), transpiration rate (E) and stomatal conductance (gs) were measured at ambient temperature and carbon dioxide concentration and light intensity of 1200 $\mu\text{mol m}^{-2}\text{s}^{-1}$ using a detachable light source provided by a dichroic lamp (Hansatech, UK).

Fluorescence measurements

Measurements were carried out using a fluorescence monitoring system (FMS, Hansatech instruments) according to Sharma *et al.* (1997) using Modfluor32 software. The maximum fluorescence (Fm), variable fluorescence (Fv) and the maximum quantum yield (Fv/Fm) ratio was calculated. The relative contributions for photochemical and non-photochemical energy dissipation measured as the photochemical quenching (qP) and non-photochemical quenching (qNP) were also calculated according to Schreiber *et al.* (1986).

Extraction and analysis of photosynthetic Pigments

Plant tissue (0.1 g) was ground in 100 % Acetone (Merck HPLC grade) making a final volume of 1.5 ml and incubated overnight at 4°C. The homogenate was centrifuged at 4°C for 10 mins at 4000 x g. 1 ml of supernatant was collected and filtered through 0.2 μm Ultipor[®]N66[®]Nylon 6, 6 membrane

filter and 10 µl of sample was analyzed in a Waters HPLC system, according to Sharma and Hall (1996). The HPLC profile was extracted at 445 nm with a Waters 2996 photodiode array detector and peaks were identified based on RT and their spectral characteristics. β-carotene was used as an external standard for peak quantization.

Lipid per oxidation

Lipid peroxidation of the cell membrane was determined according to Sankhalkar and Sharma (2002). Peroxidation of lipids was measured as malondialdehyde (MDA) content using an extinction coefficient of 155 mM⁻¹cm⁻¹ at 532 nm.

Proline determination

Proline accumulation in fresh leaves was determined according to the method of Bates *et al.* (1973). L-Proline (Sigma ultra ≥ 99 % pure) was used as a standard for quantification by plotting a standard graph against concentration at 520 nm.

Ascorbate assay

Ascorbate (ASA) and dehydroascorbate (DHA) was estimated according to Kampfenkel *et al.* (1995). Ascorbic acid (sigma) was used as standard.

Statistical analysis

Data obtained was statistically analyzed using the procedure of ANOVA: Two-Factor without Replication and unpaired two-tailed student's t-test. Statistically significant difference 'a' is reported when the *p* < 0.05.

RESULTS

Nanoparticle characterization

The TiO₂ NPs were characterized under scanning electron microscope (SEM) for their shape and was observed to be spherical to round (Fig 1a). X-ray diffraction (XRD) patterns were analyzed using Scherrer's equation and the average crystalline size was measured to be 15 ± 2 nm (Fig 1b). Using dynamic light scattering (DLS) analyzer, a narrow distribution of the particle size of nano-TiO₂ powder in Hoagland's solution was measured to be 23 ± 2 nm (Polydispersity of 0.074) and in distilled water was in the range of 12 ± 2 nm (Polydispersity of 0.191) which were in agreement with the XRD measurements. The sizes obtained were as specified by the supplier (TiO₂ NPs, size <25 nm; Sigma-Aldrich, USA). The TiO₂ powder resulted in a suspension that appeared cloudy and did not seem to settle over the sampling time.

Table 1 Percent germination (%G), Root and shoot length of rice plantlets (6 day old) treated with TiO₂ NP at different concentration.

TiO ₂ NPs (in ppm)	% G	Root length (mm)	Shoot length (mm)
0	94.3 ± 0.9	51.31 ± 4.0	37.9 ± 1.7
2.5	93.1 ± 0.2	51.82 ± 2.6	36.4 ± 2.9
10	92.1 ± 1.4	53.04 ± 4.2	36.8 ± 2.9
50	90.9 ± 2.5	52.67 ± 1.7	36.3 ± 0.1
100	92.9 ± 2.5	47.93 ± 5.5	37.0 ± 5.3
1000	91.8 ± 1.4	39.29 ± 7.4	33.7 ± 8.7

Values are the mean (± S.D) of 7 replicates.

Percent germination and root/ shoot length measurements

The percentage germination was unaffected while shoot and root length decreased by approximately 11% and 23% respectively as a result of 1000 ppm TiO₂ NP treatment (Table 1). The shoot biomass (f.w. & d.w.) showed no change up to

100 ppm but decreased by approximately 9% at 1000 ppm (Table 2). The root biomass (f.w.) decreased slightly at higher concentration of TiO₂ NP (Table 2). However, in contrast to these results, the root biomass on dry weight basis increased by 476% at the highest concentration of TiO₂ as compared to control (Table 2). Plants grown at 1000 ppm of TiO₂ also showed necrosis at the leaf tips (data not shown).

Table 2 Biomass of rice plantlets (30 day old) treated with TiO₂ NP at different concentration.

TiO ₂ NPs (ppm)	Biomass (g)			
	Shoot (F.W)	Shoot (D.W)	Root (F.W)	Root (D.W)
0	0.74 ± 0.03	0.076 ± 0.02	0.33 ± 0.03	0.026 ± 0.003
2.5	0.72 ± 0.09	0.075 ± 0.02	0.32 ± 0.02	0.028 ± 0.003
10	0.76 ± 0.07	0.075 ± 0.01	0.29 ± 0.05	0.021 ± 0.003
50	0.76 ± 0.01	0.075 ± 0.01	0.30 ± 0.01	0.023 ± 0.001
100	0.77 ± 0.05	0.076 ± 0.02	0.30 ± 0.03	0.15 ± 0.02
1000	0.67 ± 0.15	0.069 ± 0.02	0.32 ± 0.13	0.13 ± 0.02

Values are the mean (± S.D) of 7 replicates.

Accumulation of TiO₂ NPs using ICO-OES

Plants showed a 3-fold increase in the Ti content up to 10 ppm as a result of the treatment (Table 3). Further increase in the TiO₂ concentration during treatment showed little difference in Ti content as observed in control shoots. Ti content in roots, however, showed a linear increase. 50 ppm TiO₂ NP treatment resulted in 3-fold increase in Ti content in roots, which was increased to 23.5 fold at 1000 ppm concentration (Table 3).

Table 3 Shoot and root Ti content of 30 day old plantlets exposed to TiO₂ NP treatment.

TiO ₂ NP (ppm)	Ti content (mg/L)	
	Shoot	Root
0	0.9 ± 0.0009	0.9 ± 0.0003
2.5	3.0 ± 0.0034	1.1 ± 0.0224
10	3.0 ± 0.0038	2.0 ± 0.0073
50	0.9 ± 0.0015	3.1 ± 0.0295
100	1.0 ± 0.0028	21.2 ± 0.914
1000	1.2 ± 0.0062	21.3 ± 0.034

Values are the mean (± S.D) of 3 replicates.

Table 4 Carotenoid and chlorophyll content of TiO₂ NP treated rice plants at 0-1000 ppm concentration after 30 days of growth.

Pigments (conc. in µg)	Treatment with TiO ₂ NP (in ppm)				
	0	2.5	10	100	1000
Neoxanthin	0.82	0.87	1.63	1.34	1.10
Violaxanthin	1.67	1.82	3.39	2.97	2.41
Antheraxanthin	0.25	0.31	0.50	0.50	0.32
Lutein	3.44	3.07	7.25	6.09	4.57
Chlorophyll b	6.72	6.77	13.54	11.87	8.93
Chlorophyll a	5.62	5.67	11.88	10.36	7.76
β-Carotene	1.51	1.32	3.61	3.09	2.17

Photosynthetic studies

Chlorophyll fluorescence indicative of light reaction of photosynthesis was not significantly affected on treatment with high concentration of TiO₂ NP (Fig 2). The photosynthetic efficiency of PSII, measured as F_v/F_m ratio and photochemical quenching was similar to that of control, however, a 12% increase in non- photochemical quenching (qNP) indicative of dissipation of absorbed light energy in the form of heat was seen as a result of TiO₂ treatment (Fig 2).

The rate of CO₂ exchange measured as net photosynthesis (A), transpiration rate (E) and stomatal conductance (gs) decreased at higher concentrations of TiO₂ NP treatment (Fig 3). A slight increase in the rate of net photosynthesis (11%), transpiration rate (46%) and stomatal conductance (70%) was observed at low concentration (2.5 ppm) of TiO₂ NPs (Fig 3), however, an

increase in the concentration of TiO₂ resulted in decreased photosynthesis, transpiration and stomatal conductance. Net photosynthesis declined to 53% at 1000 ppm of TiO₂ concentration as compared to control. Likewise, transpiration rate and stomatal conductance also declined to 77% and 66% respectively at 1000 ppm TiO₂ compared to control (Fig 3).

The HPLC chromatogram obtained at 445 nm showed no qualitative changes (Fig 4). However, quantitative changes in the pigments were observed (Table 4). Chlorophyll *a* and *b* as well as carotenoid content (neoxanthin, violaxanthin, antheraxanthin, lutein, and β-carotene) increased on treatment with TiO₂ NP as compared to control (Table 4). A linear increase of up to 5% in Chl *a/b* ratio was observed as compared to control at high concentration. The Chl: Car ratio also increased at low concentration (2.5 ppm) but was not significantly different from control at high concentrations.

Lipid peroxidation and Osmotic stress

The malondialdehyde (MDA) content indicative of osmotic stress did not change significantly up to 50 ppm, however, an increase of 29% at 100 ppm and above concentration of TiO₂ NP was observed (Fig 5a).

The treatment also resulted in osmotic stress indicated by the increase in proline content (Fig 5b). Proline level increased more than 2-fold as compared to the control as a result of the TiO₂ treatment (Fig 6b).

Content of ascorbate, a non-enzymatic antioxidant, was also determined and was found to increase by 260% as a result of 1000 ppm TiO₂ treatment (Fig 5c).

Figure Legends

Figure 1 Scanning electron micrograph of TiO₂ NP at 30000X magnification (a), X-Ray Diffraction pattern of TiO₂ NP (b) recorded at room temperature in the range 2θ=20°-80° with a step of 0.02°, speed= 2°/min using Cu Kα radiation (λ=0.15406 nm).

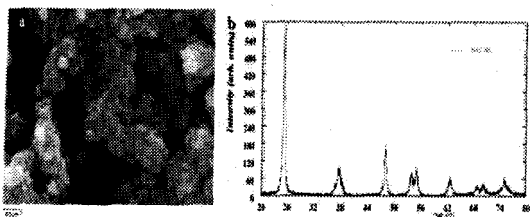


Figure 1 Scanning electron micrograph and XRD pattern of TiO₂ NP

Figure 2 Photosynthetic efficiency of photosystem II (Fv/Fm), photochemical quenching (qP) and non-photochemical quenching (qNP) of rice plants treated with TiO₂ NPs after 30 days of growth. The error bars represent the mean (± S.D) of 7 replicates. The statistical analysis was performed using the procedure of Students t-test, 'a' representing statistically significant values when p < 0.05.

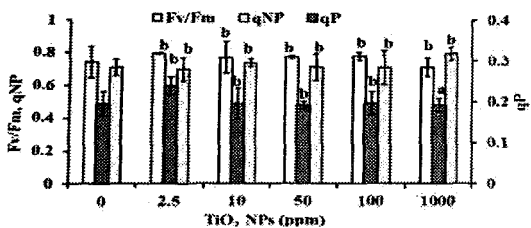


Figure 2 Light reactions of photosynthesis

Figure 3 Net photosynthesis rate (A), transpiration rate (E) and stomatal conductance (gs) of rice plants treated with TiO₂ NPs after 30 days of treatment. The error bars represent the mean (± S.D) of 7 replicates. The statistical analysis was performed using the procedure of Students t-test, 'a' representing statistically significant values when the p < 0.05.

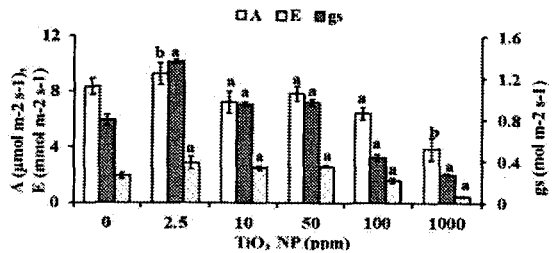


Figure 3 Dark reaction of photosynthesis

Figure 4 HPLC profile of carotenoid and chlorophyll content of rice plants at 445 nm treated with TiO₂ NP after 30 days of treatment [a= Control and b= 1000 ppm TiO₂ NPs].

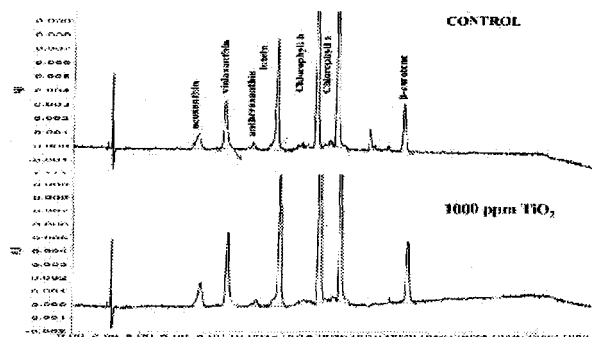


Figure 4 HPLC chromatogram of photosynthetic pigments

Figure 5 The MDA content (a), proline content (b) and ascorbate content (c) of rice plants treated with TiO₂ NP after 30 days of treatment. The error bars represent the mean (± S.D) of 7 replicates. The statistical analysis was performed using the procedure of Students t-test, 'a' representing statistically significant values when the p < 0.05.

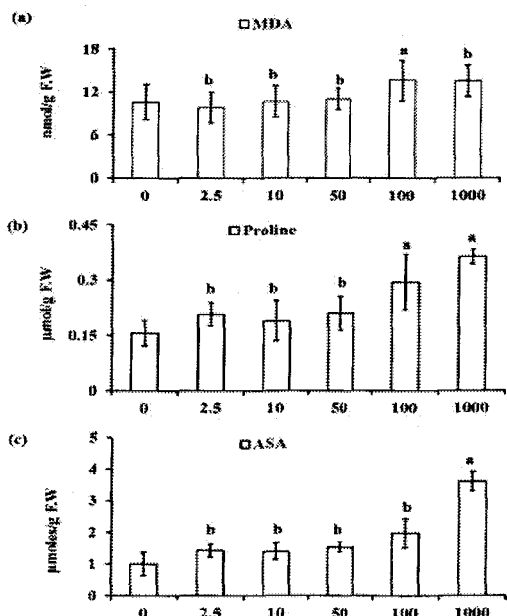


Figure 5 The MDA content (a), proline content (b) and ascorbate content (c) of rice plants treated with TiO₂ NP

DISCUSSION

Our result showed no effect of TiO₂ NP treatment on seed germination of *Oryza sativa* var. Jyoti plants (Table 1). This may be due to the impermeability of rice seed coat to the nanoparticles till the radicle emerges. Wierzbicka and Obidzinska (1998) have also shown impermeability of seed coat to NPs. We also observed that the shoot and root length was uninfluenced up to 100 ppm, while toxicity was observed at highest concentration of TiO₂ NPs (Table 1). Shoot and root biomass showed no changes on fresh weight (f.w.) basis, however an increase in the root dry weight (d.w.) was observed at high concentration (Table 2). Increase in root d.w. probably may be as a result of significant accumulation of Ti in the plant roots treated with 100 and 1000 ppm TiO₂ NPs. Kurepa *et al.* (2010) reported that roots of *A. thaliana* released mucilage forming a hydrogel capsule either inhibiting or facilitating the entry of TiO₂ NPs. Watanabe (2008) reported that mucilage released may absorb, inactivate or accumulate toxic heavy metals in the rhizosphere depending on the plant species. Our data revealed massive accumulation of Ti particles in roots (Table 3), but little accumulation in shoots at high concentration. This accumulation indicates active exclusion of Ti by root cells in order to protect the shoots and more importantly the photosynthetic tissue. Ti accumulation has been reported in parenchyma of wheat root and vascular tissue (Laure *et al.*, 2011) and roots and outer leaves of cabbage plants (Hara *et al.*, 1976).

TiO₂ NPs did not show toxicity to light reaction of photosynthesis probably because it behaves more like metal oxides, rather than like free metal ions (Farrè *et al.*, 2009) which are known to cause toxicity. In our study, no significant changes in the PSII quantum efficiency (Fv/Fm ratio) and photochemical quenching (qP) were observed (Fig 2), however, CO₂ fixation rate, transpiration rate and stomatal conductance declined significantly (Fig 3) at high concentration. Our results indicate that decrease in the net CO₂ fixation is probably a result of reduction in the stomatal conductance rather than metabolic limitation. TiO₂ NP treatment results in blocking pores in addition to decreasing root pores (Asli and Neumann, 2009). This may bring about lowering of water uptake causing osmotic stress, as observed in our study (Fig 5b). This osmotic stress could lead to stomatal closure which in turn would lower the CO₂ fixation. In contrast to our result, Yang and Watts (2005) have reported improved growth in spinach due to TiO₂ treatment, in addition to, better absorption of nitrate. This then accelerates the biosynthesis of proteins and chlorophyll and enhances photosynthesis and plant biomass. Lu *et al.* (2002) also observed that TiO₂ NPs increased nitrate reductase activity in soyabean. We observed an increase in photosynthetic pigments as a result of TiO₂ but negligible increase in shoot biomass or CO₂ fixation.

TiO₂ NPs are known to produce reactive oxygen species (ROS) due to its photocatalytic property (Hund-Rinke and Simon, 2006) resulting in lipid peroxidation, damaging DNA, proteins and lipids (Kelly *et al.*, 1998). Increased levels of MDA observed in our study indicate oxidative stress and peroxidation of biological membrane (Fig 5a). Report by Ghosh *et al.* (2010) showed an increase in MDA content in *Allium cepa* as a result of TiO₂ NP treatment. They also

reported geno-toxicity potential of TiO₂ NPs in both plant and human lymphocytes.

Exposure to heavy metals is known to cause water imbalance in the plants, suggesting that proline accumulation induced by metals depends on the development of metal-induced water stress in plant leaves (Chen *et al.*, 2001). In our study, we observed that proline, an osmo-protectant increased with increase in TiO₂ NP concentration, indicating osmotic stress (Fig 5b). As a consequence of the osmotic stress, stomatal limitation was observed (Fig 3) which probably limited the CO₂ fixation and transpiration rate (Fig 3) as reported in this study.

ASA is an important component of the antioxidant defense system in plants serving as a reductant for the peroxidative removal of H₂O₂ (Noctor and Foyer, 1998). Increase in the non-enzymatic antioxidant, ascorbic acid (ASA) (Fig 6c), observed in this study was probably in order to mitigate, oxidative as well as osmotic stress induced by TiO₂ NPs. Guo *et al.* (2005) reported that ASA decreased the electrolyte leakage in rice roots subjected to Al toxicity and alleviated the inhibition of Al on root growth, indicating that ASA and its precursor increased the resistance of rice seedlings to Al toxicity. They also suggested that ASA decreased the H₂O₂ and MDA level in rice seedlings exposed to chilling, drought and Al stress. Our results infer that a significant increase in ascorbate content at high TiO₂ NP treatment (Fig 5c) caused a lesser amount of lipid peroxidation (Fig 5a) in *Oryza sativa* var. Jyoti.

CONCLUSION

Titanium dioxide nanoparticle effect (TiO₂ NPs) on plant growth (root, shoot length and biomass) and photosynthesis was investigated. TiO₂ NPs used in this study showed no effect on seed germination, root and shoot length and light reaction of photosynthesis (Fv/Fm ratio and qP), however, it decreased carbon dioxide assimilation (A), transpiration rate (E) and stomatal conductance (gs) in *Oryza sativa* var. Jyoti at high concentration. TiO₂ NP treatment resulted in an increased MDA, proline and ascorbate content at high concentration indicating oxidative as well as osmotic stress to plants. Overall, TiO₂ NPs caused little or no effect on light reaction of photosynthesis and pigment biosynthesis but led to a phytotoxic effect on the dark reaction of photosynthesis (carbon dioxide fixation).

Acknowledgements

The authors would like to thank the Department of Science & Technology (DST), New Delhi (SR/SO/PS-63/2009) and UGC- SAP (F. 3-50/2009 (SAP-II) for funding this work. The authors also thank, NIO, Goa for SEM imaging and ICP-OES analysis. The authors are thankful to the Physics Department, Goa University using X-ray Diffractometer and the Centre for Nano Science and Engineering (CeNSE), Indian Institute of Science, Bangalore, India for NP size determination. The authors appreciate the valuable suggestions given by the reviewers.

References

- Asli, S., Neumann, P.M., 2009. Colloidal suspensions of clay or titanium dioxide nanoparticles can inhibit leaf growth and transpiration via physical effects on root water

- transport. *Plant. Cell Environ.* 32, 577–84. doi:10.1111/j.1365-3040.2009.01952.x
- Bates, L.S., Waldren, R.P., Teare, I.D., 1973. Rapid determination of free proline for water-stress studies. *Plant Soil* 39, 205–207. doi:10.1007/BF00018060
- Baun, A., Hartmann, N.B., Grieger, K., Kusk, K.O., 2008. Ecotoxicity of engineered nanoparticles to aquatic invertebrates: a brief review and recommendations for future toxicity testing. *Ecotoxicology* 17, 387–395. doi:10.1007/s10646-008-0208-y
- Boxall, A. B. A., Chaudhry, Q., Sinclair, C., Jones, A., Aitken, R., Jefferson, B., & Watts, C., 2007. Current and future predicted environmental exposure to engineered nanoparticles. Central Science Laboratory, Department of the Environment and Rural Affairs, London, UK, 89.
- Cai, R., Van, G.M., Aw, P.K., Itoh, K., 2006. Solar-driven self-cleaning coating for a painted surface. *Comptes Rendus Chim.* 9, 829–835. doi:10.1016/j.crci.2005.04.007
- Chen, C.T., Chen, L.-M., Lin, C.C., Kao, C.H., 2001. Regulation of proline accumulation in detached rice leaves exposed to excess copper. *Plant Sci.* 160, 283–290. doi:10.1016/S0168-9452(00)00393-9
- Fang, J., Shan, X., Wen, B., Lin, J., Owens, G., 2009. Stability of titania nanoparticles in soil suspensions and transport in saturated homogeneous soil columns. *Environ. Pollut.* 157, 1101–9. doi:10.1016/j.envpol.2008.11.006
- Farré, M., Gajda-Schrantz, K., Kantiani, L., Barceló, D., 2009. Ecotoxicity and analysis of nanomaterials in the aquatic environment. *Anal. Bioanal. Chem.* 393, 81–95. doi:10.1007/s00216-008-2458-1
- Franklin NM, Rogers NJ, Apte SC, Batley GE, Gadd GE, C.P., 2007. Comparative toxicity of nanoparticulate ZnO, bulk ZnO, and ZnCl₂ to a freshwater microalga (*Pseudokirchneriella subcapitata*): the importance of particle solubility. *Env. Sci Technol* 41, 8484–90.
- French, R.A., Jacobson, A.R., Kim, B., Isley, S.L., Penn, R.L., Baveye, P.C., 2009. Influence of Ionic Strength, pH, and Cation Valence on Aggregation Kinetics of Titanium Dioxide Nanoparticles. *Environ. Sci. Technol.* 43, 1354–1359. doi:10.1021/es802628n
- Ghosh, M., Bandyopadhyay, M., Mukherjee, A., 2010. Genotoxicity of titanium dioxide (TiO₂) nanoparticles at two trophic levels: Plant and human lymphocytes. *Chemosphere* 81, 1253–1262. doi:10.1016/j.chemosphere.2010.09.022
- Guo, Z., Tan, H., Zhu, Z., Lu, S., Zhou, B., 2005. Effect of intermediates on ascorbic acid and oxalate biosynthesis of rice and in relation to its stress resistance. *Plant Physiol. Biochem.* 43, 955–62. doi:10.1016/j.plaphy.2005.08.007
- Guzman, K. a D., Finnegan, M.P., Banfield, J.F., 2006. Influence of surface potential on aggregation and transport of titania nanoparticles. *Environ. Sci. Technol.* 40, 7688–93.
- Hara, T., Sonoda, Y., Iwai, I., 1976. Growth response of cabbage plants to transition elements under water culture conditions. *Soil Sci. Plant Nutr.* 22, 307–315. doi:10.1080/00380768.1976.10432993
- Hong, F., Yang, F., Liu, C., Gao, Q., Wan, Z., Gu, F., Wu, C., Ma, Z., Zhou, J., Yang, P., 2005. Influences of nano-TiO₂ on the chloroplast aging of spinach under light. *Biol. Trace Elem. Res.* 104, 249–60. doi:10.1385/BTER:104:3:249
- Hug, S.J., Sulzberger, B., 1994. In situ Fourier Transform Infrared Spectroscopic Evidence for the Formation of Several Different Surface Complexes of Oxalate on TiO₂ in the Aqueous Phase. *Langmuir* 10, 3587–3597. doi:10.1021/la00022a036
- Hund-Rinke, K., Simon, M., 2006. Ecotoxic Effect of Photocatalytic Active Nanoparticles (TiO₂) on Algae and Daphnids (8 pp). *Environ. Sci. Pollut. Res. - Int.* 13, 225–232. doi:10.1065/espr2006.06.311
- Kaegi, R., Ulrich, A., Sinnet, B., Vonbank, R., Wichser, A., Zuleeg, S., Simmler, H., Brunner, S., Vonmont, H., Burkhardt, M., Boller, M., 2008. Synthetic TiO₂ nanoparticle emission from exterior facades into the aquatic environment. *Environ. Pollut.* 156, 233–9. doi:10.1016/j.envpol.2008.08.004
- Kahru, A., Dubourgui, H.-C., Blinova, I., Ivask, A., Kasemets, K., 2008. Biotests and Biosensors for Ecotoxicology of Metal Oxide Nanoparticles: A Minireview. *Sensors* 8, 5153–5170. doi:10.3390/s8085153
- Kampfenkel, K., Vanmontagu, M., Inze, D., 1995. Extraction and Determination of Ascorbate and Dehydroascorbate from Plant Tissue. *Anal. Biochem.* 225, 165–167. doi:10.1006/abio.1995.1127
- Kelly, K.A., Havrilla, C.M., Brady, T.C., Abramo, K.H., Levin, E.D., 1998. Oxidative stress in toxicology: established mammalian and emerging piscine model systems. *Environ. Health Perspect.* 106, 375–84.
- Klaine, S.J., Alvarez, P.J.J., Batley, G.E., Fernandes, T.F., Handy, R.D., Lyon, D.Y., Mahendra, S., McLaughlin, M.J., Lead, J.R., 2008. Nanomaterials in the environment: behavior, fate, bioavailability, and effects. *Environ. Toxicol. Chem.* 27, 1825–1851.
- Kurepa, J., Paunesku, T., Vogt, S., Arora, H., Rabatic, B.M., Lu, J., Wanzer, M.B., Woloschak, G.E., Smalle, J.A., 2010. Uptake and distribution of ultrasmall anatase TiO₂ Alizarin red S nanoconjugates in *Arabidopsis thaliana*. *Nano Lett.* 10, 2296–302. doi:10.1021/nl903518f
- Larue, C., Khodja, H., Herlin-Boime, N., Brisset, F., Flank, a M., Fayard, B., Chaillou, S., Carrière, M., 2011. Investigation of titanium dioxide nanoparticles toxicity and uptake by plants. *J. Phys. Conf. Ser.* 304, 012057. doi:10.1088/1742-6596/304/1/012057
- Lu, CM., Zhang, C.Y.W., Tao, M. X., 2002. Research of the effect of nanometer on germination and growth enhancement of Glycine max L. and its mechanism. *Soybean Sci.* 21, 168–172.
- Maynard, A.D., Aitken, R.J., Butz, T., Colvin, V., Donaldson, K., Oberdörster, G., Philbert, M.A., Ryan, J., Seaton, A., Stone, V., Tinkle, S.S., Tran, L., Walker, N.J., Warheit, D.B., 2006. Safe handling of nanotechnology. *Nature* 444, 267–269. doi:10.1038/444267a
- Mu, L., Sprando, R.L., 2010. Application of nanotechnology in cosmetics. *Pharm. Res.* 27, 1746–9. doi:10.1007/s11095-010-0139-1
- Mueller, N.C., Nowack, B., 2008. Exposure modeling of engineered nanoparticles in the environment. *Environ. Sci. Technol.* 42, 4447–53.
- Navarro, E., Baun, A., Behra, R., Hartmann, N.B., Filser, J., Miao, A.-J., Quigg, A., Santschi, P.H., Sigg, L., 2008. Environmental behavior and ecotoxicity of engineered nanoparticles to algae, plants, and fungi. *Ecotoxicology* 17, 372–86. doi:10.1007/s10646-008-0214-0

- Noctor, G., Foyer, C.H., 1998. Ascorbate and glutathione: Keeping Active Oxygen Under Control. *Annu. Rev. Plant Physiol. Plant Mol. Biol.* 49, 249–279. doi:10.1146/annurev.arplant.49.1.249
- Ojamäe, L., Aulin, C., Pedersen, H., Käll, P.-O., 2006. IR and quantum-chemical studies of carboxylic acid and glycine adsorption on rutile TiO₂ nanoparticles. *J. Colloid Interface Sci.* 296, 71–78. doi:10.1016/j.jcis.2005.08.037
- Rico, C.M., Majumdar, S., Duarte-Gardea, M., Peralta-Videa, J.R., Gardea-Torresdey, J.L., 2011. Interaction of nanoparticles with edible plants and their possible implications in the food chain. *J. Agric. Food Chem.* 59, 3485–98. doi:10.1021/jf104517j
- Rosenbluh, J., Singh, S.K., Gafni, Y., Graessmann, A., Loyter, A., 2004. Non-endocytic penetration of core histones into petunia protoplasts and cultured cells: a novel mechanism for the introduction of macromolecules into plant cells. *Biochim. Biophys. Acta* 1664, 230–40. doi:10.1016/j.bbamem.2004.06.003
- Sankhalkar, S., Sharma, P.K., 2002. Protection against photooxidative damage provided by enzymatic and non-enzymatic antioxidant system in sorghum seedlings. *Indian J. Exp. Biol.* 40, 1260–1268.
- Schreiber, U., Schliwa, U., Bilger, W., 1986. Continuous recording of photochemical and non-photochemical chlorophyll fluorescence quenching with a new type of modulation fluorometer. *Photosynth. Res.* 10, 51–62. doi:10.1007/BF00024185
- Sharma, P.K., Hall, D.O., 1996. Effect of photoinhibition and temperature on carotenoids in sorghum leaves. *Indian J. Biochem. Biophys.* 33, 471–7.
- Sharma, P.K., Shetye, R., Bhonsle, S., 1997. Effect of supplementary ultraviolet-B radiation on young wheat seedlings. *Curr. Sci.* 72, 400–405.
- Tourinho, P.S., van Gestel, C.A.M., Lofts, S., Svendsen, C., Soares, A.M.V.M., Loureiro, S., 2012. Metal-based nanoparticles in soil: fate, behavior, and effects on soil invertebrates. *Environ. Toxicol. Chem.* 31, 1679–92. doi:10.1002/etc.1880
- Watanabe, T., Misawa, S., Hiradate, S., Osaki, M., 2008. Root mucilage enhances aluminum accumulation in *Melastoma malabathricum*, an aluminum accumulator. *Plant Signal. Behav.* 3, 603–5.
- Wierzicka, M., Obidzińska, J., 1998. The effect of lead on seed imbibition and germination in different plant species. *Plant Sci.* 137, 155–171. doi:10.1016/S0168-9452(98)00138-1
- Wiesner, M.R., Lowry, G. V., Alvarez, P., Dionysiou, D., Biswas, P., 2006. Assessing the Risks of Manufactured Nanomaterials. *Environ. Sci. Technol.* 40, 4336–4345. doi:10.1021/es062726m
- Yang, L., Watts, D.J., 2005. Particle surface characteristics may play an important role in phytotoxicity of alumina nanoparticles. *Toxicol. Lett.* 158, 122–32. doi:10.1016/j.toxlet.2005.03.003
- Yuranova, T., Laub, D., Kiwi, J., 2007. Synthesis, activity and characterization of textiles showing self-cleaning activity under daylight irradiation. *Catal. Today* 122, 109–117. doi:10.1016/j.cattod.2007.01.040
- Zheng, L., Hong, F., Lu, S., Liu, C., 2005. Effect of nano-TiO₂ on strength of naturally aged seeds and growth of spinach. *Biol. Trace Elem. Res.* 104, 83–92. doi:10.1385/BTER:104:1:083

AWARDS

Conference Details	Awards
103rd Indian Science Congress 2016 “Science & Technology for Indigenous Development in India” University of Mysore, Mysore, 3 rd -7 th January 2016 SECTION: PLANT SCIENCES	Young Scientist Award
1st International Conference on “Trends in Cell and molecular Biology” TCMB 2015 , BITS Pilani KK Birla Goa Campus, 19 th –21 st December 2015	Best Poster Award
3rd International Plant Physiology Congress (IPPC 2015) “Challenges and Strategies in Plant Biology Research” , Jawaharlal Nehru University (JNU), New Delhi, India 11th–14 th December 2015	Best Poster Award
National Seminar on “New Frontiers in Plant Sciences and Biotechnology” , Department of Botany, Goa University, 29–30 th Jan 2015	Best Poster Award

The Indian Science Congress Association



14, Dr. Biresh Guha Street, Kolkata 700 017

ISCA YOUNG SCIENTIST AWARD

This is to certify that *..... Maria Vera Jesus Da Costa*

..... participated in the 103rd Indian Science Congress

..... held at University of Mysore, Mysuru during

..... January, 3-7, 2016

..... He / She is a recipient of

ISCA Young Scientist Award

..... of The Indian Science Congress Association, Kolkata

..... in the Section of Plant Science

.....
Nilangshu Bhushan Basu

General Secretary (Membership Affairs)

Arun Kumar

General Secretary (Scientific Activities)

January 7, 2016



International Conference on
TRENDS IN CELL AND MOLECULAR BIOLOGY
December 19 - 21, 2015



CERTIFICATE

This is to certify that

Prof. / Dr. / Mr. / Ms. Maria Vera J. Da Costa, Department of Botany, Goa University

has received best poster award in the poster session of the conference.

Dr. Sukanta Mondal

Jt. Secretary

TCMB 2015

Dr. Angshuman Sarkar

Organizing Secretary

TCMB 2015

INDIAN SOCIETY FOR PLANT PHYSIOLOGY



Best Poster Award-2015

Dr./Mr./Ms. Maria Vera Da Costa, Panaji, Goa for poster presentation on *"Size effect of zinc oxide nanoparticles on photosynthesis and oxidant response in Oryza sativa"* at the 3rd International Plant Physiology Congress at New Delhi, India from 11-14 December, 2015.

(Dr. Madan Pal)
Hon. Secretary

(Dr. S.K. Sopory)
President

DEPARTMENT OF BOTANY, GOA UNIVERSITY



Certificate

This is to certify that Dr. / Mr. / Ms. Maria Vera J. Da Costa, Goa University, Goa.


has ~~Attended~~ / Chaired Session / Lead Lecture / Presented a Paper (Oral/Poster) entitled "Influence of titanium..... in Oryza sativa". (session-III) secured 1st place.

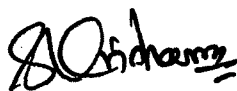
in the National Seminar on 'New Frontiers in Plant Sciences and Biotechnology' organized by UGC-SAP

Department of Botany, Goa University, Goa, during 29 - 30th January, 2015.

Date: 30th January 2015

Silver Jubilee Year (2014-15)
(Department of Botany)


(Prof. B. F. Rodrigues)
Convener


(Prof. S. Krishnan)
Organizing Secretary